THE UNIVERSITY OF SALFORD

SCHOOL OF SCIENCE, ENGINEERING AND ENVIRONMENT

OVERCOMING DRUG RESISTANCE: TARGETING THE BCL-2 FAMILY AND THE LONG NON-CODING RNA HCP5 IN MEDULLOBLASTOMA AND COLORECTAL CANCER

ISEGHOHIMEN J ADESUWA

@00476072

SUBMITTED IN PARTIAL FULFILMENT OF THE REQUIREMENTS FOR THE DEGREE OF DOCTOR OF PHILOSOPHY

AUGUST 2022

Table of Contents

List of Figures

v

List of Tables

ACKNOWLEDGMENTS

DECLARATION

I hereby declare that the following dissertation is entirely my own work and has not been submitted, in whole or in part, for any award to any other academic institution.

ABSTRACT

Colorectal cancer (CRC) is one of the most common cancers in the UK and medulloblastoma is a common cancer found in children. While there has been a progressive improvement in treatment outcomes, success has been marred by drug resistance and severe side effects. Therefore, this project focused on two aspects of chemotherapeutic drug resistance, the first using the antimitotic agent vincristine in combination with inhibitors of the anti-apoptotic Bcl-2 family proteins, while the second investigated the role of the long non-coding RNA (lncRNA), HCP5 in the resistance of cells to genotoxic agents. In the first part, three medulloblastoma cell lines (DAOY, MB03, ONS76) were analysed for the expression of Bcl-xL and ONS76 cells found to have the highest level of this anti-apoptotic protein. Subsequent results indicated that Bcl-xL encourages mitotic slippage and stemness and that knockdown of Bcl-xL in the high expressing ONS76 cells, reduces these and sensitizes the cells to the anti-mitotic agent vincristine. Thus, pharmacological inhibition of Bcl-xL should sensitize medulloblastoma cells to low doses of vincristine. Regarding the lncRNA HCP5, results showed that HCP5 was generally more highly expressed in a panel of CRC cell lines than the three medulloblastoma cell lines, corroborating data from an *in-silico* analysis for the corresponding tumours. One function of HCP5 is to translocate the multifunctional YB-1 protein from the cytoplasm to the nucleus where it carries out many of its functions. Knockdown of HCP5 followed by immunofluorescence indicated a reduction in the amount of YB-1 in the nucleus, confirming this function. Subsequently, HCP5 silencing sensitized all cell lines tested to the DNA damaging agents, cisplatin, oxaliplatin and *tert*-butyl hydroperoxide and also resulted in an increase in double-strand breaks as determined by γH2AX formation. Finally, fluorescence activated cell sorting using Annexin V and propidium iodide confirmed a decrease in cell viability in HCP5 knockdown cells following treatment with genotoxic agents and that this was mirrored by an increased apoptotic fraction. Together, these studies indicate the possibilities of using novel therapeutics to increase the functionality of existing treatments to combat acquired drug resistance in cancer patients.

ABBREVIATIONS

ANOVA   Analysis of variance

APAF-1   Apoptotic protease activating factor 1

APC   Anaphase-promoting complex/cyclosome

APS   Ammonium persulfate

ASO   Anti sense oligonucleotide

ATM   Ataxia–Telangiectasia mutated

ATP   Adenosine triphosphate

BAD   Bcl-2 associated death promoter

BAK   Bcl-2 homologous antagonist killer

BAX   Bcl-2 associated X protein

BCL-XL   B-cell lymphoma extra large

BCL-2   B-cell lymphoma 2

BER   Base excision repair

BID   BH3 interacting domain death agonist

BIK   Bcl-2 interacting killer

BOK   Bcl-2 related ovarian killer

BRCA1   Breast cancer type 1 susceptibility protein

bp   Base pair

ceRNA   Competing endogenous RNA

CDK1   Cyclin dependent kinase 1

cDNA   complementary DNA

CIN   Chromosomal instability

CMS   Consensus molecular subtypes

CRC   Colorectal cancer

CRS   Cytoplasmic retention signal

CSC   Cancer stem cells

CtIP   CtBP-interacting protein

CTNNB1   Catenin Beta 1

DDB   DNA damage binding protein

DDR   DNA damage response

DMEM   Dulbecco's Modified Eagle's Medium

DNA   Deoxyribonucleic acid

DNA-PK   DNA-dependent protein kinase

DSB   Double-strand break

ERCC1   Excision repair cross-complementation group 1

FapyG   2,6-diamino-4-hydroxy-5-formamidopyrimidine

FBS   Foetal bovine serum

FEN1   Flap endonuclease 1

Fpg   Formamidopyrimidine DNA glycosylase

FSTL5   Follistatin-like 5

GAPDH   Glyceraldehyde-3-phosphate dehydrogenase

HhH   Helix-hairpin-helix

HLA   Human leukocyte antigen

HCP5   Human histocompatibility leukocyte antigen (HLA) complex P5

HOTAIR   HOX transcript antisense RNA

HR   Homologous recombination

H2TH   helix-2turn-helix

H2AX   H2A histone family member X

ICL   Inter-strand crosslink

IC50   Inhibitory concentration at 50%

kDa   kilo Dalton

LncRNA   Long non-coding RNA

MALAT1   Metastasis Associated lung adenocarcinoma transcript 1

MCL-1   Myeloid cell leukaemia 1

MHC   Major histocompatibility complex

MSI   Microsatellite instability

MLH1   MutL homolog 1

MOMP   Mitochondrial outer membrane permeabilization

MRE11   Meiotic recombination 11 homolog A

MRN   Mre11-Rad50-Nbs1 complex

MSH5   MutS protein homolog 5

NBS1   Nijmegen breakage syndrome 1

NEIL1/2/3   Endonuclease VIII-like 1/2/3

NER   Nucleotide excision repair

NHEJ   Non-homologous end joining

NLS   Nuclear localisation sequence

NTH1   Nth like DNA glycosylase 1

OGG1   8-oxoguanine DNA glycosylase 1

PARP   poly(ADP-ribose)polymerase

PBS   Phosphate buffered saline

PCNA   Proliferating cell nuclear antigen

PCR   Polymerase chain reaction

PGCC   Polyploid giant cancer cells

PI   Propidium iodide

PI3K   Phosphoinositide 3-kinase

PTCH1   Patched-1

PVDF   Polyvinylidene difluoride

qPCR   Quantitative polymerase chain reaction

RNA   Ribonucleic acid

RNF8   Ring finger 8

ROS   Reactive oxygen species

RPA   Replication protein A

RPMI   Roswell Park Memorial Institute

RT   Reverse transcription

SAC   Spindle assembly checkpoint

SHH   Sonic hedgehog

siRNA   Small interfering RNA

SMI   Small molecule inhibitor

ssDNA   Single-stranded DNA

SRCC   Signet ring cell carcinoma

SUFU   Suppressor of fused homolog

TBH   *tert*-butyl hydroperoxide

TEMED   N,N,N′,N′-Tetramethyl ethylenediamine

TFIIH   Transcription factor II H

TP53   Tumour suppressor protein 53

UV   Ultraviolet

WNT   Wingless type

XPG   Xeroderma pigmentosum complementation group G

XRCC1   X-ray repair cross-complementing protein 1

YB-1   Y box binding protein 1

γH2AX   phosphorylated H2A histone family member X

53BP1   p53-binding protein

5-FU   Fluorouracil

CHAPTER 1: INTRODUCTION

1.1 Cancer

Cancer is one of the top five causes of death in the United Kingdom (WHO, 2022). In England, 327,174 new cancer cases were identified in 2019, with men having a 23% higher occurrence rate than women (Caswell, 2022). Cancer claimed the lives of 137,234 persons in England in 2020. Since 2001, the number of fatalities has risen by 8% (Cancer registration statistics NHS, 2021). Cancer is also the most common cause of death in children and accounts for 20% of deaths in children between 1-14 years (Cancer Research UK, 2015). Although a single source has not been identified as a causative agent for cancer in general, however certain lifestyle choices and infections has been shown to result in the development of cancer (Anand *et al*., 2008). The World Health Organisation (WHO) published in 2021 that people who smoked, drank excessive alcohol and practised an unhealthy lifestyle in general were more predisposed to developing cancer (WHO, 2022). It was also discovered that viral infections such as hepatitis B and C, HIV and the human papillomavirus, increase the risk factor of cancer development, with 13% of cancers accredited to have developed from pre-existing infections (de Martel *et al*., 2012).

Cancer is a group of disorders characterised by abnormal cell proliferation that can infiltrate or migrate to other parts of the body (Lujambio & Lowe, 2012). Cell development and division is a tightly controlled process comprising of growth factors and signalling pathways that regulate whether a cell divide (Sitas *et al*., 2006). These processes are governed by numerous proteins and mutations in these proteins can cause the cell to divide in an unpredictable and uncontrolled manner, resulting in a mass of cancerous cells (Cairns, 1975). In general, mutation in protein coding genes can be hereditary or acquired. Acquired mutations can either arise from external factors such as ionising radiation and the presence of a mutagen or the incomplete replication of DNA during cell division (Children with Cancer UK, 2018).

1.2 Colorectal cancer (CRC)

Colorectal cancer (CRC) is the development of a malignant tumour from the cells that line the colon (large intestine) or rectum (part of the large intestine) (Mármol *et al*., 2017). CRC often occurs due to WNT signalling pathway mutation which leads to the upregulation of signalling

1

activity. This mutation can be passed down to an offspring or attained naturally over time (Markowitz & Bertagnolli,2009).

CRC is one of the most common cancers in the UK as it accounts for about 11% of novel cancer cases. It is also the third most popular cancer in male and female, with 18,600 new cases for females and 23,500 new cases for males in 2017 (Cancer Research UK, 2017). CRC cases were sparse in the early decades of the 20th century, however, a rise in cases began and it was prevalently in the western countries, such as USA and UK (Fearon, 2011). CRC is common in older people with people aged 75 and above accounting for 44% of new cases in that age range in the UK (Bowel cancer UK, 2022).

1.2.1 Histological variants of CRC

CRC was classified by the WHO based on the appearance of the tumour. There are different histological variants of CRC, however only four of these variants will be reviewed. The four variants are Signet ring cell carcinoma, Adenocarcinoma, Mucinous carcinoma and Medullary carcinoma (WHO, 2022). Adenocarcinoma is a type of cancer that originates from the epithelial cells that line the mucous gland in organs such as the colon and lungs and accounts for 79% of all CRC (Figure 1.1) (Ryan *et al*., 2014). Adenocarcinoma usually begin as a growth of tissue in the inner lining of the colon, these growths are called polyps (Parkin *et al*., 2005). Some polyps can get cancerous over time (typically many years), however not all polyps turn cancerous. The likelihood of a polyp developing into cancer is determined by the type of polyp (Muto *et al*., 1975).

Mucinous carcinoma is known as a type of CRC where mucus is produced in more than half of the tumour and they are mainly situated in the right colon. CRC accounts for 40% of mucinous carcinoma, however only 10% of CRC are mucinous carcinoma (Figure 1.1) (Benesch *et al*., 2020). The epithelial mucosal cells create mucin to lubricate and also to serve as a barrier to prevent entry of pathogens and other harmful material (Lee *et al*., 2011). When there is a mutation in the protein that regulates mucus production in the cell, this leads to a change in the quality and quantity of mucus produced and this encourages cancer cells to sabotage and convert their regulatory and signalling function into a means of protection from the immune system (Kufe,2009). The increase in the amount of mucin produced interferes with interaction between cells and encourages plasticity of the cell and anchorage independent growth which are both factors that play an important role in metastasis and invasion (Hollingsworth *et al*., 2004). Prognosis for mucinous carcinoma is still undetermined as

although mucinous carcinoma was originally thought to be a negative prognostic biomarker, there has been no significant difference between the rate of survival of patients with mucinous carcinoma and patients with tumours located in the gland (Leopoldo *et al*., 2008). Rectal mucinous carcinoma is contentious as it doesn't respond to chemotherapy and the success rate of the complete removal of the tumour via surgery is low (Nagteegal *et al*., 2015).
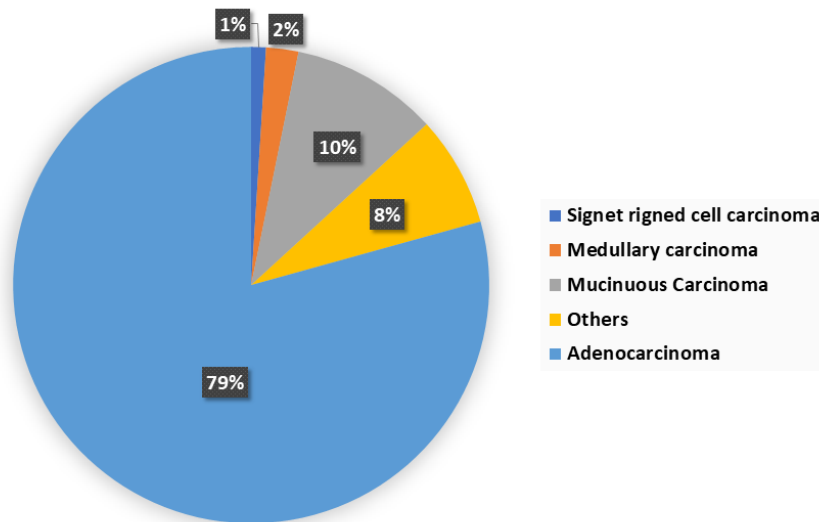
Figure 1.1- **Graphical representation of the occurrence of the types of colorectal cancer.** Adenocarcinoma is the most prevalent type of CRC accounting for 79% of all CRC cases and signet ring cell carcinoma is the least prevalent as it accounts for just 1% of all CRC cases.

Medullary carcinomas are confined carcinoma which are made up of cells that are not properly differentiated (Fatima *et al*., 2021). These malignant cells have limited stroma and they are characterized by the absence of gland formation and neuroendocrine markers. These carcinomas are uncommon and only occur at a rate of 1 in 20,000 cases (Testa *et al*., 2018). Medullary carcinomas are not aggressive, are situated proximally and they present with the absence of CDX2 and MutL homolog 1 (MLH1), so they can be easily differentiated from other adenocarcinomas that are present in the right colon (Cunningham *et al*., 2014). Medullary carcinomas are not aggressive and are situated proximally and they present with the absence of CDX2 and MutL homolog 1 (MLH1), so they can be easy differentiated from other adenocarcinomas that are present in the right colon (Cunningham *et al*., 2014). The presence of the lymphocytes in medullary carcinoma encourages an inflammatory response that curtails the distribution of the tumour to other sites (Fatima *et al*., 2021). The presence of medullary

carcinoma can also serve as a positive biomarker for prognosis as it has the best prognosis among similar carcinomas present in the colon (Thirunavukarusu *et al*.,2010).

Signet ring cell carcinoma (SRCC) is a malignant carcinoma that is rare in CRC as it accounts for about 1% of all colorectal cancers (Belli *et al*., 20014). It is more common in female patients below 40 years old and distinct features of the carcinoma is the presence of fibrosis and metastasis favours the peritoneum instead of the liver (Benesch & Mathieson, 2020). The name SRCC originates from the cells found in this carcinoma which look like signet rings, this morphology of the cells is due to the presence of a lot of mucus granules that secrete mucin in the cytoplasm (El Hussein & Khader, 2019). The presence of these mucus granules leads to the accumulation of mucin in the vacuole, which results in increase of the size of the vacuole and moves the nucleus closer to the cell's border (Portnoy, 2006). The mechanism by which signet ring cells develop is not clear, however recent studies have shown that certain pathways play a vital role in the development of signet ringed cells. The activation of ErbB2/ErbB3 controls phosphatidylinositol 3-kinase (PI3K) and of p38 MAP kinase activation (Figure 1.2) (Fukui, 2014).
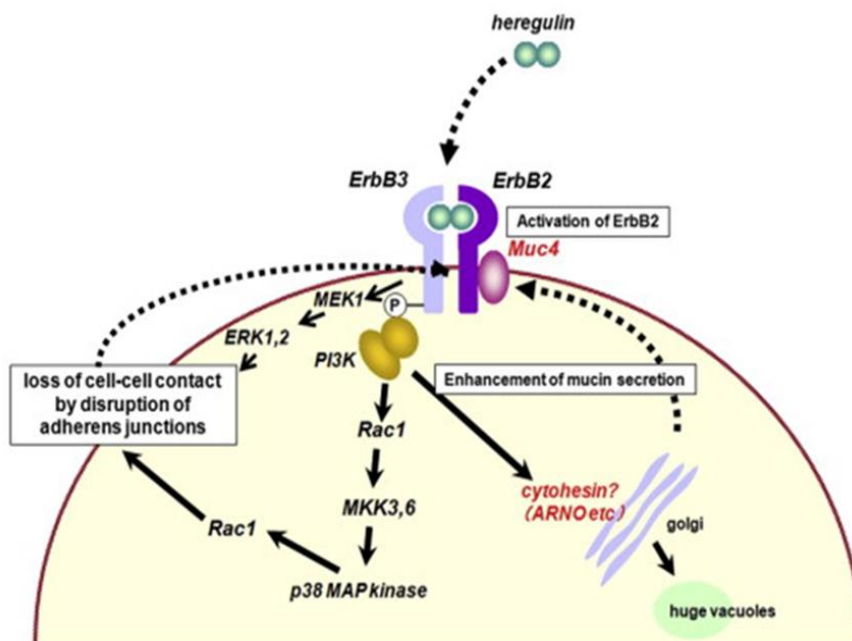
Figure 1.2- **The development of signet ring carcinoma** (adapted from Fukui, 2014). The activation of Erb2/Erb3 pathway commences signet ring carcinoma development, this results in the activation of p38 MAP kinase and MEK1pathways which disrupts adheren junctions. This this causes a lack of cell-cell connections. The activation of PI3K increases mucin secretion. ErbB2 is activated by one of the mucins, Muc4. As a result, an activation loop made up of ERbB2/ErbB3-Muc4-ErbB2/ErbB3 is created.

SRCC has distinct pathological characteristics that separate it from regular colonic AC and bestow aggressiveness on the cells. Malignant cells with signet rings can be detected floating in extracellular mucin pools as clusters or single cells (Fukui, 2014). When compared to conventional adenocarcinoma, these cells had a lower KRAS mutation rate but an increased BRAF mutation rate, and the prognostic implications are uncertain (Al-Taee *et al*., 2016). As the cells acquire stem cell-like features, loss of E-cadherin expression has been noted to contribute to the high-grade and invasive nature of SRCC (Hamilton *et al*., 2013). Prognosis for SRCC is poor and this is attributed to late diagnosis of the cancer as symptoms do not present until the cancer is at an advanced stage. SRCC can be inherited and typically manifests in young adults (Sun *et al*., 2018).

1.2.2 Subtypes of CRC

Extensive epigenomics studies showed that all CRC are different with the presence of an average of 76 expressive mutations (Wood *et al*., 2007). The consensus molecular subtypes (CMS) were established in 2014 by the Colorectal Cancer Subtyping Consortium (Dienstman et el., 2014). The CMS subtypes account for 87% of the CRC cases examined, while the remaining 13% were without a subtype as they had features that corresponds to all the CMS subtypes (Guinney *et al*., 2015). The CMS subtypes were distinguished based on gene expression signature, clinical manifestation and molecular evolution as shown in Table 1.1 (Frackowiak *et al*., 2019). Clinical evaluation of the four CMS subtypes detected significant variations amongst the subtypes based on the site of the tumour, sex of the patient, histological stage and grade of tumour at diagnosis and survival of patient (with or without relapse) (Guinney *et al*., 2015).

There are four subtypes of CRC, they are CMS1, CMS2, CMS3 and CMS4

Table 1.1- Subtypes of colorectal cancer showing the location, pathways, mutations and gene expression signature of each subtype.

Subtype	CMS1 Immune	CMS2 Canonical	CMS3 Metabolic	CMS4 Mesenchymal
Occurrence	14%	37%	13%	23%
Molecular features	Hypermutations, MSI, strong immunogenic activation	Epithelial, activation of WNT and MYC pathways	Epithelial, metabolic regulation disturbed	High TGFβ expression; epithelial invasion and angiogenesis
Gene expression signature	MSI, high number of mutations, low number of copies	CIN, low-moderate mutation and copy index	CIN, moderate no. of mutations, and low no. of copies	CIN, low no. of mutations, and high no. of copies
Mutations	MSH6, RNF43, ATM, TGFbR2, BRAF, PTEN	APC, KRAS, TP53, PIK3CA	APC, KRAS, TP53, PIK3CA	APC, KRAS, TP53, PIKC3CA, TOP1, CES2
Pathways	Inflammatory activation, JAK-STAT, caspases	WNR trail, MYC, EGFR, SRC, VEFG/VEGRF activation; integrins, TGFβ, IGF, IRS2, HNF4a and HER2 and cyclin activation	DNA repair, glutaminolysis, lipogenesis	Stroma activation, immunosuppression, integrins
Immunogenicity	Immune activated CD8, CD4 T cells, Th1, NK cells, DC, M1 macrophages, PD-1, PD-L1, CTLA4, LAG3	Immune desert Naïve CD4 T/B cells, resting NK cells	Immune mixed Enriched in cells expressing PD-1, Th17 and naïve T/B cells	Immune suppressed Tregs, MSDCs, few CD8, CD4 T cells, M2 macrophages
Location	Proximal colon	Distal colon to rectum	No specific location	Distal colon to rectum

CMS1 accounts for 14% of all CRC cases. Approximately 12% of CMS1 cases are acquired, while the rest are genetic (e.g., Lynch syndrome) (Okita *et al*., 2018). CMS1 subtype are known to originate from serrated polyps (Stintzing *et al*., 2019). Carcinogenesis in CMS1 occurs via the serrated pathway which has the following attributes: 1) loss of tumour suppressor function (CpG island methylator phenotype [CIMP]) due to hypermutable CpG islands, 2) Hypermutation of *BRAF* V600, 3) proximal colon site (occurs in the right colon) 4) affiliation with a damaged DNA mismatch repair (MMR) pathway, 5) lymphocytic infiltration into the tumour environment (Thanki *et al*., 2017).

CMS1 has high microsatellite instability due to the promoter regions of repair genes the DNA mismatch repair genes undergoing frequent methylation or mutation (Randrian *et al*., 2021). Cancers that belong to the CMS1 subtype are regarded as hypermutated as they have about 47 mutations for every 1 million bases, in comparison to cancers that lack microsatellite instability like the CMS2 subtype which have about 28 mutations for every 1 million bases (Boland and Goel, 2010). However, even though CMS1 cancers are hypermutated, they are also shown to have a low copy number of the affected genes (Smeets *et al*., 2018). When early detected before

the cells have metastasized, CMS1 tumours respond well to treatment and have good prognosis (Lenz *et al*., 2019). Studies have shown that this may be due to the tumour microenvironment of CMS1 cancers which has good immunogenicity with the presence of different T cells such as helper T cells, CD8 and cytotoxic T lymphocytes which boost immunity and the absence of cancer associated fibroblasts (CAFs) which encourage proliferation (Roelands *et al*., 2017). After treatment, CMS1 cancers are unlikely to reoccur, however if the patients do relapse, the prognosis is worse as the survival rate after relapse (SAR) is 9 months. The five-year survival rate for CMS1 subtype is 73% (Sinicrope *et al*., 2011).

CMS2 (also known as canonical) is the most common out of all the subtypes, as it accounts for 37% of all CMS subtypes (Okita *et al*., 2018). CMS2 cancers frequently present (59%) in the left side of the colon (distal) and originate from the canonical adenocarcinoma pathway (Fontana *et al*., 2019). CMS2 cancers are associated with chromosomal instability, they have a high level of chromosomal instability which usually occurs in conjunction with aneuploidy, loss of heterozygosity and addition or removal of substantial portions of the chromosome (Rebersek, 2020). This subtype has been shown to exhibit high expression of the MYC transcription factor and the WNT/β-Catenin pathway (Berg *et al*., 2019). Elevated copy number variations were discovered in CMS2 cancers with recurrent copy number addition discovered in oncogenes and copy number deletion in tumour suppressor genes like APC (Dienstman *et al*., 2017). However, the rate of mutation was low with less than 8 mutations for every 1 million bases, thus it was termed non-hypermutated (Danielsen *et al*., 2016). The prognosis for CMS2 cancer is good, with a five-year survival rate of 77% and survival after relapse (SAR) is 35 months (Berg *et al*., 2019).

CMS3 is also called the metabolic subtype and it accounts for 13% of CRC cases (Okita *et al*., 2018). Hypermutation occurs in about 30% of CMS3 tumours, KRAS mutation is ubiquitous in CMS3 with 68% of cases having KRAS mutation (Rebersek, 2020). Chromosomal instability is present in CMS3, however in comparison to CMS2 and 4, the amount of somatic copy number alteration is lower (Stintzing *et al*., 2019). Microsatellite instability is intermediate, it is however, more than that found in CMS2 and 4, but less when compared to CMS1 (Eide *et al*., 2021). Based on gene expression, CMS3 is considered the most akin to heathy colon tissue compared to other subtypes (Abdelkader *et al*., 2017). Prognosis of CMS3 cancers is good irrespective of what stage the cancer is diagnosed. The five-year survival rate is 75% (Guinney *et al*., 2015).

Studies have shown that the amount of transforming growth factor β (TGFβ) available in the microenvironment of premalignant serrated adenoma determines which subtype the cells evolve into, with high levels evolving into CMS4 and low levels CMS1 (Fessler *et al*., 2016). CMS4 also called mesenchymal accounts for 23% of CRC cases. It is characterised by low hypermutation and microsatellite stability due to low methylation and high somatic copy number alterations (Coebergh van den Braak *et al*., 2020). PIK3CA, KRAS, APC and TP53 are often mutated in CMS4 (Yang *et al*.,2022). CMS4 subtype have a mesenchymal phenotype and gene signatures are similar to an activated stroma, this includes high carcinoma-associated fibroblasts (CAFs) with TGFβ signalling, angiogenesis and binding to matrix proteins integrin (Guinney *et al*., 2015). The tumour microenvironment is inflammatory with the presence of principal innate immune cells such as macrophages, helper T cells, Treg cells and interleukin 17 and 23 which are immunosuppressive cytokines that connects this subtype to a unique type of CRC called colitis-associated colorectal carcinoma (Thanki *et al*., 2017). This cancer arises from ulcerative colitis in inflammatory bowel disease where inactivation of TP53 occurs early in the angiogenesis pathway compared to the angiogenesis of CMS2 subtype where TP53 inactivation occurs downstream of the transformation of the adenoma to carcinoma (Fessler *et al*., 2017). CMS4 occurs more in men, with men accounting for 55% of cases. Prognosis is poor and this is primarily due to diagnosis occurring at a later stage (De Sousa E Melo *et al*., 2013). CMS4 patients are known to often relapse, the five-year survival rate is 62% and the five-year relapse free survival rate is 60% (Guinney *et al*., 2015). Chemotherapy is usually recommended for stage 3 colorectal cancer, however stage 3 CMS4 do not respond well to adjuvant chemotherapy (Roepman *et al*., 2014).

1.2.3 Mutations in CRC

Fearon and Vogelstein identified certain pathways crucial to the progression of CRC in 1990. These pathways were made up of accumulating mutations in a number of genes that control cell proliferation and differentiation (Fearon & Vogelstein, 1990). The inactivation of tumour suppressor genes and consequent encouragement of neoplasia are caused by both genetic and epigenetic alterations, the latter of which results in aberrant methylation of tumour suppressor genes (Armaghany *et al*., 2012). Mutations in CRC can be attained due to lifestyle, external factors or it can be passed from a parent to its offspring. The Adenomatous polyposis coli (*APC)* gene is the gene usually mutated in most CRC cases (Fodde, 2002).

Adenomatous polyposis coli (*APC*) -This gene encodes for the APC protein which is a tumour suppressor protein that regulates the amount of beta-catenin produced/present in the cell and

when beta catenin is regulated by APC (Khalek *et al*., 2010), it prevents the genes that encourage cell replication from being over activated, thus preventing uncontrollable growth of cells (Zhang & Shay, 2017). When APC is absent, β-catenin is amassed in the cell, it then relocates to the nucleus where it initiates proto-oncogenes activation and creates a bond with DNA (Valenta *et al*., 2012). *APC* is essential for differentiation and renewal of stem cells, however when it is upregulated, this can result in cancer (White & Lowry, 2015).

P53- p53 is a transcription factor that inhibits the growth of tumours by controlling a large number of target genes with various biological roles (Sammons *et al*., 2020). The TP53 locus mutations or other oncogenic factors that reduce the activity of the wild-type protein, like the overexpression of the p53 repressor MDM2, inactivate this master transcription factor's activity in nearly all cancers (Sullivan *et al*., 2018). Mutation of p53 also plays a role in CRC, this protein activates the apoptosis pathway if a cell has been damaged beyond repair or if there is a defect in the WNT pathway (Abraha & Keteha, 2016). Other proteins in the apoptosis pathway are also mutated in CRC such as pro- apoptotic protein BAX, DCC and TGF-β.

Deleted in colorectal carcinoma (DCC)- This is a tumour suppressor gene that is a receptor for netrin-1, however when not bound to netrin-1, it inhibits cell growth and when netrin-1 is bound to its active site, DCC encourages the survival of the cell (Meijers *et al*., 2020). Netrin bound DCC has numerous pathways that encourage the development of cancer such as the MAPK1/3 AND CDC42-RAC1 pathways (Duman-Scheel, 2012). Therefore, DCC can act as a proapoptotic or antiapoptotic protein, depending on if it is activated by Netrin-1 (Kang *et al*., 2018). Inhibition of DCC is not considered to play a role in the formation of tumours, however it is thought to contribute to the growth of tumours already present (Arakawa *et al*., 2004).

Transforming growth factor beta (TGF-β)- It is a signalling protein with many other functions as it controls inflammatory processes and also participates in the differentiation of stem cells and the differentiation and regulation of T-cells (Massague *et al*., 2000). Mutation of TGF-β in CRC leads to the inability of it to carry out its regulatory function in the cell cycle which is to arrest the cell at the G1 phase of mitosis to stop replication or encourage apoptosis (Xu & Pasche, 2007). However, in its mutated state, cancer cells can replicate while the neighbouring cells such as fibroblast replicate, resulting in the increase of the amount of TGF-β synthesized in both cells thus leading to a ripple effect to all other neighbouring cells such as the endothelial and stroma cells (Itatani *et al*., 2019). It also results in suppression of the activity

of the immune system and the production of blood vessels in tumours, which increases the invasiveness of the tumour (Blobe *et al*., 2000).

Bcl-2 associated X protein (BAX)- BAX belongs to the Bcl-2 family of anti or pro apoptotic proteins that regulate apoptosis. BAX binds with Bcl-2, which results in the activation of apoptosis (Carberry *et al*., 2018). It increases the mitochondrial outer membrane permeabilization (MOMP) which leads to the escape of cytochrome c, thus triggering apoptosis (Pryczynicz *et al*., 2014). BAX expression is regulated by p53 and it is observed to mainly take part in apoptosis activated by p53 (Shi *et al*., 2003). Bax mutation is present in about 50% of CRC and it has been discovered to be the source by which cancer cells deactivate apoptosis and BAX is the primary apoptotic protein that regulates apoptosis in epithelial cells (Miquel *et al*., 2005). Therefore, when there is a mutation in BAX that deactivates its function, the cells can evade apoptosis, which leads to tumour progression (Theodorakis *et al*., 2002).

Genomic instability- There are three major pathways by which genomic instability occurs and they are microsatellite instability (MSI), chromosomal instability (CIN) and CpG island methylator phenotype (CIMP) (Rajagopalan *et al*., 2003). Chromosomal instability (CIN) pathway accounts for about 85% of all CRC cases and it involves the deletion or duplication of the chromosome or parts of it, thus resulting in unequal numbers of chromosomes which then leads to mitosis failure and aneuploidy (Pino & Chung, 2010). Chromosome instability originates due to faulty DNA damage response, where double stranded DNA breaks are not repaired properly, therefore resulting in the recombination of DNA sequence on the chromosome with that of a non-homologous chromosome (Bakhoum *et al*., 2017). It can also be caused by degeneration of telomere and irregularities in the spindle assembly checkpoint (SAC), when a kinetochore is attached to microtubules from each spindle pole, the SAC doesn't acknowledge this, thus resulting in the cell exiting mitosis with this abnormality which prevents the separation of the chromatids, thus resulting in CIN (Geigl *et al*.,2008).

Microsatellite instability (MSI) pathway- Short repetitive DNA segments are called microsatellites. These sequences can be composed of repeating, contiguous units in the genome that range in size from one to six base pairs (Nikanjam *et al*., 2020). Each person has microsatellites of a specific length, albeit they can differ from person to person and influence one's unique DNA "fingerprint." (Li *et al*., 2020)This pathway is a result of a genetic bias to mutation (hypermutability) that arises from faulty DNA mismatch repair mechanism (Nojadeh *et al*., 2018). The mismatch repair pathway fixes faults that arise during DNA replication (such

as addition or deletion of a base) (Kang *et al*., 2018). If the mismatch repair pathway is not functioning properly, this can lead to an accumulation of DNA with errors in their sequence which produces a repeated sequence of DNA (microsatellites) (Boland *et al*., 2010). The presence of MSI in CRC results in inadequate tissue differentiation, infiltration of tumours by lymphocytes and high mucinogens (Popat *et al*., 2005). Patients are classified into three groups based on the amount of microsatellite instability present i.e., high, low and stable (Li *et al*., 2020). Patients with MSI- high tumour in CRC had a 15% better prognosis compared to the others as the rate of metastasis is lower in MSI-high tumours and they usually present in stage II cancer (Beucher *et al*., 2013).

Epigenetic instability – Colorectal neoplasms tend to frequently exhibit epigenetic instability (Requena & Garcia-Buitrago, 2020). In general, the term "epigenetics" refers to the regulatory, heritable parts of a genome that are not part of the basic DNA sequence (Puttiri & Robertson, 2010). The two epigenetic markers that are best understood are DNA methylation and post-translational modification of the core histone proteins. DNA methylation is an epigenetic process that occurs in the mammalian genome and involves adding a methyl group to the cytosine's C5 position to create 5-methylcytosine (Skvortsova *et al*., 2019). It mostly occurs at the C5 position of cytosine nucleotides after a guanine (CpG) (Zhao *et al*., 2020). DNA methylation controls gene expression by attracting proteins that are involved in gene repression or by preventing transcription factors from interacting with DNA (Nishiyama & Nakanishi, 2021). The majority of the human genome is covered by DNA methylation, which is kept in very stable patterns that are formed during development (Ziller *et al*., 2013). In humans, about 70% of CpG dinucleotides carry this epigenetic alteration. CpG islands, which are found in the 5′ region of about 50%–60% of genes, are areas that are enriched with CpG dinucleotides and are typically kept in an unmethylated form (Pachano et al., 2021). A lot of these CpG islands exhibit abnormal methylation in malignancies, which may also be accompanied by transcriptional suppression (Ehrlich, 2019). This process has resulted in the silencing of some tumour suppressor genes in CRC, such as *HLTF, MGMT* and *CDKN2A/p16* (Baylin *et al*., 2000).

1.2.4 Diagnosis of CRC

There are different diagnoses for CRC, however it is mostly diagnosed by computerized tomography (CT) scan which is performed on the pelvis, chest or abdomen. Magnetic

resonance imaging (MRI) could also be used in cases where the cancer is present in the rectum, this is used to determine its location and the stage of the cancer before operating on it (Labianca & Merelli, 2010). Diagnosis can also be done by carrying out a biopsy, which involves the excision of the tumour through surgery for analysis, where a histopathology report is carried out to determine the characteristics and function of the tumour (Zhang *et al*., 2002). Staging can also serve as a good diagnostic tool and it determines the evasiveness of the cancer, it is usually done after a histopathology report has been generated or after surgery (Cunnigham *et al*., 2010). Staging in colorectal cancer is dependent on the amount of which the cancer has evaded the surrounding cells and organs and if it has progressed to the lymph nodes. It is a quantification of how far metastasis has occurred (Compton & Greene, 2004).

1.2.5 Treatment of CRC

There are various treatments for CRC, however treatment is dependent on the stage of the tumour, health of the patient and what treatment option the patient decides to go for (Ciombor & Goldberg, 2015). If the cancer is detected early, surgery can be carried out to remove the tumour, however, if it is detected late and has metastasised to other parts of the body, treatment is usually palliative to keep the person alive for as long as possible and help ease the symptoms of the cancer. (Cunnigham *et al*., 2010).

Surgery is carried out to excise the tumour if detected early, however, the size and location of the tumour determines how much of the tumour can be removed (Cancer.net, 2022). In cases where the cancer is still at its source the whole area where the tumour is located is excised including the blood vessels (Carrato, 2008). If mild metastasis has occurred to neighbouring organs such as the liver, this can also be excised through surgery. Sometimes, surgery is used in combination with chemotherapy, where the patient is initially treated with chemotherapy to reduce the size of the tumour before surgery is carried out (Fantola *et al* 2011).

Chemotherapy- This is a common treatment for CRC, it is often used in combination with surgery or radiation (Phillips & Fu, 1976). The stage of the cancer determines if chemotherapy is administered. Chemotherapy is not needed in stage 1 CRC as surgery is sufficient (Esquivel *et al*., 2007). In stage 2, chemotherapy is only administered if the patient has an aggressive tumour such as T4 tumour which means the tumour has increased in size and is protruding from the wall of the bowel (Rebuzzi *et al*., 2020). In stage 3 and 4, chemotherapy is essential as the tumour has metastasized to other organs such as the lymph nodes and chemotherapy such as cisplatin, oxaliplatin and fluorouracil are administered (Sugarbaker *et al* 2016). Several

drugs have been approved for the treatment of CRC and their functions and mode of action varies. They include, fluorouracil (5-FU), oxaliplatin, lonsurf, camptosar and capecitabine. Once in the blood stream**,** capecitabine is converted to fluorouracil, this chemotherapeutic drug is often used to treat metastatic CRC or in combination with radiotherapy. Fluorouracil works as a thymidylate synthase inhibitor, among other things (Thirion *et al.*, 2004). The pyrimidine thymidylate (dTMP), a nucleotide necessary for DNA replication, is blocked when this enzyme's function is disrupted (Longeley *et al.*, 2003). Deoxyuridine monophosphate (dUMP) is methylated by thymidylate synthase to produce thymidine monophosphate (dTMP). Because 5-FU induces a shortage of dTMP, rapidly dividing malignant cells undergo apoptosis due to the absence of thymidine (Vodenkova *et al.*, 2020). Calcium folinate acts as an exogenous source of reduced folinates, stabilising the 5-FU-TS combination and thereby increasing the cytotoxicity of 5-FU (Alvarez *et al.*, 2012). Irinotecan works by binding to a fraction of topoisomerase-1-DNA cleavage complexes, specifically those containing a guanine +1 in the DNA sequence (Vanhoefer *et al.*, 2001). Irinotecan deactivates the topoisomerase 1 enzyme by stacking on the base pairs surrounding the topoisomerase-induced cleavage site. Hydrolysis converts irinotecan to SN-38, a topoisomerase I inhibitor (Saltz *et al.*, 2000). Addition of glucuronic acid by uridine diphosphate glucuronosyltransferase 1A1 inactivates it (UGT1A1). The active metabolite SN-38 inhibits topoisomerase I, which eventually inhibits both DNA replication and transcription (Pommier, 2013). Oxaliplatin, (dach = (*trans-R,R*)cyclohexane-1,2-diamine) also known as Eloxatin is a third generation platinum-based chemotherapy drug commonly used in the treatment of CRC and is frequently used in combination with other drugs such as fluoracil and folinic acid in advanced stages of CRC (Raymond *et al.*,2002). After chemotherapy and targeted treatments have failed, lonsurf is a fixed-dose combination drug that serves as a third- or fourth-line treatment for metastatic CRC (Kish & Uppal, 2016). It is made up of two pharmacologically active ingredients: the pyrimidine analogue trifluridine and the thymidine phosphorylase inhibitor tipiracil. Tipiracil inhibits trifluridine from being rapidly metabolised, enhancing its bioavailability (Temmink *et al.*, 2007).

Radiotherapy – Radiotherapy is carried out in conjunction with chemotherapy, it is however not sought after due to the fragility of the bowels. Chemoradiation therapy is frequently performed before surgery in rectal cancer to avoid colostomy or lower the risk of recurrence (Tam & Wu, 2019). Chemoradiation therapy provided before surgery functioned better and had fewer adverse effects than the same radiotherapy and chemotherapy given after surgery (Simpson & Scholefield, 2008). The key advantages of chemoradiotherapy are: lower rate of

cancer recurrence in the original site, fewer patients requiring permanent colostomies, and less difficulties with colon scarring where radiation therapy is administered (Haraldsdottir *et al.*, 2004). The aim of radiation in stage 1 and 2 CRC is to reduce the size of the tumour before surgery and it also reduces the possibility of the cancer reappearing. It can also be administered after surgery to kill any cancer cells that may remain (Häfner & Debus, 2016). It is also used in stages 3 and 4 where surgery cannot be carried out (Cao *et al.*, 2019). There are different types of radiotherapy. Stereotactic radiotherapy is used in the treatment of metastasized CRC (Kim *et al.*, 2008). When the tumour has migrated to the liver or lungs, stereotactic radiation treatment is a type of external-beam radiation therapy that may be employed. This type of radiation therapy targets a small area with a large, precise dosage of radiation (Dagoglu *et al.*, 2015). Brachytherapy may be utilised to treat some CRCs; however, further research is needed to determine how and when to use it (Lee *et al.*, 2007). A radioactive source is placed inside the colon near to or into the tumour for this treatment. This permits the radiation to get to the colon without passing through the skin and other tissues of the abdomen (abdomen), reducing the risk of tissue damage (Rivard *et al.*, 2009). The radioactive material employed (iodine, palladium, cesium, or iridium) is determined by the treatment method. Irrespective of the treatment method used the radiation source must be encapsulated (Hoskin *et al.*, 2004). This denotes that it is stored inside a non-radioactive metallic capsule known as a "seed." This prohibits the substance from spreading throughout the patient's body (Skowronek, 2017).

Immunotherapy- Immunotherapy is commonly used with patients that have mutated or non-functioning mismatch repair pathway, this is done using inhibitors of the immune checkpoint such as ipilimumab which inhibits CTLA-4 a checkpoint protein (Boland *et al.*, 2017). Also, patients with microsatellite instability benefit from immunotherapy (Syn *et al.*, 2017). Pembrolizumab is an antibody that binds to and inhibits the protein PD-1 on lymphocytes (Flynn & Gerriets, 2021). This receptor, also known as an immunological checkpoint, is crucial for stopping the immune system from attacking the body's own tissues (Buque *et al.*, 2015). T cells defend the body against cancer by killing malignant cells. Cancer cells, on the other hand, develop proteins to defend themselves against T cells. Nivolumab works by inhibiting these protective proteins (Borghaei *et al.*, 2009). Nivolumab mechanism of action is by preventing the interaction of PD-L1 on the cancer cell with the PD-1 receptor on the T lymphocytes (Gunturi & McDermott, 2015).

1.3 Medulloblastoma

Medulloblastoma is a malignant brain tumour in children that starts in the cerebellum and spreads via the cerebrospinal fluid to other areas of the brain and spinal cord (Smoll, 2012). The second most prevalent brain tumour in children is medulloblastoma and it makes up 20% of all paediatric brain tumours (Dhall, 2009). However, it is the most common malignant (high grade) brain tumour in children. In the United Kingdom, about 55 children are diagnosed with medulloblastoma each year (Cancer Research, UK, 2019). 70% of medulloblastoma cases occur in children under the age of ten (Kijima & Kanemura, 2016).

Harvey Cushing and Pervical Bailey identified medulloblastoma in 1925 (Bailey & Cushing, 1925). Surgical excision of the tumour was the standard treatment for medulloblastoma during Cushing's time, and patients had a 30% death rate after surgery (Kunschner, 2002). In a paper published in 1953 by Patterson and Farr, craniospinal irradiation was introduced as a treatment for medulloblastoma and it had a 65% three-year survival rate for patients (Patterson & Farr, 1953). While these results were promising, the treatment had some negative side effects on younger patients, including endocrine dysfunction and neurocognitive impairment (Rutka *et al*., 1996). In 1970, adjuvant chemotherapy was incorporated with radiation and surgery to increase patient survival rates, lowering the use of irradiation as a treatment option and limiting its usage to incidences where the patient has relapsed. (Wang *et al*.,2015).

Based on transcriptional profiling investigations, medulloblastoma was split into four subtypes in 2010. Wingless (WNT), sonic hedgehog (SHH), group 3, and group 4 are the four subgroups of medulloblastoma (Gilbertson & Ellison, 2008). Each subgroup was defined by a distinct set of demographic and clinical characteristics, as well as gene expression and genetics (Taylor *et al*.,2012). The ability to define which subgroup of medulloblastoma patients belongs to has resulted in more precise patient and therapy outcomes (Ramaswamy *et al*.,2013). The different medulloblastoma subgroups are thought to originate from different cells, which illustrates why the medulloblastoma subgroup of a patient remains the same even after recurrence of the cancer or when the cancer undergoes metastasis (Ramaswamy *et al*., 2013). This distinguishes medulloblastoma from other cancers where recurrence or metastasis results in a change in the subgroup (Gibson *et al*.,2010).

1.3.1 Subgroups of medulloblastoma

 The identification and discovery of distinctive molecular subgroups of this medulloblastoma has been made possible in recent years by numerous independent initiatives

at mapping the medulloblastoma transcriptome (Northcott *et al*., 2012). The current idea of transcriptionally distinct subgroups of medulloblastoma was initially introduced in 2006 by Thompson *et al*., who described five different subgroups in a cohort of 46 patients (Thompson *et al*., 2006). In a series of 62 cases, Kool *et al*. effectively repeated Thompson's discovery of five medulloblastoma subgroups two years later. This time, the letter designations A-E were once again allocated, although there was no continuity with the nomenclature used in the Thompson study (Kool *et al*. 2008). While the remaining "C," "D," and "E" subgroups were revealed to be more closely related, the WNT and SHH subgroups, referred to respectively as "A" and "B" by Kool *et al*., were easily distinguished as freestanding sample clusters (Cho *et al*., 2011). A conclusion was finally achieved in late 2010 at a meeting in Boston based on the findings given as well as confirmation in later published and unpublished reports by independent organisations (Remke *et al*., 2011). It was decided that the existing data is most supportive of four main medulloblastoma subgroups, to be called WNT, SHH, Group 3 and Group 4. (Taylor *et al*., 2012). Until the biology of these subgroups is better known, it was considered that Group 3 and Group 4's rather generic designations would be more suitable (Ellison *et al*., 2011).

1.3.2 Wingless Pathway Tumours- The Wingless pathways tumour (WNT) subgroup accounts for 10% of all medulloblastoma cases (Taylor *et al*., 2012). Activation of the canonical Wnt/Wg signalling pathways is the hallmark of Wingless pathway tumours (Gajjar & Robinson, 2014). The WNT/β-catenin pathway is made up of a set of signalling proteins that control specific aspects of embryogenesis (Ellison *et al*., 2011). Adenomatous polyposis coli (APC) is a tumour suppressor protein that suppresses the WNT signalling pathway (Borowsky *et al*., 2018). Turcot syndrome is caused by a mutation in the APC protein, which raises the risk of developing medulloblastoma (Vijapura *et al*., 2017). In the majority of cases (60%), pathway activation is facilitated by the anchoring and build-up of β-catenin in the nucleus (Eberhart *et al*., 2000), a transcriptional activator, which is linked with activating mutations in its equivalent CTNNB1 gene (Ellison *et al*., 2005). When the WNT pathway is activated in an unregulated manner, β-catenin, a protein produced by the CTNNB1 gene accumulates (Silva *et al*., 2013). This build-up of β-catenin leads to aberrant transcription activation and subsequently cancer (Taylor *et al*., 2005). WNT medulloblastomas usually develop in the brain's midline and populate the fourth ventricle (Gallard, 2022). WNT tumours are characterised genetically based on the presence of chromosome 6 monosomy (although they

seldom express chromosome 17 abnormalities, which is a frequent occurrence with the other subgroups), β-catenin gene mutation, and immunohistochemistry to confirm positive nuclear β-catenin (Goschzik *et al*., 2015). WNT tumours are essentially absent in infants, but they predominantly affect children, with an increased incidence in children between the ages of 10 and 12 and the male-to-female ratio of WNT tumours is 1:1 (Parsons *et al*., 2011). WNT tumours rarely have metastases at the time of diagnosis, and patient outcomes for WNT medulloblastoma have been excellent, with a 5-year survival rate of over 95% (Clifford *et al*., 2006).

It was discovered that the activation of the WNT pathway is an autonomous sign of good prognosis in medulloblastoma (Thompson *et al*., 2006). An analysis of 109 patients involved in the SIOP PNET3 clinical trial showed that the overall survival rates for β-catenin nucleopositive medulloblastomas were significantly greater than that of nucleonegative medulloblastomas at five years post diagnosis (92.3% vs. 65.3%), and all children with β-catenin nucleopositive medulloblastomas presenting with clinical or histopathological adverse-risk attributes (metastasis or large cell/anaplastic morphology) lived for at least five years after diagnosis (Ellison *et al*., 2005). Another mutation observed in WNT tumours is the TP53 mutation; however, the effect of TP53 on prognosis is minimal (Pomeroy *et al*., 2002).

Table 1.2 - Subtypes of medulloblastoma, showing the rate of occurrence, survival and gene expression of each subtype.

SUBTYPE	WNT	SHH	GROUP 3	GROUP 4
OCCURENCE	10%	25%	25%	40%
SURVIVAL	VERY GOOD RARELY UNDERGOES METASTASIS (M+)	INTERMEDIATE METASTASIS IS UNCOMMON (M++)	POOR VERY FREQUENTLY UNDERGOES METASTASIS (M+++)	INTERMEDIATE FREQUENTLY UNDERGOES METASTASIS (M++)
GENE EXPRESSION	WNT SIGNALLING (MYC+)	SHH SIGNALLING (MYCN+)	PHOTORECEPTOR/ GABAERGIC (MYC+++)	NEURONAL/ GLUTAMATERGIC (VERY LITTLE MYC/MYCN)

1.3.3 Sonic hedgehog pathway tumours

The sonic hedgehog pathway is involved in development and formation of embryo and tissue polarity preservation (Zheng *et al*., 2019). Sonic hedgehog medulloblastoma tumours make up 30% of all medulloblastomas and are characterized by sonic hedgehog signalling pathway abnormalities (Garcia-Lopez *et al*., 2021). The patched-1 (PTCH1) protein is a SHH receptor that acts as a tumour suppressor. It is expressed by the PTCH1 gene, and germline mutations in this gene cause Gorlin syndrome, which makes people prone to medulloblastoma (Briggs *et al*., 2008). In addition, suppressor of fused homolog (SUFU) is a protein that inhibits the SHH signalling system; it is produced by the *SUFU* gene, and its germline suppression causes medulloblastoma in newborns (Guerrini-Roussea *et al*., 2018). The failure to perform tumour suppressor tasks is caused by the absence or mutation of these genes, resulting in carcinogenesis (Kijima & Kanemura, 2016). SHH medulloblastoma is associated to monosomy of chromosome 9q (located on the *PTCH1* gene) (Taylor *et al*., 2012). Patients with mutations in any portion of the SHH signalling pathway (PTCH1, SMO, SUFU, GLI1 and GLI2) are included in the SHH medulloblastoma subgroup (Rossi *et al*., 2008). SHH tumours are seen in

the cerebral hemisphere in adults and in the midline in babies (Tamayo-Orrego & Charron, 2019). SHH tumours are essentially non-existent in children, although they primarily afflict adults and newborns; the male-to-female ratio of SHH tumours is 1:1. (DeSouza *et al*., 2014).

SHH medulloblastomas are transcriptionally different depending on the patient's age bracket (Skowron *et al*., 2021). While most infants with SHH medulloblastoma have germline mutations of the *PTCH1* and *SUFU* genes, children have a broader range of heterogeneity, such as amplification of SHH, MYCN, and GLI2, as well as germinal and somatic TP53 mutations with PTCH1 gene mutation (Kool *et al*. 2014). Mutations in the *PTCH1* and *SMO* genes indicate the occurrence of SHH medulloblastoma in adults (Gajjar & Robinson, 2014). Majority of nodular/desmoplastic medulloblastomas belong to the SHH subgroup. Furthermore, considering that 50% of SHH subgroup medulloblastomas are not nodular/desmoplastic, this is not a reliable diagnostic biomarker for the subgroup (Taylor *et al*., 2012). SHH tumours rarely have metastasis at the time of diagnosis, and patients with SHH medulloblastoma had a 75% 5-year survival rate (Dasgupta *et al*., 2019). The TP53 mutation has a crucial impact in the prognosis and survival of patients with SHH medulloblastoma, as individuals with TP53 mutations have a 5-year overall survival rate of 41%, compared to 81 % for patients lacking TP53 mutations (Zhukova *et al*., 2013).

1.3.4 Group 3 Medulloblastoma

MYC expression and amplification are upregulated in group 3 medulloblastoma tumours, which represents about 25% of all medulloblastoma tumours (Menyhárt *et al*., 2019). Adults are seldom affected by Group 3 tumours, whereas children and new-borns are frequently affected (Hatten *et al*., 2011). In relation to MYC expression, Group 3 tumours are divided into two categories: 3α and 3β, 3α tumours have MYC amplification, whereas 3 β tumours do not (Quin *et al*., 2021). Trisomy 1q or monosomy 5q or 10q are more common in Group 3 tumours (Kool *et al*., 2008). Trisomy 17q affects 26% of people with group 3 tumours (Northcott *et al*., 2012). MYC amplification seems to be limited to Group 3 tumours, whereas OTX2, an MB oncogene, is amplified in both Group 3 and Group 4 malignancies (Stromecki *et al*., 2018). The MYC and OTX2 amplicons are mutually exclusive, implying that the malignancy in Group 3 MB is caused by two separate pathways (Northcott *et al*., 2012). Males are more likely than females to get Group 3 tumours, with a 2:1 ratio. LCA histology is common in Group 3 tumours, and they are commonly metastatic (Northcott *et al*., 2011). Additionally, it has been argued that earlier recognition of metastatic status as a potential cause for poor prognosis in

medulloblastoma was really distinguishing a subset of patients who were more likely to be in Group 3 (Cho *et al*., 2011). Group 3 medulloblastoma tumours have a dismal prognosis, with around half of group 3 medulloblastoma patients having metastasis at diagnosis, which commonly results in relapse (Kool *et al*., 2012). Group 3 medulloblastomas have a 5-year survival rate of 43% in new-borns and 48% in children (Kijima & Kanemura, 2016).

1.3.5 Group 4 Medulloblastoma

Group 4 tumours are the most common molecular subtype of medulloblastoma, accounting for approximately 35% of all medulloblastomas (Maier *et al*., 2021). 80% of women who have group 4 medulloblastoma possess a chromosomal X deletion (Cho *et al*., 2011). MYCN overexpression and isochrome 17q are used to categorize tumours in Group 4 (Kijima & Kanemura, 2016). Group 4 tumours are uncommon in babies and are more common in men, with a 3:1 male-to-female ratio (Taylor *et al*., 2012). Nearly 35% of group 4 tumours patients already have metastases at the time of diagnosis (Northcott *et al*., 2011). Tumors in Group 4 can be characterised dependent on their expression of follistatin-like 5 (FSTL5), with tumours that express FSTL5 having a worse prognosis than those that do not (Remke *et al*., 2011). Group 4 medulloblastoma patients with intermediate risk have an 80% 5-year survival rate, while patients with high risk medulloblastoma have a 60 percent 5-year survival rate (Kool *et al*., 2012).

1.3.6 Gene mutations in medulloblastoma

TP53 - The discovery that 17p is commonly deleted as part of isochromosome 17q in more than 40% of medulloblastoma samples prompted the inquiry into the involvement of p53 in medulloblastoma (Zhukova *et al*., 2013). Further research, however, revealed that only a few somatic mutations were found in limited groups of medulloblastoma patients, especially those with 17p deletion (Gilbertson & Ellison, 2008). This suggested that 17p deletion and TP53 mutations are unconnected therefore, an alternate tumour suppressor exists on 17p (Lindsey *et al*., 2011). The role TP53 plays in the prognosis of medulloblastoma has been investigated recently with varying theories on how p53 affects prognosis (Ramaswamy *et al*, 2016). It was discovered that the effect of TP53 mutation on prognosis is subgroup dependent with patients with somatic TP53 mutations in WNT malignancies having a favourable prognosis (Lindsey *et al*., 2011). While patients with SHH tumours carrying somatic TP53 mutations on the other hand, had poor prognosis (Pfaff *et al*. 2010). In patients with group 3 and 4 tumours, where

isochromosome 17q is a prevalent abnormality, TP53 mutations were nearly never found (Ramaswamy & Taylor, 2015).

CTNNB1 (Catenin Beta 1)- Zurawel *et al* discovered that the exon 3 of the *CTNNB1* gene had mutations present on its GSK3β phosphorylation sites (Zurawel *et al*., 1998). This mutation inhibits the breakdown of β-catenin in the cytosol by the ubiquitin proteasome, thereby resulting in the nuclear translocation of β-catenin (Kikuchi, 2003). CTNNB1 mutation is present in 10% of all medulloblastoma cases and is present in the WNT subgroup (Rubin and Rowitch, 2002). Tumours with CTNNB1 mutation have a chromosome 6 loss, but no chromosome 17 modifications or chromosome 7 gain, which are the most common abnormalities in medulloblastoma, the tight link between CTNNB1 mutation (on chromosome 3) and chromosome 6 deletion (Kool *et al*., 2008), as well as the resulting gene dosage impact, shows that both changes are involved in medulloblastoma development (Thompson *et al* 2006). This mutation is prevalent in older patients and prognosis is usually good for patients with this mutation (Sengupta *et al*., 2017). Ellison *et al* using immunohistochemistry discovered that the nuclear expression of β-catenin, a crucial downstream effector of the WNT/-catenin pathway, was related to successful outcome in 109 medulloblastoma patients (Ellison *et al*.,2005).

PTCH1- *PTCH1* has long been considered the 'quintessential' tumour-suppressor gene in medulloblastoma, having been discovered to be mutated in 8–10% of sporadic cases and being the foundational genetic factor of Gorlin syndrome (Gilbertson & Ellison 2008), a congenital cancer syndrome in which people with a PTCH1 germline mutation are genetically programmed to develop medulloblastoma (Taylor *et al*., 2000). PTCH1 mutations encoding the PATCHED transmembrane receptor (leading in constitutive activation of the SHH signalling cascade) are tied closely to the SHH subgroup, similar to how CTNNB1 mutations characterise the WNT subgroup (Slade *et al*., 2011). PTCH1 sequence analysis has altered the definition of the SHH subgroup as research by Kool and Thompson showed that PTCH1 mutation was present in nine of the 27 SHH tumours investigated but absent in all the other subgroups (Kool *et al*., 2008; Thompson *et al*., 2006). Other SHH pathway elements, such as SUFU and SMO, are reported to be mutated in medulloblastoma and influence the disease's aetiology (Taylor *et al*., 2002). While mutations in these genes are thought to be limited to the SHH subgroup, this relation has however not been thoroughly investigated (Yauch *et al*., 2009).

MYC-The MYC family of proto-oncogenes, which includes MYCN, MYC, and MYCL1, are the most common targets of elevated amplification in medulloblastoma (Pfister *et al*., 2009). Furthermore, patients with MYC or MYCN amplification have been demonstrated to have considerably lower progression-free survival and overall survival rates spanning numerous patient and clinical trial groups (Korshunov *et al* 2012). Despite the fact that MYC and MYCN were among the initial oncogenes to be identified as being elevated in medulloblastoma (Northcott *et al*., 2011), the link between these oncogenes and a specific subgroup has only recently been discovered. Almost all MYC amplifications have been connected to Group 3 malignancies to date (Cho *et al*., 2011). MYCL1 amplifications are extremely infrequent in medulloblastoma and have yet to be linked to a specific subgroup (Roussel *et al*., 2013). While early findings suggested that both MYC and MYCN amplifications had a universally bad prognosis (Pfister *et al*., 2009), subsequent research has revealed that tumours with MYCN amplifications exhibit far more genetic and clinical polymorphism than previously thought (Korshunov *et al* 2012).

MLL2 & histone-modifying genes - Frequent copy number alterations and DNA sequence variants that target genes encoding histone-modifying proteins have been discovered in a series of recent genomic profiling initiatives (Roussel *et al*., 2018). On chromosome 9q34, Northcott *et al* discovered repeated homozygous deletions of EHMT1, a histone 3, lysine 9 methyltransferase and repeated amplification of a jumonji family histone lysine demethylase called JMJD2C, on chromosome 9p24 (Northcott *et al*., 2009). Although information on patient subgroups was non-existent at the time of the research, the detected somatic deletions of EHMT1 happened in the setting of monosomy 9q, a genetic event unique to the SHH subgroup (Kleefstra *et al*., 2006). Loss of function mutations of MLL2 and MLL3 and both histone lysine methyltransferases, were found in 16 % of medulloblastomas in a seminal work by Parsons *et al*., which comprised of whole-exome sequencing of 22 medulloblastomas (Parsons *et al*., 2011). ARID1A, SMARCA4 and KDM6B, among other chromatin-modifying genes, have also been discovered to be somatically altered in this study, albeit at a considerably lower rate (Parsons *et al*., 2011). Despite the lack of evidence about molecular subgroup status in this study, mutations in MLL2 and MLL3 seemed to be spread throughout subgroups (Northcott *et al*., 2011).

1.3.7 Treatment

Surgery, radiotherapy, and adjuvant chemotherapy are the current treatment available for medulloblastoma (Lazow *et al*., 2022). The type of treatment is dependent on the tumour's

subgroup and stage. Surgery is a common first-line treatment for medulloblastoma, and typically entails the removal of the tumour as well as some healthy tissue surrounding it (Geyer *et al*., 2005). If the tumour does not severely invade the cerebellum and brainstem, then most medulloblastoma tumours are receptive to complete excision (Gilbertson *et al*., 2004). However, due to the position of some tumours, they cannot be operated on and in these cases, an alternative treatment must be used (Rossi *et al*., 2008).

Radiotherapy is the most effective postoperative treatment for medulloblastoma tumours because they are radiosensitive (Laprie *et al*., 2015). Due to the spine and cerebrospinal fluid serving as a possible repository of tumour cells, it is common practice to irradiate the entire craniospinal axis (Packer *et al*., 2016). Radiotherapy given to the entire craniospinal axis resulted in the greatest increase in survival for children with medulloblastoma, regardless of the amount of disease at the time of diagnosis (Packer *et al*., 2012). Proton beam radiation therapy is frequently advised due to difficulties with bone marrow and surrounding organs caused by brain and spine radiation (Grosshans, 2016). Proton beams are distinguished by a low entrance dosage, in which the protons dissipate energy along the path and the dose peaks in depth at a specific and well-defined range known as the Bragg peak right before they arrive at the designated site of treatment (Vitti & Parsons, 2019). This form of radiation protects the neighbouring tissue and organs to the site of treatment from being affected by the radiation treatment, thereby reducing the risk of unfavourable side effects (Hughes & Parsons, 2020). Depending on the subtype and extent of the tumour's dissemination, chemotherapy may be used as part of the treatment plan (Branganca & Packer, 2013).

1.4 RNA

The important role of RNA in the transmission of genetic information was discovered in 1961 (Gros *et al*., 1961), and the development of whole-genome sequencing technology over the next 50 years has substantially expedited our knowledge of both coding and non-coding RNAs (Bertone *et al*., 2004). Coding RNAs are RNAs that code for proteins, the RNA that transports information from the DNA to the ribosome, the cell's site for protein synthesis (translation), is known as messenger RNA (mRNA) (Sharma, 2022). The amino acid sequence of the protein that is generated after translation is determined by the coding sequence of the mRNA (Mauger *et al*., 2019). However, a large number of RNAs do not encode proteins (in eukaryotes, non-protein coding RNAs account for around 97% of transcriptional output) (Ponting & Haerty,

2022). Some of these non-coding RNAs can be produced from intron sequences found in precursor mRNA or by their respective genes (RNA genes) (Baptista *et al*., 2021). Transfer RNA (tRNA) and ribosomal RNA (rRNA), two of the most common types of non-coding RNAs, are both required in translation (Lambert *et al*., 2019).

Non-coding RNA can be divided into two groups based on the length of the RNA chain (Fatica, & Bozzoni, 2014). These are long RNAs such as long non-coding RNA (lncRNA) (longer than 200 nucleotides) and the small RNA (less than 200 nucleotides long) such as miRNA and siRNA.

1.4.1 Long non-coding RNA

Many regulatory RNAs of varying sizes, particularly lncRNAs, have been found (Ponting *et al*., 2009). LncRNAs are RNAs longer than 200 nucleotides (usually 1000–10,000 nucleotides long) that are not translated into functional proteins and are produced in large quantities through genome transcription (Esteller *et al* 2011). This wide definition includes a huge and extremely varied group of transcripts with varying biogenesis and genetic origins (Bushati *et al.,* 2007). According to Human GENCODE, the human genome has around 16,000 lncRNA genes, however other estimates put the number at over 100,000 (Ruan *et al*., 2020). Recent studies have revealed that non-coding RNAs play important roles in the development and regulation of a lot of diseases including cancer (Luo *et al*.,2017). The human genome contains about 58700 lncRNAs and about 1% of these lncRNAs are transcribed from ultra-conserved regions and contain ultra-conserved elements and 7% of these ultra-conserved lncRNAs contain disease associated single nucleotide polymorphism (Iyer *et al*., 2015).

Ultra-conserved regions comprise of 481 sequences that are entirely 100% conserved within orthologous portions of the human, rat, and mouse genomes and are longer than 200 base pairs (Pereira Zambalde *et al*., 2021). These 481 ultra-conserved components are divided into three groups; exonic, non-exonic, and potentially exonic. Ultra-conserved regions have distinct fingerprints in various tissues, and they are typically found in genomic areas linked to cancer (Cancer associated genomic regions) and at chromosomal fragile points (Gibert Jr *et al*., 2022). These areas have been speculated to be potential candidate genes for cancer susceptibility (Satake *et al*., 2018). Most ultra-conserved regions can be transcribed to produce lncRNAs and are therefore called transcribed ultra-conserved region (Mudgapalli *et al*., 2019). Dysregulation of transcribed ultra-conserved regions is linked to a number of human disorders, including

cancer and conditions related to the nervous system, the heart, and development (Fiorenzano et al., 2018; Fabris & Calin, 2017).

Most lncRNA are made up of a poly A tail at its 3´end and a 5´ guanine cap at the other end but is however devoid of an open reading frame (Figure 1.3) (Cheng *et al* 2005). LncRNAs are present in different loci of the genome and controls the expression of genes in the nucleus and in the cytoplasm (Balas & Johnson, 2018). Nuclear lncRNAs control the activation of chromatin modification proteins such as DNA methyl transferase which alter epigenetic markers, while cytoplasmic lncRNAs function as a miRNA decoy, regulators of splicing and translation. (Lepoivre *et al*.,2013).

It is still up for debate how many functional lncRNAs there are, due to the unavailability of proof to demonstrate the functionality of most lncRNAs (Moore *et al*., 2020). LncRNAs were once assumed to be RNA polymerase II by products void of biological function (Gao *et al*., 2020). However, as high-throughput sequencing technology has advanced, a growing percentage of lncRNAs have been characterized, and their roles in carcinogenesis and tumour progression have been significantly explained (Uszczynska-Ratajczak *et al*., 2017). LncRNAs have been implicated in the regulation of cell survival, proliferation, invasion, and metastasis, as well as the preservation of stemness and tumour angiogenesis, according to previous research (Balas & Johnson, 2018). These findings emphasise the importance of lncRNAs in cancer formation and progression, and also their prospects as novel therapeutic targets for a variety of cancers (Huarte *et al*., 2010).
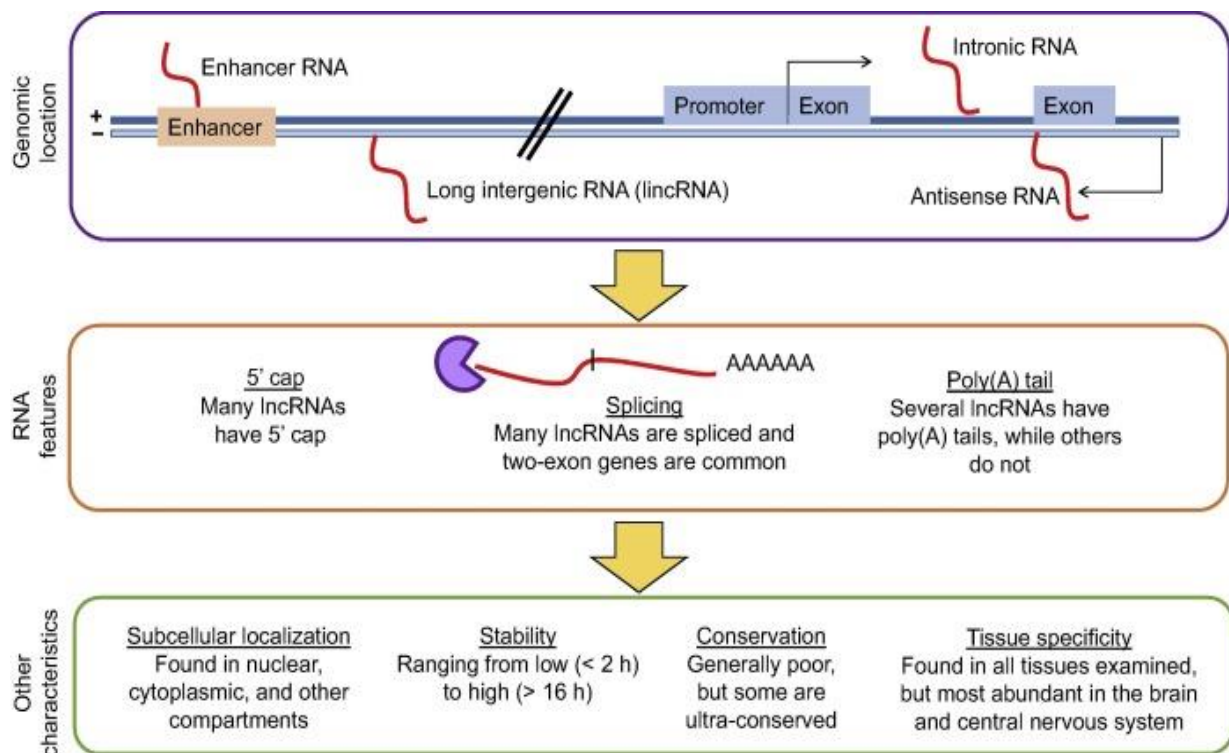
Figure 1.3- **Location and characteristics of lncRNAs** (adapted from Fang *et al*., 2016)
The classification of lncRNA based on their location on the genome, key features of lncRNAs which are similar to those found in protein-coding genes, like the 5′ cap and alternative splicing.

1.4.2 Location of lncRNA

Non-coding sections (which make up 98–99 percent of the human genome) are distributed throughout the coding regions (Figure 1.3) (Landers *et al*., 2001). Therefore, intergenic lncRNAs are transcribed wholly from intergenic regions of protein-coding genes, whereas intronic lncRNAs are produced totally from introns of protein-coding genes (Osielska & Jagodziński, 2018). LncRNA can be classified based on their location and there are four main locations within the genome where lncRNA might occur, they are

Intergenic lncRNA -They are non-coding RNAs that are independently produced and do not overlap identified coding genes (Ma *et al*., 2013). Intergenic lncRNAs are similar to lncRNA transcripts and account for more than half of all lncRNA transcripts in humans (Statello *et al*., 2021). They are found in intergenic regions, which are large stretches of DNA between two genes' protein-coding sequences (Ransohoff *et al*., 2018).

Intronic lncRNA - Small noncoding RNAs like miRNAs and snoRNAs have been discovered to reside in introns (Wu *et al*., 2017). Large-scale transcriptomic or computational investigations have currently revealed that many lengthy transcripts are contained within the

introns of annotated genes (Zhang *et al*.,2013). Many of them have been shown to have distinct expression patterns, respond to stimuli, or be dysregulated in cancer, but just a few have been thoroughly investigated (Louro *et al* 2009). Examples include COLDAIR, which is found in the first intron of the flowering repressor locus FLC which plays a role in plant vernalization (Heo *et al*., 2011).

Sense and antisense lncRNA- Sense lncRNAs, which contain exons from protein-coding genes, are transcribed from the sense strand of protein-coding genes (Zhang *et al*., 2014). They can encompass the entire sequence of a protein-coding gene or overlap with parts of it (Liu *et al*., 2015). On the other hand, antisense lncRNAs are produced from the antisense strand of protein-coding genes (Derrien *et al*., 2013). Antisense lncRNAs can exist in three contexts, according to GENCODE annotation (a repository of hand curated lncRNAs): (1) Antisense strand transcripts overlap an exon of a sense gene via lncRNA exons, (2) transcripts from a sense gene's intron are devoid of exon-exon overlap with this sense gene, and (3) transcripts encompass the complete sequence of a sense gene through an intron (Kampa *et al*., 2004).

Using next generation sequencing, qRT-PCR validation, and sequencing the 5′ and 3′ ends of full-length cDNA, sense and antisense lncRNAs are proven to be real transcripts and not truncated coding DNA sequences or transcriptional noise (Ma *et al*., 2013). Several antisense lncRNAs work via a variety of methods (like intergenic lncRNAs). In the mouse genomic sequence, about 87% of coding transcripts possess antisense partners, and in human lncRNAs only 32% are antisense to coding genes, this indicates that antisense regulation is likely to be more prevalent (Carinici *et al*., 2005).

Intergenic lncRNAs and antisense lncRNAs (particularly intergenic lncRNAs) are the focus of current research, whereas intronic lncRNAs and sense lncRNAs are less well understood (Guttman *et al*., 2010). Some biological characteristics of lncRNA are notable, including elevated conservation among animals (Khalil *et al*., 2009). Another piece of proof, although not conclusive, may point to the unique coding capacity of sense lncRNAs (Liu *et al*., 2015). Furthermore, because antisense and sense lncRNAs have different coding gene correlations, they are expected to have different impacts on gene loci or mRNAs (Wu *et al*., 2014). As a result, genomic localization and context can be utilised to classify lncRNA, albeit a classification of lncRNA based just on genomic localization and context may be inadequate (Leygue *et al*., 2007).

1.4.3 Functional classification of lncRNA

LncRNA have diverse functions in the cell, they are known to participate in the regulation of genes via various mechanisms such as controlling the role of transcription factors, regulating RNA polymerase and they also regulate post transcription processes and translation (Tehrani *et al*., 2018). The integrity of the chromatin structure and communication between proteins, proteins and DNA and proteins and RNA is also regulated by lncRNAs (Statello *et al*., 2021). Several lncRNAs have been functionally linked to various diseases in human, especially in cancer (Ma *et al*., 2013). Dysregulation of some lncRNAs has been linked to poor prognosis, metastasis, evading tumour suppressor genes such as p53, and conferring of apoptosis resistance on cells (Shi *et al*., 2013). LncRNA play functional roles in cancers such as CRC, thyroid cancer, pancreatic cancer and gastric cancer (Hao *et al*., 2017).

Due to the enormous number of discovered transcripts and the variety of biological situations in which they are involved, it has been difficult to accurately define and characterise lncRNA function (Moore *et al*., 2020). Nevertheless, four major models for characterising lncRNA function have been developed: They are signal, guide and scaffold, and molecular decoy (Mercer *et al*., 2009). Furthermore, the most of the well-studied lncRNAs function in numerous forms, indicating the intricacy of their function. Understanding the common threads that run through these processes could help anticipate lncRNA function and biological effects (Richard & Eichhorn, 2018).

Signal lncRNA - LncRNAs are frequently believed to influence downstream gene transcription by acting as signalling molecules (Kung *et al*., 2013). Previous research has shown that lncRNAs are transcribed specifically and impact certain signalling pathways under various stimulation settings (Fang & Fullwood, 2016). Transcripted lncRNAs mediate downstream gene transcription either alone or in conjunction with other proteins (such as transcription factors) (Gao *et al*., 2020). Signal lncRNA play an important role in transcription as they act as molecular indicators to adjust transcription according to different stimuli (Wang *et al*., 2011). This means that whenever the lncRNA is produced or whenever it is present, transcription is taking place examples of signal lncRNA include HOTAIR and COLDAIR lncRNA (Pandey *et al*.,2008).

Decoy lncRNA- The primary purpose of decoy lncRNA is to act as a molecular sink, limiting the amount of certain regulatory components present by binding to them, thereby inhibiting them from performing their regulatory activity (Gao *et al*., 2020). RNA-binding proteins,

transcription factors, microRNAs, catalytic proteins, and components of larger modifying complexes are sequestered by this type of RNA, which affects gene expression (Fan *et al*., 2015). Decoys work by adversely controlling effector factors by titrating these factors away from interacting with their natural target (Wang & Chang, 2011) .For example, the lncRNA PANDA which is induced by DNA damage binds to and inhibits the nuclear transcription factor NF-YA, thereby limiting the production of apoptosis-related genes and as a result, blocking the NF-YA-dependent apoptosis pathway (Hung *et al*., 2011).

Several lncRNAs, including as MEG3 and TUG1, have also been demonstrated to sequester different microRNA from protein and mRNA targets, causing changes in protein translation and breakdown (Li *et al*., 2016). The competitive endogenous RNA (ceRNA) theory is a critically discussed hypothesis around microRNA sponge function in lncRNAs (Salmena *et al*., 2011). It suggests that certain transcripts can reduce microRNA activity by sequestering it, thus preventing it from binding to its targets (Kartha & Subramanian, 2014). This hypothesis has been met with uncertainty, owing to the contention that physiological expression levels of a single lncRNA are insufficient to limit microRNA activity (Lanzillotti *et al*., 2021).

Scaffold lncRNAs – They participate in the assembly of RNA and proteins as they serve as a foundation upon which these RNA and proteins can be assembled. Examples include HOTAIR (Grote *et al*., 2013).

Guide lncRNA - LncRNAs can help certain proteins reach their desired destination and perform their biological functions by acting as guide molecules (Gao *et al*., 2020). LncRNAs frequently interact with transcription factors, which are proteins that are found on certain DNA sequences that govern gene transcription (Wang & Chang, 2011). Multiple studies have shown that lncRNAs can affect gene transcription via cis regulation, hence regulating neighbouring mRNA transcription process (Ma *et al*., 2013). They also recruit ribonucleoprotein complexes to their appropriate targets, such as the recruitment of chromatin modification enzymes to DNA. Examples include Xist lncRNA. (Li *et al*., 2013).

1.4.4 Role of lncRNA in CRC

LncRNAs play an important role in the differentiation and proliferation of cells, thereby dysregulation of these lncRNA could lead to cancer (Hu *et al*., 2018). Due to the recent improvement in genomic sequencing, some lncRNAs have been identified in cancer, especially CRC (Rinn *et al*.,2012). In CRC, lncRNAs participate in tumorigenesis by mimicking tumour

suppressor genes and these genes (such as MYC) are therefore upregulated when these lncRNAs are overexpressed (Iaccarino, 2017). LncRNA are also involved in RNA degradation, splicing, translation and transcription in CRC (Cao *et al*., 2014). LncRNA were shown to participate in the resistance of chemotherapy in CRC by controlling the expression of p53-dependent genes under normal conditions (Chaleshi *et al*., 2020). Therefore, when these lncRNA are downregulated, the genes that are been regulated by these lncRNAs are not expressed properly, the cells are therefore able to evade apoptosis which in turn leads to an increase in proliferation (Mercer *et al*.,2009).

LncRNAs can be detected in blood serum and plasma and other body fluids thereby making them an idle biomarker for the detection and prognosis of CRC (Kishikawa *et al* 2015). A couple of lncRNAs in CRC have been shown to be successful biomarkers in diagnosis, this can assist in detecting and treating CRC early and also stop colorectal adenomas from metastasizing into malignant tumours (Wang *et al*., 2019). Examples of lncRNA that can be used as early biomarkers in diagnosis include CRNDE (Ye *et al* 2015). The presence of lncRNA CCAT1 in the plasma could be used as a biomarker to predict CRC as patients highly express it in their blood plasma (Xie *et al* 2016). The presence of HOTAIR lncRNA signifies metastasis (especially metastasis to the liver) as it is known to be overexpressed in stage four CRC tissues (Kogo *et al* 2011). Svoboda *et al* carried out a study on blood and tissue samples of colorectal patients and showed that HOTAIR is linked to high rate of mortality (Svoboda *et al*., 2014).

LncRNAs have immense potential for the detection, prognosis, and treatment of cancer (Snyder *et al*., 2022). However, PCA3 is the only lncRNA that has been authorised for clinical use, it is used for the diagnosis of prostate cancer (Chen *et al*., 2022). LncRNAs need to be researched further not just as a potential cancer diagnosis tool but also in cancer treatment. It will be of benefit to utilize and integrate their varied functions in the clinical front in fighting drug resistance. This study aims to investigate the possible role of lncRNA HCP5 in cell response to chemotherapy.

1.4.5 HCP5

Human leukocyte antigen complex P5 (HCP5) is a 2547 nucleotide long lncRNA that is found on chromosome 6 of the human genome (Kulski *et al*., 2019). It is made up of a 5′ guanine cap and a poly A tail at its 3′ end and was reported in 1993 by Vernet *et al*. They discovered a sequence within the HLA class 1 region that expresses a 2500 nucleotide transcript in lymphocytes, spleen, hepatocellular carcinoma and other non-lymphoid tissues but this

sequence was not expressed in T-cells (Kulski *et al*., 2019). They showed that HCP5 was produced through the non-homologous recombination of two pseudogenes that do not encode for proteins (Vernet *et al*.,1993). HCP5 is situated in a region between the MHC class I Polypeptide-Related Sequence A and MHC class I Polypeptide-Related Sequence B genes (Zou *et al*., 2021). Although it is located in the MHC region, there is no structural similarity between HCP5 and the MHC1 proteins (Matrazaki *et al*., 2017). HCP5 is considered to be an endogenous retrovirus present in human, this indicates that it is the remains of a prehistoric virus which has now been integrated into the human genome (Lane *et al*., 2020).

 Kulski and Dawkins demonstrated in 1999 that the HCP5 gene sequence and transcripts were primarily made up of the 3′ long terminal repeats (LTR) and polymerase sequences of a primitive HERV16 insertion (Kulski & Dawkins, 1999), which was an associate of the HERVL or class III category of endogenous retroviruses (ERVs) in human and mammalian genomes (Ito *et al*., 2017). Within the α and β blocks of the MHC class I region, the primitive endogenous retroviral sequence HERV16 is recurrent at least twelve repeats (Sznarkowska *et al*., 2020), along with the HLA class I coding and non-coding sequences, and it appears to have been a recombination location for many of the unequal crossover duplication events, along with other retroelements (Kulski *et al*., 1999a). The HCP5 gene consists of an RNA polyA tail made up of 8 adenines, two exons (exon 1 is 100 base pairs long and exon 2 is 2355 base pairs long) and an intron 91bp long (Kulski *et al*., 2019). In the genomic databases, there are at least four variants of the HCP5 gene sequence, the first variant is 2630bp long, the second variant is 23kb long, third is 575bp long and the fourth is 465bp long (Crosslins *et al*., 2015). HCP5 has a unique gene structure as it contains a fragment of the HLA class I gene in exon 1 and fragmented sections of the 3′LTR and internal sequence of ERV16 in exon 2 (Kulski *et al*., 1999a).

HCP5 is largely expressed in immune system cells and is involved in both adaptive and innate immune responses (Hu *et al*., 2021). Various studies have suggested that HCP5 may act as a competitive endogenous RNA (ceRNA), sequestering the distribution of microRNAs on their targets and hence contributing to the development and progression of cancers (Chen *et al*., 2019; Zou *et al*., 2021). In a sequence of biological stages involving dosage compensation, genomic imprinting, and cell cycle disruption, HCP5 appear to influence the transcription and translation of local and distant genes via cis and trans-regulatory roles, resulting in cancer and its development (Jiang *et al*., 2015; Yan *et al*., 2015). The role of lncRNAs in binding with regulatory miRNA that regulate normal cell development pathways and cancerous cell

development pathways has emerged as a key mechanism by which they carry out their regulatory roles and this interaction is known as the competitive endogenous RNA network (Xu *et al*., 2021). The mechanism/network is a three-way binding interaction involving lncRNA, miRNA, and regulatory protein coding genes, such as those coding for regulatory transcription factors (Gu *et al*., 2020). Interactions between HCP5 and transcription factors disrupt cellular regulatory activities, which may lead to various cancers (Lanzós *et al*., 2017). Recent research on the interaction between HCP5 and Runx family proteins reveals that they may play an important part in stem cell biology, especially in controlling apoptosis and the progression between the G0/G1 phase via competitive endogenous RNA networks (Teng *et al*., 2016). Runx1 promotes HCP5 promoter activity and expression, as well as suppressing HIV reactivation in T cells, possibly through HCP5 interaction (Klase *et al*., 2014). HCP5 has been affiliated with diseases such as acquired immunodeficiency syndrome (AIDS), where a variant of this lncRNA prevents or interrupts the progression of HIV to AIDS upon infection (Zou *et al*., 2021). HCP5 is usually present in combination with Histocompatibility complex class I B (HLA-B) which is a regulatory protein present in the immune system (Rodríguez-Nóvoa *et al*., 2010).

1.4.6 HCP5 and cancer

The role of HCP5 in cancer has been studied extensively and HCP5 is abnormally expressed in numerous cancer types, according to data from the Cancer Genome Atlas (TCGA) (Zou & Chen, 2021). Based on the form of HCP5 allele and type of cancer present, HCP5 can either promote or repress cancer (Chen *et al*., 2021). Since 2016, the HCP5–miRNA–gene regulator interactions or the ceRNA pathway has been identified to cause and/or advance at least 10 distinct cancer types, including CRC (Zou *et al*., 2021). Furthermore, in several malignancies, HCP5 dysregulation is linked to cell proliferation, migration, invasion, cell death, lymphatic metastasis, and resistance to treatment (Liang *et al*., 2015). As a result, HCP5 could be exploited as a biomarker and a therapeutic target in human cancer (Qin *et al*., 2021; Hu *et al*., 2021). In most malignancies, HCP5 over-expression increased the chance of shorter overall survival (Wei *et al*., 2019). Furthermore, the link between HCP5 expression levels and clinical characteristics has been investigated for different cancer types and there were no statistically significant associations between HCP5 over-expression and age, gender, or tumour size (Hu *et al*., 2021). One the other hand, HCP5 over-expression was linked to poor histological differentiation, as well as positive lymph node metastases and progressed TNM stage (Yang *et al*., 2019; Zhao *et al*., 2019). Qin *et al.,* (2021) showed that HCP5 was highly expressed in the

blood serum of gastric cancer patients compared to healthy patients and when compared to current clinical diagnostic markers CEA and CA199, HCP5 had a higher diagnostic efficiency and would be better at distinguishing healthy patients from patients suffering from gastric cancer (Qin *et al*., 2021).

According to publicly accessible cancer gene expression data, a search of the TCNG Cancer Network Galaxy Database by Kulski (2019) yielded 206 networks for genes regulating or regulated by the HCP5 gene (shown in Figure 1.4) (Hu *et al*., 2021). A total of 1010 genes have been reported to interact with HCP5 as a regulated or regulatory gene. HCP5 was the regulatory gene in around 590 interactions, and was the gene being regulated in the remaining (420 interactions). HCP5 regulated HLA family genes downstream of HCP5 in four experimental arrays on breast cancer and one experiment on CRC (Kulski, 2019). NLRC5, a member of the NOD-like receptor family that serves as a transcriptional activator of MHC class I genes, was predicted to control HCP5 (Downs *et al*., 2016).

Furthermore, clinicopathological variables revealed that elevated serum HCP5 expression in gastric cancer was significantly associated with differentiation ($P<0.05$), lymph node metastasis ($P<0.05$), and nerve invasion ($P<0.05$), implying that serum HCP5 expression was associated with certain gastric cancer clinicopathological factors (Chen *et al*., 2020).

HCP5 has been shown to play a role in DNA damage repair as it regulates the expression of MSH5 which is a protein that is involved in the mismatch repair pathway, it regulates MSH5 by controlling the interaction between a transcription activating protein YB-1 (Y box binding protein 1) and MSH5 (Wang *et al* 2020). Das *et al*, (2007) however showed that YB-1 interacts with DNA glycosylase NEIL2 and that the activity of NEIL2 in base excision repair is decreased in cells where YB-1 has been silenced (Das *et al*., 2007). Therefore, if HCP5 regulates YB-1 and YB-1 regulates NEIL2 activity, it can be hypothesised that regulation of HCP5 might have a direct effect on NEIL2 activity, which is one of the aims this project hopes to discover.

1.5 Anti-mitotic drugs

Antimitotic drugs are chemotherapeutic treatments that target cells in mitosis and prevent the mitotic spindle from assembling, thus stopping the chromosomes from aligning during metaphase and initiating the spindle assembly checkpoint (SAC) (Shi & Mitchison, 2017). Antimitotic drugs have been shown to be quite efficient in the treatment of cancer, and they

are frequently used as the initial therapeutic option in many cancer cases (Jordan & Wilson, 2004). Classification of anti-mitotic drugs is dependent on how they interact with the microtubule. There are two types of antimitotic drugs, vinca alkaloids and taxanes (Perez, 2009).

Vinca alkaloids are a group of cell cycle–specific cytotoxic drugs that function by preventing cancer cells from dividing (Moudi *et al*., 2013). These compounds were originally developed from the periwinkle plant *Catharanthus roseus* (Gascoigne & Taylor, 2009). They work by preventing tubulin from generating microtubules, which are required for cellular division. Thus, the coupling of the microtubule to the kinetochore and the development of the mitotic spindle are prevented (Zhou & Rahmani, 1992). Examples of vinca alkaloids are vinorelbine, vincristine and vinblastine. Taxanes are a type of diterpene that inhibit microtubule activity by stabilising GDP-bound tubulin in the microtubule and preventing depolymerization that results in the inhibition of cell division (Mohammadgholi *et al*., 2013). Examples of taxanes include Docetaxel, Cabazitaxel and Pacitaxel.
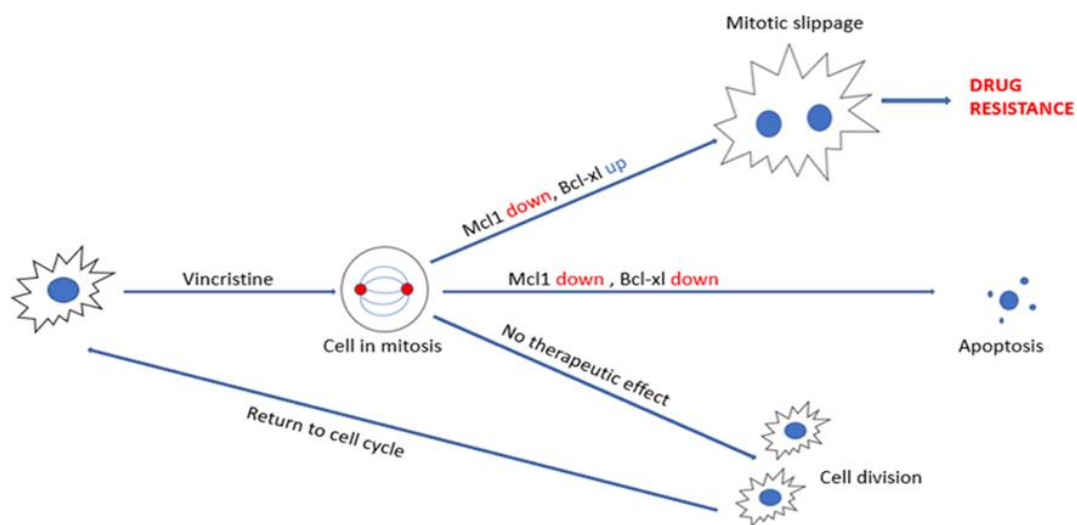
Figure 1.4- Mode of action of vincristine
The effect of the expression level of the Bcl-2 anti-apoptotic proteins on cell fate after vincristine treatment. Upregulation of anti-apoptotic proteins such as Bcl-xL results in mitotic slippage and in turn drug resistance. Downregulation of the anti-apoptotic proteins results in cell death.

According to previous studies, precise function of the mitotic spindle was found to be critical for a successful mitosis (Rieder & Maiato, 2004). Mitotic arrest occurs when the SAC inhibits the anaphase-promoting complex (APC), which prevents incorrect chromosomal dissociation (LaraGonzalez *et al*., 2012). APC-induces exit from mitosis via cyclin B1 breakdown and Cdk1

inactivation. Therefore, APC's major function is to regulate the levels of cyclin B1 during mitosis (Musacchio & Ciliberto, 2012). As a result, APC inhibition causes mitotic arrest. There are three possible outcomes for cells trapped in mitosis depending on the cancer cell line: i) mitotic catastrophe, ii) apoptosis and iii) mitotic slippage (Lok *et al*., 2020). Antimitotic therapies should cause mitotic cell death; however, the fate of the cells post treatment varies (Galan-Malao *et al*., 2012). Mitotic catastrophe was identified as a type of cell death caused by an abnormal mitosis and it usually occurs in cells without a functional apoptosis pathway (Castedo *et al*., 2004). It differs from apoptosis in that it is characterised by the presence of many micronuclei in the cells (Roninson *et al*., 2001). Apart from mitotic cell death, cells can also undergo mitotic slippage as a result of a SAC-induced mitotic arrest (Sinha *et al*., 2019). The SAC weakens during an extended mitotic arrest, leading to the progressive breakdown of cyclin B1, which might culminate in cells departing mitosis without dividing (tetraploid cells) (Brito & Rieder, 2006).

1.5.1 Vincristine

Vincristine is a vinca alkaloid discovered in the Madagascar periwinkle (*Catharantus roseus*) and is commonly used as an anticancer medicine to treat a variety of tumours (Gascoigne & Taylor, 2009). It attaches to β-tubulin at a region proximal to the GTP-binding site called the vinca domain. Vincristine's chemical structure comprises of two multi rings: vindoline and catherantine (Mousavi *et al*., 2013). This compound inhibits microtubules spindles and prevents chromosome alignment and mobility, which results in the non-dissociation of chromosomes during metaphase (Dhyani et al., 2022).
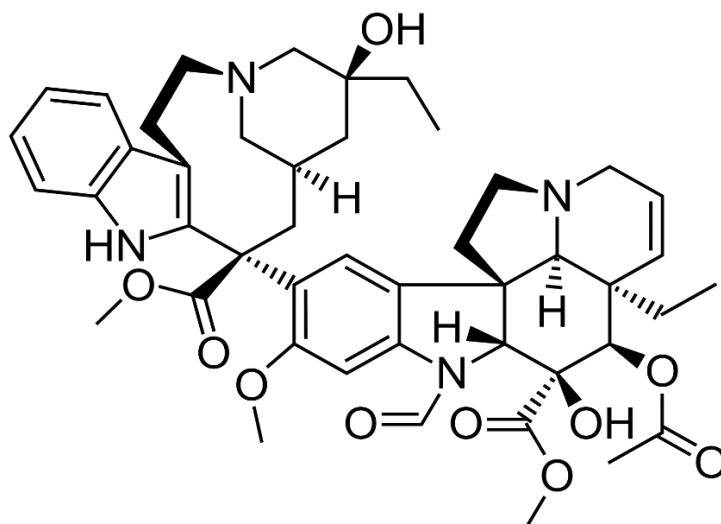
Figure 1.5- Structure of vincristine

1.5.2 Mode of action of vincristine

Vincristine's mode of action is concentration dependant; it can inhibit growth at a variety of concentrations and observing how these substances affect microtubule dynamics has provided valuable information regarding its mode of action (Kumar, 2016). Vincristine engages with ß-tubulin in the vinca domain, which is close to the GTP-binding site (Haider *et al*., 2019). The vincristine attaches to tubulin at the plus-tip of the microtubules at concentrations that prevent proliferation (Alam *et al*., 2017). This suppresses microtubule dynamics without changing polymer levels at the low end of this range but stimulates microtubule depolymerization at greater concentrations (Dhyani et al., 2022). In both circumstances, the development of the mitotic spindle is interrupted, preventing the cells from completing a normal mitosis (Liu et al., 2019). As the quantity of vincristine rises, the quality of microtubules decreases, causing spindle organisation to be disrupted and chromosomes to cluster into a ball (Gascoigne & Taylor, 2009).

Vincristine inhibits microtubule formation, causing the mitotic spindle to disassemble, preventing the cells from aligning at metaphase and initiating the activation of the SAC (Kothari *et al*., 2016). It stops the cells from entering anaphase until all sister chromatids are connected to the spindle and positioned on the metaphase plate (Havas *et al*., 2016). Due to this, the cells are unable to divide and therefore trapped in mitosis leading to cell death (Škubník *et al*., 2021). Tubulin heterodimers form microtubules, which are polymeric fibres (Graham *et al*., 2012). The α- and β-subunits of the protein tubulin create dimers, and the binding site for vincristine is situated on the β-subunit at the heterodimer's interface (Cordelia

& Lobert, 2001). Vincristine and other vinca alkaloids are therefore the only tubulin-binding drugs that do not exclusively bind to a single tubulin heterodimer (Field *et al*., 2014). This critical characteristic is essential to the vinca alkaloids' unique mechanism of action. The compounds have the ability to split microtubule fibres especially at higher dosages, the fibres then unite with one another, always bound by the vinca alkaloid (Silvestri, 2013). In the mitotic spindle, which is responsible for the separation of chromatids during mitosis, such unevenly organised, often spiralling fibres are unable to fulfil their purpose (Dhyani *et al*., 2022). At lower concentrations of vincristine, this function is also impeded as the compound binds to the terminals of microtubule fibres and maintain microtubule dynamics (Liu *et al*., 2019).

1.6 DNA damage

DNA damage is a modification in the physical or chemical structure of DNA, this includes breaking of the DNA strand and inclusion or removal of a base in the DNA strand (Yousefzadeh *et al*., 2021). Damage to the DNA causes alterations in the structure of the genetic material, prohibiting the replication cycle from operating correctly (Kohler *et al*., 2016). DNA damage can be caused by a variety of natural and man-made factors (Lord & Ashworth, 2012). DNA damage is a contradiction in relation to diseases as it can be either harmful or beneficial to the cell depending on the circumstances preceding its occurrence (Chatterjee & Walker, 2017). When one analyses the genesis and treatment of cancer, a disease that is frequently linked to DNA damage, this contrast becomes clear (Marnett, 2000).

Mutations can occur as a result of nucleotide alteration from DNA damage and when a mutation occurs in the section of DNA that codes for a certain gene, it can result in cancer (Clancy, 2008). Ionizing radiation and several chemotherapeutic drugs, on the other hand, carry out their function via DNA damage to treat cancer (O'Connor, 2015). DNA damage can be endogenous (natural) which is usually caused by the accumulation of metabolic by-products such as reactive oxygen species (ROS) which are produced during mitochondrial oxidative metabolism (Visconti & Grieco, 2009), alkylating agents and lipid peroxidation (Hoeijmakers, 2009). DNA damage can also be exogenous which indicates it originates from an external source such as radiation, environmental factors or it can be induced by chemotherapeutic agents (Morgan & David 2006). There are different types of DNA damage and they include cross linking, base alterations and strand breaks.

DNA cross linking ensues when ROS cause linkage between two nucleotides of a DNA molecule via covalent bond, this can occur on the same strand or between two complementary

strands, hence the strands are unable to separate and DNA replication cannot proceed (Huang *et al*., 2013). Some chemotherapy drugs carry out their function via this method of action. Alkylating compounds, for example, cause cross-linking, while platinum-based medicines cause strand breakage and the effects of radiation are comparable (Lawley & Brookes, 1967).

Base alterations are a common source of DNA damage, it results in the DNA strand unable to transcribe appropriately (mutation) (Ciccia, & Elledge, 2010). The end product could be illegible (nonsense mutation) or erroneously read (missense mutation) (Lindahl & Barnes, 2000). Gene-functioning segments of DNA are translated into "pre-mRNA," which is subsequently edited and spliced to create mature messenger RNA (mRNA) (Mandel *et al*., 2008). The genetic code from the nucleic acid is subsequently translated by the ribosomes into amino acids that create the polypeptide chain or chains that fold to form protein (Huang *et al*., 2013). Any change in the sequence of bases in DNA has the ability to change the structure of proteins for which it codes and the bases in DNA and RNA have a sequence that determines the sequence of amino acids (Ciccia, & Elledge, 2010). Examples of base alterations includes oxidation, methylation and alkylation (Zhao *et al*., 2021).

DNA strand breaks occur when one or both strands of the DNA molecule is severed. DNA strand break is a typical side effect of radiation and some chemotherapeutic agents Rulten, & Caldecott, 2013). In single-strand breaks where only one strand is severed, the repair process is easily achieved and carried out precisely as the other strand lacking a defect can be used as a template to repair the damaged strand (McKinnon & Caldecott, 2007).

1.7 DNA repair

If DNA damage is not recognised and repaired, the cell retains the damage and evades apoptosis (Hoeijmakers, 2001). If the damage occurs on a single-strand and that strand is replicated, the damaged base may be replaced by a different base on the complementary strand and this error would be carried on in consecutive replications, thereby resulting in a permanent mutation (O'Hagan *et al*., 2008). If both strands of the DNA are damaged, this could result in the realignment of the chromosome which in turn can result in the abnormal regulation of a gene or alter the function of a gene (Cahill *et al*., 2006). This could lead to mutation and diseases such as cancer, thus why the presence of DNA damage in cells is a hallmark of cancer (Macheret & Halazonetis, 2015).

Thus, the presence of DNA damage in cells triggers the activation of the DNA damage response pathway and the repair of DNA damage is dependent on the magnitude of the damage *i.e.,* if

one strand or both strands have been damaged (Burma &Chen, 2004). When DNA damage occurs on only one strand of the DNA, the complementary strand is used as a template in the repair of the affected strand this process is carried out by a number of different mechanisms which involve the removal and replacement of the affected nucleotide (Caldecott, 2007). If both strands of the DNA are damaged a similar sequence is used in the repair process as none of the strands can serve as a template (Krejci *et al*., 2012). There are five major pathways by which cells carry out DNA repair and these are, mismatch repair, base excision repair, nucleotide excision repair, non-homologous end joining and homologous recombination.

1.7.1 Base excision repair

Base excision repair (BER) is used to remove a single damaged DNA base that does not disrupt the DNA double helical structure (Baiken *et al*., 2021). A number of processes in the cell, such as oxidation, deamination and alkylation can cause single base damage in DNA (Jun & Kool, 2022). Most of this damage arises due to natural degeneration of DNA, however, comparable damage may also be triggered by environmental genotoxins (Huffman *et al*., 2005). These alterations can disrupt the hydrogen bonding capacity of the base leading to erroneous base pairing and mutation, or cause DNA polymerase stalling resulting in cytotoxicity (Kay *et al*., 2019).

The initiation of the base excision repair pathway by one of the eleven DNA glycosylase is dependent on the type of lesion. DNA glycosylases are small in size (35 to 50 kDa) and are monomeric proteins that do not need cofactors to carry out their enzymatic activity (Mullins *et al*., 2019). A specific DNA glycosylase identifies the lesion and the damaged base is flipped out of the DNA helix and placed in the active site of the DNA glycosylase, where the N-glycosylic bond is cleaved, which produces a free base and leaving behind an abasic site (base less sugar) (Betti & McCann 2006). There are two types of DNA glycosylases, monofunctional and bifunctional (Hans *et al*., 2020). Monofunctional DNA glycosylases carry out removal of the base only, while bifunctional DNA glycosylases have an additional activity and cleave the resulting abasic site either on the 3´ side only leaving a phosphoglycolate group (β lyase activity) or on both the 5´ and 3´ side leaving 5´ and 3´ phosphate groups (β-δelimination) (Fromme *et al*., 2004).

Bifunctional DNA glycosylase carries out its function without needing an AP endonuclease which is the enzyme that cleaves the abasic site when monofunctional glycosylase are

present (Svilar *et al*., 2007). Also, the monofunctional DNA glycosylase attacks the C1 of the sugar in the nucleotide using an activated water molecule nucleophile, while the bifunctional glycosylase active site nucleophile is usually the NH_2 group of lysine or the N terminal proline (Mcneill *et al*., 2020). The resulting products of a bifunctional glycosylase cleavage and AP endonuclease cleavage are different as bifunctional glycosylase cleavage of the abasic site produces a α,β-unsaturated aldehyde at the 3´ terminus and a phosphate residue at the 5´ terminus (Zhu *et al*., 2009). On the other hand, the AP endonuclease cleavage of the abasic site produces a 3´ OH adjacent to a 5´ deoxyribose phosphate (Thompson & Cortez, 2020). This cleavage of the abasic site results in single-strand break.

Poly(ADP-ribose)polymerase 1 (PARP1) is activated upon the development of a single-strand break, protecting the strand break and promoting the recruitment of other BER proteins to the site via its accompanying polyADP-ribosylation activity (Grundy & Parsons, 2020). The transient ADP-ribose polymers destabilise the chromatin structure at the site of damage, increasing the rate of BER (Ray Chaudhuri & Nussenzweig, 2017). This mode of action has been targeted by scientists wishing to delay the repair of strand breaks formed either directly following ionizing radiation or as repair intermediates after alkylating agent treatment to increase cancer cell death (Kelley *et al*., 2014). This ultimately led to the development of clinically relevant PARP inhibitors (PARPi) such as olaparib (Lynparza) that has been found to be particularly effective in certain forms of breast cancer (Tangutoori *et al*., 2015). The resulting strand break can either be repaired by long-patch or short-patch base excision repair (Fortini & Dogliotti, 2007).
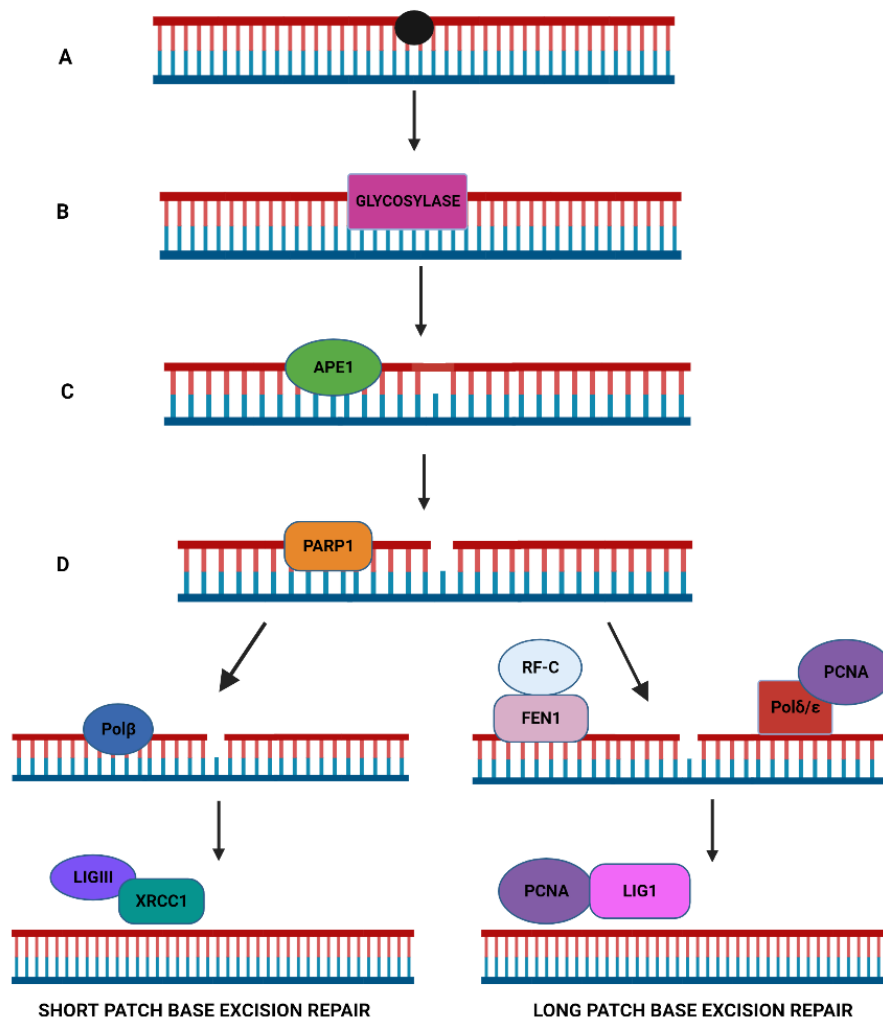
Figure 1.6- Overview of the base excision repair pathway.
A) DNA damage occurs. B) Base damage is recognised by DNA glycosylase, which then creates an apurinic or apyrimidinic site. C) A single-strand break incision is made by AP endonuclease 1. D) The single-strand break sites is recognised by PARP1, which encourages poly(ADP-ribosyl)ation of acceptor proteins at the DNA strand ends. The condition of the 5' deoxyribose phosphate terminal determines whether short-patch BER or long-patch BER should be utilised. The final stage involves the ligation of the repaired strand by DNA ligase 1or 3.

In short-patch base excision repair, one nucleotide is removed, replaced and the new nucleotide ligated, while in long-patch excision repair 2-10 nucleotides are removed and replaced (Chaudhari *et al*., 2021). The enzyme DNA polymerase plays an important role in the short and long-patch base excision repair, the short patch is catalysed by DNA polymerase β but can be compensated with DNA polymerase λ if DNA polymerase β is not

present, while the long patch is catalysed by DNA polymerase ε and DNA polymerase δ (Fortini & Dogliotti, 2007). DNA polymerase β also has deoxyribophosphatase activity as it excises the deoxyribose phosphate left behind at the 5′ terminus in short-patch base excision repair (Albelazi *et al*., 2019). The final step, which is nick sealing, is catalysed by DNA ligase III and cofactor X-ray repair cross-complementing protein 1 (Nazarkina *et al*., 2007). However, in long-patch base excision repair, the replicative DNA polymerases ε and δ are associated with proliferating cell nuclear antigen and both displace the 5′ terminus of the DNA to form a flap, which is then removed by the enzyme Flap endonuclease1 (Dasari *et al*., 2016). The resulting nick in the DNA strand is joined by DNA ligase I (Hindi *et al*., 2021). The choice of short or long-patch base excision repair is influenced by the cell cycle stage and the type of damage, for example abasic sites that are oxidised or reduced must be repaired by long-patch base excision repair as they are resistant to the dRPase activity of DNA polymerase β (Jankowska *et al*., 2008).

DNA glycosylases

DNA glycosylases play an important role in base excision repair as they initiate the process (Hindi *et al*., 2021). This family of enzymes were first discovered in *Escherichia coli* and called uracil N-glycosylase as they were responsible for the removal of the uracil base by breaking the uracil-deoxyribose bond by hydrolysis (Lindahl, 1974). DNA glycosylases have since been discovered in other prokaryotic and eukaryotic organisms (Schärer & Jiricny, 2001). As stated above, DNA glycosylases are divided into two categories, the mono functional and bifunctional glycosylases (Jacobs & Schär, 2012). Based on their substrate specificity, DNA glycosylases are classified into four superfamilies; the first monofunctional DNA glycosylases are classified as uracil DNA glycosylases as they excise uracil from DNA (Zhang *et al*., 2021). The second super family are the helix-hairpin-helix (HhH) DNA glycosylases comprising of methyl purine glycosylase and methyl binding domain glycosylase 4 (Trasvina-Arenas *et al*., 2021). The 3-methyl-purine glycosylase super family is the third super family and they carry out the removal of alkylated bases (Squillaro *et al*., 2019). They are structurally unique when compared to the other super families as they do not have an α-β fold structure like the uracil DNA glycosylase superfamily, neither do they have a HnH motif (Hindi et al., 2021).

Table 1.3 – The eleven mammalian DNA glycosylases, their function and substrates.

	Name	Substrate	Mono/ Bifunctional
1	Methylpurine glycosylase **MPG**	3-meA(3-alkyladenine), hypoxanthine	Monofunctional
2	MutY homolog glycosylase **MYH**	Double strand DNA, Adenine:8-oxoguanine	Monofunctional
3	8-OxoG DNA glycosylase 1 **OGG1**	8-oxoguanine, FapyG(2,6-diamino-4-hydroxy-5-formamidopyrimidine)	Bifunctional
4	Endonuclease III-like protein 1 **NTHL1**	FapyG, double strand DNA, thymine glycol, 5-hydroxyuracil	Bifunctional
5	Endonuclease VIII-like glycosylase 1 **NEIL1**	Thymine glycol, FapyG, FapyA, 8-oxoguanine, 5-hydroxyuracil, single and double strand breaks	Bifunctional
6	Endonuclease VIII-like glycosylase 2 **NEIL2**	Thymine glycol, FapyG, FapyA, 8-oxoguanine, 5-hydroxyuracil, single and double strand breaks	Bifunctional
7	Endonuclease VIII-like glycosylase 3 **NEIL3**	FapyG, FapyA and single strand DNA	Bifunctional
8	Single strand specific monofunctional uracil DNA glycosylase 1 **SMUG1**	Uracil, 5-formyluracil, 5-hydroxymethyluracil	Monofunctional
9	Uracil- N glycosylase **UNG**	Uracil	Monofunctional
10	Methyl- binding domain glycosylase 4 **MBD4**	5-formyluracil, Uracil, Thymidine	Monofunctional
11	Thymine DNA glycosylase **TDG**	5-formyluracil, Uracil, Thymidine, 5-hydroxymethyluracil, 5-carboxylcytosine	Monofunctional

The endonuclease VIII-like DNA glycosylases are a superfamily of DNA glycosylases that recognises oxidised bases (Prakash *et al*., 2012). Endonuclease VIII was first discovered in

Escherichia coli (nei) as an enzyme that cuts the DNA strand at the site of oxidised pyrimidines (Chetsanga & Lindahl, 1979). The protein sequence obtained after the gene was cloned showed similarity to that of formidopyrimidine (Fpg) DNA glycosylase (Melamede *et al*., 1994). Years after these findings, Fpg/Nei orthologs were discovered in mammalian cells and were named Nei-like (NEIL)1, NEIL2 and NEIL3 (Bandaru *et al*., 2002). The trademark of this superfamily is the presence of a zinc finger domain, conserved residues in the helix-two-turn helix (H2TH) domain and the active site nucleophile which is proline in NEIL1 and 2 and valine in NEIL3 (Ide *et al*., 2004). Although NEIL1 is a part of this superfamily, it does not possess a zinc finger domain, rather it has a domain devoid of the four cysteine that hold the zinc ion (Theriot *et al*., 2010). NEIL 2 and 3 however both have a zinc finger domain, the zinc finger domains differ, with NEIL3 having a Ranbp type zinc finger domain which is identical to the zinc finger domain found in bacteria Fpg (Rodriguez *et al*., 2020). It has been suggested that NEIL2 and 3 evolved from the same source, while NEIL1 evolved independently (Prakash *et al*., 2014).

 NEIL1 interacts specifically with some proteins involved in DNA replication such as replication protein A (RPA), flap endonuclease (FEN-1) and PCNA, which indicates that NEIL1 is likely to participate in replication coordinated base excision repair (Zhao *et al*., 2010).   This is further indicated by the fact that NEIL1 and NEIL3 gene expression are cell cycle regulated as expression peaks in S phase for NEIL1 and late S/G2 phase for NEIL3 (Hildrestrand *et al*., 2009). NEIL2 is however different as it is constitutively expressed in all stages of the cell cycle (Dou *et al*., 2008). All three have DNA glycosylase activity with an unusual preference for single-stranded DNA (ssDNA) and other DNA open structures found during DNA replication and transcription (Banerjee *et al*., 2011). These proteins have been shown to use the β/δ-elimination process to cleave the DNA at the abasic site (Dou *et al*., 2003; Wallace *et al*., 2003; Albelazi *et al*., 2019).

1.7.2 Nucleotide excision repair
Nucleotide excision repair (NER) is a process that involves the removal of bulky helix distorting DNA lesions which include cyclobutene pyrimidine dimers and are usually caused by UV light, chemicals or oxidative damage (Schärer, 2013). A functioning NER pathway is important as hereditary genetic mutation of some NER proteins results in diseases such as Cockayne's syndrome and Xerodema pigmentosum (DiGiovanna & Kraemer, 2012). NER in eukaryotes is made up of two subpathways, which are transcription coupled nucleotide excision repair (TC-NER) and global genomic excision repair (GG-

NER) (Hanawalt & Spivak, 2008). The GG-NER repairs damage anywhere in the genome and repairs both transcribed and untranscribed strands of DNA, while TC-NER fixes damages on the transcribed strand of DNA present in active genes (Spivak, 2016). The GG-NER functions independent of transcription and identifies DNA damage by using proteins such as the XPC-RAD23B complex and DNA damage binding protein (DDB) to monitor the genome, while the TC-NER identifies DNA damage through the RNA polymerase II complex (Friedberg *et al*., 2005).

The NER pathway is divided into four steps: 1) Identification of DNA damage 2) incision on both sides of the DNA damage and excision of the affected DNA 3) Filling of the gap by DNA synthesis 4) ligation of open DNA ends (Reardon & Sancar, 2005).

The GG-NER is initiated by the DDB and the XPC-RAD23B complex which help scan the genome and identify lesions for repair, the XPC-RAD23B identifies distortion of the helix (Sugasawa *et al* 2001), while the XPE DDB1 and DDB2 identify UV induced damages (Reardon & Sancar 2003). TC-NER is initiated when RNA polymerase is stalled at a site of damage on the DNA, this stationary RNA polymerase signifies to the TC-NER that damage is present at that site (Scharer, 2013). The only difference between the GG-NER and TC-NER sub pathways is how the DNA damage is identified (Friedberg *et al*., 2005).
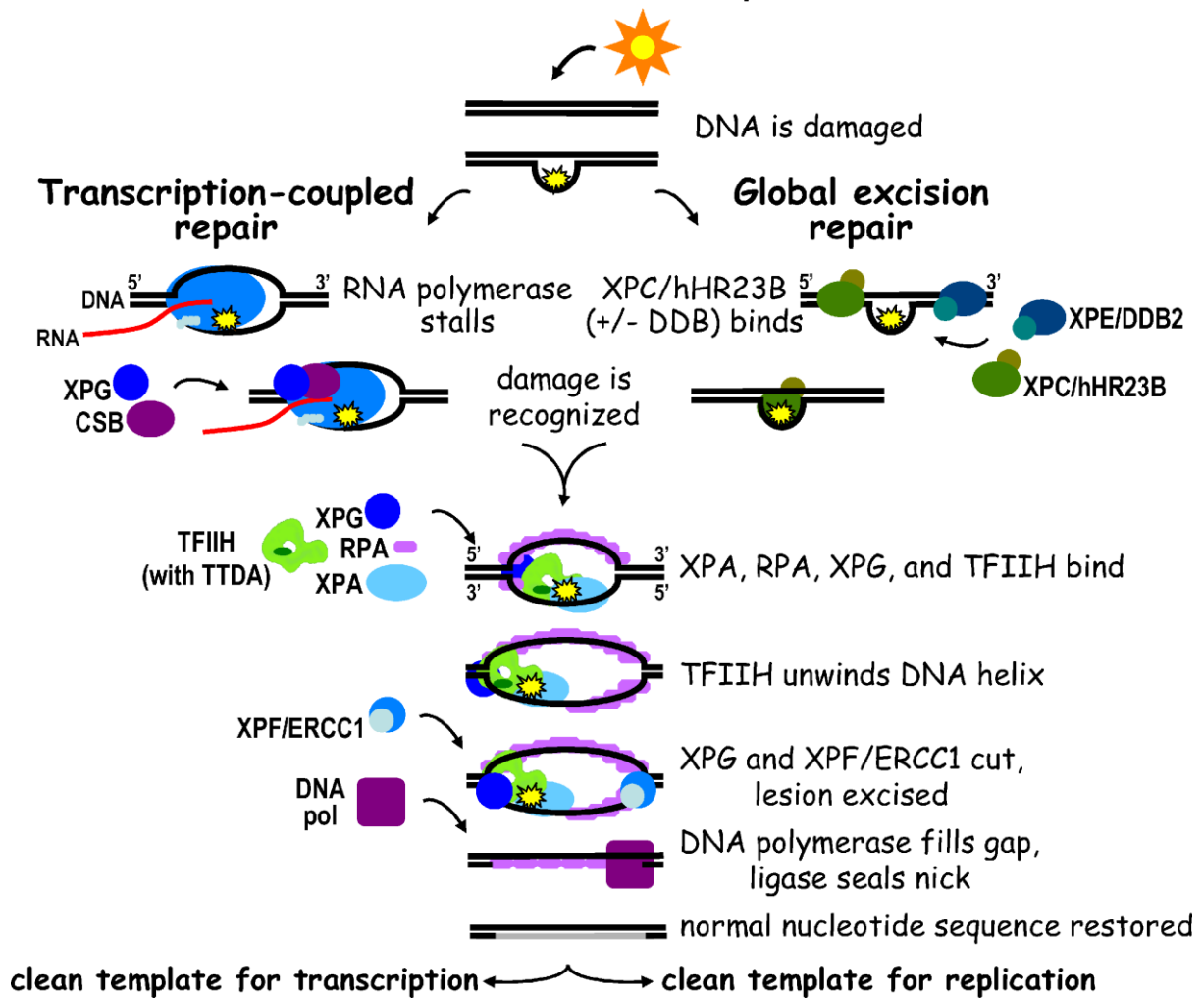
Figure 1.7 - Nucleotide excision repair pathway (adapted from Fuss & Cooper, 2006) Subsequent to DNA damage, identification of the damage is dependent on whether the DNA is transcriptionally active (transcription-coupled repair) or not transcriptionally active (global excision repair). Following the initial phase of identification, the damage is fixed in a similar manner, with the restoration of the original nucleotide sequence as the end result.

After identification of the site of damage, the transcription factor II H (TFIIH) is recruited to the DNA damage site (van der Weegen *et al*., 2020). TFIIH consists of two subunits, XPB and XPD which serves as anchors that open the helix of the DNA at the site of the damage for the entrance of TFIIH (Coin *et al*., 2007). Once XPD is engaged at the site of DNA damage, the pre-incision complex begin to assemble with the other pre-incision components (XPA, RPA and XPG) recruited to the site individually and the XPC-RAD23B leaves the complex (Riedl *et al*., 2003). XPA is the core of the complex, it is linked to DDB,

TFIIH, XPC-RAD23B and PCNA proteins (Gilljam *et al*., 2004). ERCC1-XPF is then recruited to the complex by XPG which stabilises TFIIH and once both ERCC1-XPF and XPG are in place, the dual incision begins (Fagbemi *et al*., 2011). ERCC1 begins the incision process of the DNA damage on the 5′ side and produces a free 3′ hydroxyl group, while the XPG cuts the damaged DNA from the 3′ side and leaves a 5′ phosphate (Pal *et al*., 2022). This dual incision results in the excision of a ssDNA about 30 nucleotides long and this oligonucleotide containing the damage site is then expelled with TFIIH attached to it (Kemp *et al* 2012). TFIIH binds to ATP which then releases it from the excised oligonucleotide and RPA binds to the oligonucleotide and ultimately degrades it (Krasikova *et al*., 2018). DNA repair is initiated from the 3′ hydroxy group by DNA polymerase which is recruited to the DNA strand by PCNA and Replication factor C (RFC) (Corrette- Bennett *et al*., 2004). The DNA polymerase uses translocation to copy the other strand and the resulting nick after repair is fixed by DNA Ligase α and XRCC1 (Moser *et al* 2007).

1.7.3 Mismatch repair

DNA damage is usually instigated by exogenous (e.g., UV light) or endogenous (ROS, lipid peroxidation) factors, however sometimes, DNA damage can occur as a result of mistakes generated through standard DNA metabolism such as DNA recombination, replication or during DNA repair (Kunkel *et al*., 2005). These errors generated are usually the inaccurate addition or removal of bases and mispairing of two bases (Kunkel *et al.*, 2005). Errors that are generated during replication can be transferred to the newly synthesized daughter cells, thus resulting in mutation which can then be transferred during reproduction, thus leading to hereditary cancers (Dolce *et al*., 2022). During DNA replication a mismatch occurs on the daughter strand, therefore the mismatch repair system must be able to differentiate between the template and the daughter strand before repair can commence (Stojic *et al.*, 2004).

 In *Escherichia coli*, a number of proteins play an important role in mismatch repair and they include MutH, MutL and MutS which activate the beginning of the mismatch repair process (Sameer *et al*., 2014). Thus, MutS identifies a mismatch in the DNA and binds to the site of the mismatch by forming a dimer $MutS_2$ (Putnam, 2021). MutL then binds to the MutS bound to the DNA strand and this process signals the activation of MutH by ATP (Junop *et al.*, 2001). When a DNA strand is being replicated, the newly synthesized strand is briefly nonmethylated and the presence of the nonmethylated GATC sequence

(methylation takes place on the adenosine of a GATC sequence) on the daughter strand differentiates the daughter strand from the template (Hanaoka & Sugasawa, 2016). MutH identifies the nonmethylated GATC sequence on the daughter strand, binds to it and nicks it (O'Brown & Greer, 2022). MutL employs helicase II to the site of the nick, which then unwinds the DNA helix from the site of the nick to the site of the mismatch in a 3′ to 5′ direction (Putnam, 2021).

The MutS,H and L complex formed moves down the DNA towards the site of the mismatch, also releasing the strand to be removed as it moves, producing a ssDNA (Ramilo *et al.*, 2002). An exonuclease is recruited to the site, the exonuclease present depends on location of the MutH nick, if it is done on the 5′ terminus, then ExoVII or RecJ is recruited, if it is however on the 3′ terminus, then Exol is recruited (Lopez de Saro *et al.*, 2006). The exonuclease removes the strand from the site of the MutH nick past the site of the mismatch (Putnam, 2021). The gap produced as a result of this excision is then filled by DNA polymerase and the strand present serves as a template in the production of the daughter strand, which is then closed by DNA ligase and the new daughter strand is methylated by DNA methylase (Li *et al.*,2008).

1.8 Double-strand breaks

Double-strand breaks (DSB) in DNA occur when the two complementary strands of the DNA double helix are broken concurrently at locations that are sufficiently adjacent to one another that base-pairing and chromatin structure are unable to maintain the juxtaposition of the two DNA ends (Rodgers & McVey, 2016). This, results in the two DNA ends produced by the DSB being susceptible to physical separation from one another, making subsequent repair problematic and allowing for improper recombination with other locations in the gene (Santigny *et al.*, 2001).

Irrespective of the fact that they present a serious risk to the veracity of the genome, DSBs are occasionally created on purpose and for a specific biological function (van Gent *et al.*, 2001). The V(D)J recombination process, which arises in growing B- and T-lymphocytes to provide the antigen-binding variety of immunoglobulin and T-cell receptor proteins is probably the best-known example of this in higher eukaryotes (Roth, 2015). DNA DSBs are created at a particular locus in the V(D)J pathway by a site-specific nuclease made up of the RAG1 and RAG2 proteins (Libri *et al.*, 2022). The DSBs are then fixed by the same

proteins that are also involved in the repair of DSBs caused by mutagenic agents (Jung & Alt, 2004). Even though events like V(D)J recombination are closely monitored, they can occasionally go wrong, with potentially fatal repercussions for the cell or the organism (Roth, 2014). ROS metabolism, ionising radiation, and stalled replication forks are all sources of DSBs (Cannan & Pederson, 2016). In addition to causing significant genomic rearrangements such as translocations, inversions, duplications, and deletions, DSB repair is also crucial for maintaining DNA integrity (Bétermier *et al*., 2014). On the other hand, DSBs can also produce genetic variation in vital biological procedures including meiosis and the development of the immunological arsenal (Guirouilh-Barbat *et al*.,2014). As a result, repair of DSB must be strictly regulated. The activation and/or induction of DNA repair proteins is one of the mechanisms by which cells respond to DSBs (Dudley *et al*., 2005). The DNA repair proteins are subsequently physically enlisted to the site of the DNA damage to repair it (Mills, 2020). Furthermore, dividing cells slow down their passage through the cell cycle in response to DNA DSBs (Khanna & Johnson, 2001) and advancement through S-phase is hindered when damage occurs in the G1 or S cell-cycle phases (Bartek *et al*., 2001). This allows time for DNA repair to take place prior to the lesions been detected by a replicative DNA polymerase (Zhang *et al*., 2007). DNA DSBs occurring in G2 phase also hinder progression into mitosis, limiting chromosomal fragment mis-segregation during cytokinesis (Zhou & Elledge, 2009). The DNA damage response (DDR) a comprehensive cellular mechanism, is required to regulate DSB detection, signalling, and repair (Zhou *et al*, 2000). The ATM kinase, a phosphoinositide 3-kinase (PI3K)-related protein kinase that is swiftly mobilised to chromatin in response to DSBs via association with the MRE11-RAD50-NBS1 (MRN) complex is required for the DDR (Mladenova *et al*., 2022). This mobilisation initiates a signalling cascade that triggers cell cycle checkpoints and stimulates the migration of repair components to the damage site by phosphorylating many substrates (Abraham, 2001). The serine 139 of the carboxyl terminus of the histone variation H2AX, which is known as γH2AX in its phosphorylated form, is one of the substrates of ATM kinase activity (Kuo & Yang, 2008).

1.8.1 DNA damage response signalling

The DNA damage response (DDR) signalling pathway is initiated by DNA damage sensors such as Ku70/Ku80, MRN complexes and PARP1 (Huang & Zhou, 2020). These sensors play a vital role in how DNA damage is detected and identified, they are usually the first to

interact with the site of damage (Li & Chen, 2018), they recognise and bind to the site of damage, thereby initiating DDR (Schuh *et al*., 2013). The DNA damage sensors determine which DNA repair pathway is going to be employed with the DNA-Pk preluding non-homologous end joining (NHEJ), while MRN preludes the homologous recombination (HR) pathway which is ATM dependent (Stracker & Petrini, 2011). The MRN complex acts as a first line sensor of double strand breaks, binding the damaged DNA segments together (Rupnik *et al*., 2008). Due to the interplay between NBS1 and ATM (Ataxia–Telangiectasia mutated), ATM is initially sequestered to DSB sites (Reinhardt & Yaffe, 2013). ATM phosphorylates numerous distinct substrates involved in DDR signalling after being activated by autophosphorylation (Putti *et al*., 2021). DNA-dependent protein kinase (DNA-PK) is a standard DSB sensing and binding complex made up of Ku70, Ku80, and the catalytic component DNA-PKcs (Constantini *et al*., 2007).

DNA-PK binding shields the damaged DNA end from disintegration by endogenous nucleases while also recruiting and activating subsequent elements in the NHEJ DSB repair pathway (Jette & Lees-Miller, 2015). Meanwhile, activated ATM phosphorylates the MRN subunit NBS1 to sustain/strengthen ATM's activity by generating a positive-feedback loop (Shiloh, 2013). The production of γH2AX occurs due to the phosphorylation of the H2AX histone by ATM at the serine 139 position, which then results in the build-up of γH2AX in the region of DSBs (Siddiqui *et al*., 2012). The development of γH2AX foci causes other DDR components such as MDC1 and BRCA1 to be recruited to the locations of DNA damages (Liu *et al*.,2019). The generation of γH2AX is generally regulated by ATM, although it can alternatively be regulated by DNA-PK (Shiloh & Ziv, 2013). The γH2AX foci according to Kuo and Yang, depict DSBs in a 1:1 ratio and can be employed as a measure for DNA damage (Kuo & Yang, 2008).
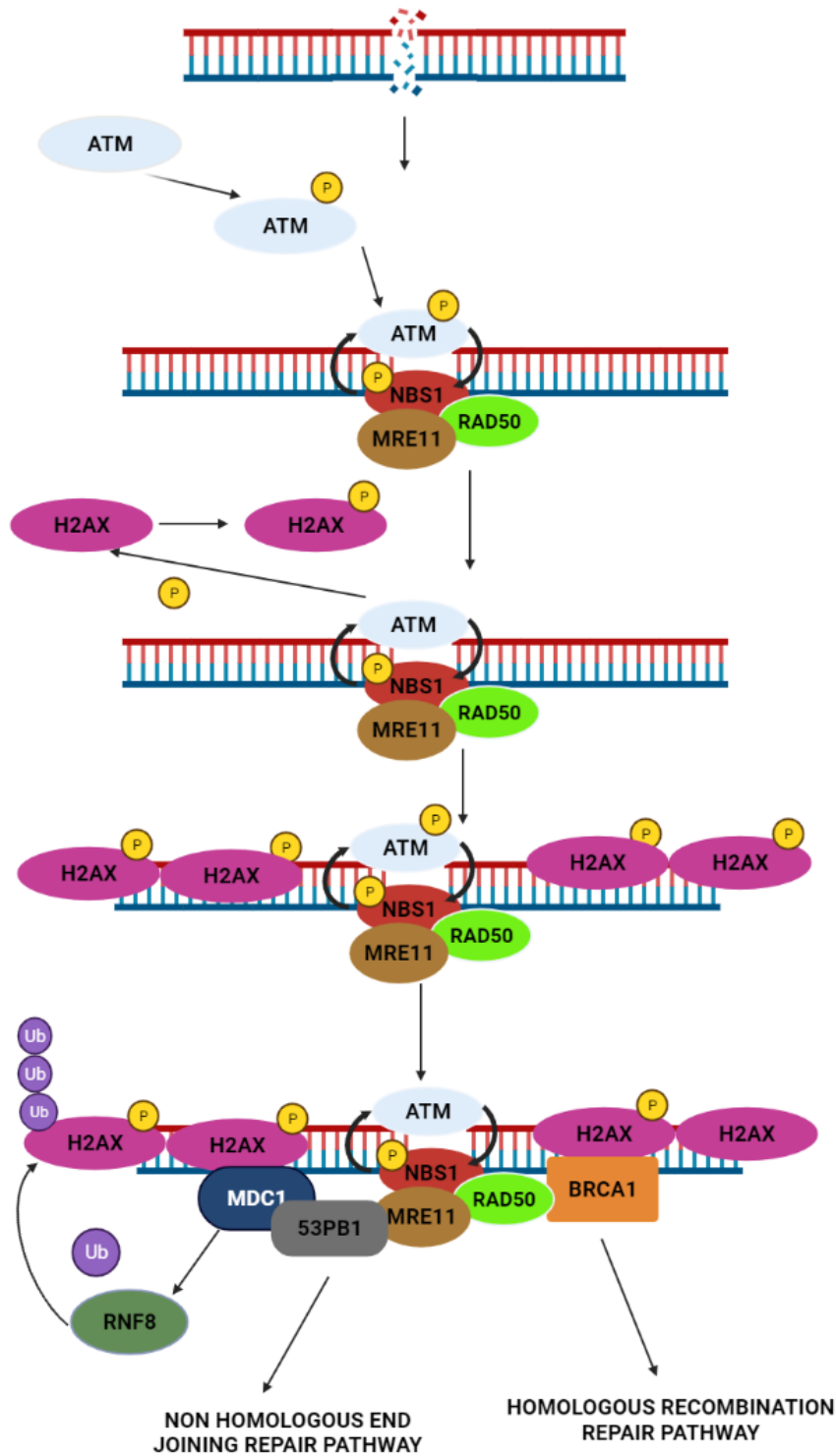
Figure 1.8 -**DNA damage response signalling.**
Graphical illustration of the DNA damage response pathway.Recruitment of ATM to the siteof DSB and its autophosphorylation of the NBS1 unit of MRN which produces a positive feedback loop, ATM phosphorylates H2AX which then recruits MDC1 and BRCA1. MDC1 recruits RNF8 which ubiquilates γH2AX which encourages the localisation of 53PB1 to the site.

In summary, MDC1 is recruited to the site of DSB by the formation of γH2AX (Liu *et al*., 2019). MDC1 then engages the RNF8 (RING finger 8) and RNF168 E3 ligases to ubiquitylate H2A in the DSB location and binds with MRN and ATM to anchor MRN and ATM at the DSB site (Fernandez-Capetillo *et al*., 2002). The methylation state of other histones is influenced by H2A ubiquitylation, which can boost 53BP1 localization to DSBs, impacting the DSB repair method (Lu *et al*., 2021). 53BP1 (p53-binding protein 1) controls which DSB repair pathway is used (Adams & Carpenter, 2006). 53BP1 NHEJ-mediated DSB repair during G1 by inhibiting long-range DNA end-resection (Wang *et al*., 2002), which is required for homologous recombination-mediated DSB repair and during S-G2 phase, BRCA1 and its binding component CtBP-interacting protein (CtIP) inhibit 53BP1-RIF1 and 53BP1-PTIP complexes, allowing homologous recombination-mediated DSB repair to occur via promotion of DNA end resection (Panier & Boulton, 2014).

DSBs can cause substantial genetic information loss, genomic rearrangements, or cell death if they are left unrepaired or fixed wrongly (Di Tullio *et al*., 2002). NHEJ and HR are the two main methods for repairing DSBs (Ensminger & Löbrich, 2020). The accuracy and template criteria of the two paths are different. NHEJ ligates the damaged DNA ends together with little or no homology, resulting in deletions or insertions (Pannunzio *et al*., 2018). HR, on the other hand, repairs the break using an undamaged DNA template from the sister chromatid or homologous chromosome, resulting in the restoration of the original sequence (Haber, 2014). Therefore, the accuracy of repair is determined by the DSB repair pathway chosen, which may impact the incidence of ageing and cancer (van Heemst *et al*., 2007). What pathway is used in DSB repair pathway is dependent on the cell cycle stage and sequence context (van Sluis & McStay, 2015). NHEJ is the major mechanism for DSB repair throughout the G1 phase, even in nonproliferating and senescent cells, while HR is primarily restricted to the S and G2 stages of the cell cycle (Hanaoka & Sugasawa, 2016). If DSBs occur near repeating sequences, HR occurrence rises and the utilization of NHEJ in DSB repair far outnumbers that of HR (Price & D'Andrea, 2014).

1.8.2 Non-homologous end joining

NHEJ is a DNA repair process that repairs double-strand breaks (Rodgers & McVey, 2016). In contrast to homology directed repair, which requires a homologous sequence to direct repair (Weterings & Chen, 2008), NHEJ is called "non-homologous" because the break ends are directly ligated without the need for a homologous template (Khanna & Johnson, 2001).). NHEJ is not bound to a specific phase of the cell cycle since it does not demand a

homologous template, while HR is thought to be functional only during the S and G2 stages of the cell cycle when a homologous template via the sister chromatid is present (vanHeemst *et al*., 2007). There are two NHEJ pathways, the canonical NHEJ (cNHEJ) and the alternative NHEJ (aNHEJ). The aNHEJ repair process is thought to be an alternative to cNHEJ. Since cNHEJ and potentially HR suppress aNHEJ, and aNHEJ has functional relevance when these other repair pathways fail (Yu *et al*., 2020). Although aNHEJ was once thought to be just a backup mechanism that only functioned when cNHEJ was inhibited, new research has shown that aNHEJ can actually be remarkably effective and operate in cells that are equipped for cNHEJ (Deriano & Roth, 2013).

1.8.2.1 Canonical non-homologous end joining

The identification and attachment of the Ku heterodimer to the DSB is the first phase of canonical NHEJ (Wang *et al*., 2006). The Ku heterodimer is made up of two monomers: Ku70 and Ku80 (also known as Ku86) (Aissaoui *et al*., 2021). Although Ku70 and Ku80 have little in common in terms of their sequence, the two Ku subunits have a comparable domain structure (Abassi *et al*., 2021), with each subunit consisting of three domains: an amino-terminal von Willebrand domain (vWA), a centralized Ku core domain, and a divergent carboxyl-terminal area (Downs & Jackson, 2004). The Ku70 and Ku80 bind to both ends of the severed DNA (Figure 1.10A).

The attachment of the Ku heterodimer serves as a scaffold for the recruitment of other essential canonical NHEJ enzymes (Yang *et al*., 2020) and supports the protection of the ends of the DSB from non-specific processing, which helps to retain their stability (Stinson *et al*., 2020). Upon attachment of the Ku heterodimer, it proceeds to recruit other enzymes to the site of the DSB such as DNA Ligase IV, DNA-PKcs, X-ray cross complementing protein 4 (XRCC4) and XRCC4-like factor (XLF) (Constatini *et al*., 2007). It has been demonstrated that upon recruitment of DNA-PKcs by the Ku heterodimer to the DSB ends, the big DNA-PKcs molecule creates a unique structure at the DNA termini (Figure 1.10B) (Weterings *et al*, 2004) which plays a part in the creation of a synaptic complex that keeps the two ends of the damaged DNA molecule together (Stinson *et al*., 2020). XRCC4 and XLF generate a filament that connects and secures the two halves of the damaged DNA molecule (Mahaney *et al*., 2013). The XRCC4-XLF filament may then form a complex with DNA-PKcs and Ku to generate a strictly controlled DNA end protection complex (Xue & Greene, 2021). The ends of the DSB have to be processed to prepare it for reattachment by the enzyme DNA Ligase IV(Altmann & Gennery, 2016).
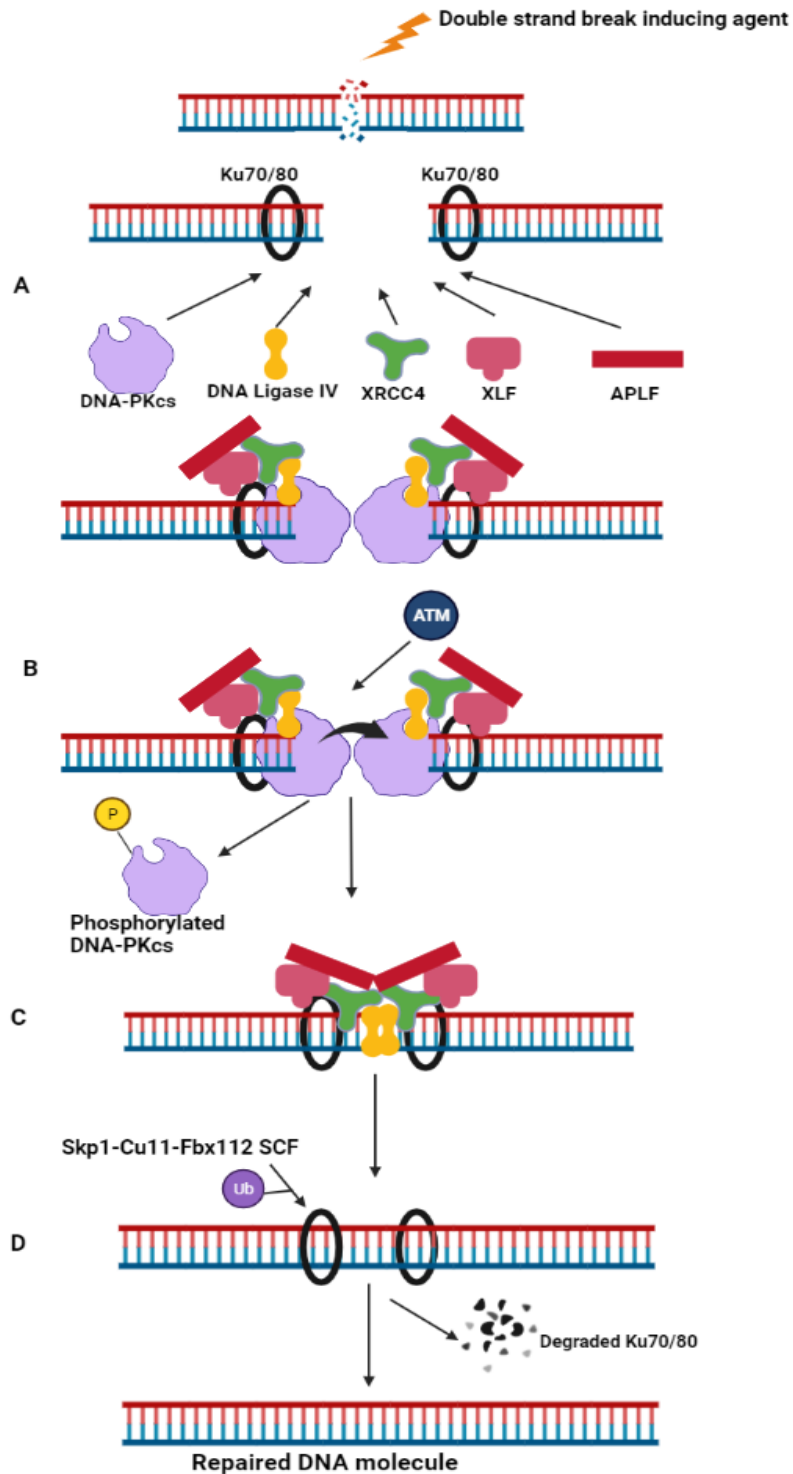
Figure 1.9- Overview of canonical non-homologous end joining. A- Attachment of the Ku heterodimer to DSB which results in recruitment of other enzymes to the site. B- DNA-PKcs which protects the severed end is phosphorylated by ATM and exits the DSB. C-Reattachment of severed DNA by DNA Ligase IV. D- Exit of all the other enzymes from the DNA molecule and ubiquitylation of the Ku heterodimer by SKP1-CU11-Fbx112 SCF.

Various DNA end processing enzymes, such as those that operate on the DNA ends, bridge the gaps and excise end groups that obstruct the function of the enzyme may be needed based on the type of DSB (Zhao *et al.*, 2020). Some enzymes listed in Table 1.4 below have been identified in being critical for preparing severed DNA ends for the canonical NHEJ pathway (Davis & Chen, 2013).

Table 1.4- List of enzymes that prepare DNA ends for the NHEJ

Enzyme	Type	Function
Apratxin	Hydrolases/transferases	Excision of covalently linked adenylated groups from the 5´ phosphate end
PKNP	Kinase/phosphatase	Elimination of 3´ phosphate group and introduction of a 5´ hydroxyl group
Artemis	Nucleolytic enzyme	endonuclease cleavage of 5´ overhang nucleotides 5´-3´ exonuclease cleavage of nucleotides.
WRN	Exonuclease	3´-5´ exonuclease cleavage of nucleotides.
APLF	Endonuclease/ exonuclease	3´-5´ exonuclease cleavage of nucleotides. Endonuclease removal of 3´ overhangs.
Ku	AP lyase	Removal of abasic sites close to the DSB.
Polymerase μ and λ	Polymerase/ lyase	Filling of gaps in the DNA strand, Polymerase μ utilizes the template and dNTP and rNTP to fill the gaps, while Polymerase λ uses its lyase function to fill it.

DNA-PKcs undergoes a conformational shift as a result of autophosphorylation and/or phosphorylation by ATM, which causes the appendages of DNA-PKcs to open, allowing it to exit the DSB (Bloct *et al*., 2004). It is unclear whether this happens before or after the final ligation phase (Davis & Chen, 2013). Upon exit of the DNA-Pkcs, DNA ligase IV arrives to reattach the severed DNA back together (Figure 1.10C) (Lieber, 2010). Although DNA ligase IV can function on its own, it needs XRCC4 and XLF to secure it to the DNA before it can carry out its function (Ghosh & Raghavan, 2021). The DNA-Ligase IV is then able to carry out its function by reattaching the ends of the DNA strands (Altmann & Gennery, 2016). XRCC4, XLF, and most likely APLF help with this final ligation step (Grundy *et al*., 2013). After the ligation process, Ku is most usually trapped on the DNA molecule (Zahid *et al*., 2021). Ku can be ubiquitylated by Rnf8 or the Skp1-Cul1-Fbx112 SCF complex (Figure 1.10D) (Postow *et al*., 2008), causing it to be freed from the repaired DSB and degraded, thus completing the repair of the DSB (Postow *et al*., 2013).

1.8.2.2 Alternative non-homologous end joining

The presence of two to twenty nucleotides of sequence homology at the ends of the DSB is required for the alternative NHEJ repair pathway to commence repair (Iliakis *et al*., 2015). The first phase involves the recognition of DNA breaks by PARP1 which activates DNA end resection (Bétermier *et al*., 2014). In the absence of the Ku70/Ku80 protection at the site of damage, the DNA ends are excised in a process that is promoted by the nuclease function of the MRN/CtiP complex exposing the ssDNA overhangs which contain the microhomology sequence at the repair site (Yang *et al*., 2018). Micro-homologies are annealed prior to joining in alternative NHEJ, which is linked to excessive deletions and insertions at junction sites and has also been linked to the creation of large-scale genomic rearrangements, including chromosomal translocations (Bunting & Nussenzweig, 2013). The short microhomologies are then used to bridge and align the ends of the DNA, while ERCC1/XPF nucleases degrade non-homologous 3′ tails (Kent *et al*., 2015). DSBs are then linked by the DNA Ligase III/XRCC1 complex after the ensuing gaps in the DNA strands have been filled by DNA polymerase θ mediated DNA synthesis which encourages the annealing of the ssDNA containing the microhomologies (Caracciolo *et al*., 2021). Additionally, DNA Ligase I could step in to catalyse the last stage of the ligation of the DNA ends in the absence of DNA Ligase III, a more efficient enzyme (Lu *et al*., 2016).
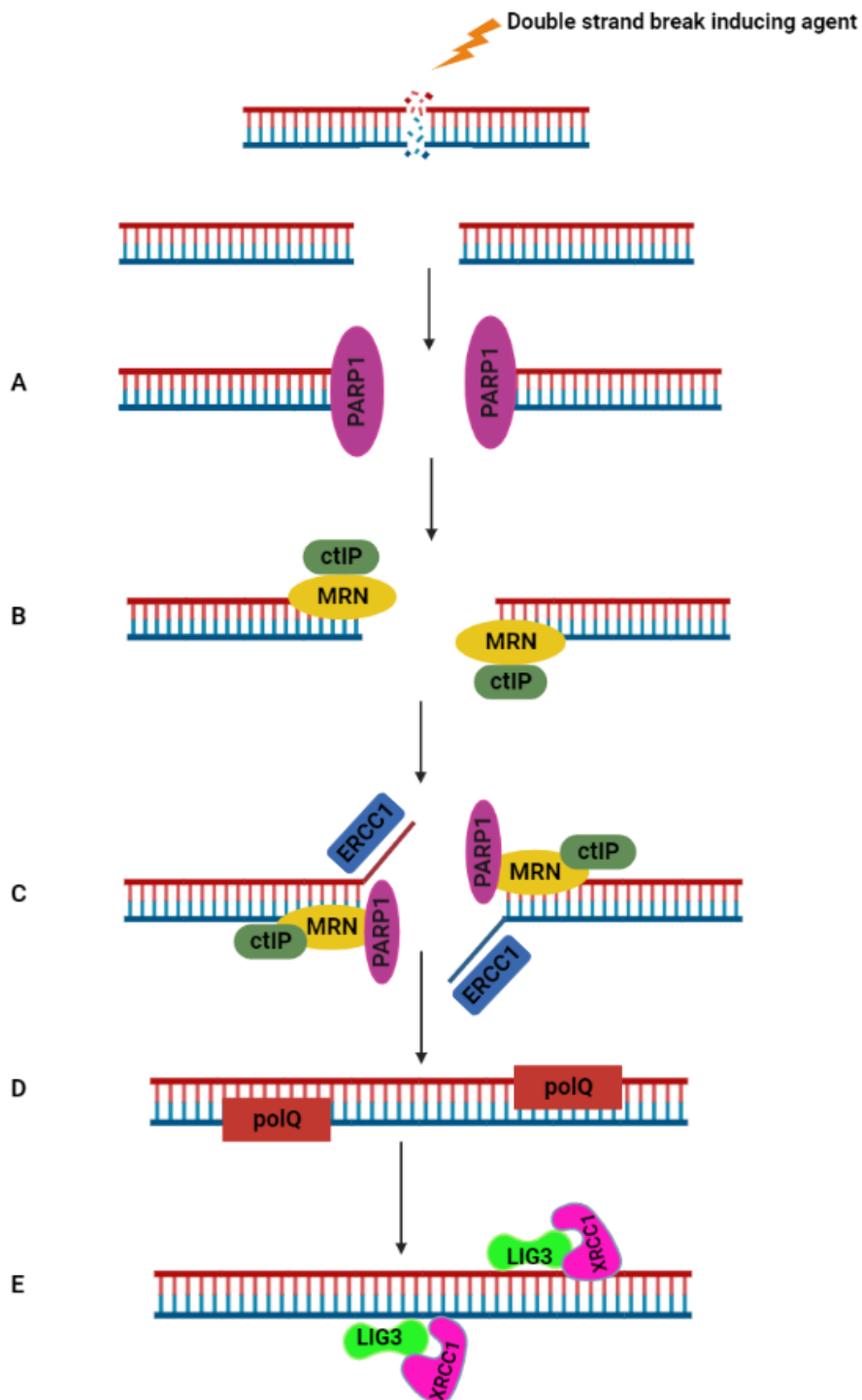
Figure 1.10- Overview of the alternative non-homologous end joining repair showing the various stages and important elements A) recognition of the DSB by PARP, B) Excision of the DNA ends by MRN/CtiP complex exposing the single-stranded DNA. C) The ends of the DNA are aligned and ERCC1XPF nucleases degrade non-homologous 3′ tails. D) The ensuing gaps in the DNA strands arefilled by DNA polymerase theta mediated DNA synthesis. E) The DNA strands are linked by the DNA Ligase III/XRCC1 complex.

1.8.3 Homologous recombination

HR is a DNA metabolic activity that occurs in all forms of life and offers reliable exchange of genetic information, template-dependent repair or acceptance of compound DNA damages such as DSBs, gaps in DNA and DNA interstrand crosslinks (ICLs) (Sung & Klein, 2006). HR plays an essential part in accurately copying the genome by offering valuable assistance during replication of the DNA and also telomere preservation, in addition to its role in preserving the genome (Zhao *et al.*, 2017). The phase of cell cycle the cell is in determines what repair pathway fixes the DSB (Oh *et al.*, 2022). HR is used to fix DSB in the S and G2 phase prior to the cells progression into mitosis as sister chromatids which have an identical template to the damage DNA is readily accessible at these phases (Mathiasen & Lisby, 2014). In order to guarantee genome integrity, DSB repair by HR operates through a series of subsequent stages that must be carefully regulated (Krejci *et al.*, 2012). The four sequential stages are 1) identifying the DSB, 2) resection of the DSB, 3) RAD51- regulated search for homology and strand exchange and 4) Resolution of the outcomes of the holiday junction and homologous recombination (San Filippo *et al.*, 2008). The early steps are maintained, but the resolution of the HR routes varies (Ragu *et al.*, 2021). The HR process is initiated by the identification of the DSB which is regulated by the MRN complex and ATM which in turn activate the DNA damage response (Hauer *et al.*, 2017). Upon the detection of a DNA DSB, modifications to the chromatin structure are initiated, which promotes the enlistment of DNA repair proteins and chromatin decondensation (Price & D'Andrea, 2014). The phosphorylation of the histone modification of H2AX close to the lesion is particularly important as MDC1 which interacts directly with phosphorylated H2AX at serine 139 (Stucki *et al.*, 2005), is one of the repair proteins that are more easily recruited to the damaged location as a result of H2AX phosphorylation (Salguero *et al.*, 2019). The ubiquitin ligases RNF8 and RNF168 alter chromatin structure as a result of the build-up of the MDC1-stabilized MRN complex (Mailand *et al.*, 2007).
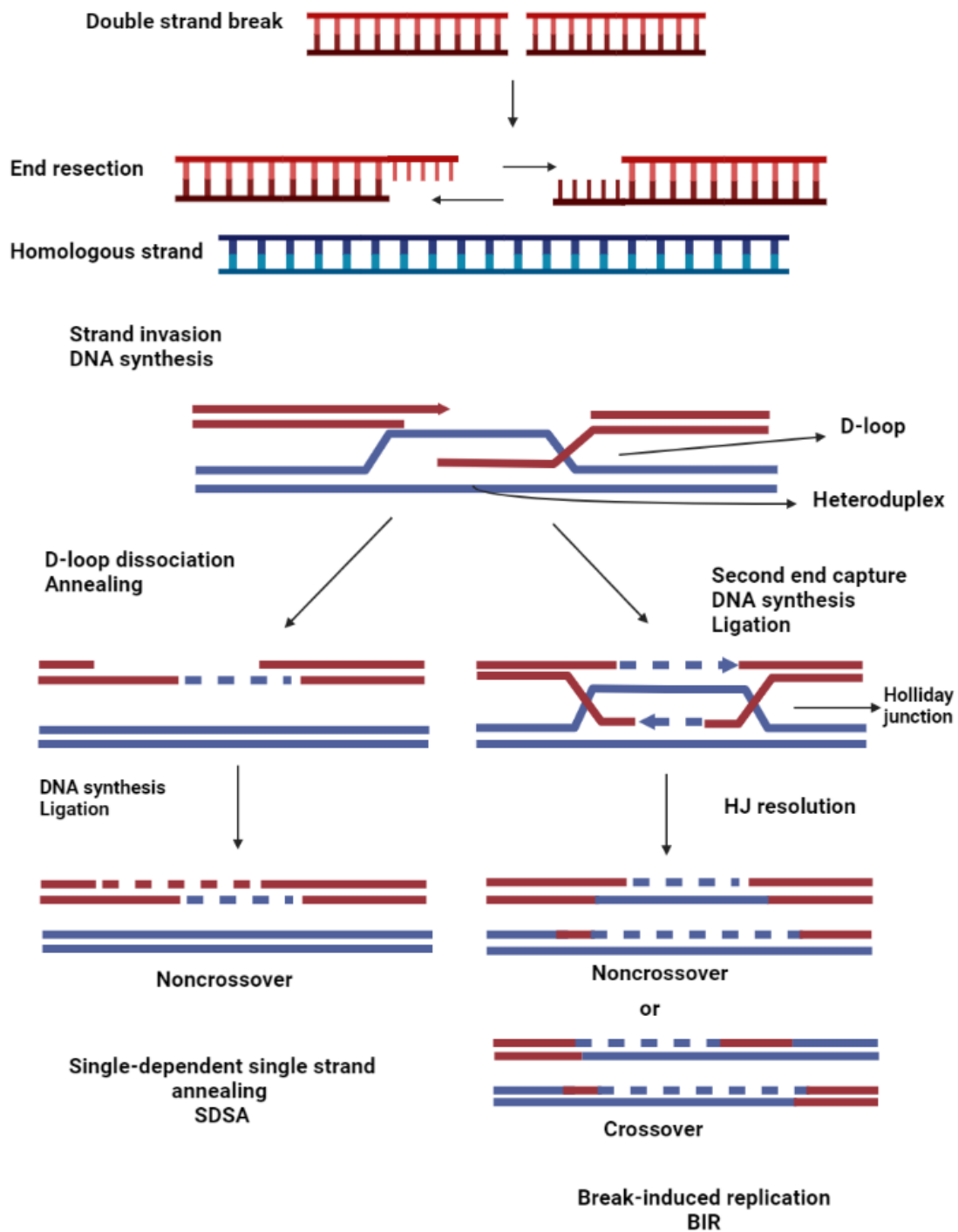
Figure 1.11- **Overview of the homologous recombination repair pathway of DSBs**.
The detection of double-strand DNA breaks by ATM and ATR signals the start of
homologous recombination. A lengthy 3′ single-strand DNA tail is produced by DNA end
resection, and this tail might encroach upon the homologous DNA strand. RAD51 is placed
onto the single-strand DNA tail following end resection. The DNA repair is then carried out
when the strand invades the homologous DNA strand.

BRCA1 and its cofactors are drawn to the DSB location via their association with the NBS1 element of the MRN complex following identification of the DSB and chromatin remodelling (Ragu *et al*., 2021). In order to counteract BRCA1's action in the activation of resection, 53BP1 binds with the shieldin complex (Jasin & Rothstein, 2013). The elimination of the 53BP1-shieldin complex from the DSB site is a crucial function of BRCA1 during HR commencement (Noordermeer *et al*., 2018). Initiation and extension are the two steps that make up the resection process (Mirman & de Lange 2020). The MRE11 subunit of the MRN complex works with the endonuclease CtIP to catalyse commencement of resection (Yu *et al*., 2006). The BRCT domain of the BRCA1 protein facilitates interactions with phosphorylated proteins, thus resulting in the formation of a complex with BARD1 which confers ligase activity to the complex (Jasin & Rothstein, 2013). As a result, this combination permits the ubiquitination of the CtIP nuclease, which works with MRN to start the resection of the DSB. A DNA nick is formed as a result of the interaction between CtIP and MRE11 which activates the endonuclease activity of MRE11 and MRE11 degrades in a 3′ to 5′ direction away from the nick (Rass *et al*., 2009). The BLM/DNA2 complex and exonuclease1 then ensure that the 3′ strand is lengthened to produce a lengthy 30 nucleotide overhang (Krejci *et al*., 2012). Finally, RPA stabilises and protects the 3′ ssDNA stretch produced by resection (Nimonkar *et al*., 2011). The replacement of RPA on the ssDNA with RAD51 which is facilitated by BRCA2 and PALB2 results in the formation of a presynaptic complex (Kelso *et al*., 2017). The homologous pairing and strand intrusion of a 15 nucleotides homologous duplex sequence are encouraged by the ssDNA/RAD51 filament (Krejci *et al*., 2012). This results in the beginning of the homologous matrix's replication and the production of cruciform precursors known as Holliday junctions (HJ) (Ashton *et al*., 2011). Among the elements that resolve HJ via cleavage of the intermediate are the nucleases GEN1, the heterodimer MUS81/EME1 and the SLX1-SLX4 complex (Wyatt *et al*., 2013). Through the concurrent transit of the two double HJs (dHJs) towards one another, which results in their collapse, topoisomerase III (TOP3A) and BLM resolve both dHJ substrate. RMI2 (a crucial component of the "dissolvasome" complex) promotes dHJ resolution, and TOP3 engages RMI1 to catalyse dHJ disintegration (Bizard & Hickson, 2014). This technique could lead to an interchange of adjacent sequences depending on how the HJ resolution is oriented (Ashton *et al*., 2011). Gene conversions with or without cross over are hence the by-products of HR (contingent on the resolution of the intermediate structure) (Sobhy *et al*., 2019). However, if the HJ is not resolved, this will result in synthesis-dependent strand annealing (SDSA) or break-induced replication (BIR) (Elbakry & Löbrich, 2021).

1.9 Platinum compounds

There was an increase in research looking at anticancer chemicals that reacted chemically with DNA in the 1960s and 1970s (Rosenberg *et al*., 1969; Cleare & Hoeschele, 1973). Compounds that modify DNA bases directly, intercalate between bases, or generate DNA crosslinks were among those researched (Cleare & Hoeschele, 1973). Goodman and Gilman discovered that nitrogen mustards cause delayed replication fork advancement and cell death via apoptosis by direct alkylation of DNA located on purine bases (Kahlin *et al*., 2013). The first platinum compound cisplatin was discovered in 1884 but it wasn't until the early 1960s was it discovered that platinum compounds were able to inhibit bacterial cell division and were thus recommended for the treatment of different malignancies (Dasari & Tchounwou, 2014). Platinum compounds have shown outstanding cytotoxicity across different types of cancers with about 50% of all patients undergoing chemotherapy for cancer treated with a platinum based antineoplastic compound (Galanski *et al*., 2004). Despite the widespread use of platinum medicines in cancer treatment regimens, there are a number of associated drawbacks (Brabec & Kasparkova, 2005). For instance, not all cancer types respond to treatment with a single agent consistently, and some cancer forms seem to be innately resistant to treatment with any of the platinum drugs that are now licenced (Hartmann, & Lipp, 2003). Furthermore, populations of cancer cells may develop resistance to platinum compounds over time through a process known as somatic evolution (Marine *et al*., 2020). Additionally, the use of platinum drugs is accompanied with a number of adverse effects, ranging in severity from modest to dose-limiting in toxicity (Kelland, 2007). Numerous platinum complexes have been created and examined for anticancer activity in an effort to get around these issues (Desoize & Madoulet, 2002). The development of target compounds that differ greatly from those recommended by the conventional structure-activity relationships established in the 1970s has been one tactic employed by chemists to improve platinum drugs (Lovejoy & Lippard, 2009). The approved platinum-based compounds used in chemotherapy are cisplatin, oxaliplatin, nedaplatin and carboplatin. However, this study focuses on cisplatin and oxaliplatin

1.9.1 Cisplatin

Cisplatin (cis-diaminedichloroplatinum [II]) is a platinum-based antitumor drug that is used for the treatment of different types of cancer which includes cervical cancer, sarcoma, carcinoma, bladder and testicular cancer (Kartalou & Essigmann, 2001). Michele Peyrone initially created

the compound cis-[Pt(NH3)2Cl2] in 1845, and it was termed Peyrone's salt for a long time (Arnesano & Natile, 2009). Alfred Werner correctly identified the structure of Peyrone's salt in 1893 (Ghosh, 2019). However, Barnett Rosenberg, a biophysicist established the capacity of cisplatin to suppress sarcoma 180 and leukaemia L1210 in mice in 1969 and it was demonstrated to be effective against a wide range of animal tumour systems in later experiments (Makovec, 2019). Finally, the National Cancer Institute began trial 1 in 1971, and the US Food and Drug Administration authorised the use of cisplatin for testicular and ovarian cancer in 1978 (Ciarimboli, 2021). The United Kingdom approved it a year later, in 1979 (Wiltshaw, 1979).

The cisplatin molecule is made up of a central platinum ion with two chlorine ligands and two amine ligands attached to it (Rohdenburg *et al*., 2019).

$$\text{Cl}_{\text{,,,}}\text{Pt}^{\text{,,,}}\text{NH}_3$$
$$\text{Cl}\quad\text{NH}_3$$
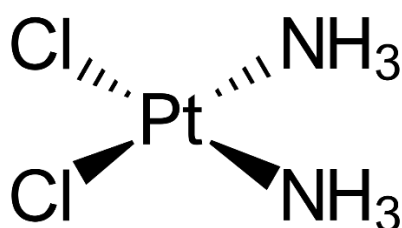
Figure 1.12- Structure of cisplatin

1.9.2 Mechanism of action of cisplatin

Cisplatin carries out its function by disrupting DNA replication and it does this by forming covalent bonds with DNA during S-phase which prevents DNA replication (Ahmad, 2017). This involves a process called aquation where the chloride ion on the cisplatin molecule is replaced by water which results in cis-[PtCl(NH$_3$)$_2$(H$_2$O)]$^+$ (Dasari & Tchounwou, 2014). This process is possible due to the low concentration of chloride ion in the cell (Johnstone *et al*., 2006). The water molecule in the new cisplatin complex can therefore be displaced by one of the DNA bases when it interacts with DNA, forming covalent bonds with the DNA which leads to cell cycle arrest, thus preventing the cell from leaving the S/G2 phase (Fuertes *et al*., 2003). Cell cycle arrest triggers DNA repair process activation which in turn triggers the activation of apoptosis when DNA repair is not successful (Fuertes *et al*., 2002). Crosslinking of DNA by cisplatin occurs through different mechanisms with the most common one being disrupting cell division during mitosis (Ghosh, 2019). In this process, once cisplatin is activated in the cytoplasm of the cell, it then binds to an open nitrogen atom on the DNA molecule, preferably on a guanine base and then binds to another guanine base resulting in

DNA crosslink (Florea & Büsselberg, 2011). If both guanine bases cisplatin bound to are on the same strand, then this is known as intrastrand crosslink, however if the guanine bases are on different strands, then this is known as interstrand crosslink (Ghosh, 2019). The most common crosslinks produced in DNA by cisplatin are the 1,2-Pt-d(GpG) intrastrand crosslinks which makes up about 70% of all cisplatin induced crosslinks (Gentilin *et al*, 2019). Other crosslinks include 1,3-Pt-d(GpXpG) and 1,2 -Pt-d(ApG) interstrand crosslinks (Rycenga & Long, 2018). These crosslinks can result in unwinding of the DNA, inhibition of transcription and replication, bending of the DNA all of which can in turn result in DNA strand breaks (Siddik, 2003). Although DNA is considered to be a key target for cisplatin, only 5-10% of the intracellular concentration of cisplatin is detected in the DNA fraction, while the remaining 75-85% interacts with nucleophilic sites of intracellular elements such as thiol-containing peptides, proteins, replication enzymes, and RNA (Timerbaev *et al*., 2006). Cisplatin resistance, as well as its severe toxicity, can be attributed to this preferential binding to non-DNA targets (Gómez-Ruiz *et al*., 2012).

1.9.3 Oxaliplatin

Oxaliplatin oxalatoplatinum(II) (*trans-R,R*)-cyclohexane-1,2-diamine also known as Eloxatin is a third generation platinum-based chemotherapy drug commonly used in the treatment of CRC and is frequently used in combination with other drugs such as fluoracil and folinic acid in advanced stages of CRC (Raymond *et al*.,2002). Professor Yoshinori Kidani of Nagoya City University discovered oxaliplatin in 1976, when the need for development of a new platinum-based drug arose due to some of the limitations of cisplatin (Culy *et al*., 2000). Cisplatin was known to be significantly toxic; cells were seen to have acquired resistance against it after treatment and it was also not effective in the treatment of CRC which is one of the most prevalent cancers in the world (Huerta *et al*., 2003). Oxaliplatin is considered to have the least toxicity among the platinum compounds (cisplatin and carboplatin) (Levi *et al*., 2000).

1.9.4 Structure of oxaliplatin

Oxaliplatin is made up of a platinum ion at its core and compared to cisplatin, the two amine groups have been replaced with a bidentate 1,2-diaminocyclohexane carrier ligand, while the two chlorine ligands have been substituted with an oxalate group (Figure 1.13) (Apps *et al*., 2015). This oxalate group is also called a "leaving group" as the activation of oxaliplatin

involves the displacement of the oxalate group which enhances the solubility of the drug (Mehmood *et al*., 2014). Kidani *et al* showed that there are three isomeric forms the DACH–Pt complex of oxaliplatin can occur and the most effective isomer against cisplatin resistant/sensitive cell lines was the trans-1(R,R) isomer (Kidani *et al*, 1978). The chemical properties of oxaliplatin plays a key role in its biotransformation as the chemically inert DACH ligand is not displaced upon activation, while the oxalate group upon hydrolysis serves as a carrier which enhances the solubility of the molecule in water (Kweekel *et al*., 2005). These features of oxaliplatin explains why majority of the biotransformation products of oxaliplatin have a Pt(DACH) core.
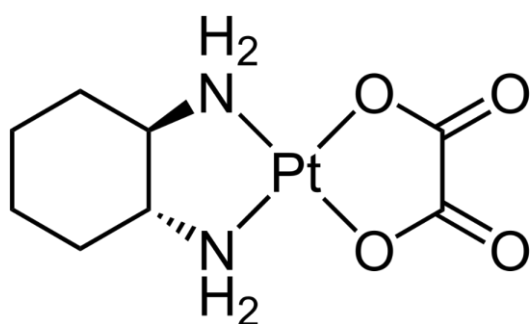
Figure 1.13 - Structure of oxaliplatin

1.9.5 Mechanism of action

Oxaliplatin exercises its activity by exchange reaction with nucleophile species such as water, chloride, glutathione and methionine that it comes in contact with within biological fluids (Misset *et al*., 2000). Oxaliplatin undergoes a non-enzymatic transformation into reactive compounds by the displacement of the oxalate group (Mehmood *et al*., 2014). Oxaliplatin has several biotransformation products (Figure 1.15), however the products that have been shown to play a key role in its mechanism of action are the products formed when the displaced oxalate group is replaced with chloride ions and then aquated (Ahmad, 2017). The hydrolysis of the molecule is known to take place intracellularly at physiological concentrations of bicarbonate ion (HCO3-) and dihydrogen phosphate (H_2PO_4) (Dasari *et al*, 2022). This reaction is considered to be the major pathway by which oxaliplatin is activated (Gao *et al*., 2003). Oxaliplatin has been shown to carry out its cytotoxicity through DNA damage, however cell death caused by oxaliplatin can be credited to different factors such as DNA and RNA synthesis inhibition, DNA lesions and activation of immunological reactions (Alcindor & Beauger, 2011).
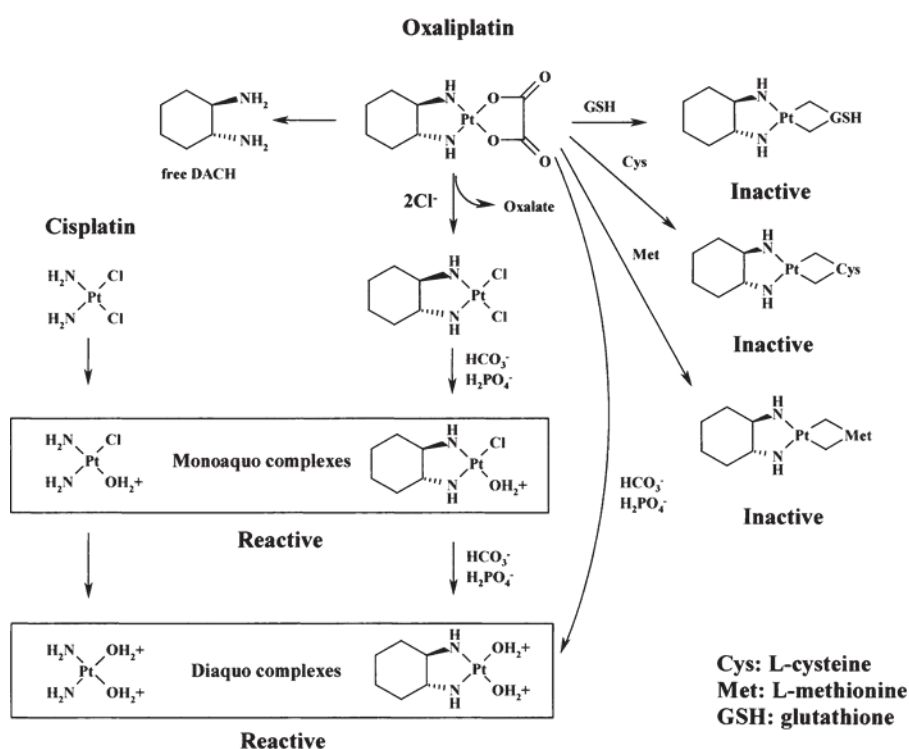
Figure 1.14 – **Overview of the mechanism of action of oxaliplatin and cisplatin**
The major metabolites produced by these platinum compounds are highlighted above, the active metabolites are the products formed when the chloride ions are aquated. The biotransformation of cisplatin and oxaliplatin both produce monoaquo complexes which undergo hydrolysis in the presence of bicarbonate ion (HCO3-) and dihydrogen phosphate (H₂PO₄).

DNA Lesions -The dichloro Pt(DACH) compound generated from the biotransformation of oxaliplatin in the plasma proceeds to the nucleus of the cell where the first chloride is replaced with a water molecule producing a monoaquochloro compound, which has a high affinity for GC rich sites, thus binding with the N7 of Guanine of DNA to produce a monoadduct (Spingler *et al*., 2001). The second chloride is also replaced with a water molecule which produces a diaquo compound (Figure 1.15) which also binds to Guanine or Adenosine forming a diadduct which completes the process of platination (Mezencev, 2014). There are three types of crosslinks that can be produced by oxaliplatin (Woynarowski *et al*., 2000).

1) DNA intrastrand crosslinks- This is the primary pathway by which DNA lesions/platination is induced, this involves the binding of the Pt(DACH) to two adjacent guanine bases or occasionally guanine and adenine bases on the same strand (Andrezálová & Országhová, 2021).

2) DNA interstrand crosslinks- Interstrand crosslinks occurs in oxaliplatin treatment, this only however accounts for a small percentage of the total adducts produced, this process occurs when a covalent bond is formed between the activated oxaliplatin molecule and the guanine bases on opposite strands of a DNA molecule (Faivre *et al*., 2003).

3) DNA protein crosslink- When an activated oxaliplatin molecule produces a crosslink (covalent bond) between DNA and a protein molecule, this is called a DNA protein crosslink (Stingele *et al*., 2017).

Monoadducts lack cytotoxic properties and unless nucleotide excision repair has happened, lethal DNA biadducts impede both DNA replication and transcription, triggering apoptosis after cell cycle arrest (Gentilin *et al*., 2019). With cisplatin, the formation of these DNA adducts is larger and faster compared to oxaliplatin (DiFrancessco *et al*.,2002). The therapeutic actions of oxaliplatin certainly do not rely solely on the platinum moiety's alkylating–intercalating activities (Alcindor & Beauger, 2011).

DNA and RNA synthesis inhibition-Experiments exploring the process of synergism between oxaliplatin and 5-fluorouracil (5-FU) have revealed that oxaliplatin possess a direct inhibitory impact on thymidylate synthase, blocking thymidine insertion in nucleic acid synthesis (Fischel *et al*., 2002). The mitotic process is stopped due to its antimetabolite-like action and because oxaliplatin is generally given in combination with 5-FU, which is also a thymidylate synthase inhibitor, it's debatable if this mode of action of oxaliplatin plays a significant role *in vivo* (Todd & Lippard, 2009).

Immunological reactions- In mouse and human cell lines, oxaliplatin has recently been reported to promote immunogenic apoptosis of CRC cells (Zhu *et al*., 2020). Before initiating apoptosis, CRC cells generate multiple immunogenic markers on their surface after being exposed to oxaliplatin (Tesniere *et al*., 2010). These signals cause T cells to produce interferon and engage with dendritic cells' toll like receptor 4 (TLR4), resulting in a kind of tumour vaccination (Apetoh *et al*., 2007). Individuals with a mutant allele of the TLR4 gene that causes loss of function were found to have a reduced advantage from oxaliplatin chemotherapy in the metastatic state, with a statistically significant shorter progression-free and overall survival (Tesniere *et al*., 2010).

1.9.6 Resistance to oxaliplatin

Although oxaliplatin showed increased sensitivity to cancer cells over the course of treatment some cancer cells were shown to develop resistance to oxaliplatin (Martinez-Balibrea *et al*., 2015). Different mechanisms have been hypothesized to be responsible for the resistance of some tumours to oxaliplatin, which includes the uptake of the drug intracellularly (if the uptake is low and the efflux of the drug is high this can result in lower bioavailability of the drug in the cell) (Di *et al*., 2020). Overexpression of certain DNA repair proteins such as ERCC1 can lead to an increase in DNA damage repair level in the cell, increased acceptance of DNA lesion and platinated DNA (Wu *et al*., 2004). Faulty apoptosis response machinery and the build-up of oxaliplatin in the cell can generate side reactions (such as binding to the sulphydryl group of gluthathione) that results in the deactivation and trapping of oxaliplatin which prevents it from carrying out its cytotoxic function (Rottenberg *et al*., 2021).

1.10 Apoptosis

A multicellular organism's cells are part of a tightly knit family and in this family, the number of cells present in a given period is strictly regulated, not only by regulating the rate of cell division but also by regulating the amount of cell death (Alberts *et al*., 2002). Cells that are no longer required start an intracellular death programme and end their lives (Pérez-Figueroa *et al*., 2019). As a result, this process is known as programmed cell death, although it is often referred to as apoptosis (D'arcy, 2019). Apoptosis is a natural process that happens throughout growth and ageing as well as a homeostatic mechanism to keep cell populations in tissues stable (Mahoney & Rosen, 2005). Additionally, apoptosis happens as a protective process, such as in immunological responses or when diseases or toxic chemicals destroy cells (Norbury & Hickson, 2001). Despite the fact that apoptosis can be brought on by a wide range of physiological and pathological stimuli and situations, not every cell will inevitably undergo this process and die (Hengartner, 2000). Apoptosis can occur via a p53-dependent mechanism in some cells as a result of DNA damage brought on by radiation or chemotherapy medications (Green, 2022). While some cells are unaltered or even stimulated, specific hormones, such as corticosteroids, may cause apoptotic death in certain cells (like thymocytes) (Elmore, 2007). The induction, amplification, or inhibition of apoptosis is regulated by a large number of proteins and enzymes (Uzdensky, 2019). The induction of apoptosis typically results in the activation of caspases, which in turn mediates the auto destruction of the cell (Jan & Chaudry, 2019). Procaspases are the inactive precursors of caspases that are routinely cleaved to produce the active version (Wong, 2011). Cellular breakdown occurs due to the cleavage of several

intracellular and cytoplasmic membrane components by activated caspases (Santagostino *et al*., 2021). In mammalian cells, there are two main mechanisms of apoptosis: an extrinsic pathway that is started by death receptors and an intrinsic pathway that operates via the mitochondria (Figure 1.15) (Zaman *et al*., 2014). The proper external factors must attach to death receptors on the cell surface for the extrinsic pathway to function (Lowe & Lin, 2000). The intrinsic pathway, in contrast, triggers apoptotic signalling by releasing mitochondrial enzymes in response to signals that originate from inside the cell, such as damage brought on by radiation and different chemotherapeutic drugs (Sayers, 2011).

1.10.1 Intrinsic pathway of apoptosis

A variety of non-receptor-mediated stimuli are involved in the intrinsic signalling pathways that induce apoptosis (Elmore, 2007). These processes are mitochondrial-initiated and result in intracellular signals that operate directly on targets inside the cell (Jan & Chaudry, 2019). In the mitochondria, a plethora of cytotoxic stimuli and proapoptotic signal-transducing molecules congregate to cause permeabilization of the outer mitochondrial membrane (Joza *et al*., 2001). The Bcl-2 family of proteins are mitochondrial proteins that control the flux of bioenergetic metabolites while elements of the permeability transition pore also control the permeabilization of the membrane (Green & Kroemer, 2004). The proapoptotic multi-domain proteins of the Bcl-2 family have the ability to generate pores in the mitochondrial outer membrane, where this can lead to the initiation of mitochondrial outer membrane permeabilization (MOMP) (Tait & Green 2010). Some of these proteins, like Bax and Bak, possess multiple Bcl-2 homology regions and a transmembrane domain, which enable their integral or inducible incorporation into the outer membrane (Galluzzi *et al*., 2020). Numerous members of the same protein family influence how Bak and Bax execute MOMP (Peña-Blanco *et al*., 2018). Specifically, antiapoptotic proteins like Bcl-2, Bcl-xL, and Mcl-1 prevent MOMP by attaching to Bak and Bax and keeping them in a conformation that prevents them from becoming active (Youle & Strasser, 2008). The BH3-only proteins such as Bad, Puma and Noxa, which are small members of the Bcl-2 family and frequently only possess the BH3 domain, on the other hand, can encourage the pore-forming activity of Bak and Bax by a number of distinct means (Uren *et al*, 2017). Therefore, BH3-only proteins can either actively compete with Bax, Bak1, or other BH3-only proteins to remove them from inhibitory connections with Bcl-2, Bcl-xL, and Mcl-1 or directly induce the conformational activation of Bax and Bak1 in this manner (Jeng *et al*., 2018). The transcriptional level and swift post-

translational alterations (such as phosphorylation and proteolytic processing) can both affect BH3-only proteins, making them effective sensors of intracellular stress that have a direct impact on the modulation of intrinsic apoptosis (Galuzzi *et al*., 2020). The permeabilization of the outer mitochondrial membrane by proapoptotic Bcl-2 family members and caspase activation are closely related processes (Green & Kroemer, 2004).
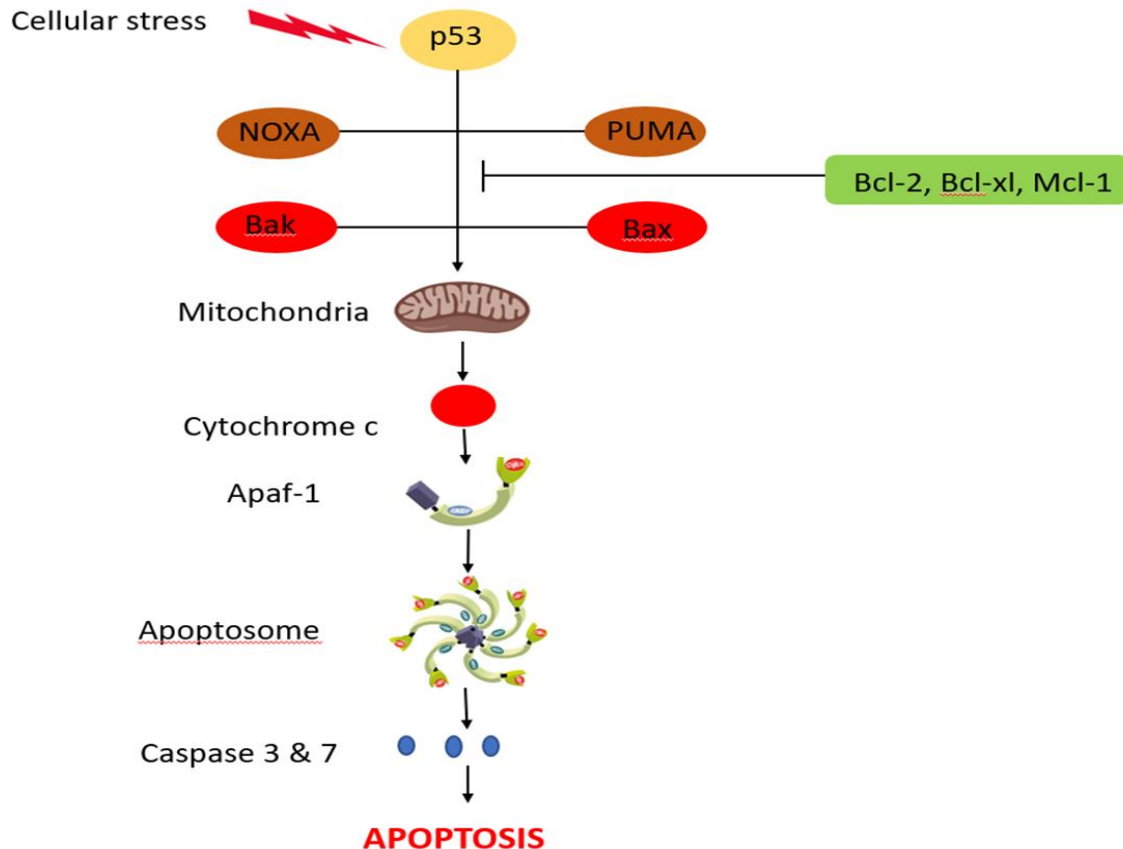
Figure 1.15- **Elements of the intrinsic pathway of apoptosis**.
In the intrinsic pathway, the tumour suppressor protein p53 is crucial in triggering apoptosis by transcriptionally activating the proapoptotic proteins. Cytoplasmic proteins BAX and BID bind to the outer membrane of mitochondria as a result of the stress signal. Cytochrome c is released due to the permeabilization of the outer mitochondrial membrane. This attaches to Apaf-1, which subsequently forms an apoptosome and causes procaspase-9 to become activated. The caspase cascade that results in apoptosis is initiated by activated caspase-9.

A group of proteins typically located in the area between the inner and outside mitochondrial membranes are released upon breakdown of the outer mitochondrial membrane, including cytochrome c (Saelens *et al*., 2004). The development of the cytochrome c/Apaf-1/caspase-9- apoptosome complex, which is immediately triggered by the release of cytochrome c from the mitochondria, activates caspase-3 (Cain *et al*., 2000). Cytochrome c enters the cytosol and

attaches to the C-terminal domain of Apaf-1, a cytosolic protein with an N-terminal caspase activation and recruitment domain (CARD) (Wolf *et al*., 2022). The interaction of dATP with Apaf-1 and the exposure of its N-terminal CARD, which may now oligomerize and serve as a platform for the recruitment and activation of the initiator caspase-9 through a CARD-CARD interaction (Shakeri *et al*., 2017). Following that, the resident caspase-9 of the apoptosome recruits the executioner caspase-3 and activates it (Bratton *et al*., 2001).

1.10.2 Spindle assembly checkpoint

The cells' protection against early anaphase is the spindle assembly checkpoint (SAC). It's a vetting process that prevents the cell from initiating anaphase until all of the chromosomes are connected to the spindle and aligned at the metaphase plate (Koyuncu *et al*., 2021). Although the name "spindle assembly checkpoint" is widely used, it is a misnomer because the SAC checks the appropriate adhesion of the microtubule to the kinetochore instead of regulating spindle assembly (Mussachio & Salmon, 2007). The SAC is turned on in the presence of unattached kinetochores, inhibiting anaphase (Manic *et al*., 2017). When all kinetochores are securely linked to microtubules, the SAC is fulfilled, hence allowing the microtubules to pull the sister chromatids away from each other and towards the spindle pole (anaphase), resulting in the progression of the cell cycle (Nezi & Mussachio, 2009).
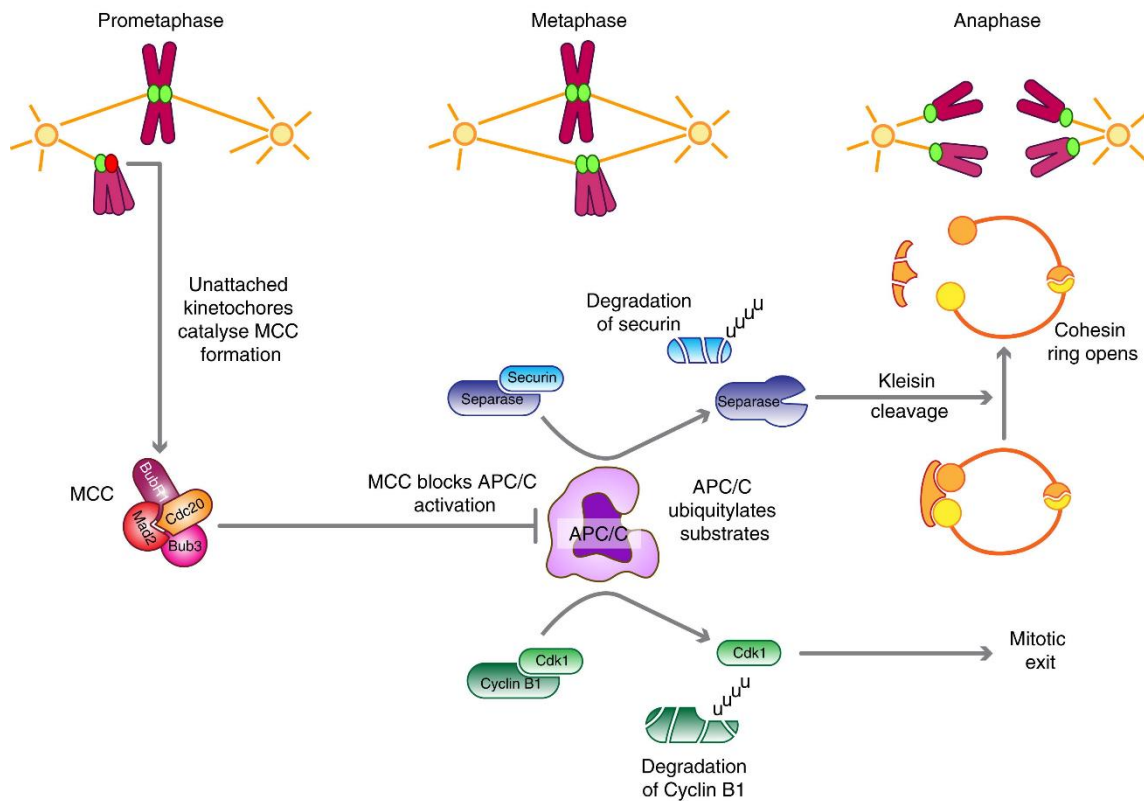
Figure 1.16 - **Principle of the spindle assembly checkpoint** (Adapted from Lara- Gonzalez *et al*., 2012). The development of the mitotic checkpoint complex (MCC), which inhibits the APC/C, is catalysed by unattached kinetochores during the early stages of mitosis. The creation of the MCC stops after all the chromosomes are lined up and their kinetochores are linked to the spindle, causing Cdc20 to activate the APC/C and induce the ubiquitylation and breakdown of securin and cyclin B1. Sister chromatids can divide as a result of the release of separase, which breaks the Scc1 kleisin subunit of the cohesin ring structure (anaphase). Cdk1 is rendered inactive by the breakdown of cyclin B1, which causes mitotic exit.

Due to the existence of unattached kinetochores at the start of mitosis (prometaphase), the mitotic checkpoint complex (MCC), which comprises of BubR1, Bub3, Mad2, and Cdc20, is created (Sudakin *et al*., 2001). This complex then proceeds to inhibit the anaphase-promoting complex/cyclosome (APC/C), an E3 ubiquitin ligase that degrades a number of proteins, including mitotic cyclins, via proteolysis (Matson & Stukenberg, 2011). The formation of the SAC ends after all of the chromosomes are aligned with their kinetochores connected to the spindle (metaphase), allowing Cdc20 to activate the APC/C, resulting in the ubiquitination and breakdown of securin and cyclin B1 (Zhou *et al*., 2002). Securin degradation releases separase,

which then cleaves the cohesin ring structure at the Scc1 kleisin subunit, allowing the sister chromatids to separate (anaphase) (Nasmyth & Hearing 2009).

By polyubiquitinating the two critical substrates, cyclin B and securin, this ubiquitin ligase induces mitotic exit and facilitates their rapid destruction by the 26S proteasome (Lara-Gonzalez *et al*., 2012). The MCC stabilises these substrates by inhibiting the APC/C, thereby effectively limiting mitotic escape. Some cells, however, depart mitosis without dividing, a condition known as mitotic slippage (Uzunova *et al* 2012).

1.10.3 Mitotic slippage

Despite their effectiveness, anti-mitotic medications have moderate to severe adverse effects, making their long-term usage in the clinic challenging (Gomber *et al*., 2010). Additionally, regular use of anti-mitotic drugs results in the development of chemotherapeutic drug resistance in malignant tumours, which causes relapse (Chan *et al*., 2012). Cancer cells frequently develop various resistance mechanisms that allow them to circumvent mitotic arrest and exit mitosis early without dividing, this process is known as mitotic slippage (Burgess *et al*., 2014). Mitotic slippage is a different path that cells can take after a SAC-enforced mitotic arrest in addition to mitotic cell death (Sinha *et al*., 2019). Cells may prematurely leave mitosis as a result of the SAC's attenuation, which causes cyclin B1 to slowly degrade over the course of a prolonged mitotic arrest (Brito & Rieder 2006). Tetraploid multinucleated cells result when cells "slip" from mitosis and enter interphase without passing through the necessary chromosomal segregation and cytokinesis (Musacchio et al., 2015). Cells then have three options: (i) continue proliferating as genomically unstable cells; (ii) die after slippage; or (iii) remain in the G1 cell cycle phase (Brito & Rieder, 2006). The tendency of a cell to either die in mitosis or experience mitotic slippage after SAC activation and mitotic arrest is best explained by the "competing networks-threshold" concept (Gaiscoigne & Taylor, 2009). According to this hypothesis, two distinct network pro-apoptotic caspase activation and cyclin B1 degradation determine a cell's fate after mitotic arrest (Gascoigne & Taylor, 2008). Each network has a threshold, and the fate of a cell depends on which threshold is crossed first. Mitotic slippage happens when cyclin B1 levels drop below the threshold for mitotic departure before caspase activation. On the other hand, mitotic cell death happens if caspase activation takes place before cyclin B1 is adequately broken down and the apoptosis threshold is crossed (Cheng & Crasta, 2017).

1.10.4 Anti-cancer drugs and apoptosis

The mode of action of most anti-cancer drugs is by the induction of apoptosis through the intrinsic pathway (van Vuuren *et al*., 2015). The Bcl-2 family controls the intrinsic pathway of apoptosis, therefore development of small molecule inhibitors (SMI) of the Bcl-2 family will be helpful in cancer treatment either in combination with other chemotherapeutic drugs or as a single treatment (Soderquist & Eastman, 2016).

The ability of cells to escape apoptosis after treatment is a hallmark of cancer and is one of the major sources by which cells become resistance to chemotherapy (Sinha *et al*., 2019). Upregulation of the anti-apoptotic Bcl-2 family proteins in cancer cells has been shown to promote resistance to chemotherapy and progression of certain cancers (Basu, 2022). Bcl-xL and Mcl-1, two members of the Bcl 2 family have been shown in a recent study to undergo regular somatic amplification in different cancers such as melanoma, and survival of these cancer cells is determined by the expression of Bcl-xL and Mcl-1 (Um, 2016). This indicates that Mcl-1 and Bcl-xL are important targets in the development of chemotherapeutic drugs (Reroukhim *et al*., 2010).

Different SMI of the Bcl-2 family have been discovered to date, ABT-737 was developed in 2005 by Abbott laboratories (Oltersdolf *et al*., 2005) as an inhibitor of Bclxl, Bcl-w and Bcl-2, this led to the development of ABT-263 (navitoclax) an analog which had better oral bioavailability (Chen *et al*., 2011). Navitoclax was effective in clinical trials, but it showed dose limiting toxicity such as thrombocytopenia (Kaefar *et al*., 2014). To solve this problem, a selective inhibitor of Bcl-2, ABT-199 (venetoclax) was developed (Souers *et al*., 2013). WEHI 539 is a SMI that inhibits Bcl-xL selectively and it was developed by disrupting the interaction between BIM and Bcl-xL, it was the first SMI to inhibit Bcl-xL at nM concentrations (Montero & Letai, 2017).

Maritoclax is a specific Mcl-1 inhibitor that binds to and targets Mcl-1 for proteasomal mediated degradation, it is also able to disturb the interaction between Mcl-1 and Bim (Doi *et al*., 2012). Muristerone A is not an SMI however, it is a small molecule that upregulates Bcl-xL by stimulating Bcl-xL mRNA transcription (Abcam, UK). These compounds were selected for this experiment as they were an ideal way to determine the effects of inhibiting or upregulating members of the Bcl-2 family.

Tert-butyl hydroperoxide (TBH), an organic peroxide utilised in a variety of oxidation processes, it is a popular substitute for H_2O_2 as a reactive oxygen species used to induce

oxidative stress. Olaparib is an inhibitor of poly(ADP-ribose) polymerase enzymes in humans (PARP-1, PARP-2, and PARP-3) (Deeks, 2015).
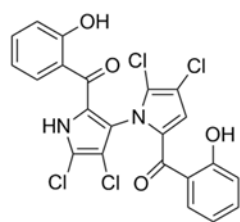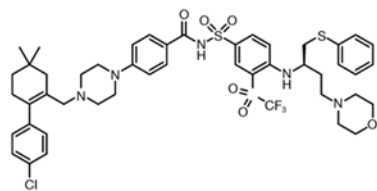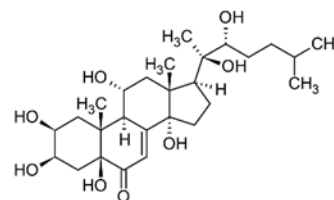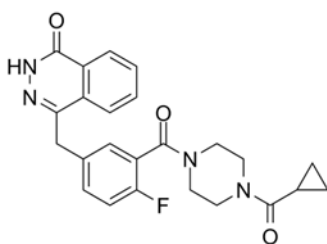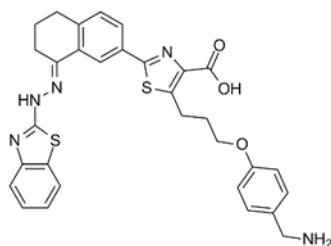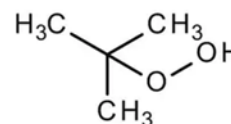
Figure 1.17- Structure of Bcl-2 family modulators, olaparib and *tert*-butyl hydroperoxide

Aims and Objectives

CRC and medulloblastoma are two of the most common cancers in the UK, and while treatment has progressively improved over the past years, however this success has been marred by drug resistance and severe side effects. The capacity of cancer cells to evade apoptosis following treatment is a hallmark of the disease and one of the primary mechanisms through which cells develop resistance to chemotherapy. Therefore, there is a pressing need for new treatments to help sensitize cancer cells to chemotherapy which would result in drug dosage reduction, fewer side effects, as well as eliminating drug resistance and in essence patient relapse. To address this, this research project was split into two parts with the same goal of sensitizing cancer cells to chemotherapy but focusing on different targets which are:

1) To sensitize medulloblastoma cells to vincristine treatment by inhibiting the expression of Bcl-2 family proteins.

2) To sensitize medulloblastoma and CRC cells to genotoxic agents by inhibiting the expression of lncRNA HCP5.

PROJECT 1- Most genotoxic anti-cancer drugs work by inducing cell death through the intrinsic apoptotic pathway. The Bcl-2 family proteins are known to regulate the intrinsic pathway, therefore, small molecule inhibitors (SMI) of the Bcl-2 family may be one way to improve treatment outcome in combination with other toxic chemotherapeutic agents (Soderquist & Eastman, 2016). Increased expression of anti-apoptotic Bcl-2 family proteins in cancer cells has been reported to promote chemotherapy resistance and cancer development (Basu, 2022). Bcl-xL and Mcl-1, two members of the Bcl-2 family have been demonstrated to exhibit frequent somatic amplification in many malignancies, including melanoma. The expression of Bcl-xL and Mcl-1 is critical for cancer cells survival suggesting that Mcl-1 and Bcl-xL are key targets for chemotherapeutic drug development (Reroukhim *et al.*, 2010). The aims of this project are as follows:

1) To determine the effect of Bcl-2 family protein expression levels on cell fate in response to vincristine treatment.

- Confirm the heterogeneity that exists between subgroups and subtypes of medulloblastoma in response to vincristine treatment.

- Quantify Bcl-2 family protein expression level in three medulloblastoma cell lines.
- Determine the cell viability of medulloblastoma cell lines after vincristine treatments alone or in combination with Bcl-2 inhibitors.

2) To identify the fate of medulloblastoma cells evading vincristine treatments and to study their response to a second vincristine treatment.

- Grow vincristine treated cells in culture to determine the fate of the cells after evading treatment.
- Determine if these cells acquire resistance to vincristine.

PROJECT 2- The role of HCP5 in cancer has been studied extensively (Qin *et al*., 2021; Zou & Chen, 2021). HCP5 is abnormally expressed in numerous cancer types, according to data from the Cancer Genome Atlas (TCGA). Furthermore, in several malignancies, HCP5 dysregulation is linked to cell proliferation, migration, invasion, cell death, lymphatic metastasis, and resistance to treatment (Zhang & Wang, 2021). As a result, HCP5 could be exploited as a biomarker and a therapeutic target in human cancer. Therefore, the objective of this project is to understand the effect HCP5 expression has on chemotherapy response. In addition, to investigate the effect of HCP5 knockdown on cell sensitivity to genotoxic agents. The aims of this project are as follows:

1) To determine the effect of HCP5 expression levels on cell response to cisplatin, oxaliplatin and TBH

- Quantify HCP5 expression levels in the medulloblastoma and CRC cell lines.
- Identify any correlation between HCP5 expression levels and response to cisplatin, oxaliplatin and TBH.
- Determine cell viability after HCP5 knockdown in combination with cisplatin, oxaliplatin and TBH treatment.

2) To investigate the interaction between HCP5, YB-1 and the DNA glycosylases.

- Quantify the expression of DNA glycosylases in medulloblastoma and CRC cell lines.
- Identify the effect of HCP5 knockdown on DNA glycosylase expression. Confirm the connection between HCP5 and YB-1.

CHAPTER 2: MATERIALS AND METHODS

2.1 Cell culture

2.1.1 Cell lines

The cell lines used in these studies were derived from either human medulloblastoma (ONS 76, HDMB03 and DAOY) or CRC (SW480, SW48, HCT116, HT29, LOVO). All cell lines were purchased from American Type Culture Collection (Virginia, USA) asides from HDMB03 which was purchased from the Leibniz Institute DSMZ (Braunschweig, Germany). Mycoplasma testing was carried out routinely every three months on all cell lines to check for possible contamination. Short tandem repeat (STR) profiling was not carried out on any of the cell lines used in both studies.

ONS76 - The cell line ONS 76 (Osaka Neurological Surgery 76) was derived from the large cerebral tumour of a two-year old girl. They are adherent human medulloblastoma cell line and belong to the sonic hedgehog subgroup and exhibit wild type TP53 (Yamada *et al*., 1989).

DAOY - The DAOY cell line was derived from a tumour excised from the posterior fossa of a four-year-old boy (Jacobsen *et al*., 1985), it is an adherent cell line which belongs to the sonic hedgehog subgroup and possess mutant TP53 (Ivanov *et al* 2016).

HDMB03- HDMBO3 cell line was derived from a tumour of a three-year-old boy with metastasized group 3 medulloblastoma (Milde *et al*., 2012). The medulloblastoma was present in the midline (fourth ventricle and vermis), and magnetic resonance imaging revealed spinal metastases. This cell line is semi adherent i.e.part of the population is adherent while the rest grows in suspension.

HT29 - HT29 was derived from the primary tumour, of a 44-year-old Caucasian woman with colorectal adenocarcinoma (Fogh *et al*., 1977), they are adherent cells which proliferate as a nonpolarized, undifferentiated monolayer in typical cell culture conditions. The HT29 cells are microsatellite stable and positive for CpG island methylator phenotype and chromosomal (Ahmed *et al*., 2013). They have wild type KRAS and PTEN, a V600E mutation wherein glutamic acid (E) replaces valine (V) at amino acid 600 of the BRAF protein (Roma *et al*., 2016), a P449T mutation where proline is substituted for threonine at amino acid 449 of the P13KCA protein (Hao *et al*., 2016) and a hotspot R273H mutation where arginine is substituted for histidine on amino acid 273 of p53 (Tan *et al*., 2015).

SW48 - The SW48 cell line was derived from 82-year-old male with Duke's type C, grade IV, colorectal adenocarcinoma (Leibovitz *et al*., 1976). SW48 is positive for CpG island methylator phenotype and negative for chromosomal instability. It has wild type phenotype for KRAS, BRAF, P13KCA, PTEN and p53 (Ahmed *et al*., 2013)

LOVO - LOVO cell line was derived from a metastatic tumour site of the left supraclavicular region of a 56-year-old male CRC patient with adenocarcinoma of the colon. They were isolated in 1971 and are adherent cells with epithelial morphology (Drewinko *et al*., 1976). They possess micro satellite instability, are negative for CpG island methylator phenotype (CIMP) and for chromosomal instability. LOVO cells have wild type phenotype for BRAF, P13KCA, PTEN and p53 (Ahmed *et al*., 2013) but has both a G13D mutation where glycine (G) is substituted for aspartic acid (D) at amino acid 13 and a A14V mutation where alanine (A) is substituted with valine (V) at amino acid 14 on the KRAS protein (Inaguma *et al*., 2017).

SW480 – SW480 was established from the primary adenocarcinoma of a 50-year-old male. The cells are adherent and have an epithelial morphology (Leibovitz *et al*., 1976). They are microsatellite stable, but are positive for chromosomal instability, and they have wild type BRAF, PTEN and PIK3CA. They are negative for CpG island methylator phenotype (CIMP) and have G12V mutation on codon 12 of KRAS (Ahmed *et al*., 2013).

HCT116 – HCT116 is a human colon carcinoma cell line; established from the primary colon carcinoma of an adult male. The cells are adherent and have an epithelial morphology. They possess micro satellite instability, are positive for CpG island methylator phenotype (CIMP) and negative for chromosomal instability. They have wild type BRAF (Roma *et al*., 2016), PTEN and p53 but have a H1047R hotspot mutation in the kinase domain of the PIK3CA protein and glycine (G) to aspartic Acid (D) mutation at amino acid residue 13 (G13D) of KRAS (Ahmed *et al*., 2013)

Table 2.1- Classification of cell lines based on morphology, subtype, source and site.

Cell line	Source	Subtype	Site	Morphology	Disease
ONS76	Primary Tumour	Sonic hedgehog (SHH)	Neural/Brain	Epithelial	Medulloblastoma
DAOY	Primary Tumour	Sonic hedgehog (SHH)	Cerebellum/Brain	Polygonal	Desmoplastic Cerebellar Medulloblastoma
HCT116	Primary Tumour	CMS1	Large intestine/Colon	Epithelial	Carcinoma Colorectal
HT29	Primary Tumour		Colon	Epithelial	Adenocarcinoma; Colorectal
LOVO	Metastasis	CMS1	Large intestine/Colon	Epithelial	Adenocarcinoma; Colorectal; Dukes' type C, grade IV
MB03	Metastasis	Group 3	Cerebellum	Epithelioid	Medulloblastoma
SW48	Primary Tumour	CMS1	Large intestine/Colon	Epithelial	Adenocarcinoma; Colorectal; Dukes' type C, grade IV
SW480	Primary Tumour		Large intestine/Colon	Epithelial	Adenocarcinoma; Colorectal; Dukes' type B

2.1.2 Growing and maintaining the cells.

Human medulloblastoma ONS76, DAOY and human colon cancer LOVO cell lines were grown in Roswell park memorial institute (RPMI) 1640 culture medium (Biosera, USA) in a T-75 flask, the culture medium was supplemented with 10% (v/v) foetal bovine serum FBS (Thermo Fisher scientific, UK), 1% (v/v) penicillin/streptomycin (Biosera, USA) and 2 mM L-glutamine. The HDM03 cell line was grown under the same conditions but was supplemented with 1% non-essential amino acids (Thermo Fisher scientific, UK). HT29 and HCT116 cells

were grown in McCoy's 5A medium (Biosera, USA), while SW48 and SW480 cells were grown in high glucose Dulbecco's Modified Eagle's Medium (DMEM) (Biosera, USA) with 10% (v/v) FBS (SW480) or 20% (v/v) FBS (SW48) and 1% (v/v) penicillin/streptomycin. All cell lines were maintained at 37ºC in a humidified incubator with 5% CO_2.

2.1.3 Routine sub-culture of cells

The cells were cultured in their respective growth medium and the medium was changed every 2 days to ensure the cells were provided with the adequate nutrients to grow. The cells were split when confluency was close to 90% and splitting was carried out by removing the culture medium from the flask and washing the cells twice with 5 ml of phosphate buffered saline (PBS). The cells were then trypsinized to detach the cells from the flask by adding 2.5 ml of trypsin (Thermo Fisher scientific, UK) to the flask and incubating it for 3 min at 37ºC and 5% CO_2 in a humidified incubator. Following agitation, detachment of cells was confirmed using a microscope and 5 ml of appropriate medium was added to the flask to deactivate the trypsin. The cells were transferred to a 15 ml Falcon tube and pelleted by centrifugation at 1200 rpm for 5 min.

For the HT29, SW480 and HCT116 cell lines, following trypsinisation and addition of 5 ml of culture medium, the cells were replated without centrifugation, as this prevented the cells growing in clumps. Instead, these cells were harvested and suspended in 10 ml of medium and 1 ml of this suspension was placed in a new T75 flask containing 10 ml of medium to obtain the subsequent passage.

2.1.4 Cell counting

To ascertain that the right number of cells was used for every experiment, the cells were counted using a haemocytometer (Figure 2.1). After every passage, 30 μl of cell suspension was mixed with an equal volume of 0.4% (v/v) trypan blue solution and 10 μl of the mixture loaded into the haemocytometer and viewed under a light microscope using the 10X objective. Dead cells were distinguished by the uptake of the dye, thus resulting in a distinctive blue colour, while the clear, viable cells in the four squares of the haemocytometer were counted. Cells on the inner side of each square were ignored and cells on the outer sides of each square were considered. The cell count from each square was determined and the average cell count was calculated.
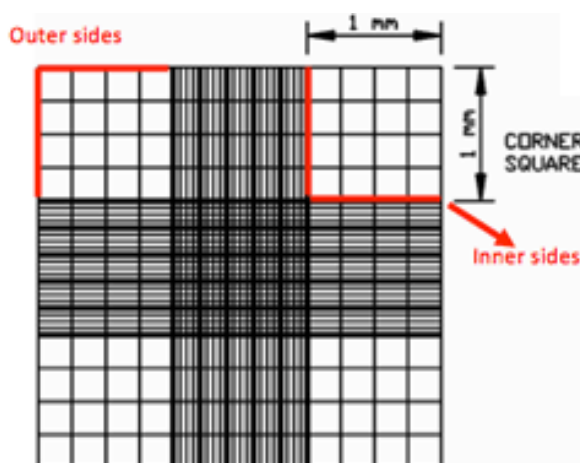
Figure 2.1 – Haemocytometer chamber showing the different quadrants used in cell counting.

This number was multiplied by the dilution factor (which was 2 in this case, as the cell suspension was diluted with trypan blue) and then divided by the volume (ml) of a single square which is 0.0001 ml.

Cell density = <u>Average of viable cells per square x dilution factor</u>
                        Volume of a single square (mL)

2.1.5 Chemical agents

Oxaliplatin, cisplatin, vincristine and TBH were purchased from Sigma Aldrich, WEHI- 539, navitoclax and maritoclax were purchased from APExBIO, USA, olaparib (Adooq, USA) and muristerone, (Abcam UK). Oxaliplatin was dissolved in 5% (w/v) glucose solution, cisplatin was dissolved in 0.9% (w/v) saline solution and olaparib, WEHI-539, navitoclax, maritoclax, muristerone and vincristine were dissolved in dimethyl sulfoxide (DMSO). Each drug was reconstituted and diluted to a working solution of 10 mM. Subsequent concentrations of each compound were achieved by dilution of the stock solution with cell culture medium. All chemicals were used at a starting concentration of 100 µM.

2.2 MTT assay

The 3-[4,5-dimethylthiazol-2-yl]-2,5 diphenyl tetrazolium bromide (MTT) assay was carried out to determine changes in cell growth in response to anti-cancer agents; oxaliplatin, cisplatin, TBH, vincristine, Bcl-2 family modulators and olaparib as single treatments or as combination

treatments such as vincristine combined with the Bcl-2 family modulators or oxaliplatin, cisplatin, TBH combined with olaparib and HCP5 knockdown.

Cells were seeded in culture growth medium in a clear flat bottomed 96-well plate (Starstedt) at 2500 cells per well and 5000 cells per well for SW48 at a volume of 100 µl and incubated for 24 h at 37ºC and 5% CO_2 before being exposed to a serial dilution of different concentrations of the chemotherapeutic drugs (either vincristine, cisplatin, oxaliplatin, TBH, the Bcl-2 family modulators or the combination treatment. The serial dilution of the drugs was prepared on a different 96-well plate, 150 µl of cell culture medium was added to wells B3 to G10 of the plate, this serves as the diluent of the drug, however, if a combination treatment was to be carried out, the second drug which concentration was to remain constant was added to the cell culture medium which serves as the diluent. 300 µl of the primary drug diluted in cell culture medium to the desired starting concentration (100 µM) is then added to wells B2- G2. Using a multi-channel pipette, 150 µl of the drug is taken from each well (B2-G2) and then mixed with the medium in the well next to it, this is continued until wells B10-G10 and the excess 150 µl of medium is discarded. 100 µl of was transferred from each well to its corresponding well on the 96 well plate containing the cells, 100 µl of culture medium was also added to wells E11-G11 as negative control (Figure 2.2) and incubated for 72 hours in a humidified atmosphere at 37ºC and 5% CO_2.
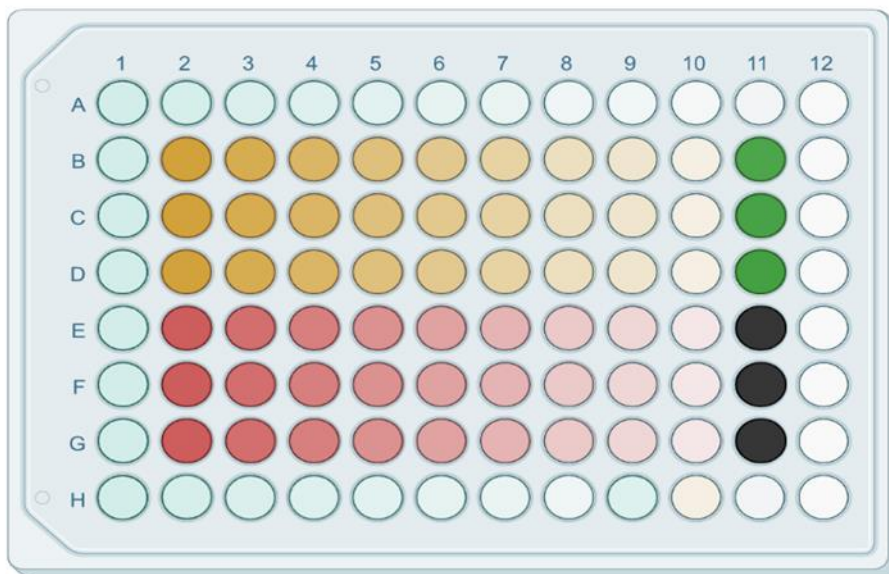
Figure 2.2- MTT plate layout for drug dilution
MTT plate layout showing drug dilution across the plate, yellow = initial concentration of drug 1, red= initial concentration of drug 2, green = wells positive control, black = negative control.

Fifty microlitres of MTT solution (5mg/ml in PBS) was added to each well and then incubated for 3 h in a humidified atmosphere at 37ºC and 5% CO_2, to allow viable cells convert the MTT reagent into insoluble purple formazan crystals. The MTT solution was carefully removed from each well and the formazan crystals were solubilized by adding 200 µl of DMSO and the absorbance was measured at 570 nM using a Varioskan lux (Thermo Fisher scientific, UK) microplate reader with a reference wavelength of 690 nM. The data was processed by subtracting the background absorbance (690 nM) from the 570 nM measurement and normalising the result to untreated control cells (Van Meerloo *et al*., 2011).

Each treatment was carried out in three replicate wells and repeated three times.

2.3 Immunofluorescence microscopy

Cells were seeded in a flat-bottomed 12-well plate (Starstedt), (100,000 cells for HCT116, SW48 and SW480 and 50,000 cells for DAOY) containing a sterilized cover slip and left to adhere on the coverslip for 48 h. Then, the cells were washed with PBS and fixed at room temperature using 4% (w/v) paraformaldehyde for 10 min at room temperature and then permeabilized using 0.25% (v/v) Triton X-100 in PBS for 10 min followed by three washes in

PBS for five minutes each. Unspecific binding of the antibodies was prevented (blocking) by incubating the cells in 1% (w/v) bovine serum albumin (BSA) in PBS for 30 min. The cells were incubated with primary antibody YB-1 (Cell Signalling, UK) which was diluted (1:100) in 1% (w/v) BSA in PBS for 30 min after which it was incubated in Alexa Fluor™ 594 rabbit secondary antibody (Thermo Fisher scientific, UK) diluted 1:1000 in 1% (w/v) BSA for 1 h at room temperature. The coverslips were taken out of the wells and mounted on slides using a mounting medium containing 4,6-diamidino-2-phenylindole (DAPI; Abcam) to counterstain the nuclei. The coverslip was sealed with nail polish and viewed at x40 magnification on an EVOS fluorescence microscope (Thermo Fisher scientific, UK). ImageJ image analysis software (available at http://rsb.info.nih.gov/ij) was used to quantify immunostaining. Images from DAPI and immunofluorescence were combined after background removal and image stacking.

2.4 Isolation of total RNA and cDNA synthesis

The cells were seeded in a 6-well plate (100,00 cells for DAOY, 250,00 cells for HCT116 and SW480 and 500,000 cells for SW48). After 24 hours. The culture medium was aspirated and the cells were washed twice with PBS, trypisinised and washed twice with PBS again before RNA isolation using an ISOLATE II RNA kit (Meridian Bioscience). First, 350 µl of lysis buffer RLY and 3.5 µl of 2-mercaptoethanol was added to the cell pellet. and vortexed vigorously for 1 minute. The lysate was loaded onto an ISOLATE II filter and centrifuged for 1 minute at 11,000 xg. The filter was discarded and 350 µl of 70% (v/v) ethanol was added to the flow-through, mixed and transferred to an ISOLATE II RNA mini column and centrifuged at 11,000 xg for 30 s. Then, 350 µl of membrane desalting buffer was added to the spin column and centrifuged at 11,000 xg for 1 min. DNA still present in the sample was removed by mixing 10 µl of DNase to 90 µl of reaction buffer for DNase (RDN) in a separate tube and then adding 95 µl of the mixture to the centre of the silica membrane followed by incubation at room temperature for 15 min. To wash the membrane, first, 200 µl of wash buffer RW1 was added to the column and centrifuged at 11,000 xg for 30 s, then 600 µl of wash buffer RW2 was added and the spin-column centrifuged at 11,000 xg for 30 s, while the third wash was carried out by adding 250 µl of buffer RW2 to the column followed by centrifugation at 11,000 xg for 2 min. To elute the RNA from the membrane, 40 µl of RNase-free water was added to the centre of the membrane and centrifuged at 11,000 xg for 1 min. This step was repeated to increase RNA

yield. A Nanodrop 2000 Spectrophotometer (ThermoScientific) was used to the determine the quantity and purity of the total RNA obtained.

Total RNA was considered pure if the 260/280 was between the range of 1.8 to 2.1. The resulting RNA was aliquoted and stored at -80°C.

For reverse-transcription, 500 ng of total RNA was converted to cDNA using a Primescript RT reagent kit (Takara Bio) in a 10 µl reaction volume with the following reaction conditions; 37ºC for 15 min (Reverse transcription) and 85ºC for 5 s (heat treatment to inactivate the reverse transcriptase). The cDNA produced with the Primescript RT Kit was quantified using a Nanodrop 2000 Spectrophotometer and used as a template for PCR and RT-qPCR (Section 2.6).

Table 2.2 – Reaction mixture for reverse transcription

Reagent	Volume
5X Prime Script Reagent	2 µl
Prime script RT Enzyme mix	0.5 µl
Oligo(dT) Primer (50 µM)	0.5 µl
Random 6mers (100 µM)	0.5 µl
Total RNA (500 ng)	Variable
RNase Free dH$_2$O	Variable
Total	10 µl

2.5 Agarose gel electrophoresis

RNA integrity was confirmed using agarose gel electrophoresis, a 1% agarose gel was prepared by dissolving 0.5 g of agarose in 50 ml of 0.5TBE and heating in a microwave for 3 minutes with consistent swirling of the mixture every 30 s until the agarose powder was completely dissolved. The mixture was allowed to cool down and 5 µl of SYBR safe was added and this was poured into a gel casting tray containing prior to crystallizing of the gel and allowed to set at room temperature. The comb was taken out and 0.5x Tris-borate-EDTA (TBE) buffer was

added and 10 µl of RNA mixed with 2 µl of loading buffer was added to each well alongside 7 µl of a 1kb DNA ladder (New England Biolab, UK). Electrophoresis was carried out at 100 V for 60 min. The bands were visualised and imaged using a UV transilluminator (Syngene, UK)

2.5 Reverse transcription polymerase chain reaction

Subsequent to the extraction of RNA and conversion to cDNA by reverse transcription, PCR was used to amplify the target genes sequences. Each reaction was prepared in a 200 µl PCR tubes containing 0.5 µl each of forward and reverse primer, 12.5 µl of OneTaq Hot Start Quick-Load 2X Master Mix, 1 µg of cDNA and made up to 25 µl with nuclease free water as shown in Table 2.3.

Table 2.3 – Reaction mixture for PCR

Component	Volume	Final concentration
10 µM Forward Primer	0.5 µl	0.2 µM
10 µM Reverse Primer	0.5 µl	0.2 µM
Template DNA	Variable	<1000ng
OneTaq Hot Start Quick-Load 2X Master Mix with Standard Buffer	12.5 µl	1X
Nuclease-free water	Variable	
Total	25 µl	

Negative controls consisting of the reaction mixture without the cDNA were included in each experiment to check for contamination and a positive control glyceraldehyde 3-phosphate dehydrogenase (GAPDH) which served as a loading control. Reaction conditions were as follows: initial denaturation at 94°C for 30 s, 30 cycles of denaturation for 15 s, annealing at 60°C for 30 s, annealing at 68°C for 30 s and final extension at 68°C for 5 min.

After completion of the PCR step, 10 µl of the amplified PCR reaction mixture were separated on a 2% (w/v) agarose gel alongside a 100 bp DNA ladder (New England Biolab, UK) at 100 V for 60 min. The bands were visualised and imaged using a UV transilluminator (Syngene, UK)

Table 2.4 – Agarose gel electrophoresis: List of reagents

Reagents (Supplier)	Dilution/Description
Agarose	Agarose powder was acquired ready to use from Sigma Aldrich, UK
Tris-Borate- EDTA	10X TBE was prepared by dissolving 108 g tris base and 55 g boric acid in 40 ml 0.5 M EDTA solution (pH 8.0) and 900 ml double-distilled H2O. To make up a 1X working solution, 100ml of 10X TBE and 900 ml of deionised water
SYBR safe	Purchased ready to use from Thermo Fisher scientific UK. 5 ml was added to agarose solution
DNA ladder	100 bp or 1 kb DNA ladder (New England biolabs, UK) was prepared by mixing 4µl of deionised water, 1 µl of loading dye and 1 µl of DNA ladder
Agarose gel electrophoresis loading buffer	0.05% bromophenol blue (w/v), 40% sucrose (w/v), 0.1 M EDTA (pH 8.0) and 0.5% SDS (v/v)

2.6 Real-time quantitative polymerase chain reaction (qPCR)

qPCR reactions were carried out using an Opticon 2 instrument (BioRad). Each reaction was carried out in triplicate with a final volume of 20 µl for each reaction. Reaction mixtures included 10 µl of 2X Sensifast SYBR no-rox kit (Meridian Bioscience), 1 µl each of the forward and reverse primer (0.5 µM per reaction volume for each primer), 5 µl of RNase-free water and 3 µl of cDNA (300 ng). Negative controls consisting of the reaction mixture without the cDNA were included in each experiment to check for contamination. Reaction conditions were as follows: 95°C for 2 min (polymerase activation) and 40 cycles of: 95°C for 5 s (denaturation) and 60°C for 30 s (annealing/extension). Data acquisition was carried out during the

annealing/extension stage and a melting curve analysis between 65°C and 95°C was carried out at the end of the experiment to ascertain amplification of desired fragments and primer specificity. The $2^{-\Delta Ct}$ method was used to calculate the gene expression level of in each sample and $2^{-\Delta\Delta Ct}$ method (Livak & Schmittgen, 2001). was used to calculate fold change in gene expression after HCP5 knockdown. Actin was used as an internal control.

The primers used in this experiment are listed in Table 3. All primers were designed on the exon-exon junction to prevent amplification of DNA using the NCBI primer BLAST and the Eurofins primer design software and purchased from Eurofins. Primers were reconstituted using deionised water to a concentration of 100 µM stock solution and stored in -20°C and then diluted to a 10 µM working solution which was aliquoted stored in -20°C.

Table 2.5 – Primers and primer sequence

Target gene	DNA sequence (5´ to 3´)	PCR product size (bp)
NEIL1 Forward primer	AGAAGATAAGGACCAAGCTGC	212
NEIL1 Reverse primer	GATCCCCCTGGAACCAGATG	
NEIL2 Forward primer	GCCTTAGAAGCTCTAGGCCA	145
NEIL2 Reverse primer	GCACTCAGGACTGAACCGAG	
NEIL3 Forward primer	CGCCTCTGCATTCTCCGAGT	147
NEIL3 Reverse primer	TGGAACGCTTGCCATGGTTG	
GAPDH Forward primer	GGTGGTCTCCTCTGACTTCAACA	127
GAPDH Reverse primer	GTTGCTGTAGCCAAATTCGTTGT	
YB-1 Forward primer	GCACAAGAAGGTCATCGCAAC	171
YB-1 Reverse primer	TCTCCATCTCCTACACTGCGA	
HCP5 Forward primer	TCGCACTTTCAGCACCAGGG	100
HCP5 Reverse primer	TGCCAGCTTTGAGTGGAGCC	
NTH1 Forward primer	GATGGCACACCTGGCTATG	165
NTH1 Reverse primer	CCACAGCTCCCTAGGCAG	

Target gene	DNA sequence (5´ to 3´)	PCR product size (bp)
ERCC1 Forward primer	CAAAACGGACAGTCAGACCCT	146
ERCC1 Reverse primer	TCAAGAAGGGCTCGTGCAG	
OGG1 Forward primer	AGCAGCTACGAGAGTCCTCA	137
OGG1 Reverse primer	CATATGGACATCCACGGGCA	
Beta actin Forward primer	TCTGGCACCACACCTTCTTAC	166
Beta actin Reverse primer	AGCACAGCCTGGATAGCAAC	

2.7 SDS-PAGE and western blotting

The protein samples were separated using sodium dodecyl sulphate polyacrylamide gel electrophoresis (SDS-PAGE). To begin the process, a 12% (w/v) SDS gel which is made up of two parts, the resolving and stacking gel was prepared. The resolving gel was prepared as described in Table 2.6 and transferred into a gel making cassette to fill up 75% of the cassette, 100% ethanol was added into the cassette to ensure a straight edge at the the top of the gel. The gel was allowed to solidify for 30 minutes, after which the ethanol was removed. The stacking solution (Table 2.6) was then added to the cassette, a 10-well comb was inserted into the cassette and the gel was allowed to solidify. The prepared gel was wrapped in paper roll, wet with dH20, wrapped with cling film and stored at 4°C. Medulloblastoma and CRC cells were grown for 24 h in a 6-well plate and were lysed at 4°C for 30 min using 100 μl of triple lysis buffer made up of 50 mM Tris-HCl pH7.5, 150 mM NaCl, 0.1% (w/v) sodium dodecyl sulphate (SDS), 1% (v/v) Nonidet p-40 and 0.5% (w/v) sodium deoxycholate, supplemented with 1 μl of proteinase inhibitor cocktail (Cell signalling, UK). The cells were then scraped off the plate using a cell scraper and transferred to a 1.5 ml microcentrifuge tube and left on ice for 30 min. The cell lysates were then centrifuged at 13000 xg for 15 min at 4°C. The supernatant was transferred into 1.5 ml microcentrifuge tubes and was quantified using the Bradford assay method where 1 ml of 5X Bradford reagent (BioRad, UK) was diluted to 1X using deionised water and 2 μl of the protein solution was added to a cuvette containing 1ml of 1X Bradford reagent. 1 ml of Bradford reagent only was used to calibrate the machine and the absorbance read at 595 nm and the resulting absorbance was converted to concentration using a standard curve generated using bovine serum albumin (BSA).

The 12% (w/v) SDS-polyacrylamide gel was assembled into a gel holding chamber and inserted into a tank, 1X SDS- PAGE running buffer (BioRad, UK) was added to the tank, the combs were removed from the gel and the wells were washed with running buffer before the samples were loaded. An equal amount of protein (30 µg) for each protein lysate was mixed with 4 µl of loading dye and heated at 100ºC for 10 min, centrifuged at maximum speed for 30 sec and then loaded alongside 7 µl of a protein marker (Thermo Fisher Scientific, UK) and separated using electrophoresis at an initial voltage of 100 V for 20 min, after which the voltage was increased to 120 V until the dye front was at the bottom of the gel.

Table 2.6 - SDS-PAGE: List of reagents

Reagents (Supplier)	Dilution/Description
Ammonium Persulfate (APS) (BioRad, UK)	Prepared a 10% (w/v) working solution by dissolving 1 g APS in 10 ml of deionised water.
10% and 12% SDS-polyacrylamide gels	The resolving gel was made with 5 ml Protogel 30%, 3.75 ml of 4X resolving buffer, 6.1 ml of deionized water, 150 µl APS and 15 µl TEMED. The stacking gel was made with 665 µl Protogel, 1.25 ml Protogel stacking buffer, 3.05 ml deionized water, 25 µl APS and 5 µl TEMED
TEMED (Sigma-Aldrich, UK)	N,N,N′,N′-Tetramethylethylenediamine
PBS-Tween 20	900 ml of deionised water, 100 ml PBS and 10 ml of 10X Tween 20
Blocking buffer	5% (w/v) skimmed milk- 2.5 g in 50 ml of PBS-Tween
Triple lysis buffer	50 mM Tris-HCl pH7.5, 150 mM NaCl, 0.1% (w/v) SDS, 1% (v/v) Nonidet P-40 and 0.5% (w/v) sodium deoxycholate
10X Tris/glycine transfer buffer (Biorad laboratories, UK)	25 mM Tris, 192 mM glycine and pH 8.3. To make up 1X working solution, 700 ml deionised water, 200 ml methanol and 100ml 10X Western blot transfer buffer

10X Tris/glycine/ SDS running buffer (Biorad laboratories, UK)	25 mM Tris, 192 mM glycine, 0.1% SDS and pH 8.3. To make up 1X working solution, 900 ml deionised water and 100ml 10X Tris/glycine/ SDS running buffer.
6X Laemmli loading buffer (Thermo Fisher scientific, UK)	375 mM Tris-HCl pH 6.8, 9% (w/v)SDS, 50% (w/v) glycerol, 9% (v/v) β-mercaptoethanol, 0.03% (w/v) bromophenol blue
Protogel 30% (National diagnostics, UK)	30% (w/v) acrylamide/ 0.8% (w/v) methylene bisacrylamide stock solution (37:5:1)
4X Resolving buffer (National diagnostics, UK)	0.375M Tris-HCl, 0.1% (w/v) SDS and pH 8.8
4X Stacking buffer (National diagnostics, UK)	0.125M Tris-HCl, 0.1% (w/v) SDS and pH 6.8
10X PBS	10X PBS tablets were acquired ready to use from Thermo Fisher scientific UK and dissolved 100 ml of deionised water to make a 1X working solution.

The separated polypeptides were transferred on to a polyvinylidene difluoride (PVDF) membrane for 90 minutes at 0.4A using the wet transfer method, where the gel containing the separated proteins is assembled in a sandwich, the sandwich was prepared (Figure 2.3) by first activating the PVDF membrane in 100% methanol and starting from the transparent side of the cassette the foam pad was placed on the cassette followed by three filter papers, ensuring bubbles are rolled out using a roller after the addition of each component the activated PVDF membrane is placed on followed by the gel (This process has to be done in a tray containing transfer buffer as all the components must be kept wet) .Three filter papers are placed on the gel and then the second foam pad is added. The cassette is closed and place in the transfer tank which is filled with 1X Tris/glycine transfer buffer.
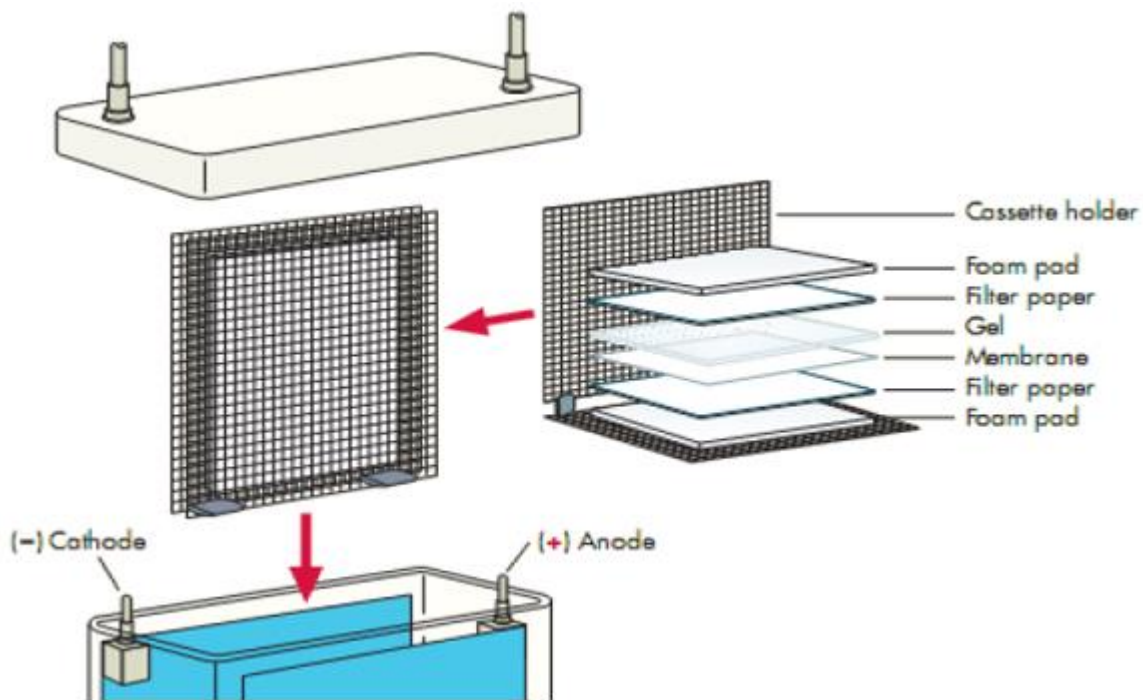
Figure 2.3 - Assembly of western blot transfer sandwich adapted from bosterbio.com

Transfer onto the membrane was confirmed using Ponceaus s solution (Sigma, UK) the membrane was then blocked with 5% non-fat milk in PBS-tween at room temperature for 1 hour and incubated in the desired primary antibody (Table 2.7) overnight at 4°C. The membranes were then treated with a secondary antibody for 1 hour at room temperature, washed three times with PBS-T for 10 minutes and a chemiluminescent detection system called West Femto (Thermo Fisher scientific, UK) was used to develop the membranes and was visualised using the G:Box (Sygene UK). Densitometric analysis was carried out using ImageJ software.

Table 2.7 - List of antibodies

Antibody (Dilution)	Supplier
BCL-XL (1:1000)	Cell Signalling (#2762)
MCL-1 (1:1000)	Cell Signalling (#4572)
YB-1 (1:1000)	Cell Signalling (#4202)
PARP-1 (1:1000)	Santa Cruz (sc-8007)
GAPDH (1:10,000)	Santa Cruz (sc-47724)

ACTIN (1:2000)	Abcam (ab8227)
LAMIN B1 (1:5000)	Santa Cruz (sc-374015)
BCL-2 (1:1000)	Santa Cruz (sc-7382)
γH2AX (Ser 139) (1:1000)	Santa Cruz (sc-517348)
Goat anti mouse IgG antibody HRP conjugate (1:5000)	Sigma Aldrich (12-349)
Anti-rabbit IgG HRP-linked antibody (1:5000)	Cell Signalling (#7074)

2.8 Spheroid formation assay

Low adhesion plates were prepared by coating 6-well plates with 1.2% 2-hydroxyethyl methacrylate (poly-HEMA) solution and dried under sterile conditions for 5 days. 5000 cells were seeded in DMEM F12 medium supplemented with Epidermal growth factor (EGF) and Vitamin B-12. Spheroids above 50 microns were considered in this experiment. The spheroids were stained with 20 µl of 100 nM Mitotracker deepred FM (Invitrogen, M22426), and two drops of Nucblue and Nucgreen LIVE/DEAD viability kit (Invitrogen, R10477), Each experiment was carried out in triplicates and the spheroids were visualized using the Evos microscope (Thermo Fisher scientific, UK).

2.9 siRNA and transfection

siGENOME Human BCL-2L1 siRNA SMARTpool and siGENOME non-targeting siRNA Pool (#2) were purchased from Dharmacon (Lafayette, CO). Five antisense oligonucleotides for HCP5, negative control A and positive control for GAPDH were purchased from Qiagen. 100,000 cells were seeded in a 6-well plate 24 h before the experiment in a medium lacking antibiotic and incubated at 37ºC. 80 nM of each siRNA and 30 nM of the antisense oligonucleotide were used to transfect cells using Opti-MEM reduced serum medium (Thermo Fisher Scientific, UK) and Lipofectamine 3000 (Invitrogen, Carlsbad, CA). 125 µl of Opti-MEM medium was added to two 1.5 ml microcentrifuge tubes, 3.75 µl of Lipofectamine 3000 was added to the first tube and mixed by vortexing. The desired concentration of siRNA / oligonucleotide was added to the second tube and mixed using a pipette. The contents of the two tubes were then combined and incubated at room temperature for 10 min. The growth medium was taken off the cells and 750 µl of cell culture medium lacking antibiotics added

and the 250 µl of transfection medium was added drop wise to the cells. The transfection medium was removed 12 h after transfection and replaced with complete growth medium and the cells were left for 48 h before analysis. The list of siRNA and oligonucleotide used for transfection is given in Table 2.8.

Table 2.8 – List of siRNA and oligonucleotides used

siRNA and Oligonucleotide	Supplier
Antisense LNA Gapmer HCP5 1	Qiagen (LG00247261-DDA)
Antisense LNA Gapmer HCP5 2	Qiagen (LG0024762-DDA)
Antisense LNA Gapmer HCP5 3	Qiagen (LG0024763-DDA)
Antisense LNA Gapmer HCP5 4	Qiagen (LG0024764-DDA)
Antisense LNA Gapmer HCP5 5	Qiagen (LG0024765-DDA)
Negative Control A	Qiagen (LG00000002-DDA)
Positive Control (GAPDH)	Qiagen (LG00000005-DDA)

2.10 Cell cycle analysis

Medulloblastoma HDMB03 and ONS76 cells were seeded in 6-well plates overnight and treated with 15.6 nM and 39.1 nM vincristine respectively, while control cells had no treatment. 24 and 48 hours after treatment, the cells were harvested with trypsin and washed with PBS. The cells were fixed with 70% ethanol and incubated on ice for 30 min. The ethanol was removed after 30 min and the cells were washed twice with PBS. 50 µl of 100 µg/ml RNase was added to each tube followed by 400 µl of 50 µg/ml propidium iodide (Abcam, Cambridge, UK) and was incubated for 10 min at room temperature and analysed on a FACSCalibur flow cytometer (BD Biosciences).

2.11 Apoptosis assay

DAOY, HCT116, SW48 and SW480 cells were grown in a 6-well plate and treated with different concentrations of oxaliplatin, cisplatin and TBH with or without HCP5 knockdown for 48 hours and untreated cells were used as control. The cells were trypsinised and harvested along with the floating dead cells spun down in a centrifuge at 2000 rpm for 5 min and washed with PBS. The cell pellet was resuspended in 500 µl of 1X Annexin V binding buffer (Thermo

Fisher scientific, UK), stained with 5 µl of Annexin V-APC (Thermo Fisher scientific, UK) and 5 µl of propidium iodide (Sigma) and incubated for 15 min at room temperature in the dark. Analysis was done using FACSCalibur flow cytometer (BD Biosciences). Early apoptotic cells were Annexin V+/PI-, late apoptotic cells Annexin V+/PI+, necrotic cells Annexin V-/PI+. Data was analysed using the Flojo software.

2.12 Colony formation assay

500 cells per well for the DAOY, HCT116 cells and 1000 cells per well for the SW48 and SW480 were seeded in a 6-well plate. The cells were allowed to adhere for 24 h and then treated with the desired drug (oxaliplatin, cisplatin or TBH). After 24 h the medium containing the drugs was removed, the cells were washed with PBS to stop drug action and fresh culture medium was added. After 14 days, the culture medium was removed and the colonies were fixed with 100% methanol at room temperature for 20 min and stained with 0.2% (w/v) crystal violet for 5 min, the cells were washed with water to remove excess dye and the plates were inverted on tissue paper and allowed to dry. Colonies were counted manually using a bright field microscope (a group/cluster of 50 or more cells was considered to be a colony). Plating efficiency for the SW480 cells were 35%, DAOY 41%, HCT116 55% and SW48 38%. Calculation of the surviving fraction was carried out by dividing the number of seeded cells with the number of colonies and normalising the result to the plating efficiency of the control.

2.13 Statistical analysis

Statistical analysis of data was performed using GraphPad prism 9 (GraphPad, USA). All experiments were performed in triplicates unless stated otherwise. The data were shown as mean ± SD and $p<0.05$ was considered to be significant. Two-way analysis of variance (ANOVA) supplemented with Tukey's multiple comparisons test was used to analyse the MTT and apoptosis data, while a student t-test was used to analyse the statistical difference in the other experiments.). ns = $p>0.05$, * = $p \leq 0.05$, ** = $p \leq 0.01$, ***= $p \leq 0.001$.

CHAPTER 3- TARGETING THE BCL-2 FAMILY IN CANCER CHEMOTHERAPY

3.1 Results

3.1.1 Determining the basal expression levels of Bcl-2 proteins in medulloblastoma cell lines

According to numerous studies, increased expression of the Bcl-2 family proteins results in resistance to chemotherapeutic treatments while decreased expression of the Bcl-2 family proteins encourages apoptotic responses to anticancer medications (Basu, 2022). It was therefore important to determine the basal level of the Bcl 2 family proteins (Bcl-xL, Mcl 1 and Bcl 2) in the different cell lines. Expression of Mcl-1, Bcl-xL and Bcl-2 was determined using western blot analysis and as seen in Figure 3.1, the ONS76 cell line is overexpressing Bcl xl when compared to the other cell lines, while the DAOY cell line has a high basal expression of Bcl 2 protein when compared to the other cell lines. The HDMB03 cell line has normal basal expression level of all three proteins.
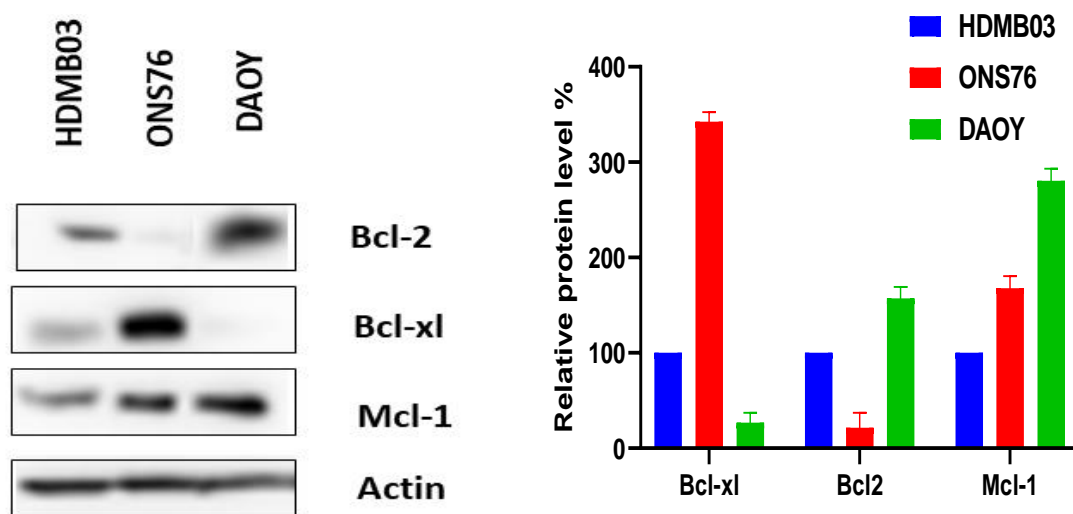
Figure 3.1- **Comparison of Bcl-2 family protein expression levels in three medulloblastoma cell lines**; HDMB03, ONS76 and DAOY using western blot analysis. Each band was quantified by densitometric analysis and measured in relation to HDMB03. Each data point represents three independent experiments (n=3). Data are represented as mean ±standard deviation of the mean.

3.1.2 Medulloblastoma cell lines respond differently to vincristine treatment.

Subsequent to establishing the variation in the expression level of the anti-apoptotic Bcl-2 family proteins in the cell lines, it was of interest to determine if this variation affects how the

cells respond to anti mitotic drug vincristine. To determine the effect of vincristine on medulloblastoma cells, the three medulloblastoma cell lines were initially treated with 5 μM vincristine using RPMI medium as the negative control and 50 μM vincristine as positive control. At the higher concentrations, a substantial loss of cell viability was observed (not shown), however, a concentration with 50% cell viability (IC50) was needed for the combination treatment, as it shows that the drug is still effective at that concentration and the effect of Bcl-2 modulator can be noticed, and not overshadowed by the toxicity of vincristine. The experiment was then repeated at 39.1 nM to get a better range of which concentration had 50% cell viability (Figure 3.2). All three cell lines responded differently to the vincristine treatment, this further confirms the heterogeneity that exists between subgroups and subtypes of medulloblastoma. At a concentration of 39.1 nM of vincristine for ONS76, 9.76 nM for DAOY and 15.26 nM for HDMB03 viability of the cells was close to 50%. This concentration was then used for the combination treatment with the Bcl-2 modulators.
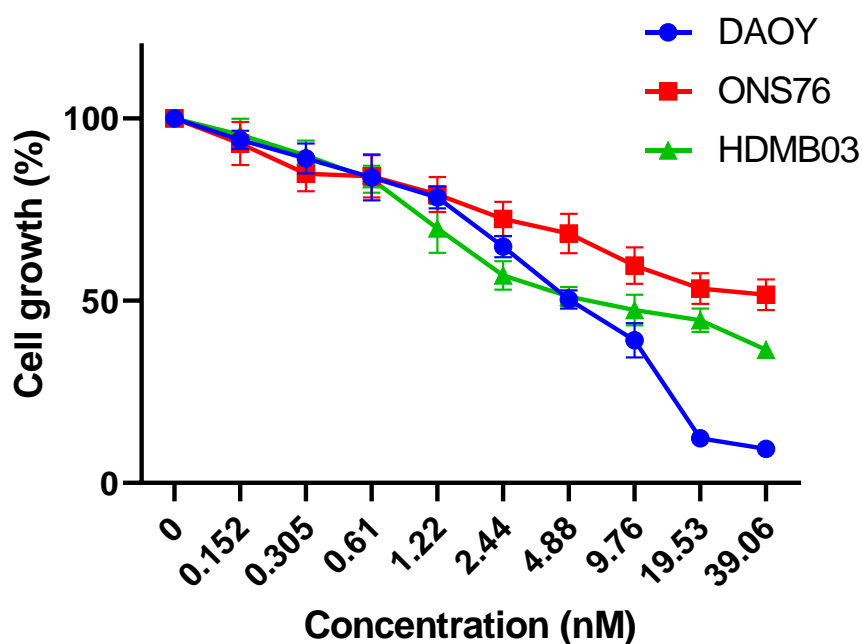
Cell line	IC50 value (nM)
DAOY	8.9 ± 0.95
ONS76	N/A
MB03	15.23 ± 0.89

Figure 3.2 -**Effect of vincristine treatment on DAOY, ONS76 and HDMB03 cell lines.** Percentage of cell growth was determined by MTT assay after treatment with Vincristine, each graph represents the effects of vincristine on DAOY, ONS76 and HDMB03 cell lines. Cells were exposed to serial dilution of vincristine for 72 hours and the results were analysed. IC50

values of combination treatment and vincristine only treatment, N/A indicates IC50 value is above highest concentration. Results shown are the average of three independent experiments carried out in triplicates. Error bars ± standard deviation.

NAVITOCLAX

The DAOY cells showed a higher expression of Bcl-2 protein as shown in Figure 3.1, therefore, to determine if Bcl-2 protein knockdown will have a better effect on sensitizing DAOY and HDMB03 cells to vincristine. Navitoclax an inhibitor of the Bcl-2 family was then used on the various cell lines, starting with a concentration of 50 μM, the three cell lines were treated with navitoclax alone. At high concentrations of navitoclax, there was about 95% mortality in all cell lines, the lowest concentration from the MTT assay which was 0.195 μM was chosen for the combination treatment for the three cell lines as it had little effect on cell viability as seen in Figure 3.3
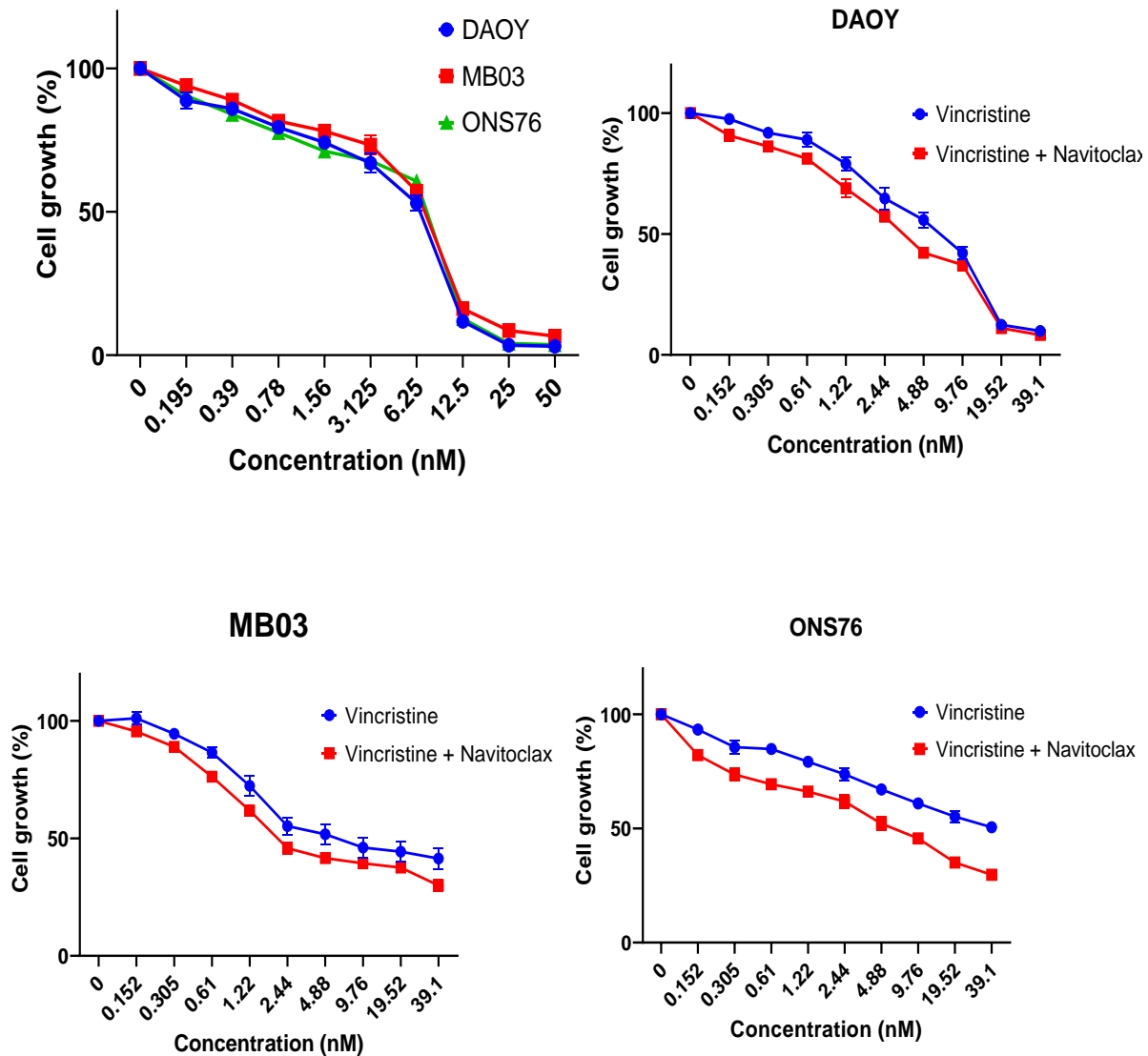
Cell line	Treatment	
	Vincristine (nM)	Vincristine + Navitoclax (nM)
DAOY	8.89 ± 0.63	6.01 ± 0.92
ONS76	N/A	10.51 ± 1.53
MB03	14.52 ± 0.75	10.33 ± 1.07

Figure 3.3- **Effect of combination treatment of navitoclax and vincristine on medulloblastoma cell lines-** DAOY, MB03 and ONS76 cells were exposed to serial dilution of Navitoclax for 72 h. B) Cells were treated with vincristine alone and with a combination of vincristine + 0.195 µM navitoclax for 72 h and the results were analysed. C) IC50 values of combination treatment and vincristine only treatment, N/A indicates IC50 value is above highest concentration. Results shown are the average of three independent experiments carried out in triplicates (n=3). Error bars ±standard deviation.

The combination treatment was carried out using the concentrations selected from the MTT assays, RPMI medium was used as the negative control for the vincristine treatment and RPMI medium + navitoclax was used as negative control for the combination treatment. In the ONS76 cell line, there was some reduction in cell viability ($p<0.05$), compared to the cells treated with just vincristine, which suggested that the cells showed increased sensitivity to low doses of the vincristine treatment in the presence of 0.195 μM navitoclax, However, in HDMB03 and DAOY cell lines, there was no significant difference in cell viability ($p>0.05$).

MURISTERONE A

To determine if upregulation of Bcl-xL has the opposite effect on vincristine compared to its inhibition, the cells were treated with muristerone A and the combination treatment experiment was repeated using muristerone A which is known to upregulate Bcl-xL expression in cells, the experiment was carried out using the same methods as the WEHI 539 and navitoclax experiments. To start with, all the cell lines were treated with 50 μM muristerone A to determine what concentration to use in the combination treatment. muristerone A did not show any toxicity to the cell, even at the highest concentration as shown in Figure 3.4, there was however an increase in cell growth when compared to the untreated control at the higher concentration of muristerone in all three cell lines. To proceed with the combination treatment 10 μM muristerone A was selected as the concentration to use in combination with vincristine.
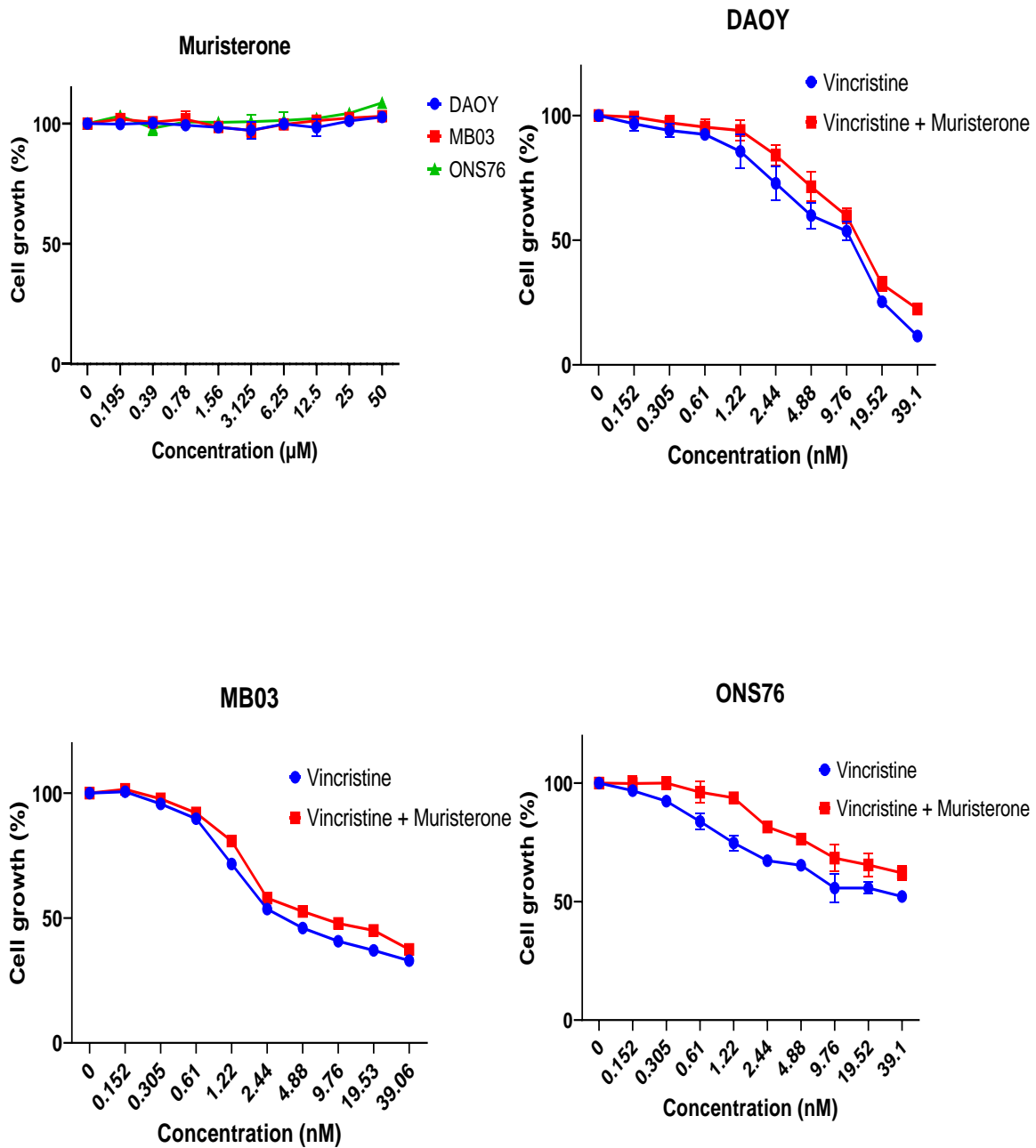
Cell line	Treatment	
	Vincristine (nM)	Vincristine + Muristerone (nM)
DAOY	9.88 ± 0.21	11.91 ± 0.47
ONS76	N/A	N/A
MB03	17.61 ± 1.81	14.25 ± 1.21

Figure 3.4- **Effect of combination treatment of muristerone and vincristine on medulloblastoma cell lines-** DAOY, MB03 and ONS76 cells were exposed to serial dilution of navitoclax for 72 hours. B) Cells were treated with vincristine alone and with a combination of vincristine + 10 µM muristerone for 72 hours and the results were analysed. C) IC50 values

of combination treatment and vincristine only treatment, N/A indicates IC50 value is above highest concentration. Results shown are the average of three independent experiments carried out in triplicates (n=3). Error bars ±standard deviation.

The combination treatment with muristerone A showed a significant increase in cell viability ($p<0.05$), in the ONS76 cell line when compared to the vincristine only treatment, while the DAOY and MB03 cell lines showed a slight but not significant increase in cell viability ($p>0.05$), compared to just vincristine treatment as expected as Bcl-xL is known to promote cell survival during mitotic arrest.

MARITOCLAX

Previous studies have shown that cells with high expression of Mcl-1 were able to escape chemotherapy induced mitotic arrest. It was imperative to determine if inhibition of Mcl-1 would sensitize the cells to vincristine as all the cell lines showed expression of Mcl-1. Maritoclax which is a selective Mcl-1 inhibitor, was used to treat the cells in combination with vincristine. The cells were first treated with maritoclax alone at a concentration of 50 μM, all the cell lines responded differently to the drug with all the cell lines having very low cell viability at 50 μM, however, the DAOY cells had the lowest viability between the three cell lines at 50 μM. Maritoclax was toxic to the cells at the higher concentrations, therefore 0.078 µM was chosen for the combination treatment as this concentration was not toxic to the cells.

Cell line	Treatment	
	Vincristine (nM)	Vincristine + Maritoclax (nM)
DAOY	10.05 ± 0.74	7.75 ± 0.92
ONS76	36.89 ± 0.56	28.5 ± 0.72
MB03	17.73 ± 1.11	14.41 ± 1.03

Figure 3.5- **Effect of combination treatment of maritoclax and vincristine on medulloblastoma cell lines-** DAOY, MB03 and ONS76 cells were exposed to serial dilution of navitoclax for 72 hours. B) Cells were treated with vincristine alone and with a combination of vincristine + 0.078 μM maritoclax for 72 hours and the results were analysed. C) IC50 values of combination treatment and vincristine only treatment. Results shown are the average of three independent experiments carried out in triplicates (n=3). Error bars ±standard deviation.

Each cell line was then treated with vincristine alone and a combination of vincristine and maritoclax, there was a little reduction in cell viability across the three cell lines, however, the reduction in cell viability in all the cell lines was not significant as $p>0.05$.

WEHI 539

Over expression of Bcl-xL has been linked to controlling pathways associated with the development of many malignancies in addition to acting as crucial indicators for cell fate determination (Trisciuoglio *et al*., 2017). Results from the western blot assay in Figure 3.1 showed that Bcl-xL expression was higher in the ONS76 cells compared to the others, so it was of interest to determine if knockdown of Bcl-xL will have the same effect on vincristine sensitivity across the three cell lines. To begin with, the effect of Bcl-xL inhibition on cell viability was determined, the three cell lines were treated with Bcl-xL inhibitor WEHI 539, with a starting concentration of 50 µM. The starting concentration of 50 µM was toxic to the cells and it was of importance to select a concentration with low toxicity to the cells, but inhibition of Bcl-xL was still effective for the combination treatment, this concentration was chosen as the purpose of WEHI 539 in the combination treatment was to inhibit Bcl-xL and not to cause cell death on its own, as this way it can be ascertained that cell death was caused by vincristine in the combination treatment and not toxicity of WEHI 539 alone. 0.195 µM WEHI539 was selected as the ideal concentration for all cell lines to be used in the combination treatment.

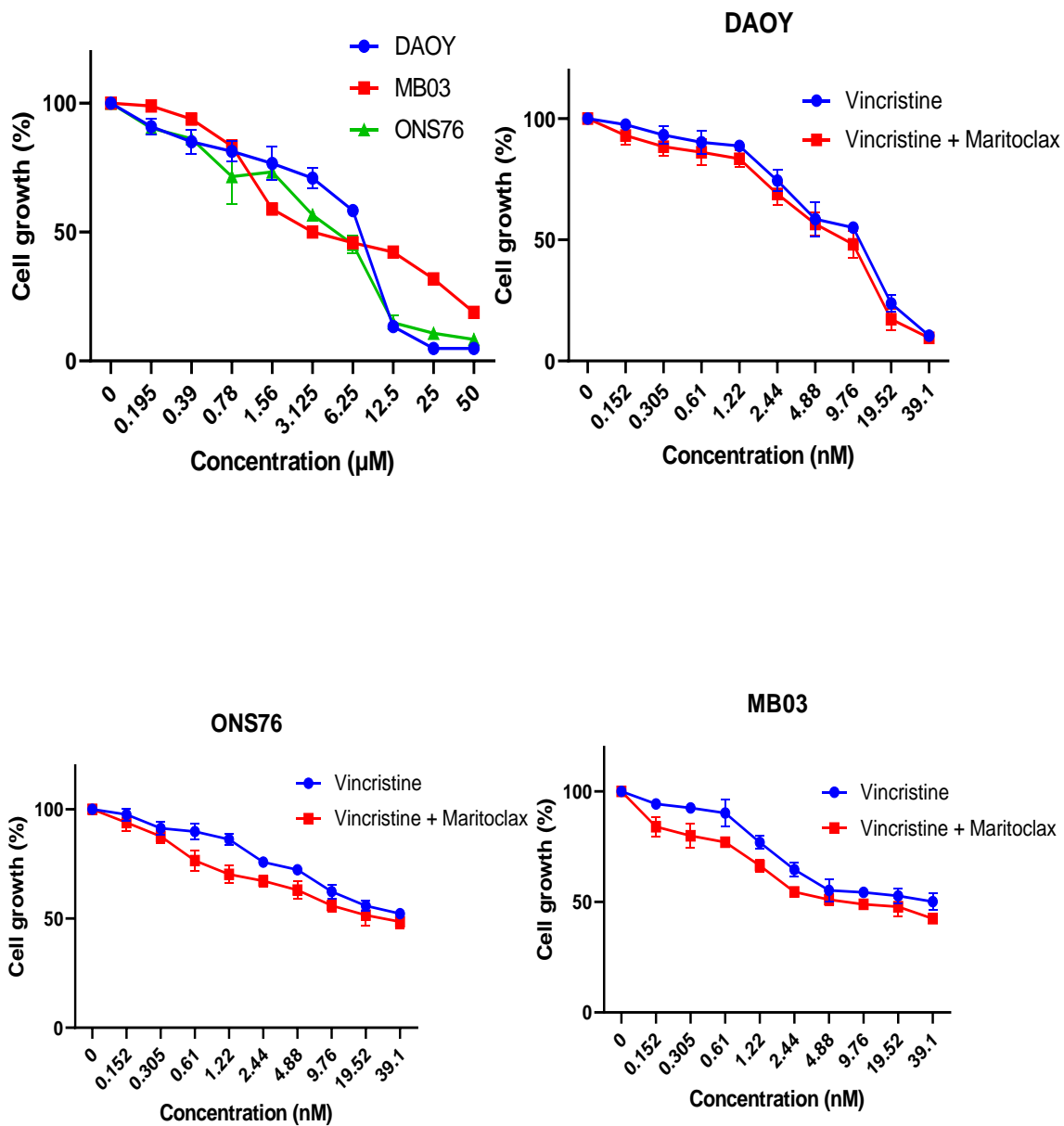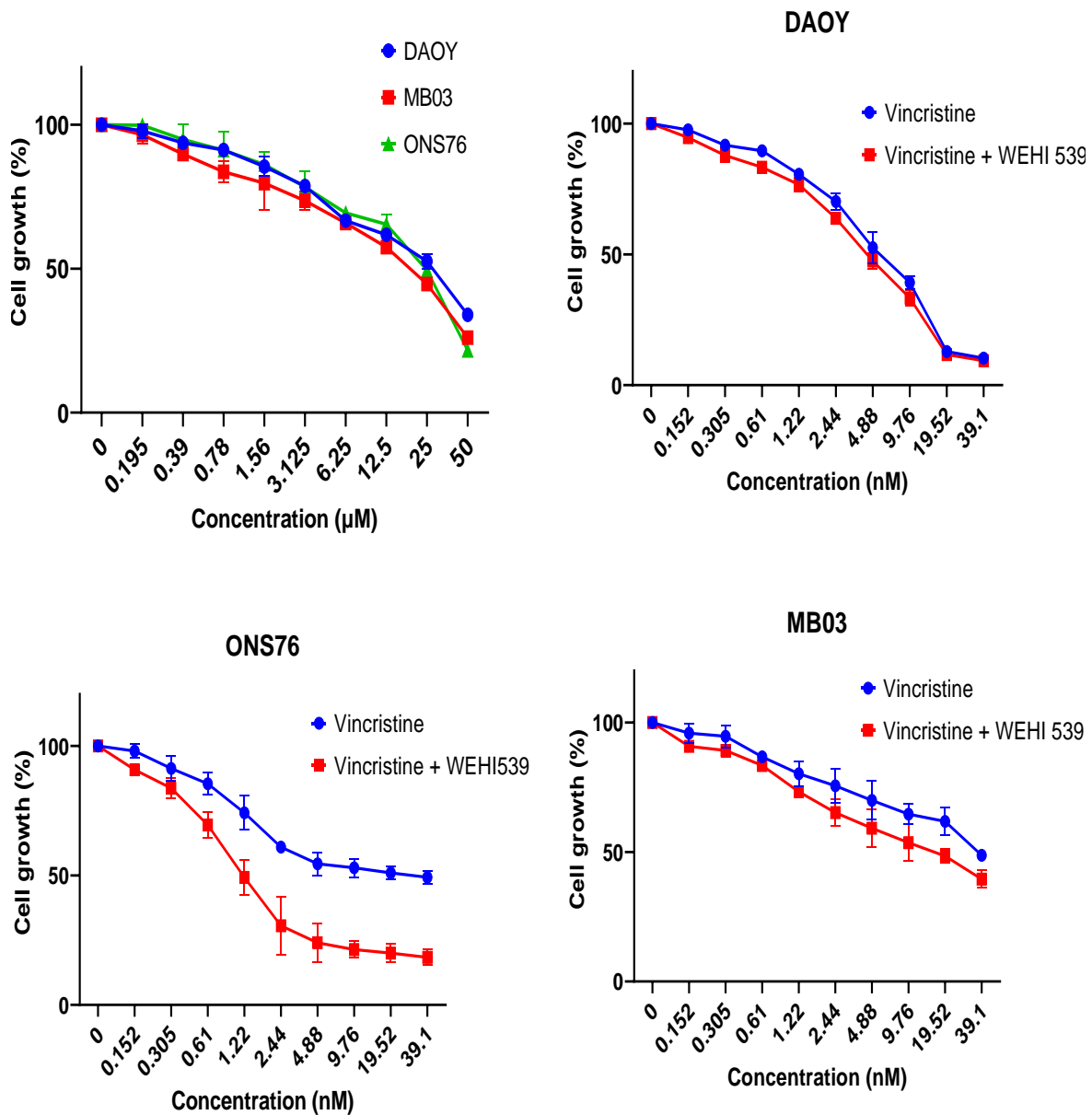| Cell line	Treatment	
	Vincristine (nM)	Vincristine + WEHI539 (nM)
DAOY	8.75 ± 1.05	6.57 ± 1.11
ONS76	37.1 ± 1.12	2.05 ± 0.72
MB03	19.59 ± 1.45	13.33 ± 0.81

Figure 3.6- **Effect of combination treatment of WEHI539 and Vincristine on medulloblastoma cell lines-** DAOY, MB03 and ONS76 cells were exposed to serial dilution of WEHI 539 for 72 hours. B) Cells were treated with vincristine alone and with a combination of vincristine + 0.195 µM WEHI539 for 72 hours and the results were analysed. C) IC50 values

of combination treatment and vincristine treatment. Results shown are the average of three independent experiments carried out in triplicates (n=3). Error bars ±standard deviation.

In the ONS76 cell line, the combination treatment was carried out using 39.1 nM vincristine and 0.195 µM WEHI539, incubated for 72 h and the cells were analysed using MTT assay. RPMI medium was used as the negative control for the vincristine only treatment and RPMI medium + WEHI 539 was used as negative control for the combination treatment. In the ONS76 cell line, there was a significant reduction in cell growth in the combination treatment ($p<0.05$), compared to the cells treated with just vincristine, which suggested that the cells showed increased sensitivity to low doses of the vincristine treatment in the presence of 0.195 µM WEHI 539 (Figure 3.6). However, in the DAOY and HDMB03 cell lines, there was no significant difference in cell viability ($p>0.05$), although a little decrease can be seen in cell viability at the higher concentrations. Based on results from the MTT assay it was decided to focus on the effect of Bcl-xL inhibition in ONS76 cells as Bcl-xL was highly expressed in ONS76 cells and its inhibition significantly suppressed the growth of ONS76 cell in a dose and time-dependent manner when combined with vincristine treatment.

To determine if knockdown of Bcl-xL would have a similar effect on the ONS76 to the inhibition of Bcl-xL with WEHI539, Bcl-xL knockdown was carried out using siRNA and knockdown efficiency was confirmed using western blot.
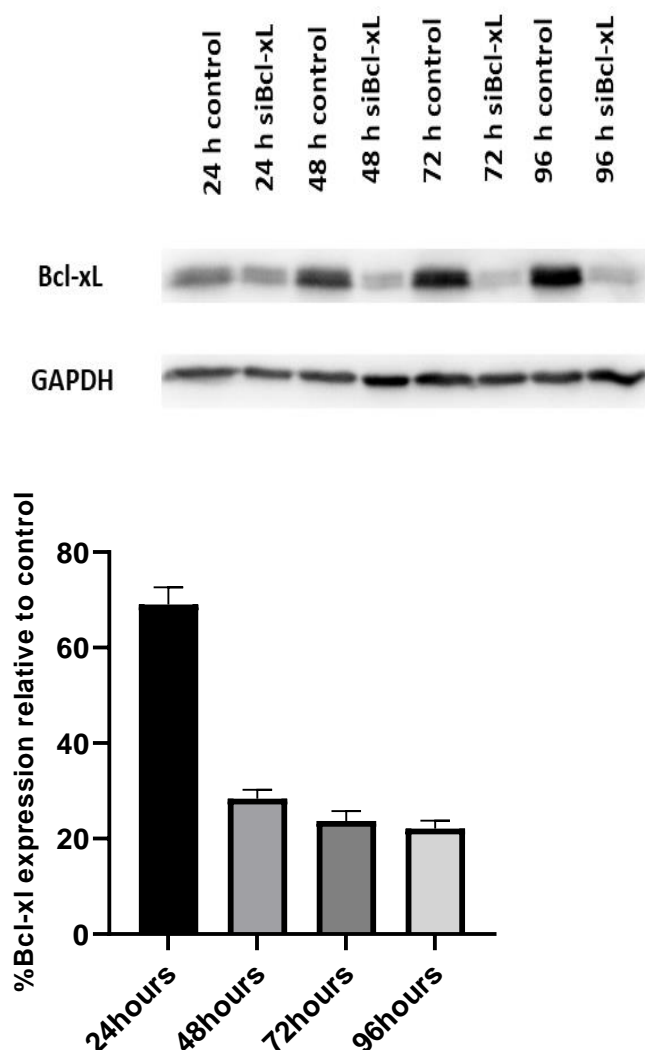
Figure 3.7 - **Western blot showing timeframe of Bcl-xL knockdown in ONS76 cells.**
Bcl-xL knockdown was carried out for 24, 48, 72 and 96 hours. Expression level of Bcl-xL
was obtained by western blot using GAPDH as a loading control. Each band was quantified by
densitometric analysis in relation to GAPDH. Each data point represents three independent
experiments (n=3). Data are represented as mean ±standard deviation of the mean.

To determine when the knockdown of Bcl-xL became effective in the cell, 100,000 ONS76
cells were seeded for 24h and transfected with 80 nM siBclxl using 3.5 µl lipofectamine for
24, 48, 72 and 96 h after which protein was extracted and subjected to western blotting as seen
in the Figure 3.7, there was no significant difference in the expression level of Bcl-xL in the
24 h control and the 24h siBcl-xL, however 48 hours after transfection, Bclxl knockdown
efficiency was more than 50% at and knockdown was still effective at 96 h. Therefore, for
further experiments, 48 h Bcl-xL knockdown was selected.
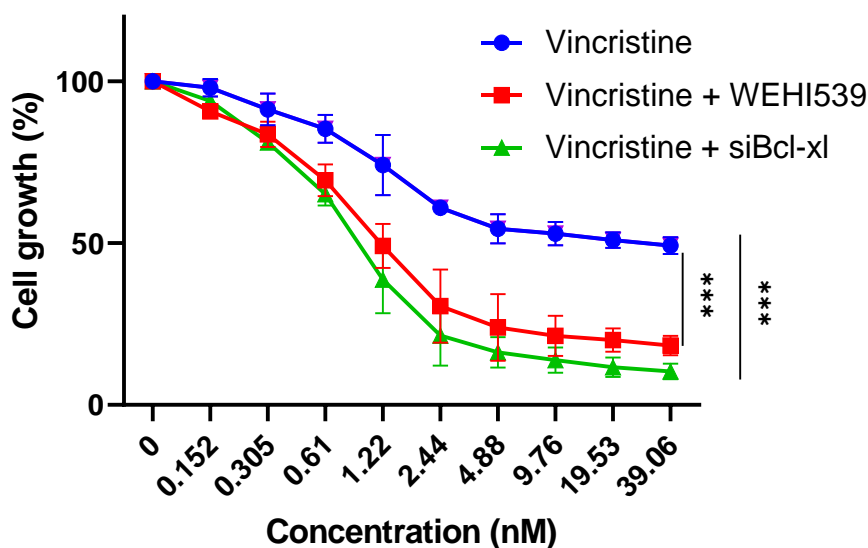
Treatment	IC50 (nM)
Vincristine	38.05±0.78
Vincristine + WEHI539	1.44± 0.36
Vincristine + siBclxl	0.89±0.29

Figure 3.8- Bcl-xL knockdown sensitizes ONS76 cells to chemotherapy.
ONS76 cells were exposed to serial dilution of vincristine for 72 hours and the results were analyzed. Results shown are the average of three experiments carried out in triplicates. Error bars ± standard deviation. Statistical analysis was carried out using two-way ANOVA supplemented with Tukey's multiple comparisons test. ***= $p \leq 0.001$.

After determination of the effect of vincristine + WEHI539 treatment on the growth of the different medulloblastoma cell lines, the effect of the combination of Bcl-xL knockdown and vincristine treatment on cell growth was investigated and this effect was compared to the vincristine + WEHI539 treatment to determine if both combinations have similar effect. The cells were divided into three groups, the first group was made up of cells treated with only the single vincristine treatment, while the second group were treated with the vincristine + WEHI539 combination treatment. The third group were cells transfected with siBcl-xL and treated with vincristine. The three groups were plated on the same 96-well plate and allowed to grow for 72 h, after which cell growth was analysed and as shown in Figure 3.8, knockdown of Bcl-xL had a similar effect to inhibition of Bcl-xL using WEHI-539, as there was a significant decrease between the percentage cell growth when comparing the group treated with only vincristine and the group treated with vincristine + siBcl-xL. There was a slight decrease

108

in percentage cell growth when comparing the group treated vincristine + WEHI539 combination and the group treated with vincristine + siBcl-xL, however this reduction in cell growth was not significant.

3.1.3 Determining the fate of cells after treatment with vincristine.

Havas *et al*. showed that following treatment with vincristine, an accumulation of polyploid cells were noticed and it was attributed to the fact that the cells slipped out of mitosis after a prolonged mitotic arrest in their tetraploid state without dividing (Havas *et al*., 2016).

MTT assays only shows the percentage of cell viability but does not indicate the fate of the cells i.e if the cells that survived the treatment undergo mitotic slippage or a normal cell division. To analyse the changes in cell morphology that define individual cell fate, ONS76, DAOY and HDMB03 cells were treated with vincristine, and monitored by time lapse microscopy for 72 h (supplementary Figures 1-3). It was discovered that in the ONS76 cell line, the predominant survival tactics for the cells after the vincristine treatment was via mitotic slippage as all the cells that survived after the vincristine treatment survived via mitotic slippage. In the DAOY cell line, slippage was not apparent, as the cells that survived were heathy cells that underwent a normal mitosis. In the HDMB03 cell line, mitotic slippage was also apparent after vincristine treatment, with most of the cells undergoing mitotic slippage.

3.1.4 Treatment with vincristine increases polyploidy.

Flow cytometry was used to determine if mitotic slippage encourages polyploidy, cells from HDMB03 and ONS76 cell lines were treated with 15.6 nM and 39.1 nM vincristine respectively and subjected to cell cycle analysis using flow cytometry after 24 and 48 hours. In HDMB03 cells after treatment with 15.6 nM vincristine for 24 and 48 h (Figure 3.10), revealed that in the cells treated for 24 h when compared to the untreated cells, showed an increase in the number of cells stuck in the subG1 phase from 2% to 20%, a reduction in the S phase from 10% to 8%, a decrease in the G0\G1 phase from 76.6% to 24.2%, increase in the G2\M phase 4.39% to 33.4% and an increase in the number of polyploid from 2.53% to 7.89%. The 48 hours treatment showed an increase in the subG1 from 0.74% to 35.48%, the S phase, 2.77% to 8.5% decrease, a decrease in the G0\G1 phase from 84.8% to 20.79%, increase in the G2\M phase 8.85% to 24.6% and an increase in the polyploid population from 1.49 to 5.81%. When comparing the polyploid population between the 24 h treatment and the 48h treatment,

there was a decrease in the polyploid population in the 48 h treated cells when compared to the cells treated with 39.1 nM vincristine (7.89% to 5.81%).

Figure 3.10- Cycle analysis of MB03 cells after treatment with 15.6 nM vincristine.
(A) 24 hours control, (B) 24 hours treated (C) 48 hours control (D) 48 hours treated (E)
Quantitation of A,B,C and D. . Results shown are the average of three independent experiments
carried out in triplicates. Error bars ± standard deviation.

The ONS76 cells were plated in a 6-well plate and treated with 39.1 nM vincristine for 24 and
48 h, cells were collected, stained and cell cycle analysis was carried out using flow cytometry
(Figure 3.11). When comparing the cells treated for 24 h to the untreated cells, there was an
increase in the number of cells stuck in the subG1 phase from 2.12% to 20.96%, a reduction in
the S phase from 10% to 8%, a decrease in the G0\G1 phase from 76.6% to 24.2%, increase in
the G2\M phase 4.39% to 33.4% and an increase in the number of polyploid from 2.53% to
7.89%. The 48 hours treatment showed an increase in the subG1 from 0.74% to 35.48%, the S
phase, 2.77% to 8.5% decrease, a decrease in the G0\G1 phase from 84.8% to 20.79%, increase
in the G2\M phase 8.85% to 24.6% and an increase in the polyploid population from 1.49 to
5.81%. When comparing the polyploid population between the 24 h treatment and the 48 h
treatment, there was a decrease in the polyploid population in the 48 h treated cells when
compared to the cells treated with 39.1 nM vincristine (7.89% to 5.81%).

Figure 3.11- **Cycle analysis of ONS76 cells after treatment with 39.1 nM vincristine.** (A) 24 hours control, (B) 24 hours treated (C) 48 hours control (D) 48 hours treated (E) Quantitation of A,B,C and D. . Results shown are the average of three independent experiments carried out in triplicates. Error bars ± standard deviation.

3.1.5 Vincristine treatment induced polyploid cells.

The introduction of polyploidy by antimitotic drugs has been linked to drug resistance (Denisenko *et al*., 2016) and the ability of polyploid cells to survive after mitotic slippage leads to aneuploidy which plays a huge role in cancer progression (Coward *et al*., 2014). It was therefore important to determine if cells that escape vincristine induced cell death are able to survive different cycles of cell division and if they do develop into polyploid cells is the combination treatment able to sensitize the polyploid cells to vincristine.

Subsequent to the cell cycle analysis experiment which showed an increase in polyploid cells population after vincristine treatment for 48 h. It was therefore imperative to investigate the fate of cells that evade apoptosis after vincristine treatment, ONS76 cells were treated with 39.1 nM vincristine for 72 h and the cells that survived were collected after treatment and grown 2D in culture, it was however noted, that the time to confluency between each passage was 7 days, which was longer compared to the 3 days of confluency by normal ONS76 cells. After the first passage, most of the cells began to show a change in phenotype and adapting a more epithelial like structure as shown in Figure 3.12B. However, in passage 3, some cells started to exhibit a different change in morphology by acquiring dendritic like structures resembling a neuron (Figure 3.12E), this indicated that the cells had differentiated which is a hallmark of stem cells.
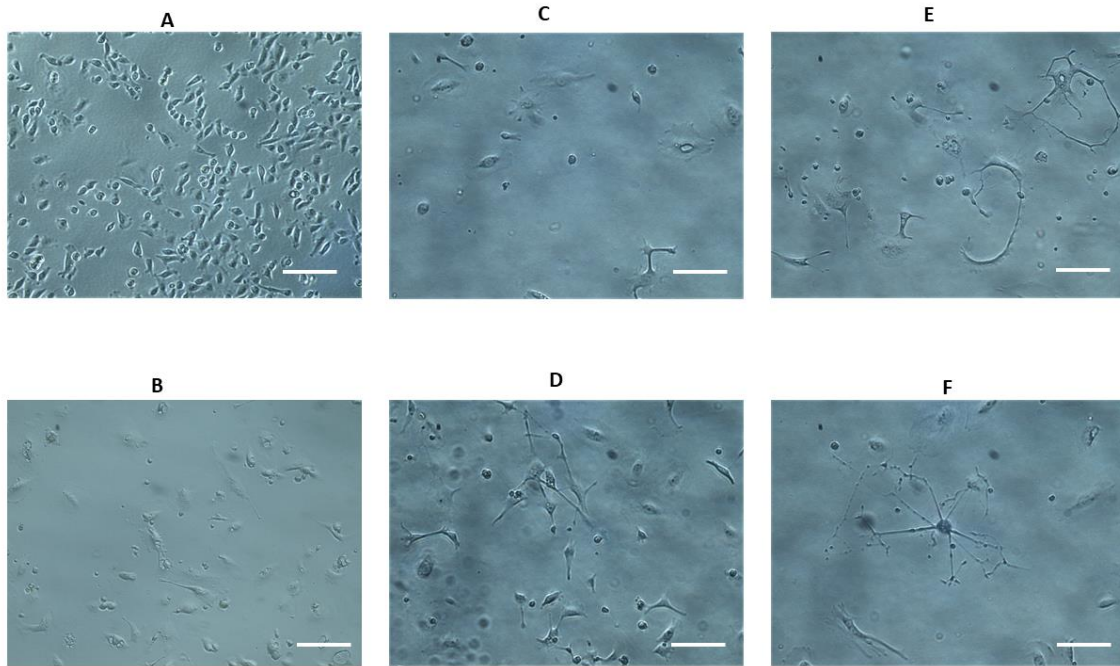
Figure 3.12- **ONS76 cells were treated with 39.1 nM vincristine for 72 hours and the surviving cells grown in culture.**
The cells were passaged once a week. A) Control cells, no treatment B) first passage after treatment, C,D) Second passage after treatment E,F) Third passage after treatment. Scale bar is 1000 µm

In Figure 3.13, some huge undivided cells with multiple nuclei can be seen, this shows that the cells have undergone mitotic slippage a couple of times, which confirms that cells can undergo slippage continuously without dying resulting in giant polyploid cancer cells (PGCC). The vast size and enormous nucleus were the two phenotypical traits of PGCCs. A cancer cell that grows at least three times larger in size than its parental cancer cells was considered to be a "PGCC." The PGCCs' average size was 3–10 times greater than that of typical cancer cells as shown in Figure 3.14.
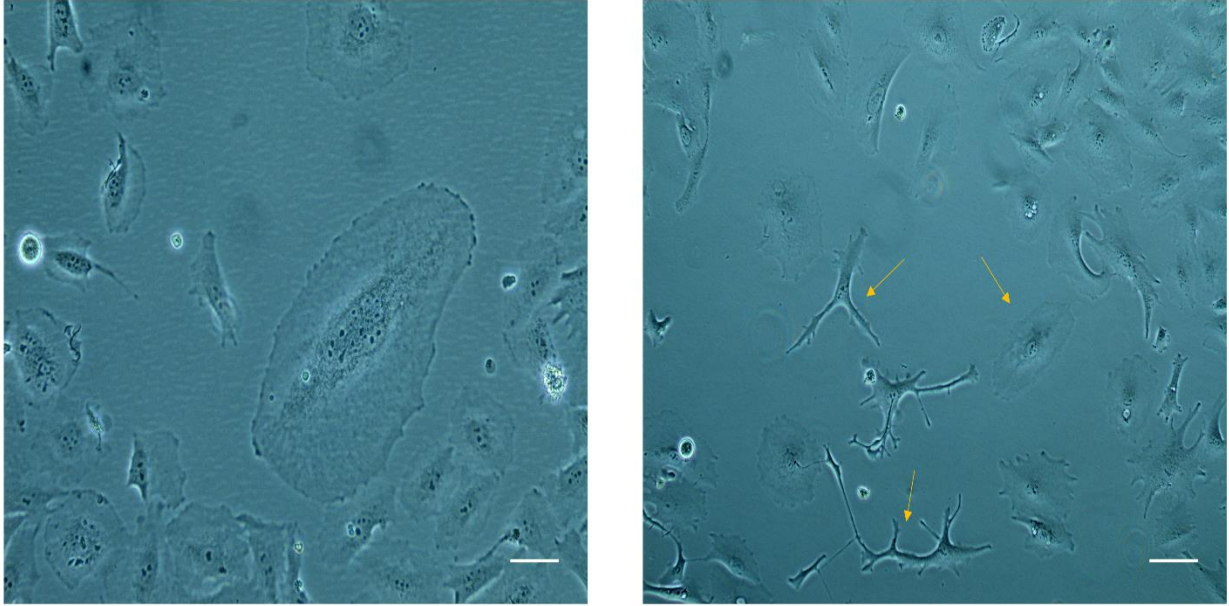
Figure 3.13- **Vincristine treatment encourages the formation of PGCCs.**
Image showing giant polyploid cells and cells undergoing budding, yellow arrows indicate cells undergoing budding. Scale bar is 100 µm.

In the PGCCs, it was discovered the cells were not dividing via mitosis, however, they were replicating via asymmetric cell division patterns known as budding and bursting. Daughter cells from PGCCs typically budded from their branches as shown in Figure 3.14 and some multinucleated PGCC were seen to "burst", thus releasing a large number of daughter cells.
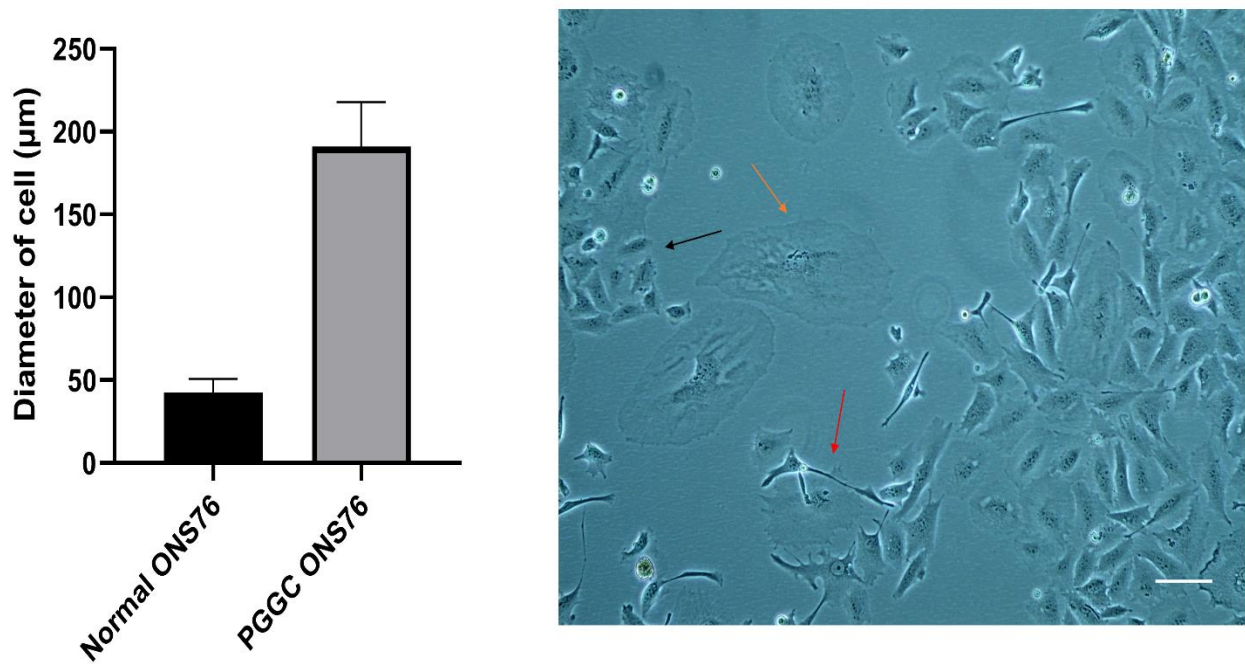
Figure 3.14 - ONS76 polyploid cells are 3-4 times bigger than normal cells. Quantification of the diameter of the polyploid cells and normal cells, measured using imagej. Twenty cells were analysed for each group. Data are represented as mean ±standard deviation of the mean (n = 3). Scale bar is 100 µm.

3.1.6 Spheroids derived from medulloblastoma cell lines possess varying spheroidization time and morphological characteristics.

Polyploid cancer cells have been shown to evolve into cancer stem cells (CSC) in ovarian cancer cells (Zhang *et al*., 2014). Therefore, it was important to investigate the stem like properties of the polyploid cells. Partly due to their capacity for self-renewal and differentiation into a variety of cancer cell lineages, cancer stem cells (CSCs) have been implicated in the development of chemoresistance and cancer relapse (Phil *et al*, 2018). A typical experiment to evaluate the amount of CSC, the self-renewal and multipotent properties of the cancer stem cell subpopulations inside a tumour or cancer cell line is the spheroid formation assay. Firstly, the capacity of the medulloblastoma cell lines to produce three-dimensional (3D) spheroids was investigated. The three medulloblastoma cell lines were grown in a low adherent plate in DMEM-F12 medium and other supplements to encourage spheroid formation. The spheroids were allowed to grow for five days and analysed. The DAOY and ONS76 cells had formed visible spheroids and the number of spheroids generated after five days were counted manually using the Evos microscope. However, the HDMB03 cell line had a few spheroids after five days, they were allowed to grow for two more days and after seven days the spheroids were

116

counted and analysed (Figure 3.15). All three cell lines could form spheroids, with the spheres formed from each cell lines having different morphology. The ONS76 cells formed more compact and round spheroids, while the DAOY and HDMB03 spheroids generated spheroids with bubble like structures.

A
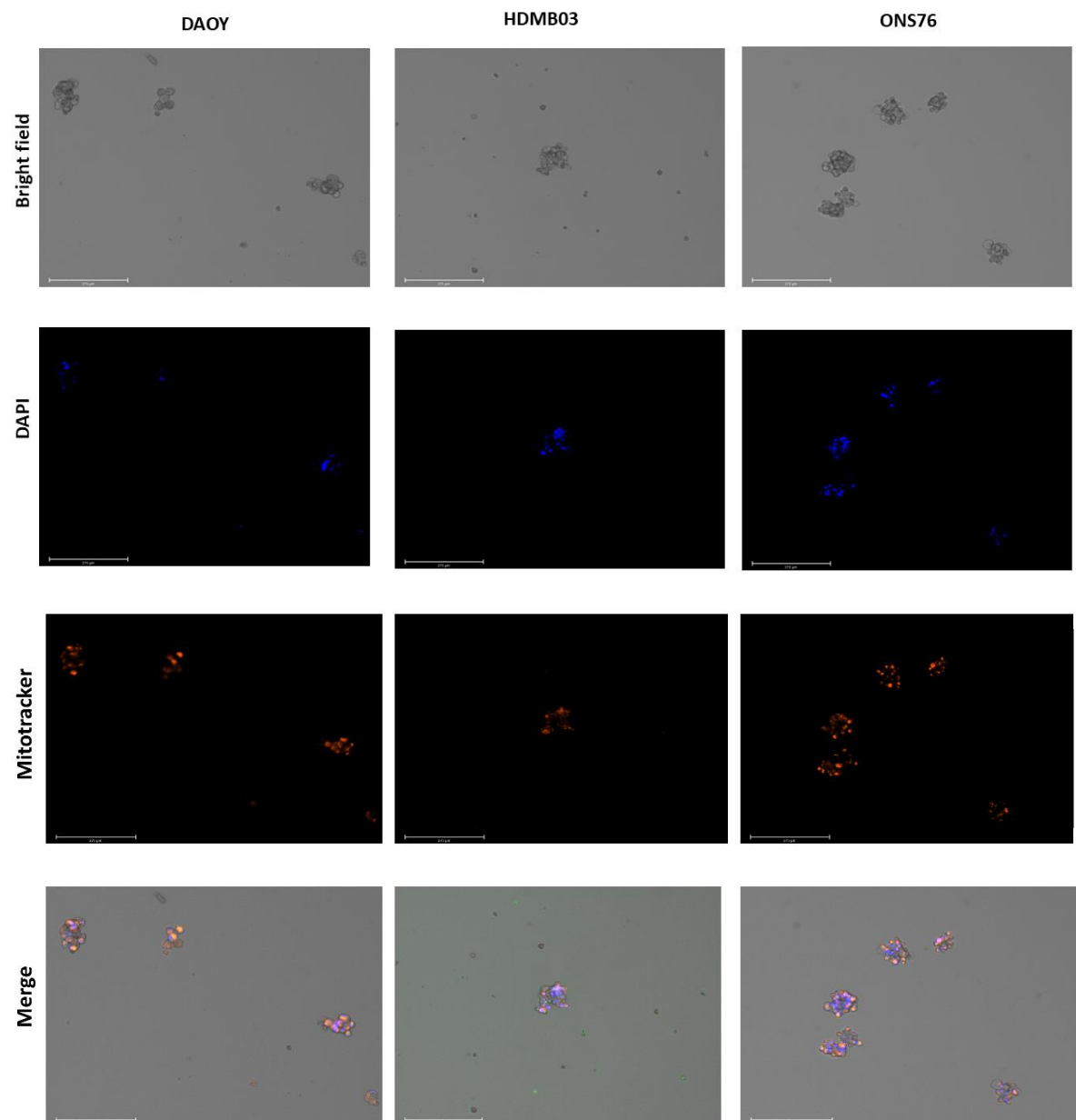
B
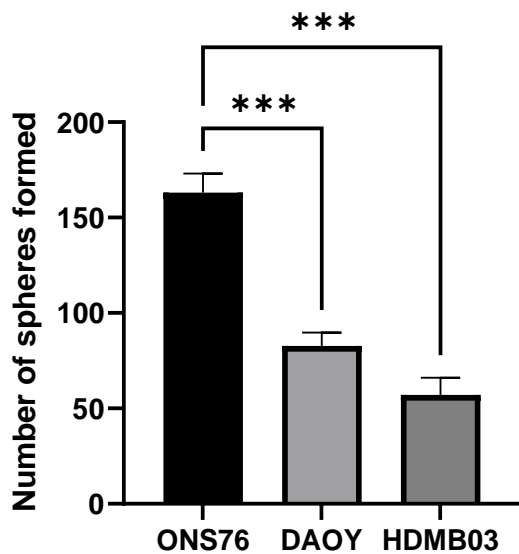
Figure 3.15- Spheroids formed from ONS76, HDMB03 and DAOY. (A) The spheroids were stained with live\dead stains and mitotracker to show viability. Scale bar is 200 μm. (B) Quantitation of the number of colonies formed from the three cell lines. Results shown are the average of three independent experiments carried out in triplicates. Error bars ± standard deviation. ***= p≤ 0.001.

To ascertain the viability of each spheroids produced, the spheroids were allowed to grow for five days (DAOY and ONS76) and 7 days (MB03) and stained with different viability dyes to determine if they were healthy spheroids. All the cell lines produced healthy spheroids as shown in Figure 3.15. However, the ONS76 cell line produced more spheroids compared to the other cell lines, while HDMB03 produced the least, as most of the spheroids produced were below 50 microns.

3.1.7 Bcl-xL encourages spheroid formation in medulloblastoma cell lines.

Inhibition of Bcl-xL has been shown in this study to sensitize ONS76 cells to vincristine and it was also discovered that ONS76 cells that escape apoptosis during vincristine treatment can evolve into polyploid cells and essentially cancer stem cells, therefore investigating the effect of Bcl-xL on the stem cell population in the ONS76 cells was important. To begin, the experiment was divided into three groups, in the first group, Bcl-xL was knocked down for 48 hours and then subjected to spheroid formation assay for 5 days. In the second group, cells from the slipped cells experiment were also plated in a non-adherent plate and subjected to spheroid formation assay. The third group consisted of the control group, where normal ONS76 cells were subjected to spheroid formation assay. After five days, the cells from each group

118

were counted and compared to the control group. As shown in Figure 3.16, there was a significant decrease in the number of spheroids produced in the siBcl-xL group, when compared to the control and comparison of the number of spheroids formed by the slipped cells and the control group revealed a significant increase in the number of spheroids.
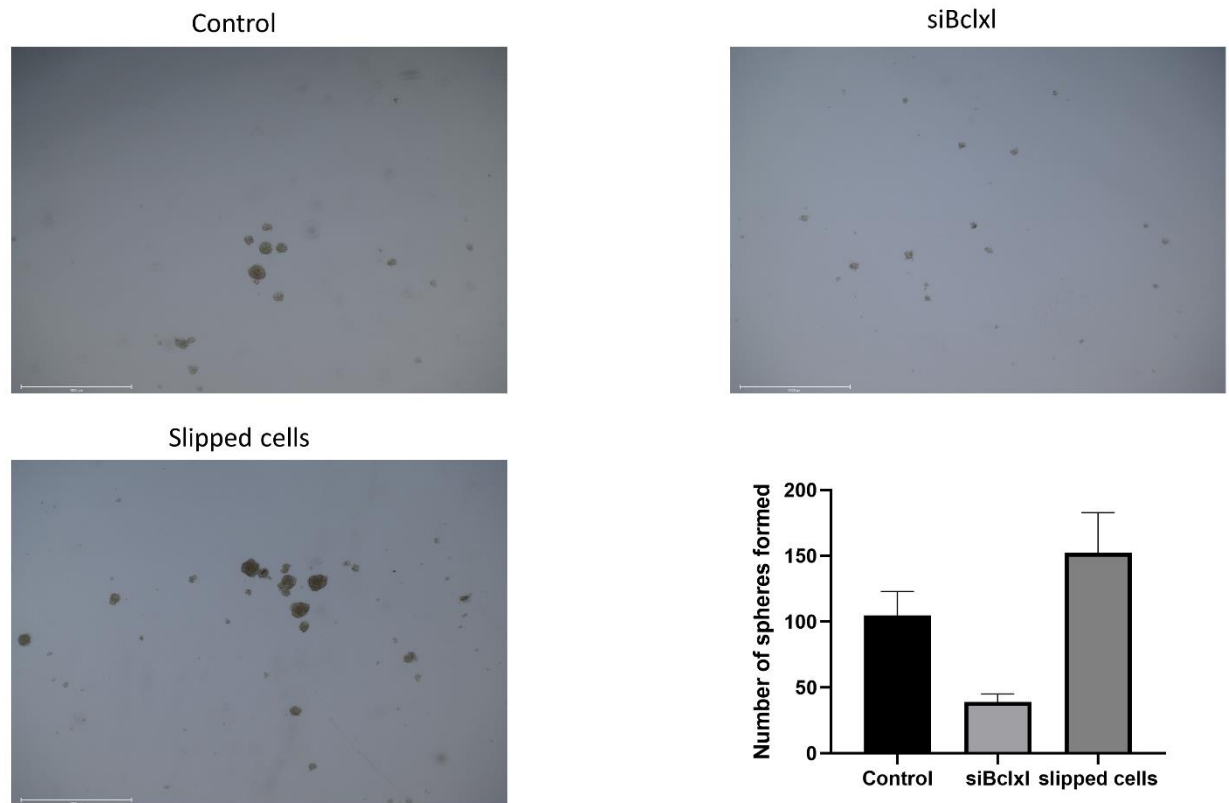
Figure 3.16- Bcl-xL knockdown reduces number of spheroids formed. The spheroids formed from the Bcl-xL knockdown cells and slipped cells were quantified and compared to the control group. Scale bar is 200 µm. Quantitation of the number of colonies formed from the three experiments. Results shown are the average of three independent experiments carried out in triplicates. Error bars ± standard deviation.
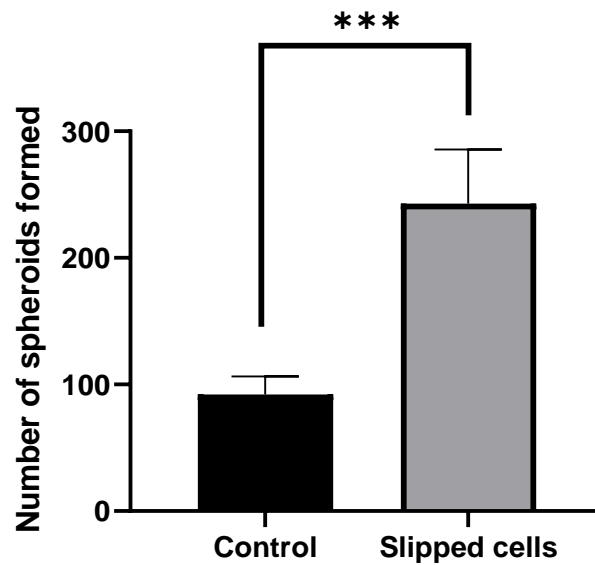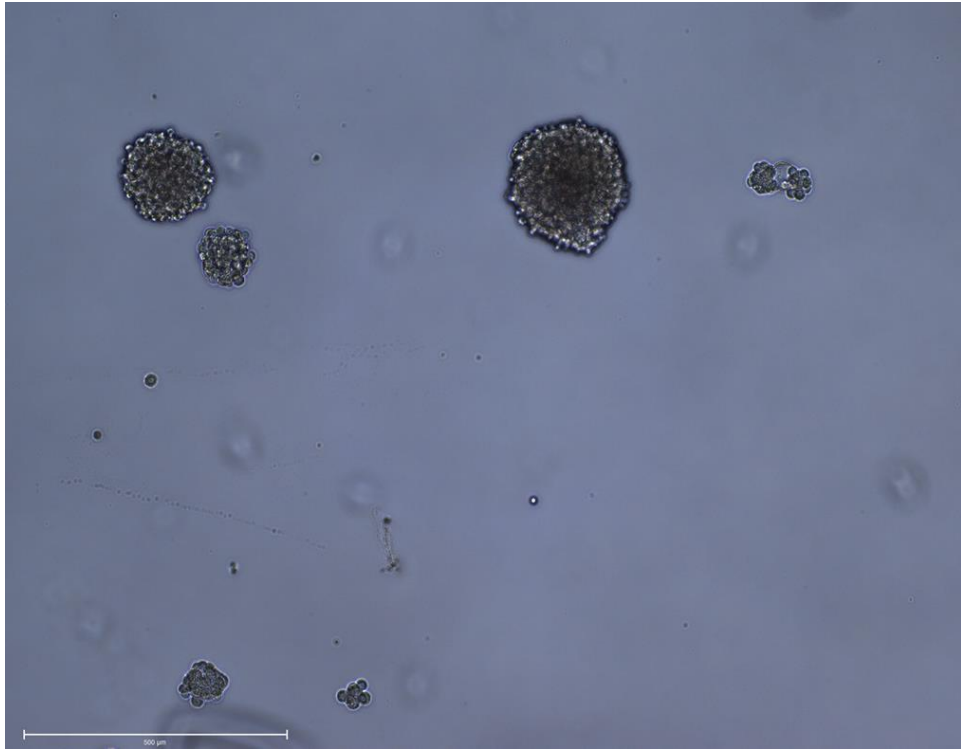
Figure 3.17- Spheroids produced from ONS76 cells.
Quantification of the diameter of the spheroids formed from ONS76 slipped cells and normal cells, measured using imagej. Twenty spheroids were analysed for each group. Scale bar is 200 μm. Data are represented as mean ± standard deviation of the mean (n = 3). ***= p≤ 0.001.

A closer look at the spheroids formed in the slipped group showed that the spheroids formed were bigger, when compared to the spheroids formed in the control group and the siBcl-xL group (Figure 3.17). A quantification of the diameter of the spheroids from each group,

120

confirmed that the spheroids from the slipped cells experiment was significantly bigger than the spheroids from the other groups.

3.1.8 Bcl-xL sensitizes slipped cells to vincristine.

The slipped cells have been shown to produce more and bigger spheroids when compared to the normal ONS76 cells, it was therefore of importance to determine if this slipped cells are more resistant to vincristine, when compared to the normal ONS76 cells.
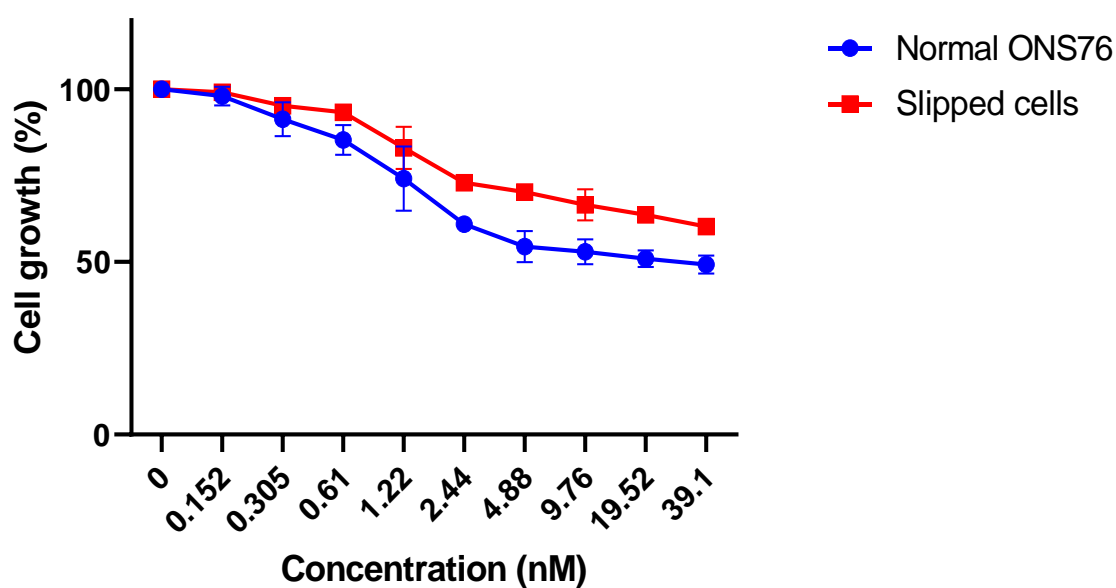
Figure 3.18- **Effect of vincristine on normal ONS76 cells and slipped ONS76 cells.**
Cells were exposed to serial dilution of vincristine for 72 hours and the results were analysed. Results shown are the average of three experiments carried out in triplicates. Error bars ± standard deviation.

To determine if the slipped cells have become resistant to vincristine, slipped cells and normal ONS76 cells were treated with 39.1 nM vincristine and the percentage cell growth was determined using the MTT assay. Results from this experiment, showed that the slipped cells were more resistant to vincristine when compared to the normal cells (Figure 3.18), with the slipped cells having a higher percentage cell growth when compared to the normal cells. The expression of the Bcl-2 family proteins has been shown to confer resistance in certain cell lines, therefore it was of interest to determine if the expression level of the anti-apoptotic proteins in the slipped cells played a role in conferring resistance to the cells. To determine this, protein was extracted from the cells at different passages and the expression level of the Bcl-2 proteins

121

was analysed (Figure 3.19). When compared to control, the slipped cells had a higher expression of Bcl-xL, however the increase in the expression of Bcl-xL did not commence until passage as the expression was similar to the control at passage 3.
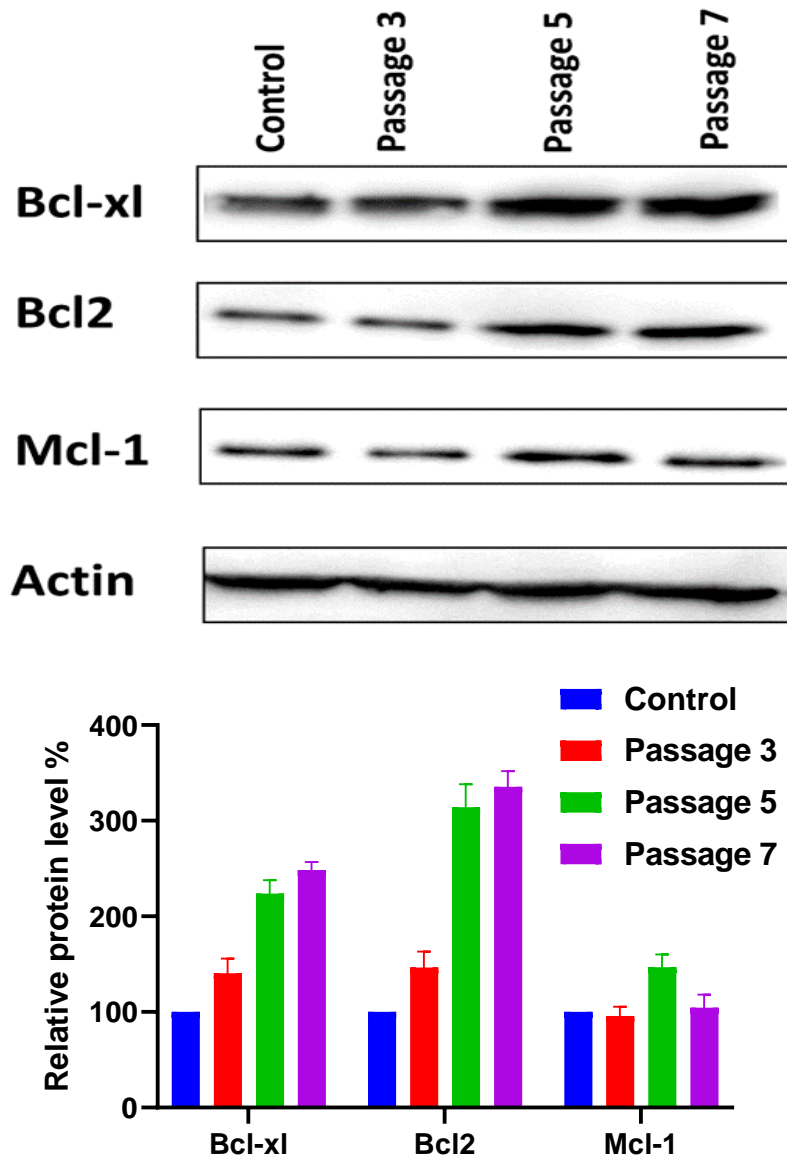
Figure 3.19- **Expression of Bcl-2 family proteins in slipped cells.**
Cells were treated with vincristine for 72 hours and surviving cells were grown in culture. Expression level of Bcl-xL, Bcl-2 and Mcl-1 was obtained by western blot using actin as a loading control after each passage. Each band was quantified by densitometric analysis and measured in relation to control. Each data point represents three independent experiments (n=3). Data are represented as mean ±standard deviation of the mean.

The expression of Bcl-2 in the slipped cells was compared to the control and similar to Bcl-xL, Bcl-2 expression was upregulated in the slipped cells at passage 5 and 7 when compared to the control. Taking the expression of Mcl-1 into consideration, there was no significant difference

between the expression of Mcl-1 in the different passages of the slipped cells when compared to the control. After confirmation of an increase in resistance to vincristine in the slipped cells, it was of interest to determine if the vincristine + WEHI 539 combination treatment, can also sensitize cells with acquired resistance to vincristine. The slipped cells were plated in a 96-well plate and treated with vincristine alone and another group treated with vincristine + WEHI 539 combination treatment for 72 hours and percentage cell growth was determined using MTT assay (Figure 3.20).
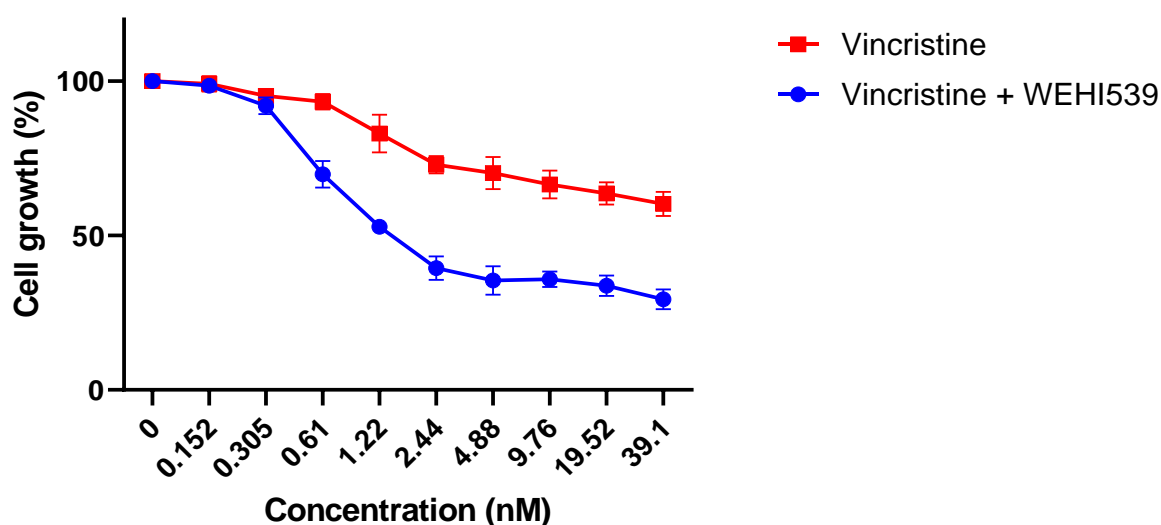
Cell line	Treatment	
	Vincristine	Vincristine + WEHI539
ONS76	N/A	1.79± 1.62 nM

Figure 3.20- **Effect of combination treatment of WEHI539 and vincristine on ONS76 slipped cells** - ONS76 slipped cells were exposed to serial dilution of vincristine alone and with a combination of vincristine + 0.195 μM WEHI539 for 72 hours and the results were analysed. C) IC50 values of Vincristine + WEHI539 treatment and vincristine only treatment, N/A indicates IC50 value is above highest concentration. Results shown are the average of three independent experiments carried out in triplicates (n=3). Error bars ±standard deviation.

When comparing the results of the vincristine only treatment to the result of the vincristine and WEHI 539 combination treatment, there was a significant reduction ($p \leq 0.001$) in cell growth in the vincristine + WEHI 539 combination treatment.

Subsequent to the discovery of the effect of Bcl-xL knockdown in reducing spheroid formation in ONS76 cells and also sensitizing slipped ONS76 cells to vincristine. It was of interest to determine if these results can be duplicated in the HDMB03 cell line, as they belong to a different and more aggressive subgroup of medulloblastoma (group 3). The MB03 cell lines showed an increase in polyploid population after treatment with vincristine and there was also an increase in mitotic slippage upon treatment with vincristine. To begin, the cells were treated with 15.6 nM vincristine for 72 h and the surviving cells were allowed to recover and continuously passaged. Prior to the spheroid formation assay, Bcl-xL knockdown using siRNA was confirmed in the MB03 cell lines, the cells were divided into four groups, the control group, the group transfected with control siRNA, the mock control group (lipofectamine only) and the group transfected with 80 nM of siBclxl. Transfection lasted for 48 hours after which protein was extracted and quantified and the expression of Bcl-xL in each group was analysed using western blot assay.
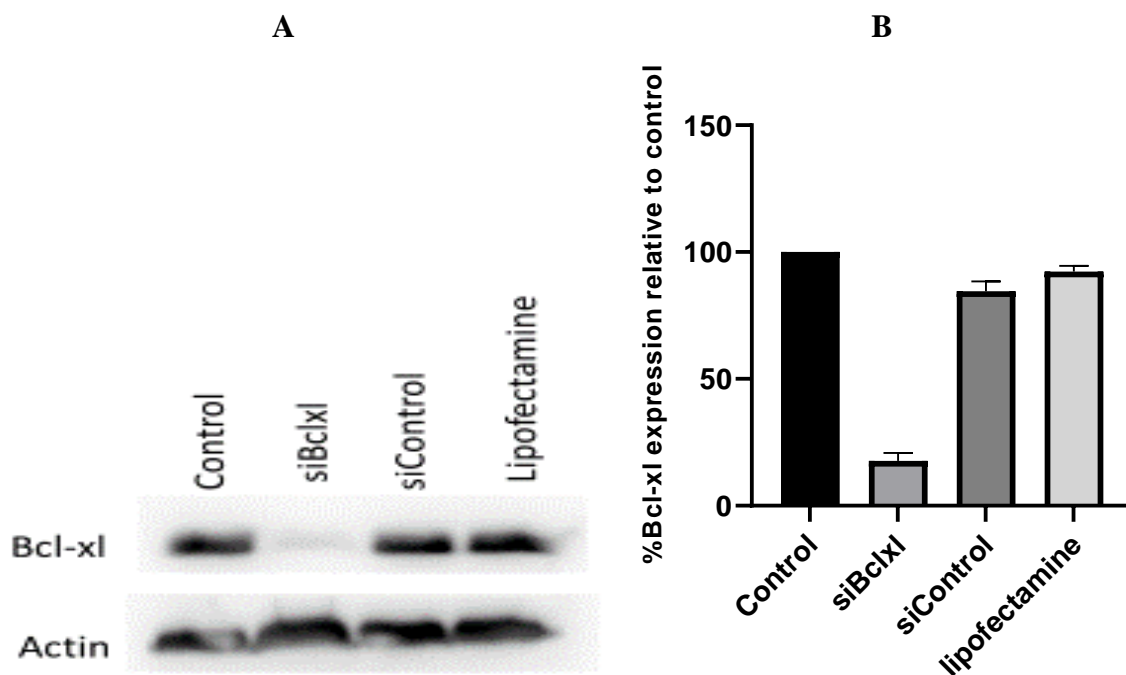
Figure 3.21 – Knockdown of Bcl-xL in HDMB03 cells- (A) Western blot analysis of Bcl-xL in HDMB03 cell line using actin as loading control. (B) Each band was quantified by densitometric analysis in relation to actin. Each data point represents three independent experiments (n=3). Data are represented as mean ±standard deviation of the mean.

When comparing the expression level of Bcl-xL in all the groups, there was a significant decrease ($p<0.05$) in Bcl-xL expression in the siBcl-xL group when compared to the control,

mock control and the sicontrol group. Thus, confirming knockdown of Bcl-xL in the HDMB03 cell lines after 48 h (Figure 3.21).

After confirmation of Bcl-xL knockdown using siRNA in HDMB03 cells and determining the effect of vincristine + WEHI539 treatment on the growth of HDMB03 cells as shown in Figure 3.6, the effect of combining siRNA knockdown with vincristine was compared to the vincristine + WEHI539 combination treatment results, to determine if both processes produce a similar effect.
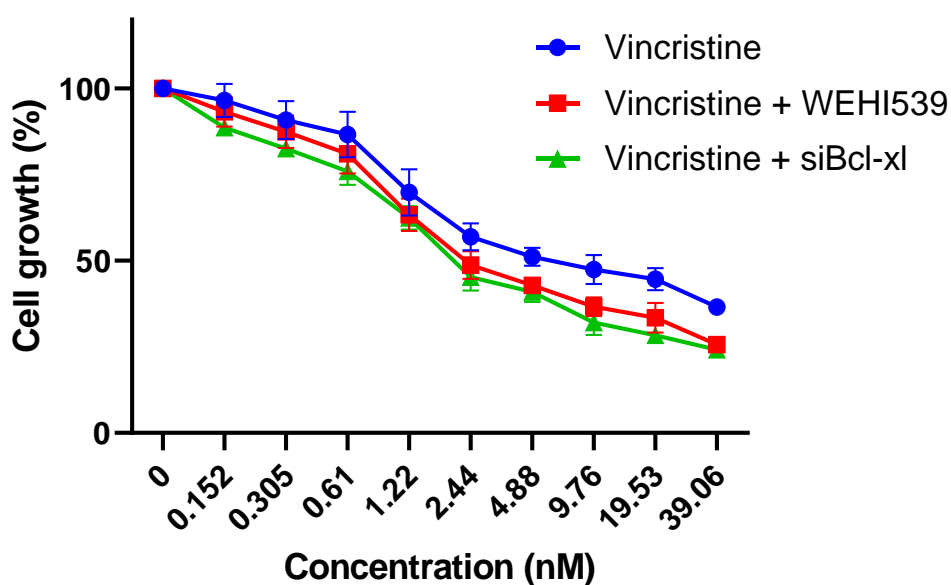
Treatment	IC50 (nM)
Vincristine	13.63±1.08
Vincristine + WEHI539	10.5± 1.55
Vincristine + siBcl-xL	9.47±1.11

Figure 3.22-**Effect of Bcl-xL knockdown on vincristine treatment in HDMB03 cells.** HDMB03 cells were exposed to serial dilution of vincristine for 72 hours and the results were analyzed. Results shown are the average of three experiments carried out in triplicates. Error bars ± standard deviation. The blue line shows cells treated with just vincristine, the red line shows cells treated with vincristine and WEHI 539 and the green line shows cells treated that Bcl-xL has been silenced with siRNA and then treated with vincristine.

The cells were divided into three groups, the first group was made up of cells treated with only the single vincristine treatment, while the second group were treated with the vincristine + WEHI539 combination treatment. The third group were cells transfected with siBcl-xL and treated with vincristine. The three groups were plated on the same 96-well plate and allowed to grow for 72 h, after which cell growth was analysed and as shown in Figure 3.22, knockdown

of Bcl-xL had a similar effect to inhibition of Bcl-xL using WEHI-539, as there was no significant decrease (p=0.25) between the percentage cell growth when comparing the group treated with only vincristine and the group treated with vincristine + siBcl-xL. There was a slight decrease in percentage cell growth when comparing the group treated vincristine + WEHI539 combination and the group treated with vincristine + siBcl-xL, however this reduction in cell growth was not significant (p= 0.14).

To determine if the slipped cells produced more spheroids when compared to normal HDMB03 cells the slipped cells and normal cells were subjected to spheroid formation assay for five days and the spheroids were counted and quantified.
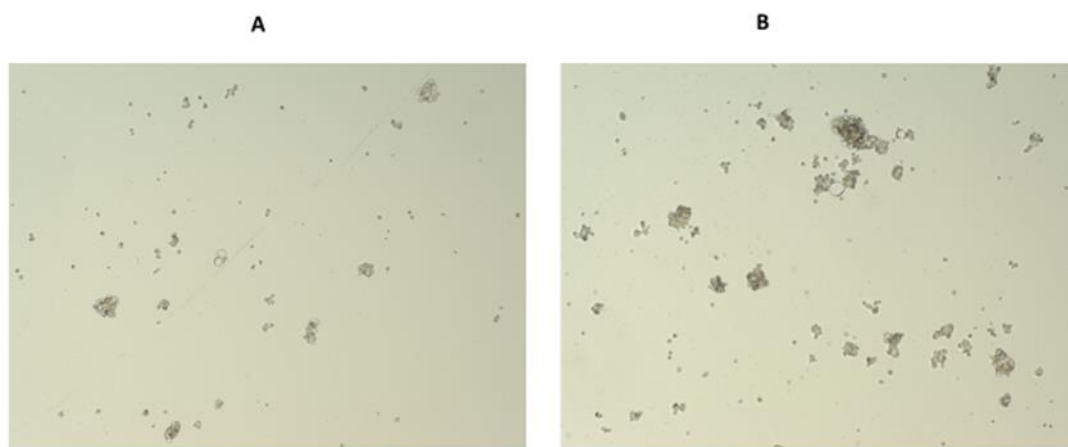
Figure 3.23- HDMB03 spheroids
(A) spheroids made from normal HDMB03 cells (control). (B) spheroids formed slipped HDMB03 cells.

Analysis of the spheroids formed from the HDMB03 cells (Figure 3.23) showed that the spheroids formed were not healthy as they disintegrated and looked like a clump of cells rather than spheroids. Due to this occurrence, it was decided to not proceed with the HDMB03 experiments.

3.2 Discussion

The main objective of anticancer treatment is to specifically induce cell death in order to achieve the highest level of tumour remission and ultimately cure the disease. The majority of current conventional treatments focus on DNA damage brought on by chemotherapy or radiation-induced apoptosis (Kastan & Bartek, 2004). Recently, novel approaches to cancer treatment, such as monoclonal antibodies or small pharmacological inhibitors that inhibit growth factor receptor signalling, have been successfully developed as single treatment or in combination with other treatments. Despite these developments, the majority of people with metastatic malignancies pass away from their illness. Chemotherapy is a crucial component of the all-encompassing care for different cancers (Fajka-Boja *et al.*, 2018). For many different forms of human cancers, including breast cancer, medulloblastoma and ovarian cancer, colchicine, vincristine, and other anti-mitotic drugs are frequently employed as first-line of treatment (van Vuuren *et al.*, 2015). Since its discovery in 1961, vincristine has been used as a chemotherapeutic drug to treat various types of cancers which includes medulloblastoma, non-Hodgkin's lymphoma and neuroblastoma. Although chemotherapeutic drugs have been very effective in the treatment of cancer, its success has been marred by patient relapse. About 20-30% of patients with standard risk medulloblastoma experience relapse after treatment with chemotherapeutic drugs, relapse arises when cancer cells become resistant to chemotherapeutic drugs. Reducing the overall dose utilised is one method that can be used to lessen the negative effects of chemotherapeutic drugs. Induction of cell death is a crucial component of cancer treatment. Certain tumour forms were shown to be responsive to this sort of medication in the clinical context, and in such instances, the tumour disappeared after numerous chemotherapy regimens. In this study, an adjuvant treatment approach to improve efficacy and possibly lessen toxicity was investigated to address this problem. During a prolonged mitotic arrest, the fate of the cell is determined by the balance between the pro survival proteins such as Bcl-xL and Mcl-1 and the pro apoptotic proteins, however previous studies have shown that in the absence of pro survival proteins, mitosis alone is stressful to the cell and can trigger apoptosis, thus highlighting the importance of pro survival proteins for cell survival during prolonged mitotic arrest (Bennett *et al.*,2016).

In light of this, it was hypothesized that the Bcl-2 family anti-apoptotic proteins might play a role in the resistance of medulloblastoma cells to vincristine.

Inhibition of Bcl-xL sensitizes cancer cells to vincristine.

The cell death pathway is significantly regulated by the Bcl-2 family of anti-apoptotic proteins and overexpression of the Bcl-2 family proteins has been documented in a wide range of malignancies ever since it was first discovered. According to studies, increased Bcl-2 expression results in chemotherapeutic treatment resistance. Recent research on the structure-function relationships between these proteins, their interactions with other nonhomologous proteins, and their control by protein phosphorylation and the design of small molecule inhibitors that can inhibit these proteins is starting to make suggestions for possible methods of reducing the relative resistance of many types of cancers to apoptotic stimuli like chemotherapy and radiation. To begin, the effect of the expression level of the Bcl-2 family proteins on cell survival after treatment with vincristine was analysed, by initially determining the basal expression level of three of the anti-apoptotic Bcl-2 family protein. The basal expression level of the anti-apoptotic proteins Bcl-xL, Bcl-2 and Mcl-1 was determined by western blot in three medulloblastoma cell lines ONS76, DAOY and HDMB03 and the results shown in Figure 3.1 showed that the expression level of Bcl-xL was highest in ONS76 while the expression level of Bcl-2 was highest in DAOY. This suggested that the main functioning anti-apoptotic protein in ONS76 cells might be Bcl-xL and in DAOY cells is Bcl-2. HDMB03 cells however did not show any preference for any of the antiapoptotic proteins as the basal expression level of all three anti-apoptotic proteins was similar.

The expression level of Mcl-1 was similar among all cell lines, this was as expected, as previous studies have shown that Mcl-1 is continuously produced and degraded during mitosis and complete degradation of Mcl-1 during mitosis heralds' apoptosis (Sloss *et al*. 2016). The three medulloblastoma cell lines were then treated with vincristine and all three cell lines responded differently to the vincristine treatment, with the DAOY cell line being more sensitive when compared to the ONS76 and HDMB03. This is indicative of why different treatments have to be tailored for different patients as although all three cell lines are medulloblastoma, they belong to different subgroups of medulloblastoma and heterogeneity exists between subgroups and within subgroups. The DAOY and ONS76 cell lines belong to the same some group (SHH), however a distinct difference between both cell lines is their p53 status, DAOY cells have a mutated p53, while the ONS76 has wild type p53. Vincristine treatment was combined with various small molecule modulators of the anti-apoptotic protein. The effect of inhibition of Mcl1 on sensitivity to vincristine treatment was determined by comparing the maritoclax + vincristine combination treatment with the vincristine treatment only, there was no significant

difference in the % cell growth across all the cell lines. This was interesting to see, as all the cell lines had a similar expression of Mcl1, however, it was important to consider that Mcl1 has been shown to be continuously degraded during prolonged mitotic arrest and knockdown of Mcl-1 can only induce apoptosis in cells that over express Mcl-1 and have low level of the other anti-apoptotic proteins (Shi *et al*., 2011), therefore inhibition of Mcl-1 would not make a huge shift in cell viability or reduce mitotic slippage as Mcl-1 is already degraded. Using WEHI 539 to inhibit Bcl-xL expression in the three cell lines, the effect of Bcl-xL on cell survival after vincristine treatment was determined. WEHI539 was combined with vincristine and when compared to the vincristine only treatment, there was a significant decrease in % cell growth in the ONS76 cell line, this was not replicated in the other cell lines as the DAOY and HDMB03 cell lines did not show a significant difference in % cell growth. Previous studies by Galan-Malo *et al* on the role of Bcl-xL and Mcl1 on vincristine-induced mitotic arrest was carried out by over expressing Bcl-xL and Mcl1 in two cancer cell lines and the response of the cells to vincristine was examined. Both cell lines showed a lag in loss of mitochondrial membrane potential ($\Delta\Psi$m), but the cell line overexpressing Bcl-xL had a lower percentage of cells with loss of ($\Delta\Psi$m). This indicates that Bcl-xL protects cells from vincristine-induced apoptosis more than Mcl-1 does, as evidenced by their higher mitochondrial membrane potential (Galan-Malo *et al*., 2012).

Bcl xl encourages stemness in medulloblastoma cell lines.

According to Havas *et al*., following treatment with vincristine, an accumulation of polyploid cells were noticed and it was attributed to the fact that the cells slipped out of mitosis after a prolonged mitotic arrest in their tetraploid state without dividing (Havas *et al*., 2016), the introduction of polyploidy by antimitotic drugs has been linked to drug resistance (Denisenko *et al*., 2016). The ability of polyploid cells to survive after mitotic slippage leads to aneuploidy which plays a huge role in cancer progression (Coward *et al*., 2014). It was therefore important to determine if cells that escape vincristine induced cell death are able to survive different cycles of cell division and if they do develop into polyploid cells is the combination treatment able to sensitize the polyploid cells to vincristine.

To begin, the fate of cells that escape apoptosis through mitotic slippage after a single vincristine treatment was explored. ONS76 cells were treated with 39.1 nM of vincristine in a 6-well plate to induce mitotic slippage. After 72 hours, these "slipped" cells were then transferred into a T-75 flask and grown in 2D culture. However, it was noticed that the growth

rate of the cells was really slow and it took about a week to reach about 50% confluency compared to the three days it takes for normal ONS76 cells take to reach 90% confluency when grown under the same conditions, this suggested that the cells might have developed a tactic to evade apoptosis by increasing the time spent in mitosis as previous studies have shown that as the time a cell spends in mitosis increases, the death signal for apoptosis diminishes and once this elapses the cell can exit mitosis (LaraGonzalez et al., 2012). It was also discovered, that due to modifications in transcription and translation, murine embryonic fibroblasts with additional chromosomal copies similar to polyploid cancer cells undergo cell division less frequently (Rao et al., 2005). Additionally, co-regulation of cell growth, size, and division ensures that cells are large enough to divide during mitosis with smaller cells postponing the G1 to S phase transition until they are large enough to retain viable progeny following cell division (Dolznig et al., 2004). However, compared to their diploid equivalents, polyploid cancer cells have a cell volume that is thrice as large (Zhang et al., 2014) and a feasible theory derived from both data, suggests that due to the size criteria cells have to meet before cell division can take place, the larger polyploid cancer cells are stuck in the G0/G1 phase. The increased and uneven chromosomal copy number imposed on polyploid cancer cells which increases transcriptional and translational demands eventually hinders the G0/G1 arrest, which results in the cell replicating (Coward & Harding, 2014).

After the third passage of the cells as shown in Figure 3.13, huge polyploid cells began to appear, these cells were 3-4 times bigger that the normal ONS76 cells, this confirms previous suggestion that mitotic slippage leads to polyploidy. This was in line with previous studies which showed that when exposed to chemotherapy, some cells in the population do not undergo apoptosis but rather evolve into polyploids (Li et al., 2014). In the clinical context, patients who have malignancies with polyploid subclones have a worse prognosis, and polyploid cancers are very resistant to conventional radiotherapy and chemotherapy treatments (Nano et al., 2019). The development of polyploids was therefore thought to be related to tumour resistance. In passage 4, some of these cells had started to change morphology and develop structures that look like dendrites, similar to neurons, this was indicative of differentiation, which is a property of stem cells, which suggests that mitotic slippage promotes stemness and that the cells differentiated as the stem cells did not have the required nutrients to grow. However, after studying the cells closely for a while and combing the literature to understand this phenomenon, it was discovered that the cells with a change in morphology were also

undergoing reproduction and creating new daughters through a process called budding which might have been responsible for the change in morphology of some of the cells to resemble neurons (Zhang *et al*., 2014) (Sundaram *et al*., 2004). This also suggests a possible answer to why the polyploid cells were taking longer to replicate as this was no longer done through mitosis but through budding which is a form of reproduction used in yeast (Knop, 2011). This is line with results from Fei *et al.,* (2019) who showed that PGCCs stimulated with CoCl2 and paclitaxel exhibit cancer stem cell characteristics and produce daughter cells asymmetrically through budding (Fei *et al*., 2019). This process of cell division will make these polyploid cells resistant to vincristine as vincristine functions through mitotic arrest. Although previous studies suggested that formation of polyploid cells can be induced by anti-mitotic drugs, however these cells were not stable and are often on the verge of mitotic catastrophe and apoptosis (Vakifahmetoglu *et al*., 2008), this was however different to what was observed in this experiment as the polyploid cells were dividing and stably passaged and by passage 5, there was an explosion of small daughter cells formed from budding of the polyploid cells, the cells were cultured for several passages and were still stable and replicating. The resulting daughter cells from the PGCC play a pivotal role in drug resistance as Zhang *et al* showed that the daughter cells produced from the PGCCs had significantly increased migratory and invading characteristics (Zhang *et al*., 2004). Another characteristic of the PGCCs to take into consideration is that although the PGCCs began to appear within 7 days post vincristine treatment, it may take several weeks after the treatment before polyploid/multinucleated giant cell offspring emerge. While their nuclear budding and depolyploidization processes can start at any time after emergence, it can take weeks or even months for a stable population of daughter cells to start dividing quickly. As a result, such cells cannot be accounted for in commonly used cell-based tests, such as the "long-term" (two-week) colony formation assay, which is regarded as the industry-standard method for evaluating chemosensitivity. Puig *et al*., (2008) showed that unless the trials are prolonged to more than 35 days after anticancer therapy, polyploid/multinucleated giant cells and their tumour-repopulating descendants might not be taken into consideration in standard *in vivo* tumour growth delay assays. However, the majority of anticancer drug discovery techniques stop at this crucial moment after administration (Puig *et al*., 2008).

The biology of medulloblastoma cancer stem cells is still poorly understood, despite the identification and isolation of cancer stem cells in different haematopoietic malignancies and other solid tumours since the 1970s (Battle & Clevers, 2017). The failure of current therapies

to reliably eradicate tumour cells may be explained by the presence of cancer stem cells within a population of medulloblastoma cells. The majority of cancer cells may be targeted by treatments, however leftover medulloblastoma cancer stem cells may replenish the cancer cell population, leading to tumour recurrence after chemotherapy. Determining and creating new treatment targets for selectively eliminating this cell type is therefore becoming more and more important. To begin it was imperative to determine the CSC population in ONS76, DAOY and HDMB03 cells as shown in Figure 3.15 the ONS76 cells formed the most spheroids when comparing all three cell lines, while the MB03 cell lines had the least number of spheroids. Variations in shape and spheroid forming capacity amongst the medulloblastoma cell lines was noted. Spheroids were generated by SHH cell lines (DAOY and ONS76), which grow continuously in conventional culture and are extremely reproducible. HDMB03 the group 3 cell line on the other hand, which often grows semi-adherently in 2D culture formed looser spheroids. Therefore, it is possible that the observed variance in 3D spheroid morphology between cell lines reflects the underlying phenotype of each cell type. It has been demonstrated in the past that invasive, aggressive cell lines like HDMB03 are more likely to produce looser 3D structures (Gayan *et al*., 2017). It was decided to investigate if the slipped cells which have adapted polyploidy show a difference in the CSC population when compared to the parent cells. After passage five which was 7 weeks after the initial treatment of the cells with vincristine, the ONS76 slipped cells were trypsinised and 5000 cells were grown in DMEM F12 medium to encourage spheroid formation, the number of spheroids produced were counted and the "slipped" cells produced more spheroids when compared to the control, however, the spheroids produced by the slipped cells were noticeably bigger than the spheroids produced from the control cells. This suggests that giant polyploid cells produce bigger spheroids.

Mitotic slippage confers resistance on medulloblastoma cell lines.

To determine if these polyploid cells were resistant to vincristine, polyploid ONS76 cells and normal ONS76 cancer cells were treated with vincristine and cell viability was determined with MTT assay. Although Havas *et al.,*(2016) showed that cells that undergo polyploidy were more sensitive to vincristine, in this study, the polyploid cells had higher cell viability when compared to the normal ONS76 cells which indicates that these slipped polyploid cells have developed some sort of resistance to vincristine. Recent research has demonstrated a connection between polyploidy and chemo-resistance: cisplatin treatment was proven to be ineffective against polyploid cancer cells, and cisplatin treatment caused the production of 4N

tetraploidy in HCT116 cisplatin-resistant clones (Mirzayans *et al.*, 2018). The ability of polyploid cells to produce viable offspring, which could result in treatment resistance or more aggressive secondary tumours, means that polyploidization is not a 100% guarantee of apoptosis. The ONS76 cells which had the highest expression of Bcl-xL also had the highest incidence of mitotic slippage post vincristine treatment, therefore it was important to determine if these ONS76 slipped cells had an increased expression in Bcl-xL. Western blot was carried out to determine the expression level of Bcl-xL in the polyploid cells compared to the normal cells. The polyploid cells showed a higher expression of Bcl-xL compared to the control and an interesting observation was the increase in Bcl-xL only began at passage 5, it is important to know that passage 5 was when there was an explosion of daughter cells from the giant polyploid cells. This result was in line with previous studies where unlike control cells, daughter cells produced by PGCCs following radiation and chemotherapy exhibited a mesenchymal phenotype and expressed proteins involved in the epithelial-mesenchymal transition, such as N-cadherin, vimentin, Twist, Slug, Snail, and CK7 (Fei *et al.*, 2019). These daughter cells were also shown to possess stronger invasion and migration ability (Zhang *et al.*, 2014a) (Zhang *et al.*, 2014b). This indicates that Bcl-xL does not just encourage stemness, but it encourages the growth and survival of polyploid cells. The result from the cell cycle analysis showed HDMB03 cells showed an increase in polyploid population after 48 hours of vincristine treatment, to investigate this even further, HDMB03 cells were treated with 15.6 nM vincristine for 72 hours and grown in DMEM-F12 medium to encourage spheroid formation. After 5 days the plates were checked for spheroids, more spheroids were formed from the slipped cells, however the spheroids formed by the HDMB03 cells were not of good quality as they looked like cells that clumped together rather than spheroids.

Conclusion

Understanding Bcl-xL and the BCL-2 family members more generally will help clarify why some malignancies are more responsive to chemotherapy than others, how conventional chemotherapy kills cancer cells in a selective manner, and how tumours advance molecularly. In conclusion, this research showed that Bcl-xL promotes cell survival in cancer polyploid cells generated by vincristine. Additionally, combining a Bcl-xL inhibitor with a polyploid inducer results in improved efficacy and anti-proliferative effect *in vitro*. Furthermore, these findings indicate the prospective therapeutic use of WEHI 539, which specifically targets and exploits

the polyploid phenotype in cancer. Results from this study further highlights the need of focusing on BCL-2 family members to eradicate CSC-resistant populations. Bcl-xL is therefore a target for polyploidy resistance, and cells that overexpress Bcl-xL are more susceptible to vincristine upon Bcl-xL inhibition, supporting the idea that WEHI539 is a promising strategy for overcoming vincristine resistance exhibited in medulloblastoma cells.

Future Work

Based on the preliminary results of this experiment, further studies will be required to validate the role of Bclxl in conferring stemness to cancer cells. This can be done by analysing the expression levels of stem cell biomarkers such as CD133, Nano g and Sox 2 in the polyploid ONS76 cells. The expression level of these biomarkers before and after slippage and also before and after polyploidy will determine if mitotic slippage encourages stemness.

From the results, Bcl-xL knockdown was able to sensitize high expressing Bcl-xL ONS76 cells to vincristine. Testing a broader range of cell lines with high expression of Bcl-xL across various cancers can also be used to determine if this efficacy of sensitization to vincristine by Bcl-xL knockdown can be reproduced across various cancer types. For cells with low expression of Bcl-xL such as DAOY and HDMB03, other inhibitors of apoptosis such as XIAP and CIAP can be explored.

Vincristine has been shown to be ineffective in the treatment of various types of cancers such as colorectal cancer. Further studies where Bcl-xL knockdown is combined with other chemotherapeutic drugs such as cisplatin and oxaliplatin could be carried out.

Finally, Bcl-xL has been identified as a promising candidate to sensitize medulloblastoma cells to vincristine *in vitro*, further studies *in vivo* using mouse models can be carried out to validate the results from this study.

CHAPTER 4: TARGETING HCP5 IN CANCER CHEMOTHERAPHY

4.1 Results

4.1.1 HCP5 is overexpressed in cancer cells.

To begin this project it was important to determine the role HCP5 plays in cancer and if HCP5 was upregulated in cancer cells. An *in silico* analysis was carried out to determine the expression of HCP5 across different cancers compared to the corresponding healthy tissue. The RNA-sequence of 16 tumours and normal corresponding tissues was analysed using the TCGA and GTEx database which was accessed using GEPIA (http://gepia.cancer-pku.cn/). The expression of HCP5 was higher in 16 different tumours when compared to the normal corresponding tissue. This was also seen in colon adenocarcinoma tumours (Figure 4.1).
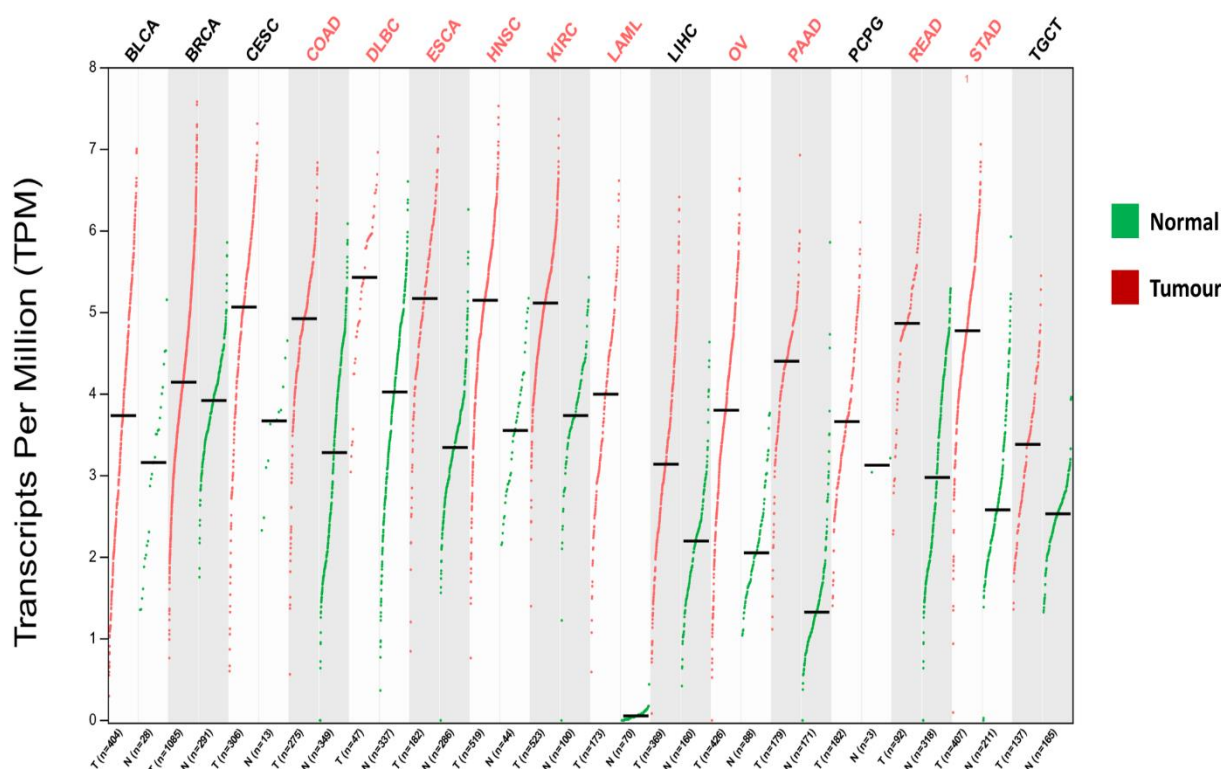
Figure 4.1- **Gene expression profile across tumour samples and paired normal tissues.** Comparison of the expression of HCP5 in normal and tumour tissues across various cancers from the TCGA database. The cancers written in red signify a significant increase in the expression of HCP5 in the tumour tissue when compared to the healthy tissue. Bars indicate the mean expression. Statistics was carried out using one way analysis of variance (ANOVA) and q-value cut off was set for 0.01. $p<0.05$ was considered to be significant. **Abbreviations** BLCA-Bladder Urothelial Carcinoma, BRCA-Breast invasive carcinoma, CESC-Cervical squamous cell carcinoma and endocervical adenocarcinoma, COAD-Colon adenocarcinoma,

DLBC-Lymphoid Neoplasm Diffuse Large B-cell Lymphoma, ESCA-Oesophageal carcinoma, HNSC-Head and Neck squamous cell carcinoma, KIRC-Kidney renal clear cell carcinoma, LAML-Acute Myeloid Leukaemia, LIHC-Liver hepatocellular carcinoma, OV-Ovarian serous cystadenocarcinoma, PAAD-Pancreatic adenocarcinoma, PCPG-Pheochromocytoma and Paraganglioma, READ-Rectum adenocarcinoma, STAD-Stomach adenocarcinoma, TGCT-Testicular Germ Cell Tumours.

HCP5 was overexpressed in the tumour tissue when compared to the healthy tissue in 10 (including CRC) of the 16 cancer types analysed, while the other six also showed an increase in HCP5 expression, however this increase was not significant. Due to the unavailability of medulloblastoma expression data on the TCGA database, comparison of the expression data of HCP5 in medulloblastoma and CRC was carried out from the R2 database, which was accessed using the R2 software (https://r2.amc.nl/).
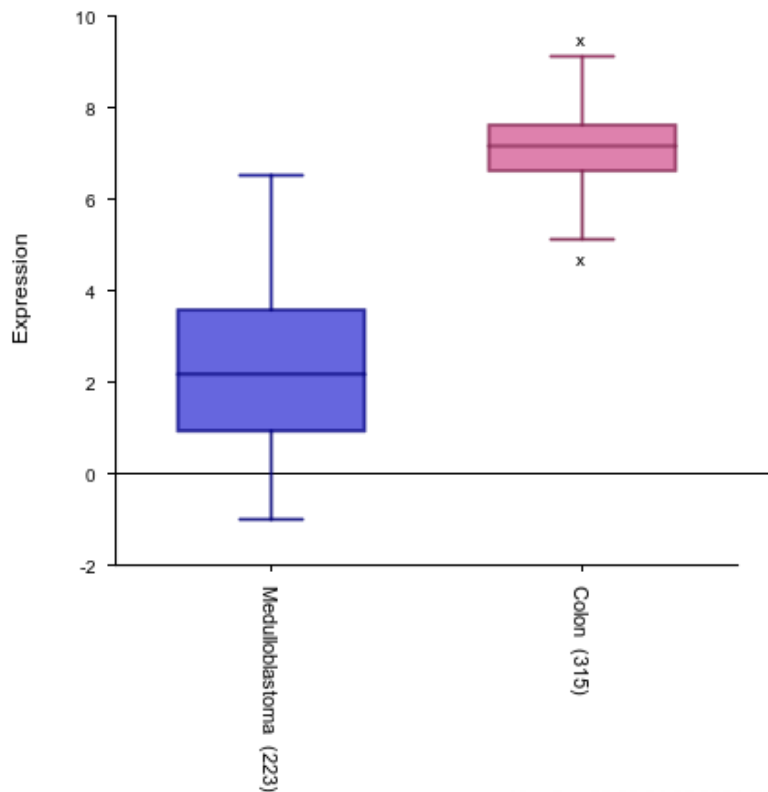
Figure 4.2- **Expression of HCP5 in medulloblastoma and colorectal cancer tumours.**
The expression data of tumour samples from 223 medulloblastoma patients obtained from Northcroft *et al* and 315 CRC patients obtained from the international genomics consortium database was analysed for the expression of HCP5 using the R2 software. Each box represents the mean expression. Error bars ±standard deviation. Statistics was carried out using one way analysis of variance (ANOVA), x indicates significant difference ($p<0.05$)

To corroborate the results from the *in-silico* analysis, the expression of HCP5 in medulloblastoma and CRC cell lines was determined using qPCR. The results shown in Figure 4.3 show that CRC cell lines SW480, LOVO, HCT116 and SW48 had higher expression levels of HCP5 compared to the medulloblastoma cell lines. This is in line with the expression of HCP5 in medulloblastoma and CRC tumours analysed from the TCGA database (Figure 4.2). SW48 had the highest expression of HCP5 in all eight cell lines used and DAOY had the highest expression of HCP5 amongst the medulloblastoma cell lines. To proceed with the project, it was decided to focus on four cell lines with the highest expression of HCP5, three CRC cell lines (SW480, HCT116 and SW48) and one medulloblastoma cell line (DAOY).
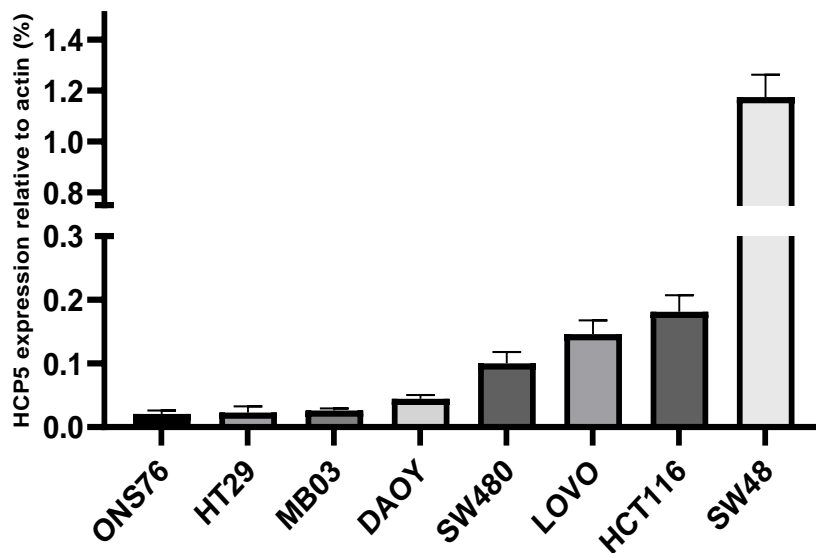
Figure 4.3 – Expression of HCP5 in colorectal cancer and medulloblastoma cell lines
Expression level of HCP5 in reference to actin was determined by qPCR. Each data point represents three independent experiments, carried out in triplicates (n=9). Analysis of data was carried out using the $2^{-\Delta Ct}$ method. Error bars ± standard deviation.

4.1.2 Expression of DNA damage repair genes in medulloblastoma and colorectal cancer cell lines.

Previous studies have shown a relationship between the lncRNA HCP5 and the YB-1 protein (Wang *et al*., 2020). However, YB-1 has also being shown to modulate the activity of some

DNA repair proteins such as the BER proteins NEIL1, NEIL2 and NTH1 *(Das et al*., 2007; Guay *et al*., 2008). Therefore, it was decided to determine if there was any direct correlation between HCP5 levels and specific DNA repair gene expression.

Initially, qualitative RT-PCR for the three *NEIL* genes was carried out on the two CRC cell lines (HCT116 and SW48) that showed the highest levels of HCP5 expression and the DAOY medulloblastoma cells. Gene specific primers were designed to anneal to different exons as described in Section 2.6, to differentiate between the mRNA and any contaminating genomic DNA in the sample. Table 2.5 indicates the size of product expected from the PCR for each gene.

4.2.1 Evaluation of the expression of *NEIL1, NEIL2* and *NEIL3.*

To begin, total RNA from three of the cell lines was converted to cDNA by reverse transcription and then subjected to RT-PCR to determine the expression level of three DNA glycosylases *NEIL1*, *NEIL2* and *NEIL3* and confirm primer specificity.
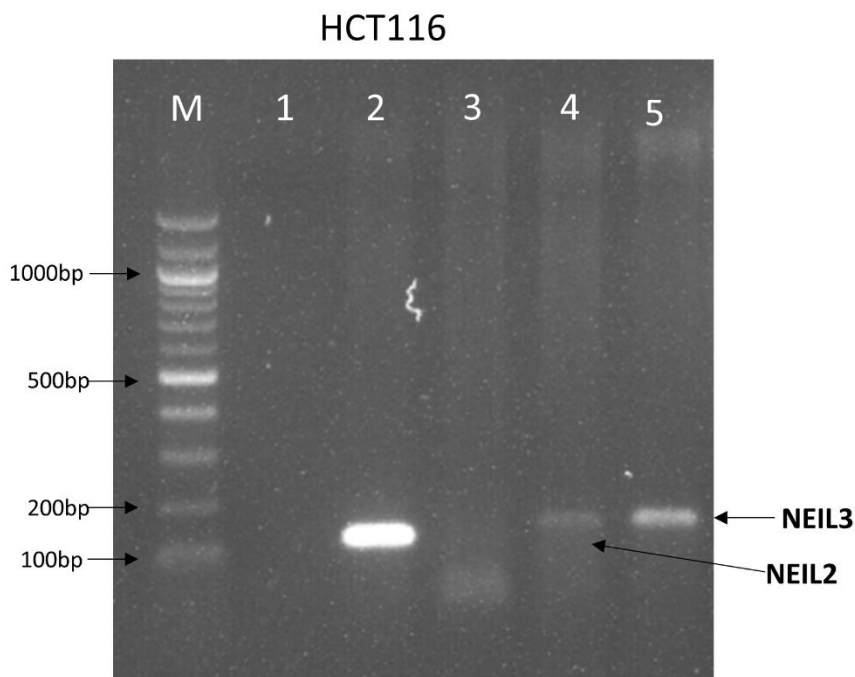
Figure 4.4 - Agarose gel electrophoresis showing *NEIL1*, *NEIL2* and *NEIL3* expression in the HCT116 cells.
Lane M showing 100 bp Hyperladder, lane 1- negative control, lane 2- GAPDH expression at 120 bp, lane 3- *NEIL1*, lane 4- *NEIL2* at 145 bp, lane 5- *NEIL3* at 147 bp.

Figure 4.4 shows an agarose gel electrophoresis of RT-PCR products of cDNA prepared from total RNA of HCT116 cells. The basal expression level of *NEIL1*, *NEIL2* and *NEIL3* in this cell line was determined. A band for *NEIL1* was absent in lane 3 which indicates it is not expressed in the cell line or it is expressed at a low level. A band which indicates expression of *NEIL2* was seen in lane 4 and a band which indicates expression of *NEIL3* was present in lane 5. *NEIL3* was expressed at a higher level compared to *NEIL2*, at least by this semi-quantitative method.
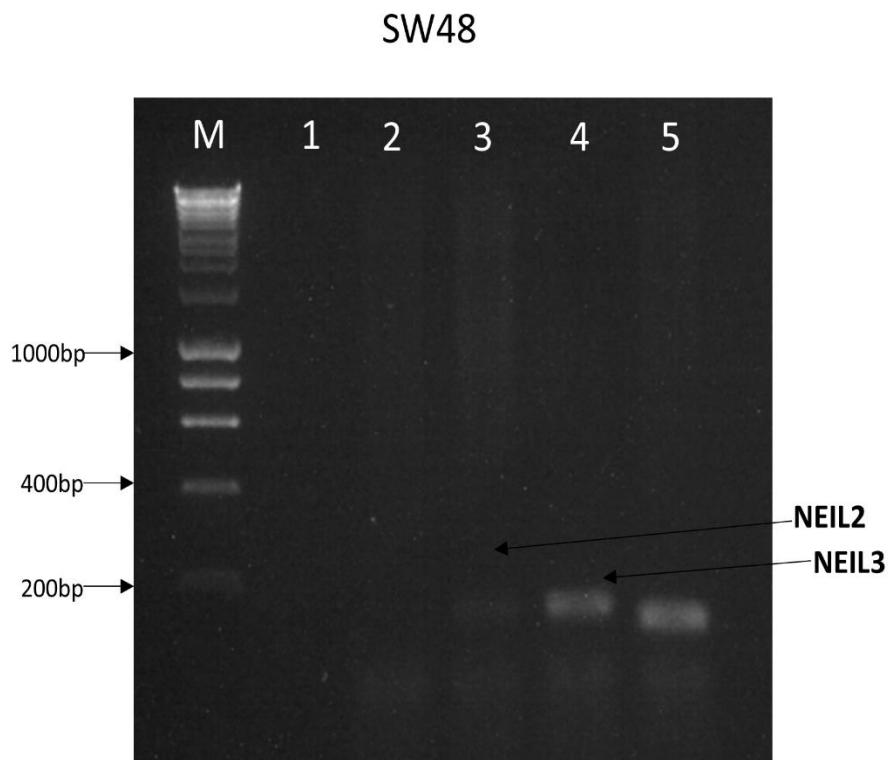
Figure 4.5 - Agarose gel electrophoresis showing *NEIL1*, *NEIL2* and *NEIL3* expression in the SW48 cell line.
Lane M showing 100 bp Hyperladder, lane 1- negative control, lane 2- *NEIL1*, lane 3- *NEIL2* at 145 bp, lane 4- *NEIL3* at 147 bp, lane 5- GAPDH expression at 120 bp.

The SW48 cell line had no visible band in lane 2 for the expression of *NEIL1*, it however showed a faint band for *NEIL2* and a more visible band for *NEIL3*, thus indicating that the expression of *NEIL3* is apparently higher in SW48 cells when compared to *NEIL2*.
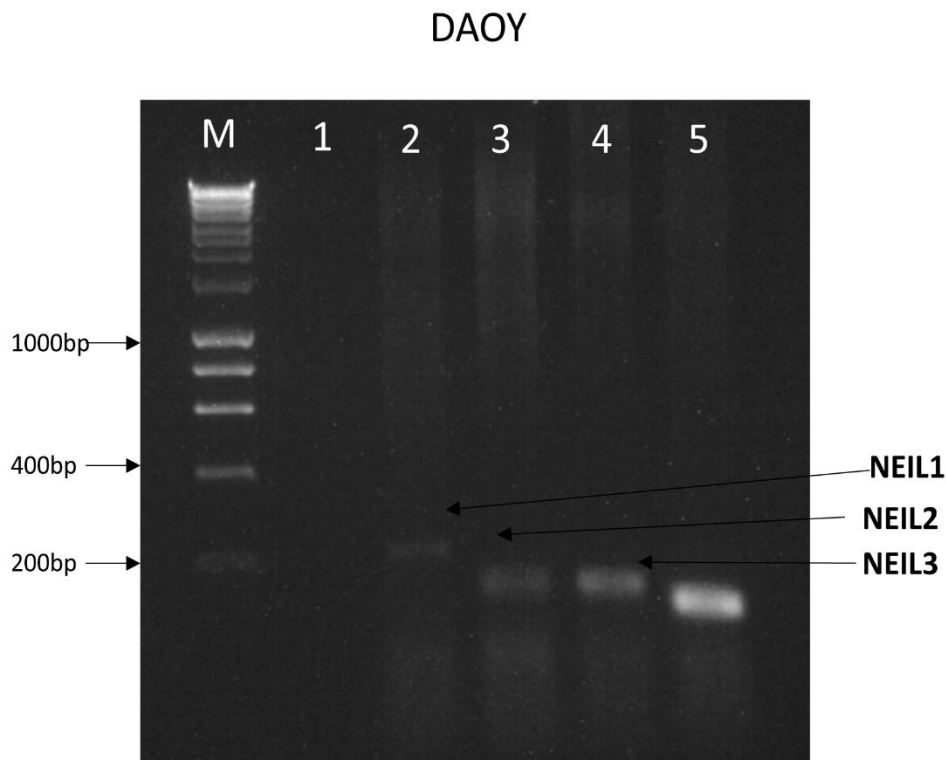
Figure 4.6 - Agarose gel electrophoresis showing *NEIL1*, *NEIL2* and NEIL3 expression in the DAOY cell line.
Lane M showing 100 bp Hyperladder, lane 1- negative control, lane 2- *NEIL1* at 212 bp, lane 3- *NEIL2* at 145 bp, lane 4- *NEIL3* at 147 bp, lane 5- positive control GAPDH expression at 120 bp.

In contrast to the two CRC cell lines tested (Figures 3.4 - 3.5), an RT-PCR product of the correct size was obtained for each of the *NEIL* genes from RNA extracted from the DAOY medulloblastoma cells (Figure 4.6). Interestingly, the band for *NEIL3* is again most prominent (as shown in lane5) compared to those for *NEIL1* and *NEIL2*.

4.1.3 Quantitative profiling of DNA repair genes in SW480, SW48, HCT116 and DAOY cells

After confirmation of the expression of the three *NEIL* genes by RT-PCR, the gene expression was quantified with a more accurate assay, qPCR, to determine the variations in the mRNA level of YB-1 and relevant DNA glycosylase genes across the different cell lines. RNA was extracted from the cell lines, converted to cDNA, quantified and analysed using actin as

reference, due to the inability to get a single peak in the melt curve analysis of GAPDH across the four cell lines.

YB1
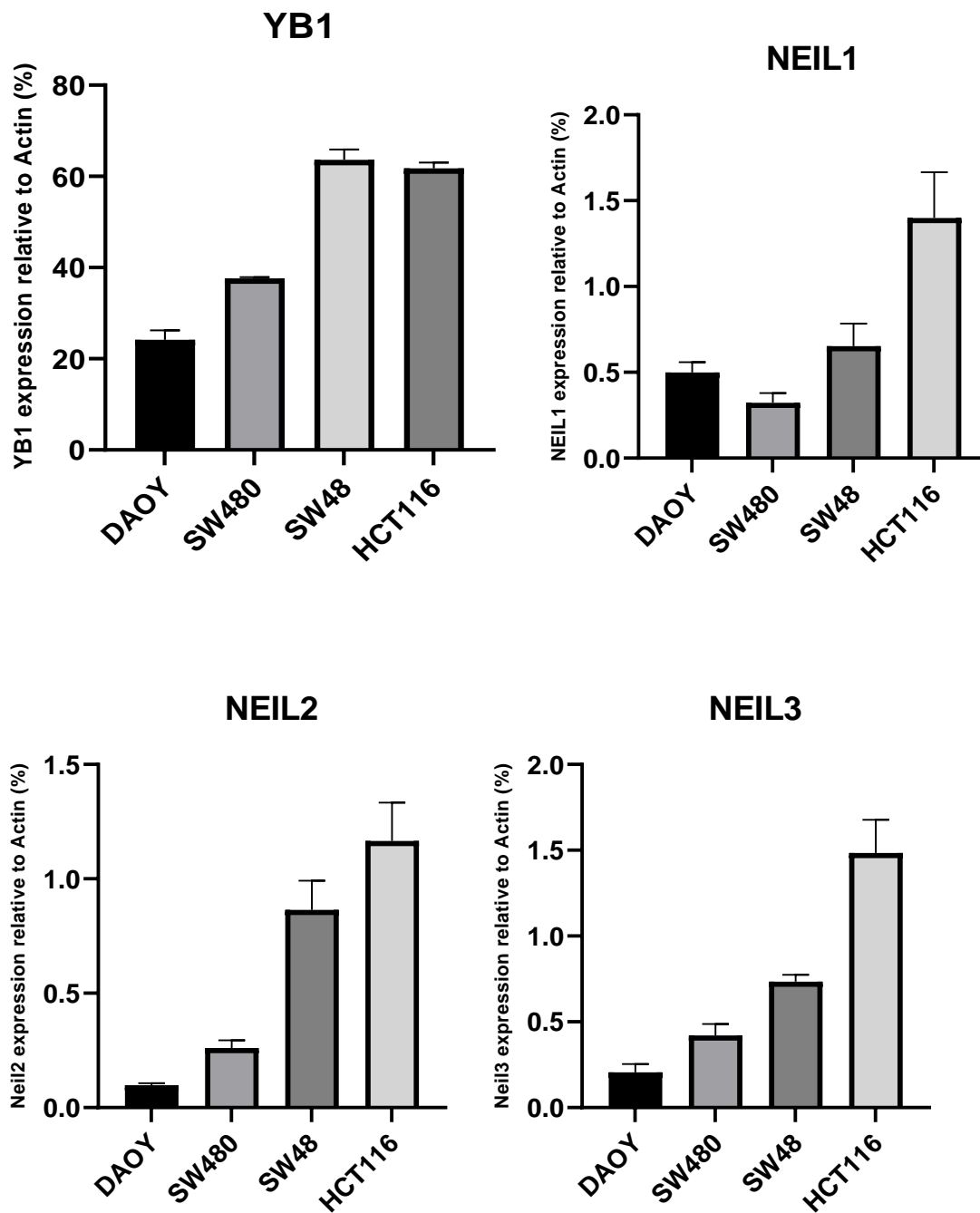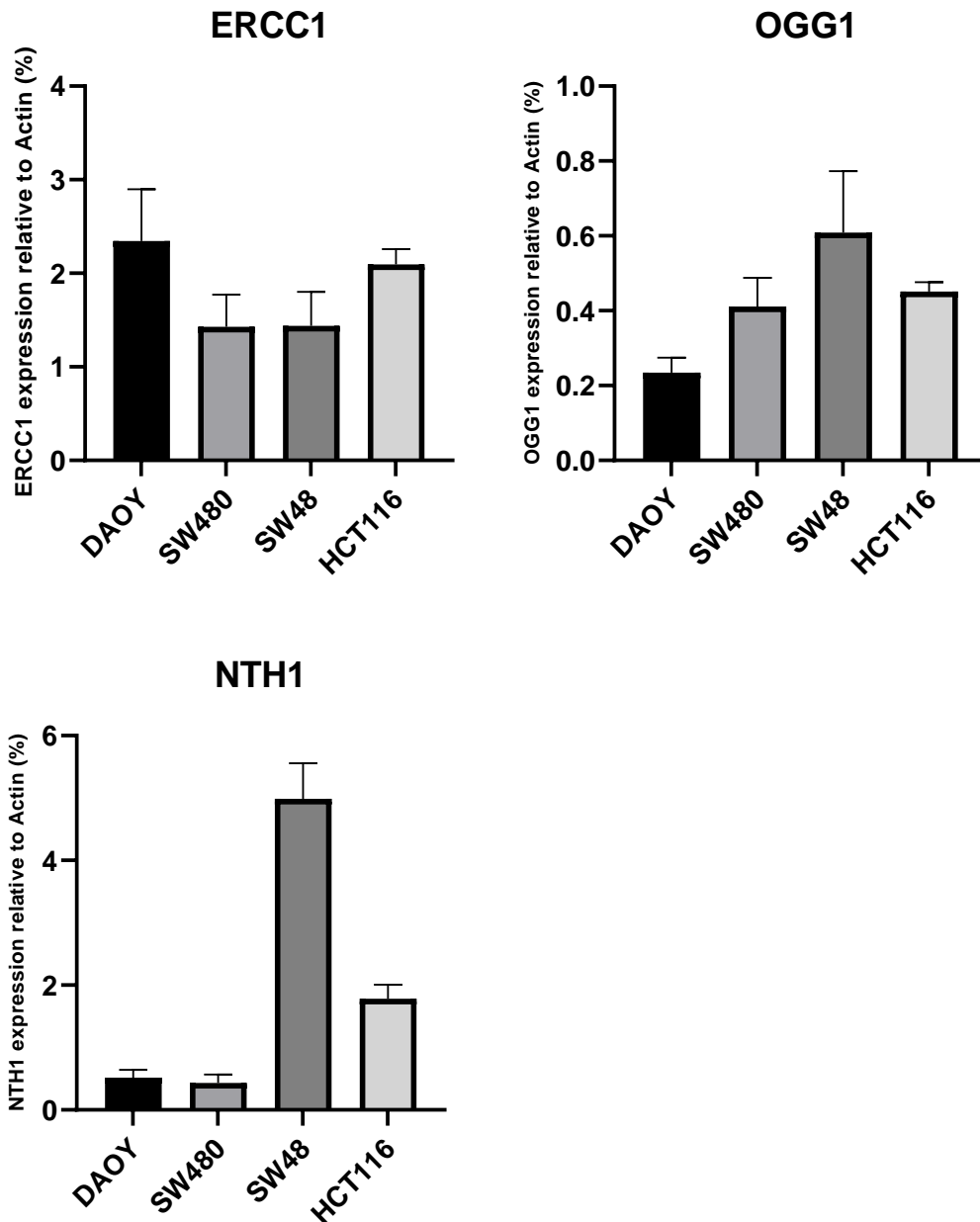
NEIL1

NEIL2

NEIL3

Figure 4.7- **Expression of DNA damage repair genes and *YB-1* in colorectal and medulloblastoma cell lines.**
mRNA expression level of *NEIL1*, *NEIL2*, *NEIL3*, *ERCC1*, *OGG1*, *NTH1* and *YB*-1 in reference to actin was determined by qPCR in DAOY, SW480, SW48 and HCT116 cell lines. Each data point represents three independent experiments, carried out in triplicates (n=3). Analysis of data was carried out using the 2−ΔCt method. Error bars ± standard deviation.

Figure 4.7 shows the expression levels for five BER–related genes, one NER-related gene (*ERCC1*) and *YB-1* that has been shown to interact with HCP5 (Wang *et al*., 2020). The DNA repair genes were chosen because, (with the exception of *OGG1* and *NEIL2*,) they have either

been shown to be involved in the repair of ICLs (*NEIL1*, *NEIL3*) or high expression levels have been shown to increase resistance to oxaliplatin (*NTH1*, *ERCC1*) (Hector *et al*., 2001, Yang *et al*., 2017, McNeil *et al*., 2013).

It is clear from Figure 4.7 that, in comparison with actin, the expression of each gene varies between each cell line and that no gene is consistently highly or weakly expressed in every cell line. In the *NEIL1* expression results, the expression of *NEIL1* was higher in the HCT116 cells when compared to the other cell lines, with a 2.15-fold difference when compared to SW48, 2.8-fold difference when compared to DAOY and a 4.4-fold difference when compared to SW480 which had the lowest expression. The *NEIL2* gene showed a high expression in the HCT116 and SW48 with a 1.34-fold difference between each cell line and lower expression in the DAOY (12-fold decrease) and SW480 (4.5-fold decrease) when compared to HCT116. HCT116 also had the highest expression of *NEIL3* when compared to the other cell lines with a fold decrease in expression of 2 when compared to SW48, 3.5-fold decrease in SW480 and 7.4-fold decrease in DAOY. The DAOY cell line had the highest expression of *ERCC1* when compared to the other cell lines, with a 1.6-fold difference when compared to SW480 and SW48 and 1.1-fold difference for HCT116. *OGG1* expression was highest in the SW48 cell line with a fold decrease of 1.3, 1.5 and 2.7, when compared to HCT116, SW480 and DAOY respectively. SW48 had the highest expression of *NTH1* and comparison with the other cell lines, revealed a fold decrease of 2.41, 7.4 and 10 when compared to HCT116, DAOY and SW480 respectively.

4.1.4 CRC cells respond differently to DNA damaging agents.

Increased cell proliferation and the suppression of apoptosis are initial underlying events in CRC carcinogenesis, a multilevel process involving several molecular events (Yang *et al*., 2009). To determine the *in vitro* effect of chemotherapy on medulloblastoma and CRC cell lines, the four cell lines were treated with a serial dilution of DNA damaging agents (oxaliplatin and cisplatin) and also the ROS inducing compound TBH with a starting concentration of 100 µM (0.39, 0.78, 1.56, 3.125, 6.25, 12.5, 25, 50 and 100 µM) and the results were analysed by the MTT assay. All the cell lines responded differently to each treatment with the DAOY cells being more sensitive to cisplatin over oxaliplatin with an IC50 of 0.84 µM for cisplatin and 11.48 µM for oxaliplatin. The ROS inducing compound TBH had the least cytotoxic effect on the DAOY cells with an IC50 of 13.88 µM.

The SW480 cell line was more sensitive to oxaliplatin with an IC50 of 1.096 µM compared to cisplatin where it had an IC50 of 7.295 µM and it showed the least sensitivity to TBH with an IC50 of 57.67 µM. The HCT116 cell line was more sensitive to oxaliplatin with an IC50 of 0.66 µM compared to cisplatin where it had an IC50 of 3.31 µM and it showed the least sensitivity to TBH with an IC50 of 18.28 µM. The SW48 cell line was more sensitive to oxaliplatin with an IC50 of 0.51 µM compared to cisplatin where it had an IC50 of 17.22 µM and it showed the least sensitivity to TBH as an IC50 value could not be determined. In comparison, the low cytotoxicity of TBH was consistent across the four cell lines with SW480 being the least sensitive to TBH, not generating an IC50 at 100 µM and DAOY being the most sensitive. For cisplatin, the DAOY cell line was the most sensitive, while SW480 was the least sensitive and for oxaliplatin, HCT116 cell line was the most sensitive and DAOY was the least sensitive, However, out of the three colorectal cell lines, SW48 was the least sensitive to oxaliplatin, this implies that out of the four cell lines, SW48 was the least sensitive to all treatment.

DAOY
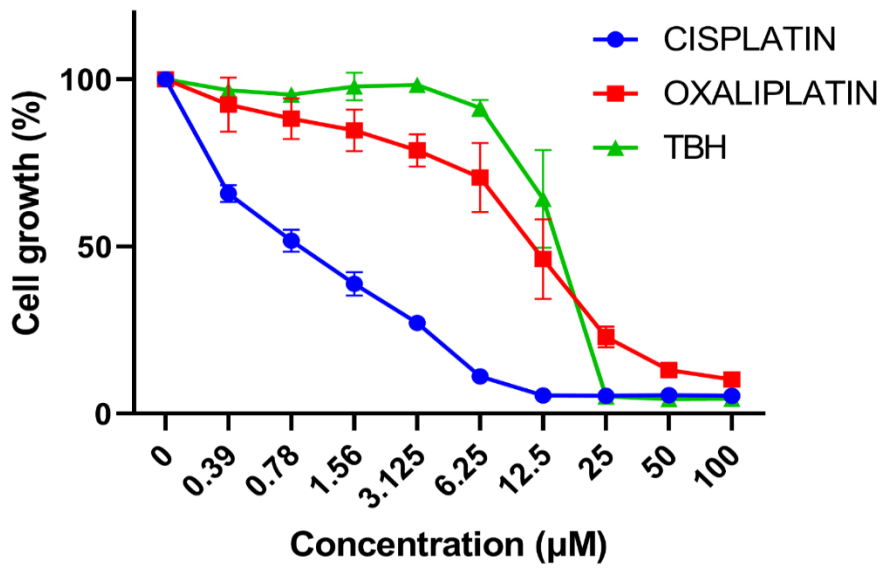
	IC50
Cisplatin	0.838 µM
Oxaliplatin	11.48 µM
TBH	13.88 µM

HCT116

	IC50
Cisplatin	3.31 µM
Oxaliplatin	0.66 µM
TBH	18.28 µM

SW480

	IC50
Cisplatin	7.295 µM
Oxaliplatin	1.096 µM
TBH	57.67 µM
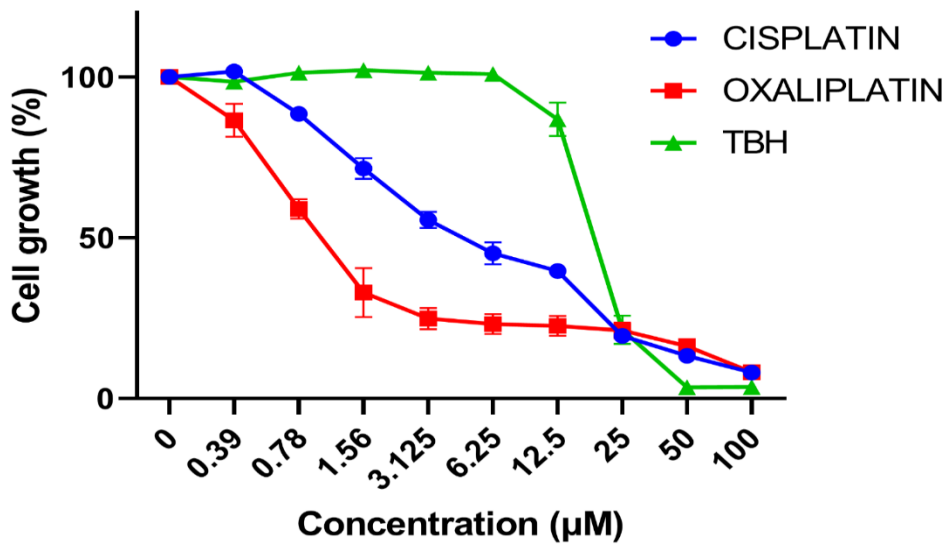
SW48

	IC50
Cisplatin	17.22 µM
Oxaliplatin	0.663 µM
TBH	N/A
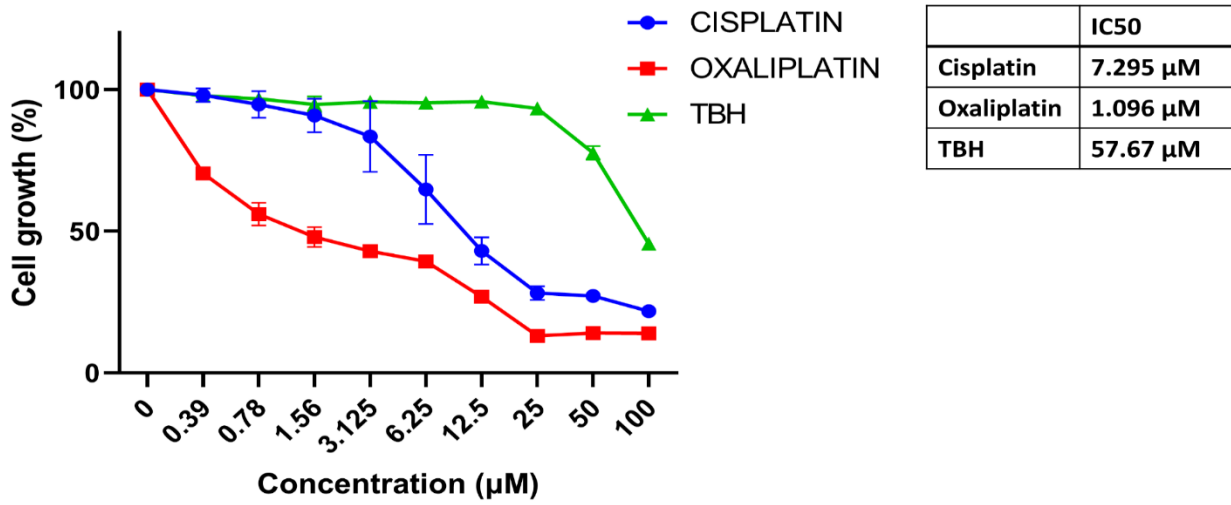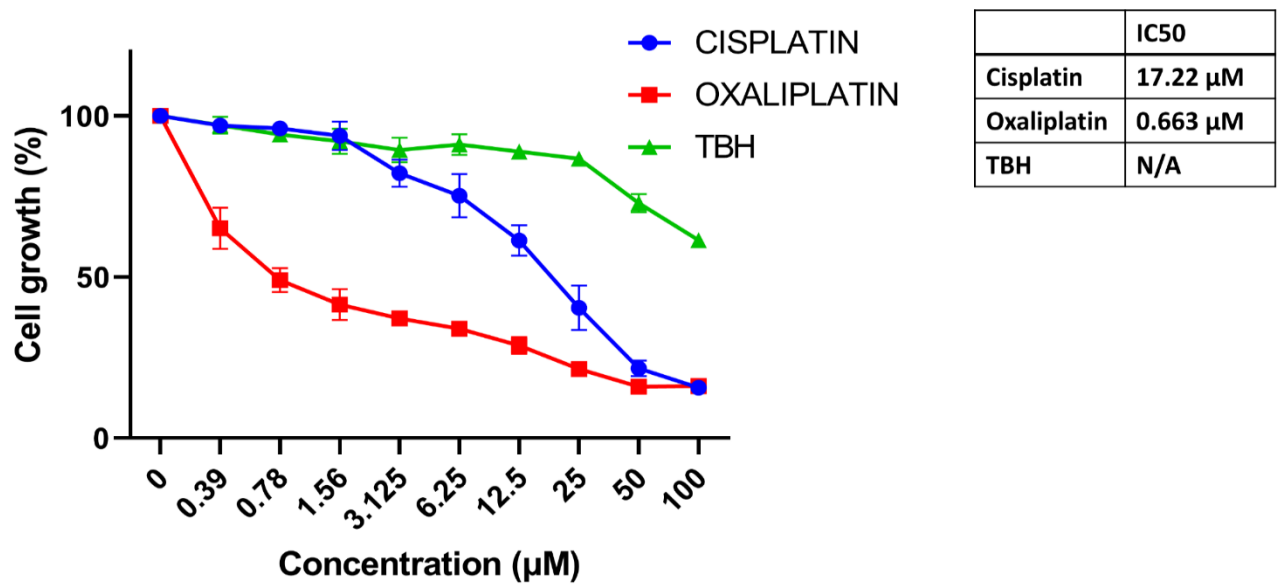
Figure 4.8- Effect of DNA damaging agents on cell growth in DAOY, SW48, SW480 and HCT116 cell lines.

Percentage of cell growth was determined by MTT assay after treatment with cisplatin, oxaliplatin and TBH, each graph represents the effects of the three treatments on SW48, DAOY, SW480 and HCT116 cell lines. Cells were exposed to serial dilution of each treatment individually for 72 hours and the results were analysed. Results shown are the average of three independent experiments carried out in triplicates. Error bars ± standard deviation.

4.1.5 Knockdown of HCP5 sensitizes cancer cells to genotoxic agents.

Following up on the determination of the expression level of HCP5 in the cell lines (Figure 4.3), it was imperative to determine the effect of HCP5 on cell sensitivity to genotoxic agents. To begin, HCP5 was knocked down in four of the cell lines with the highest expression of HCP5. The four cell lines DAOY, SW48, SW480 and HCT116 were transfected with five locked nucleic antisense oligonucleotides (ASO) (oligo 1-5), a negative control and a positive control GAPDH using lipofectamine 3000. Initially the cells were transfected with the various oligonucleotides for 48 h, but when knockdown efficiency was assessed using qPCR there was no knockdown of the lncRNA. The experiment was then repeated and HCP5 levels determined after 24 h at which timepoint knockdown was confirmed. Thus, all subsequent HCP5 knockdown experiments were conducted 24 h following transfection.

After 24 h, RNA was extracted from the transfected cells, reverse-transcribed to cDNA and the efficiency of knockdown for each ASO determined by qPCR, using GAPDH as the positive control. However, while oligo 3 routinely had one of the highest knockdown efficiencies in all cell lines tested (Figure 4.9), transfection of this ASO resulted in approximately 70% cell death across all the cell lines. Therefore, based on cell survival and knockdown efficiency in the different cell lines tested, oligo 4 was chosen as the preferred ASO for all subsequent experiments as it had a knockdown efficiency of 70% in DAOY, 80% in HCT116, 65% in SW480 and 55% in SW48.
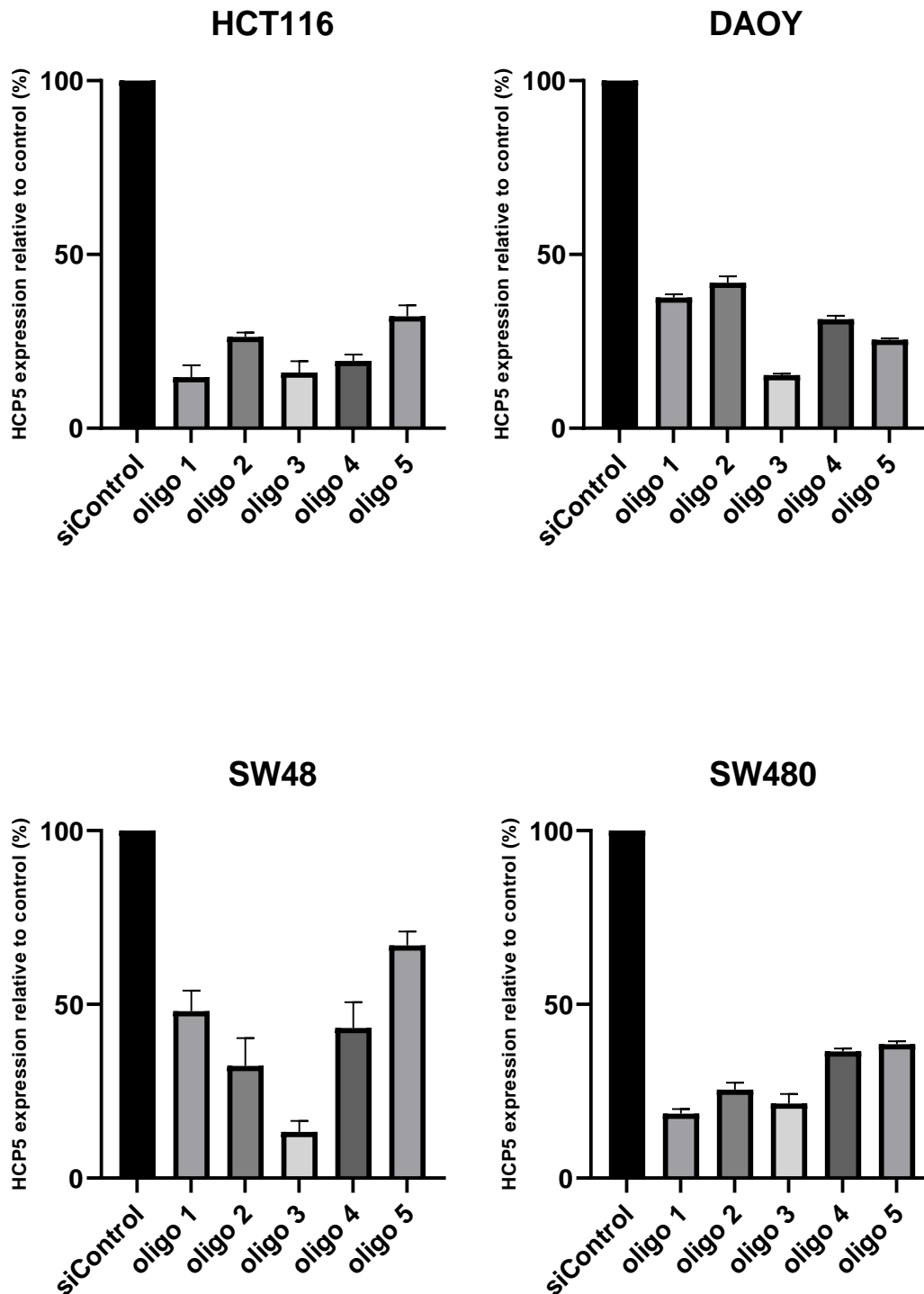
Figure 4.9 – **Confirmation of HCP5 knockdown in DAOY, HCT116, SW48 and SW480 cells.** Expression level of HCP5 in reference to actin after HCP5 knockdown was determined by qPCR. Each data point represents three independent experiments, carried out in triplicates (n=9). Analysis of data was carried out using the $2^{-\Delta\Delta Ct}$ method. Error bars ± standard deviation.

4.1.6 HCP5 knockdown has no effect on NEIL1, NEIL2 and NTH1 expression.

Subsequent to determining the expression level of the DNA glycosylases in the DAOY, HCT116, SW48 and SW480 cells it was interesting imperative to determine if knockdown of HCP5 had a direct effect on the expression of NEIL1, NEIL2 and NTH1 all of which have been shown to be activated by YB-1, which in turn is linked to HCP5. Therefore, HCP5 was knocked down in the four cell lines for 24 h using oligo 4. The RNA was extracted, converted to cDNA and expression of the three DNA glycosylase was determined using qPCR. Perhaps unsurprisingly, given the proposed mechanism of action of YB-1 on the activity of these DNA glycosylases, Figure 4.10 shows that, when compared to the control, there was no significant reduction in the expression of any of the genes tested when HCP5 was knocked down across all the cell lines.
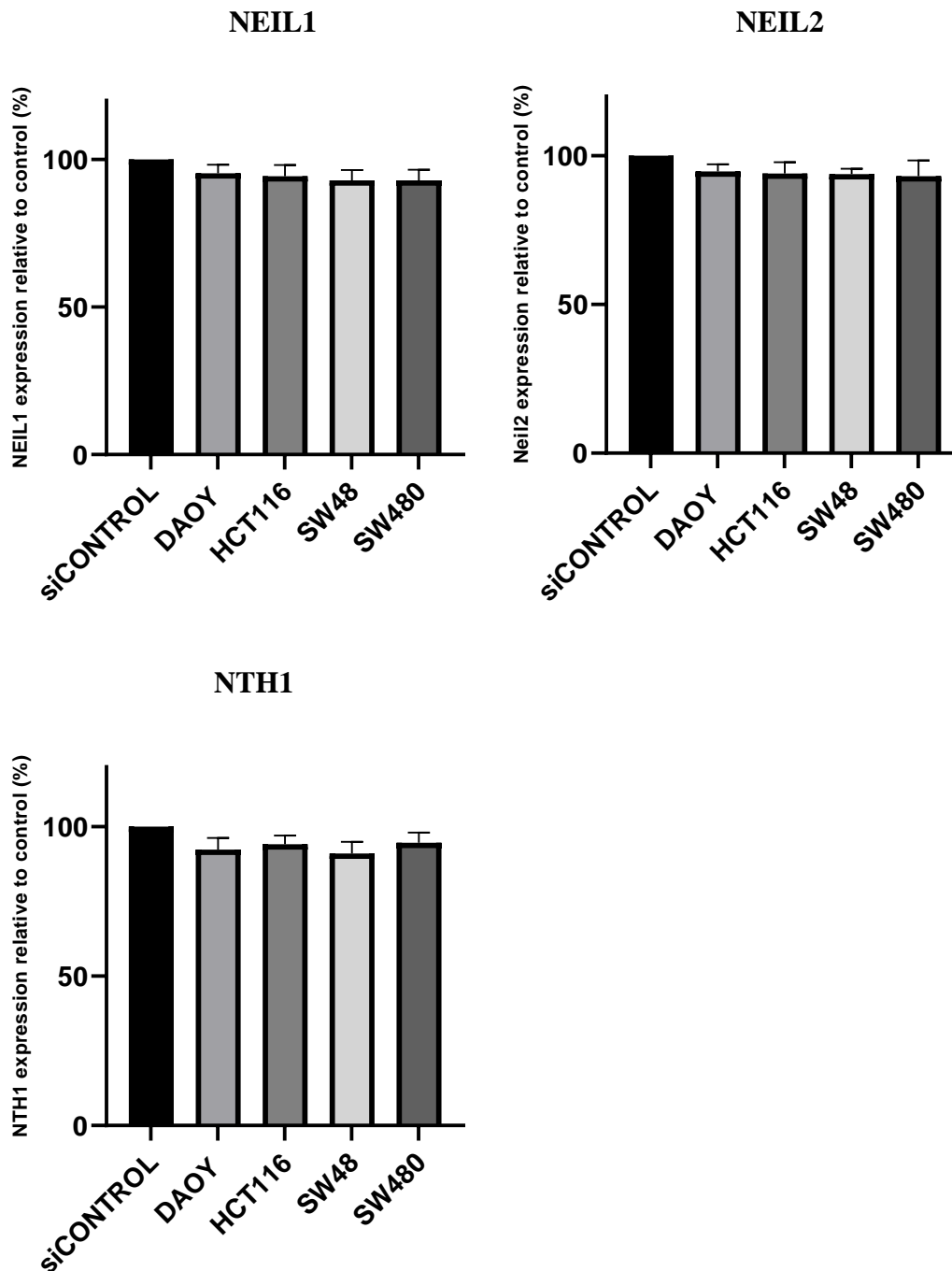
Figure 4.10 – Expression of NEIL1, NEIL2 and NTH1 in the four cell lines after HCP5 knockdown. Expression level of NEIL1, NEIL2 and NTH1 in reference to actin after HCP5 knockdown was determined by qPCR. Each data point represents three independent experiments, carried out in triplicates (n=9). Analysis of data was carried out using the $2^{-\Delta Ct}$ method. Error bars ± standard deviation.

4.1.7 Olaparib treatment has no effect on HCP5 expression.

Olaparib which is an inhibitor of PARP has been shown to sensitize cancer cells to cisplatin (Prasad *et al*, 2017) since a cross talk has been established between HCP5 and PARP 1, it was of interest to determine if inhibition of PARP using olaparib had an additive or synergistic effect to sensitizing cancer cells to chemotherapy in combination with HCP5. To begin, all the cell lines were treated with olaparib with a starting concentration of 100 µM (Figure 4.11). All the cell lines responded in a similar pattern to the PARP inhibitor with the IC50 of all four cell lines in a range of 12 µM to 17 µM, with DAOY having the least IC50 at 12.95 µM and SW480 having the highest IC50 at 17.1 µM. 5 µM olaparib was chosen to be used in the combination treatment with cisplatin, oxaliplatin and TBH as the toxicity of the inhibitor was minimal at this concentration, thus any increase in cell death in the combination treatment will be due to the drug and not olaparib.
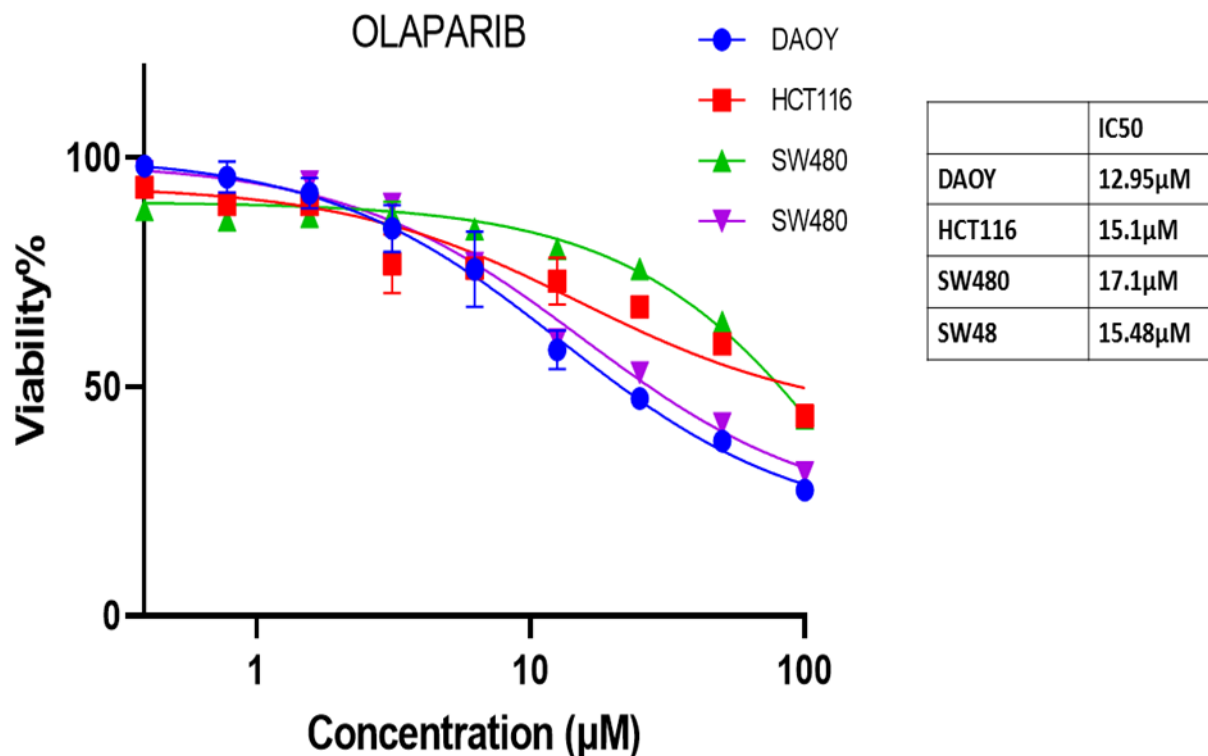
Figure **4.11 – Effect of Olaparib on cell growth of DAOY, HCT116, SW48 and SW480 cells.** Percentage of cell growth was determined by MTT assay after treatment with olaparib, each graph represents the effects of olaparib on SW48, DAOY, SW480 and HCT116 cell lines. Cells were exposed to serial dilution of each treatment individually for 72 hours and the results were analysed. Results shown are the average of three independent experiments carried out in triplicates. Error bars ± standard deviation.

To investigate if there was interaction between HCP5 and PARP, as inhibition of PARP has been shown to directly affect the expression of other lncRNAs and PARP 9,12 and 14 have been shown to be direct target genes of HCP5 (Hu *et al*, 2021), the effect of olaparib on HCP5 expression levels was determined. The cells were plated in a 6-well plate and treated with 10 μM olaparib for 48 hours, RNA was extracted and converted to cDNA and analysed via qPCR. As indicated in Figure 4.12, there was no difference in the expression of HCP5 after treatment with olaparib when compared to the expression of HCP5 in the control cells and this result was constant across the cell lines.
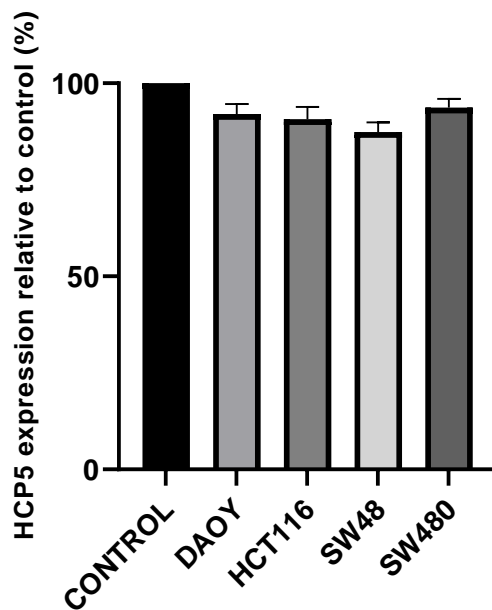
Figure 4.12- **Expression of HCP5 in all four cell lines after treatment with 10 μM olaparib.**
Expression level of HCP5 in reference to actin after olaparib treatment was determined by qPCR. Each data point represents three independent experiments, carried out in triplicates (n=9). Analysis of data was carried out using the $2^{-\Delta Ct}$ method. Error bars ± standard deviation.

4.1.8 Inhibitory effects of single anticancer agents combined with HCP5 knockdown and olaparib on HCT116, SW48, SW480 and DAOY cells.

After determination of the effect of each anticancer agents on the growth of the different cancer cell lines, the effect HCP5 knockdown on sensitizing the cells to the anticancer agents was determined. The cells were divided into three groups, the first group was made up of cells treated with only the single treatment individually which were cisplatin, oxaliplatin and TBH, while the second group which was a transfection control where cells transfected with a negative

control and treated with the individual single treatment. The third group were cells transfected with HCP5 and treated with the individual single treatment. After establishing in the experiments prior to this that treatment with olaparib had no effect on HCP5 expression and discovering in some research articles that treatment with olaparib sensitizes cancer cells to chemotherapy (Gao *et al*., 2021), olaparib was added to the combination treatment to determine if this will give an additive effect on sensitizing the cells to chemotherapy when used in combination with HCP5 knockdown. Therefore, a fourth group was created where the HCP5 was knocked down in the cells and these cells were treated with an individual single treatment and also treated with 5 µM of olaparib. The cells were treated with a sequential concentration of cisplatin/oxaliplatin/TBH, starting at 100 µM. HCP5 knockdown was carried out across all four cell lines using oligo 4 for 24 h. All four groups were set up in the same 96-well plate under the same conditions, this process was done with all four cell lines and repeated with all anti-cancer agents. The cells were allowed to grow for 72 h and cell viability was analysed using the MTT assay.
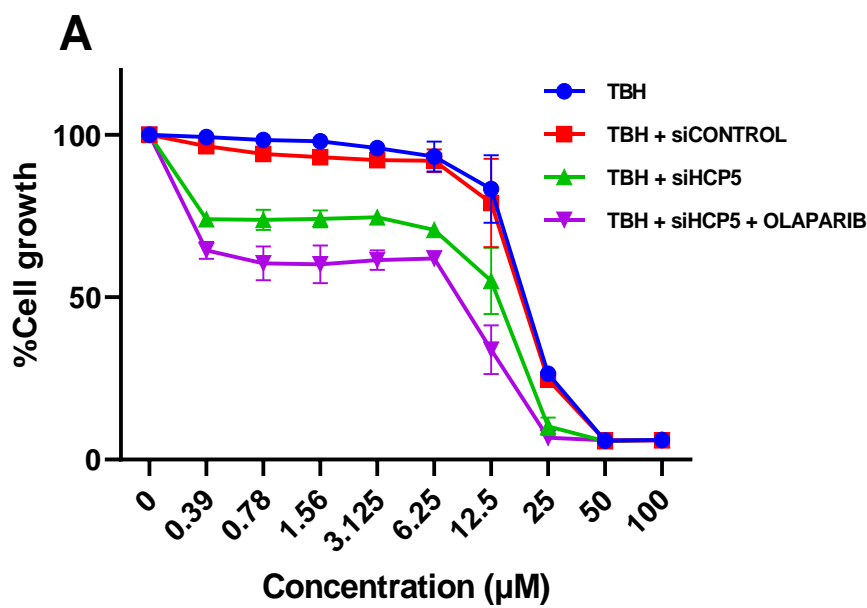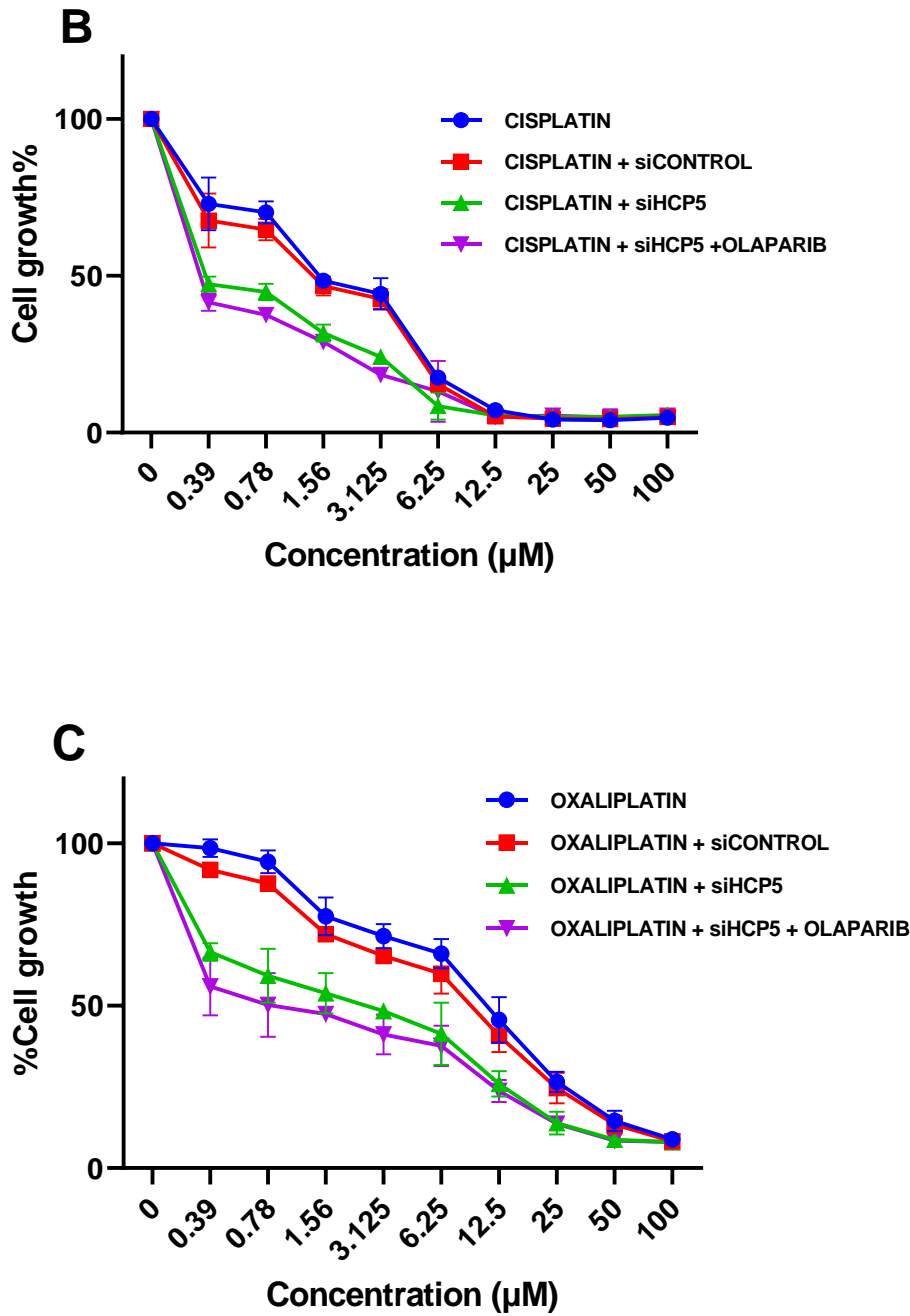
Figure 4.13 -**Effect of combination treatment of DNA damaging agents and HCP5 knockdown on DAOY cells.**

Cells were exposed to serial dilution of (A) TBH, (B) cisplatin or (C) oxaliplatin individually and in combination with HCP5 knockdown alone or HCP5 knockdown and olaparib for 72 hours and the results were analysed. Results shown are the average of three independent experiments carried out in triplicates (n=3). Error bars ±standard deviation. IC50 values for all experiment is shown in supplementary data 4

Table 4.1- Comparison of treatment groups in DAOY cells. Statistical analysis was carried out using two-way ANOVA supplemented with Tukey's multiple comparisons test.

Comparison	P value
CISPLATIN vs. CISPLATIN + siCONTROL	0.62
CISPLATIN vs. CISPLATIN + siHCP5	<0.001
CISPLATIN vs. CISPLATIN + siHCP5 +OLAPARIB	<0.001
CISPLATIN + siHCP5 vs. CISPLATIN + siHCP5 +OLAPARIB	0.35
OXALIPLATIN vs. OXALIPLATIN + siCONTROL	0.55
OXALIPLATIN vs. OXALIPLATIN + siHCP5	<0.001
OXALIPLATIN vs. OXALIPLATIN + siHCP5 +OLAPARIB	<0.001
OXALIPLATIN + siHCP5 vs. OXALIPLATIN + siHCP5 +OLAPARIB	0.42
TBH vs. TBH + siCONTROL	0.24
TBH vs. TBH + siHCP5	<0.001
TBH vs. TBH + siHCP5 +OLAPARIB	<0.001
TBH + siHCP5 vs. TBH + siHCP5 +OLAPARIB	0.13

In all the four cell lines, it was discovered there was a reduction in cell viability in the HCP5 knockdown cells combined with the single treatment when compared to the group with just the single treatment. In the DAOY cells TBH combination experiment, there was no significant difference between the TBH only experiment when compared to the TBH + sicontrol experiment as expected. However, when comparing the TBH only treatment to the TBH + siHCP5 and the TBH + siHCP5 + olaparib experiment there was a decrease in cell growth when comparing the TBH only treatment to each treatment individually as shown in Figure 4.13A. When comparing the TBH + siHCP5 treatment and the TBH + siHCP5 + olaparib treatment, there was no significant difference in cell growth. The cisplatin combination treatment results were similar to the TBH results, there was a reduction in cell growth across all treatments, but this reduction was higher in the lower concentration range (Figure 4.13B). There was no significant difference (p=0.62) the cisplatin only treatment and the cisplatin + siHCP5 treatment as expected. There was however a significant reduction (p<0.001) in cell growth when comparing the cisplatin only treatment to cisplatin + siHCP5 treatment and the cisplatin + siHCP5 + olaparib treatment individually as shown in Table 4.1. Like the TBH experiment, there was no significant reduction in cell growth between the cisplatin + siHCP5 treatment and the cisplatin + siHCP5 + olaparib. The oxaliplatin combination treatment results were similar to the TBH and cisplatin results with no significant difference between the oxaliplatin only treatment and the oxaliplatin + sicontrol treatment (Figure 4.13C). There was

also significant difference between the oxaliplatin only treatment and the oxaliplatin + siHCP5 treatment and oxaliplatin + siHCP5 + olaparib treatment when analysed separately. There was however no significant difference in cell growth when comparing the oxaliplatin + siHCP5 treatment and oxaliplatin + siHCP5 + olaparib treatment.

Figure 4.14 -**Effect of combination treatment of anticancer agents and HCP5 knockdown on SW48 cells.**

Cells were exposed to serial dilution of (A) TBH, (B) cisplatin or (C) cisplatin individually and in combination with HCP5 knockdown alone or HCP5 knockdown and olaparib for 72 hours and the results were analysed. Results shown are the average of three independent experiments

carried out in triplicates (n=3). Error bars ±standard deviation. IC50 values for all experiment is shown in supplementary data 4

Table 4.2- Comparison of treatment groups in SW48 cells. Statistical analysis was carried out using two-way ANOVA supplemented with Tukey's multiple comparisons test.

Comparison	P value
CISPLATIN vs. CISPLATIN + siCONTROL	0.23
CISPLATIN vs. CISPLATIN + siHCP5	<0.001
CISPLATIN vs. CISPLATIN + siHCP5 +OLAPARIB	<0.001
CISPLATIN + siHCP5 vs. CISPLATIN + siHCP5 +OLAPARIB	0.11
OXALIPLATIN vs. OXALIPLATIN + siCONTROL	0.27
OXALIPLATIN vs. OXALIPLATIN + siHCP5	<0.001
OXALIPLATIN vs. OXALIPLATIN + siHCP5 +OLAPARIB	<0.001
OXALIPLATIN + siHCP5 vs. OXALIPLATIN + siHCP5 +OLAPARIB	0.08
TBH vs. TBH + siCONTROL	0.97
TBH vs. TBH + siHCP5	<0.001
TBH vs. TBH + siHCP5 +OLAPARIB	<0.001
TBH + siHCP5 vs. TBH + siHCP5 +OLAPARIB	0.09

The SW48 cells were treated with the various TBH combination treatments as shown in Figure 4.14A. when comparing the TBH only treatment and the TBH + sicontrol treatment, there was no significant difference, but comparing the TBH only treatment to the TBH + siHCP5 and the TBH + siHCP5 + olaparib experiment individually indicated a significant decrease in cell growth in both instances. This was however different when comparing the TBH + siHCP5 combination treatment and the TBH + siHCP5 + olaparib combination treatment as there was no significant reduction in cell growth (Table 4.2). Analysis of the SW48 cisplatin combination treatment revealed there was no significant difference in cell growth between the cisplatin only treatment and the cisplatin + sicontrol treatment, comparison of the cisplatin only treatment and the cisplatin + siHCP5 treatment and the cisplatin + siHCP5 + olaparib treatment individually revealed a significant decrease in cell growth in both cases as shown in Figure 4.14B. However, comparison of the cisplatin + siHCP5 treatment and the cisplatin + siHCP5 + olaparib treatment showed no significant reduction in cell growth. The results for the oxaliplatin combination treatment were similar to the cisplatin and TBH combination treatment, with the oxaliplatin treatment and the oxaliplatin + sicontrol treatment not showing any significant difference in cell growth when compared (Figure 4.14C). Comparison of the oxaliplatin only treatment with the oxaliplatin + siHCP5 treatment and the oxaliplatin +

siHCP5 + olaparib treatment revealed a reduction in cell growth in both cases, but comparison of the oxaliplatin + siHCP5 treatment and the oxaliplatin + siHCP5 + olaparib treatment showed no significant in cell growth (Table 4.2).

Figure 4.15 -**Effect of combination treatment of anticancer agents and HCP5 knockdown on HCT116 cells.**
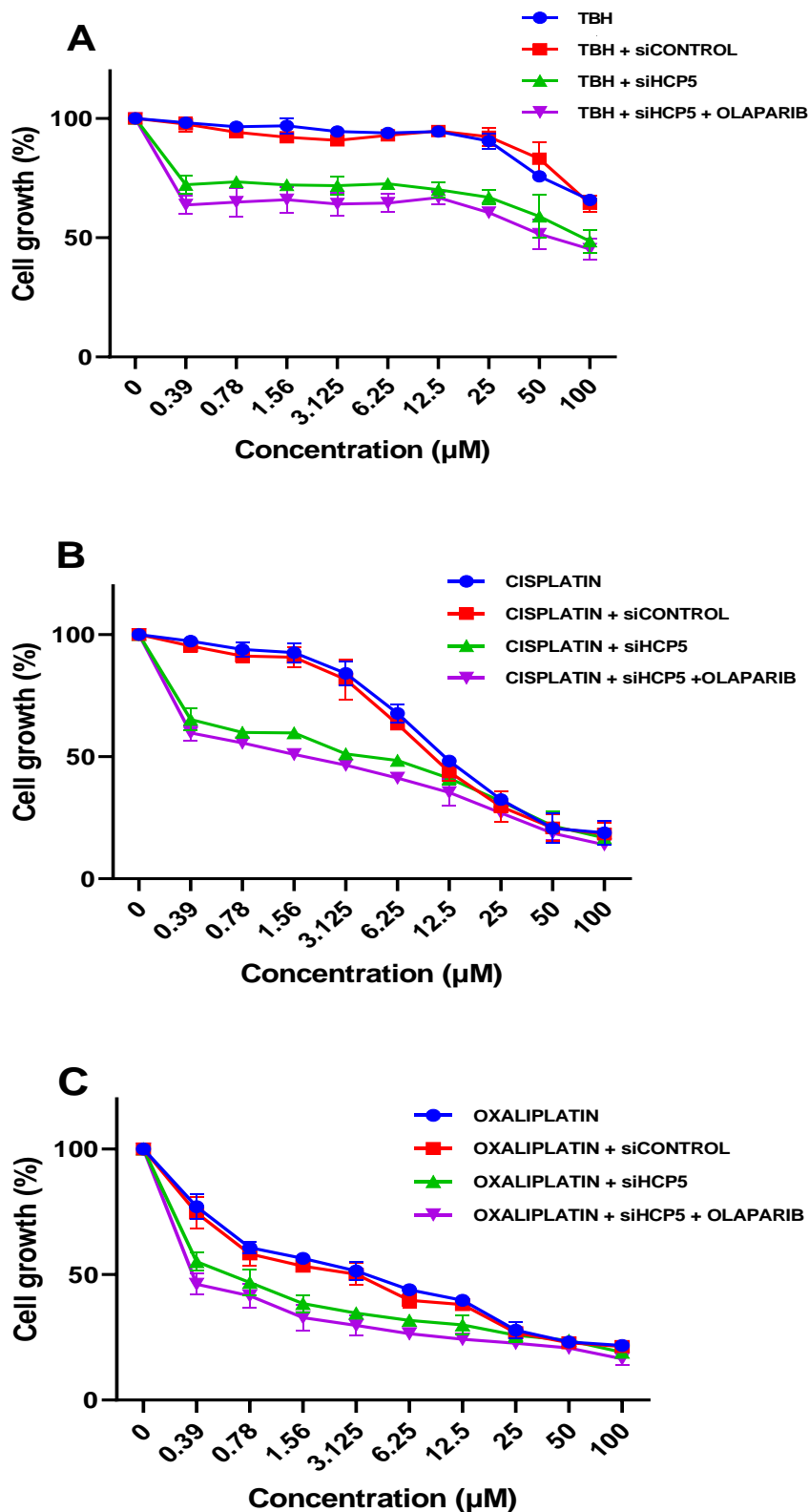
Cells were exposed to serial dilution of (A) TBH, (B) cisplatin or (C) oxaliplatin individually and in combination with HCP5 knockdown alone or HCP5 knockdown and olaparib for 72 hours and the results were analysed. Results shown are the average of three independent experiments carried out in triplicates (n=3). Error bars ±standard deviation. IC50 values for all experiment is shown in supplementary data 4

Table 4.3- Comparison of treatment groups in HCT116 cells. Statistical analysis was carried out using two-way ANOVA supplemented with Tukey's multiple comparisons test.

Comparison	P value
CISPLATIN vs. CISPLATIN + siCONTROL	0.2
CISPLATIN vs. CISPLATIN + siHCP5	<0.001
CISPLATIN vs. CISPLATIN + siHCP5 +OLAPARIB	<0.001
CISPLATIN + siHCP5 vs. CISPLATIN + siHCP5 +OLAPARIB	0.77
OXALIPLATIN vs. OXALIPLATIN + siCONTROL	0.95
OXALIPLATIN vs. OXALIPLATIN + siHCP5	<0.001
OXALIPLATIN vs. OXALIPLATIN + siHCP5 +OLAPARIB	<0.001
OXALIPLATIN + siHCP5 vs. OXALIPLATIN + siHCP5 +OLAPARIB	0.68
TBH vs. TBH + siCONTROL	0.91
TBH vs. TBH + siHCP5	<0.001
TBH vs. TBH + siHCP5 +OLAPARIB	<0.001
TBH + siHCP5 vs. TBH + siHCP5 +OLAPARIB	0.04

The combination experiment with HCP5 knockdown, olaparib and the single anti-cancer agents was repeated with the HCT116 cells (Figure 4.15). The results were similar to the other cell lines with TBH combination experiment having no significant difference in the cell growth between the TBH only treatment and the TBH + sicontrol treatment. On the contrary, the TBH only treatment showed a significant decrease in cell growth when compared to the TBH + siHCP5 treatment and the TBH + siHCP5 + olaparib treatment individually as shown in Figure 4.15A. While comparison of the TBH + siHCP5 treatment and the TBH + siHCP5 + olaparib treatment showed no significant difference in cell growth. For the cisplatin combination treatment, there was no significant difference in the percentage cell growth of cisplatin + sicontrol treatment when compared to cisplatin only treated cells (Figure 4.15B). The cisplatin + siHCP5 treatment and the cisplatin + siHCP5 + olaparib treatment when compared individually to the cisplatin only treatment, showed a decrease in percentage cell viability and when comparing the cisplatin + siHCP5 treatment with the cisplatin + siHCP5 + olaparib treatment, there was no significant difference in % cell growth (Table 4.3). The oxaliplatin combination treatment results in the HCT116 cell line were similar to that of the other anti-cancer agents (Figure 4.15C), there was no significant difference between the oxaliplatin only treatment and the oxaliplatin and sicontrol treatment and also no significant difference when comparing the oxaliplatin only treatment with the oxaliplatin + siHCP5 treatment and the oxaliplatin + siHCP5 + olaparib treatment individually and no significant difference between the percentage cell growth when comparing oxaliplatin + siHCP5 treatment with the oxaliplatin + siHCP5 + olaparib treatment (Table 4.3).

A

B
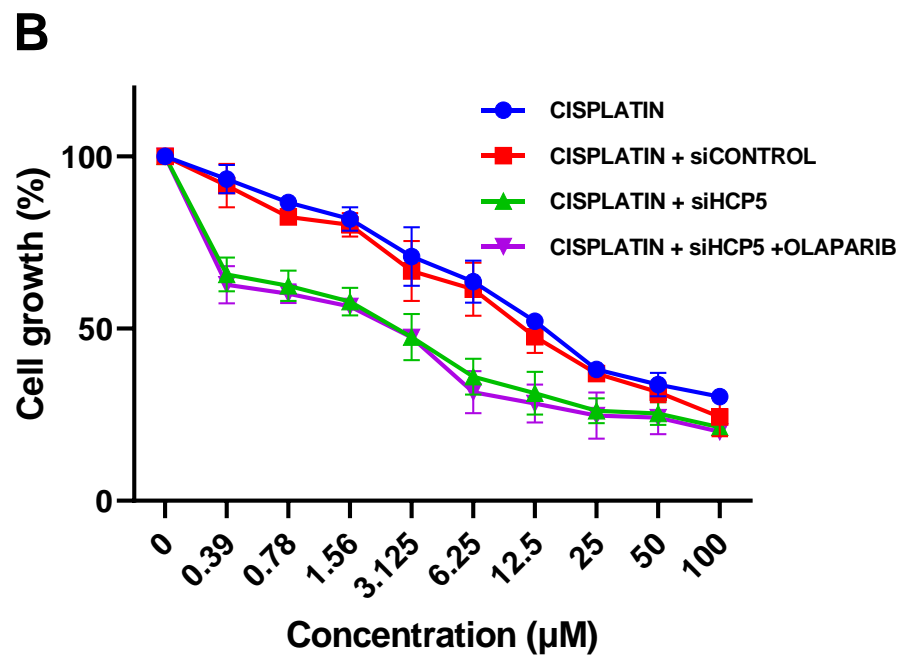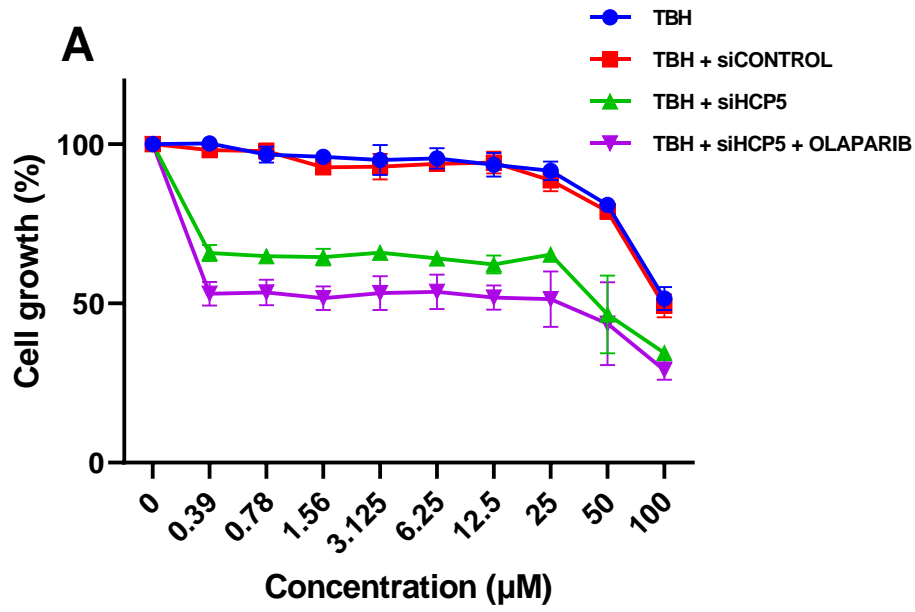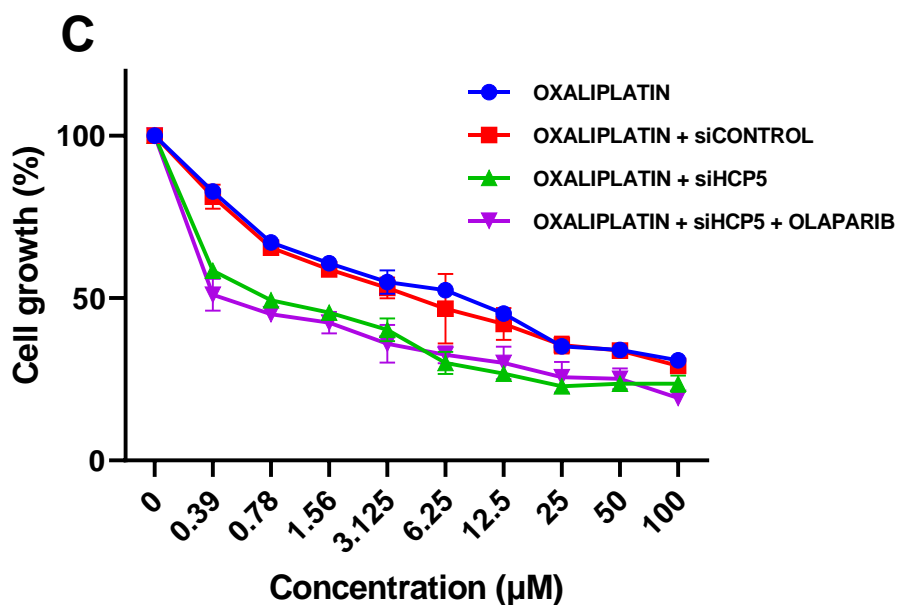
Figure 4.16 -**Effect of combination treatment of anticancer agents and HCP5 knockdown on SW480 cells.**
Cells were exposed to serial dilution of TBH, oxaliplatin, cisplatin individually and in combination with HCP5 knockdown alone or HCP5 knockdown and olaparib for 72 hours and the results were analysed. Results s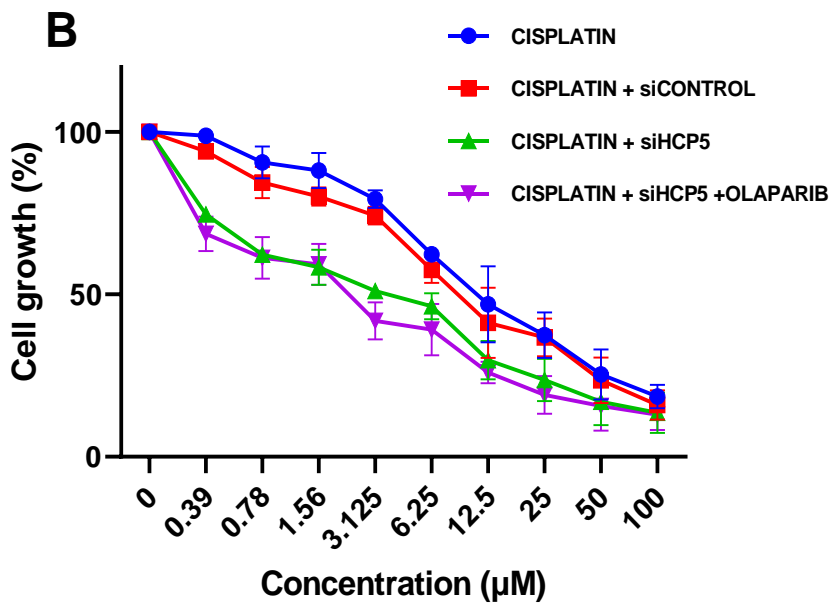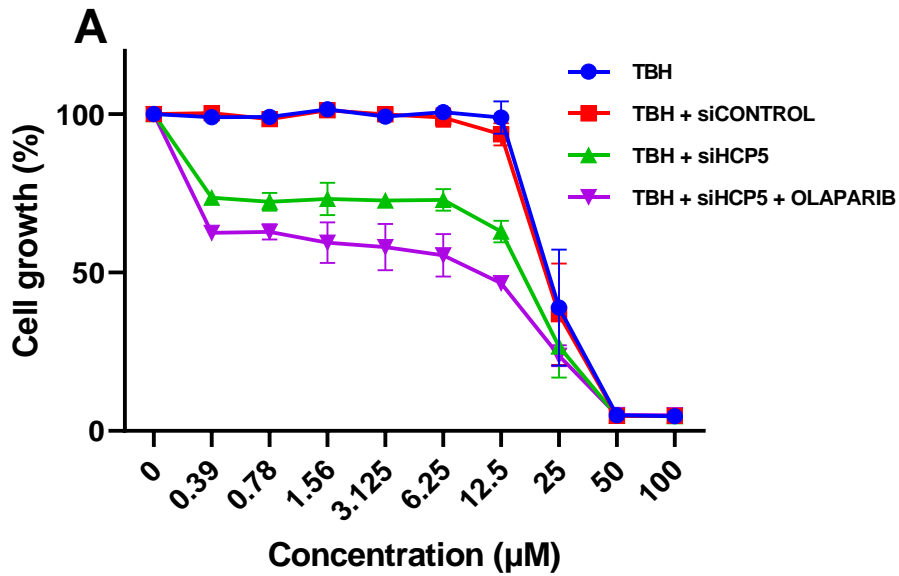hown are the average of three independent experiments carried out in triplicates (n=3). Error bars ±standard deviation. IC50 values for all experiment is shown in supplementary data 4.
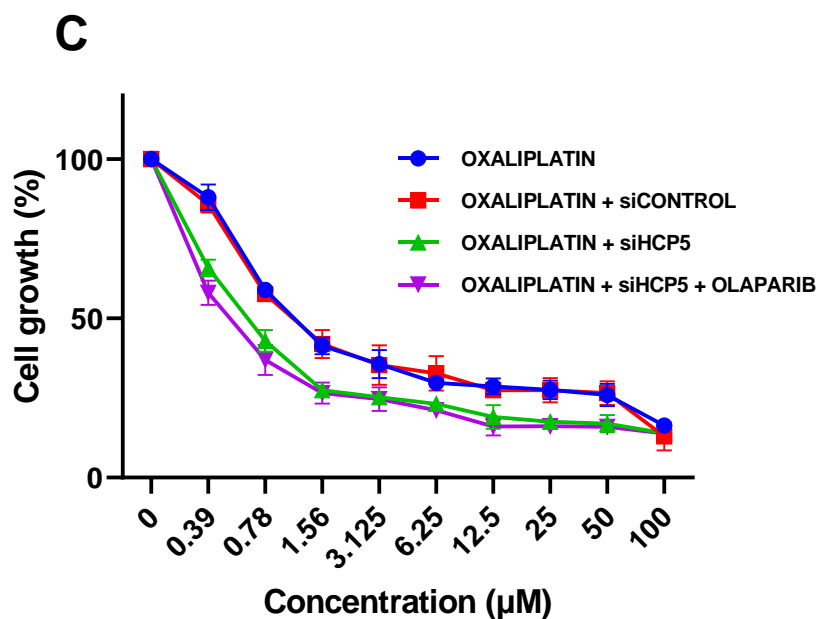
Table 4.3- Comparison of treatment groups in SW480 cells. Statistical analysis was carried out using two-way ANOVA supplemented with Tukey's multiple comparisons test.

Comparison	P value
CISPLATIN vs. CISPLATIN + siCONTROL	0.34
CISPLATIN vs. CISPLATIN + siHCP5	<0.001
CISPLATIN vs. CISPLATIN + siHCP5 +OLAPARIB	<0.001
CISPLATIN + siHCP5 vs. CISPLATIN + siHCP5 +OLAPARIB	0.6
OXALIPLATIN vs. OXALIPLATIN + siCONTROL	0.3
OXALIPLATIN vs. OXALIPLATIN + siHCP5	<0.001
OXALIPLATIN vs. OXALIPLATIN + siHCP5 +OLAPARIB	<0.001
OXALIPLATIN + siHCP5 vs. OXALIPLATIN + siHCP5 +OLAPARIB	0.51
TBH vs. TBH + siCONTROL	0.53
TBH vs. TBH + siHCP5	<0.001
TBH vs. TBH + siHCP5 +OLAPARIB	<0.001
TBH + siHCP5 vs. TBH + siHCP5 +OLAPARIB	0.063

The response of the SW480 cell line to the combination treatments was similar to the other cell lines, the TBH only treatment showed no significant change in percentage cell growth when compared to the TBH + sicontrol treatment group. There was a significant decline in percentage cell growth in the cells treated with TBH + siHCP5 and TBH + siHCP5 + olaparib when individually compared to the cells treated with only TBH. This phenomenon was however not replicated in the comparison of the TBH + siHCP5 treatment with the TBH + siHCP5 + olaparib treatment as there was no significant difference in percentage cell growth (Figure 4.16A). The cisplatin combination treatment yielded the same results as the TBH treatment with no significant difference in the cisplatin + sicontrol treatment and the cisplatin only treatment and a significant difference when comparing the cisplatin + siHCP5 treatment and the cisplatin + siHCP5 + olaparib treatment with the cisplatin only treatment independently. Comparison of the cisplatin + siHCP5 treatment with the cisplatin + siHCP5 + olaparib revealed there was no significant difference in % cell growth (Figure 4.16B). The results for the oxaliplatin combination treatment were similar to the cisplatin and TBH combination treatment, with the oxaliplatin treatment and the oxaliplatin + sicontrol treatment not showing any significant difference in cell growth when compared. Comparison of the oxaliplatin only treatment with the oxaliplatin + siHCP5 treatment and the oxaliplatin + siHCP5 + olaparib treatment revealed a reduction in cell growth in both cases, but comparison of the oxaliplatin + siHCP5 treatment and the oxaliplatin + siHCP5 + olaparib treatment showed no significant in cell growth (Figure 4.16C).

4.1.9 HCP5 knockdown acts synergistically with chemotherapy to inhibit cell proliferation and colony formation in cancer cells.

After determining HCP5 knockdown combined with oxaliplatin, cisplatin and TBH growth inhibitory abilities, the impact of the genotoxic agents on the colony forming ability (clonogenicity assay) of the various cell lines was assessed. The clonogenicity assay is a more accurate technique for examining how certain agents affect cell proliferation and viability as it gives an objective estimate of the self-renewal capacity of a single cell to form a colony. Therefore, it was important to investigate if the combinatorial treatment of HCP5 knockdown and the genotoxic agents could reduce the colony forming capacity more effectively than that of the treatment individually. The four cell lines were plated into 6-well cell culture plates with and without different concentrations of cisplatin/oxaliplatin, TBH and or HCP5 knockdown,

the DNA damaging agents were removed after 24 h to allow colonies to form. Control and treated cells were kept in culture for an additional 14 days. The quantity and size of growing colonies were decreased in both single and combination treatments, as seen in Figures 4.17-4.19. The SW480 and the SW48 cells formed smaller colonies when compared to the DAOY and HCT116 cells.

A
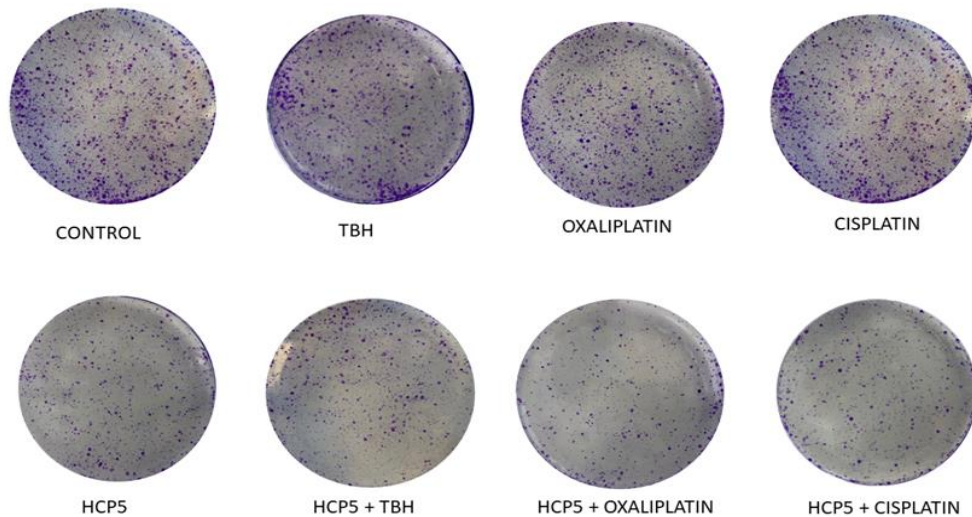
B
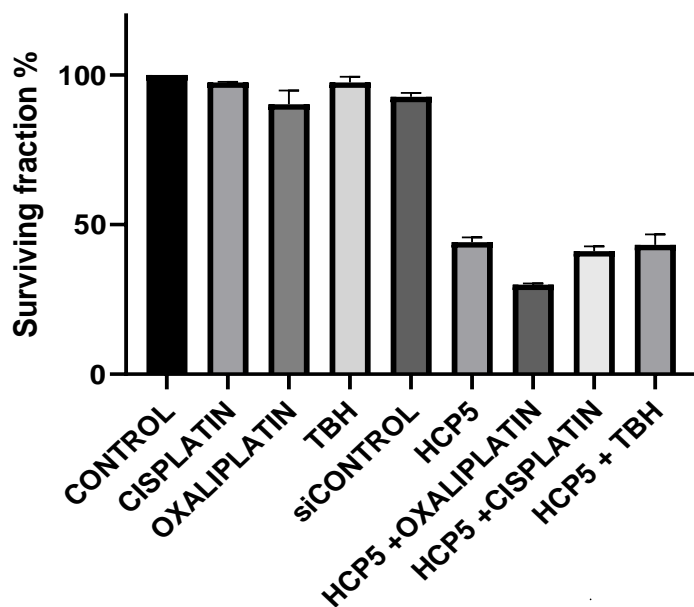
Figure 4.17 -Effect of single and combination treatments of anticancer agents and HCP5 knockdown on colony forming ability of SW480 cells.
SW480 cells were treated with cisplatin, oxaliplatin and TBH alone and in combination HCP5 knockdown for 24 hrs and allowed to grow for 14 days. (A) Colonies were fixed in methanol, stained with crystal violet, and counted. (B) The number of colonies were analysed and data are represented as mean ±standard deviation of the mean (n = 3).

Table 4.4 - Comparison of surviving fractions of the different treatment groups in SW480 cells. Statistical analysis was carried out using two-way ANOVA supplemented with Dunnett's multiple comparisons test.

Comparison	p value
CONTROL vs. CISPLATIN	0.57
CONTROL vs. OXALIPLATIN	<0.001
CONTROL vs. TBH	0.58
CONTROL vs. siCONTROL	0.003
CONTROL vs. HCP5	<0.001
CISPLATIN vs. HCP5 +CISPLATIN	<0.001
OXALIPLATIN vs. HCP5 +OXALIPLATIN	<0.001
TBH vs. HCP5 + TBH	<0.001
HCP5 vs. HCP5 +OXALIPLATIN	<0.001
HCP5 vs. HCP5 +CISPLATIN	<0.001
HCP5 vs. HCP5 + TBH	<0.001

In the SW480 cells, the cells were treated with 1 μM cisplatin or TBH and there was no significant difference between the surviving fraction when comparing the number of colonies in the control group, only the oxaliplatin treated group showed a significant reduction in the surviving fraction of the groups treated with only single agents (Figure 4.17). There was a however significant difference (p<0.001) in the number of colonies formed in the HCP5 knockdown cells compared to the siRNA-control group and when comparing the number of colonies formed from the single DNA damaging treatments compared to the combination treatments with HCP5 knockdown, there was significant decrease in the number of colonies formed with the three single treatments, when compared to their corresponding combination treatments, with (p<0.001) in all three cases (Table 4.4). When comparing the number of colonies formed from HCP5 knockdown group to the number of colonies formed in the different combination treatments, all the three combination treatment groups showed significant decrease in number of colonies (p<0.001) (Table 4.4), when compared to the HCP5 knockdown only group.
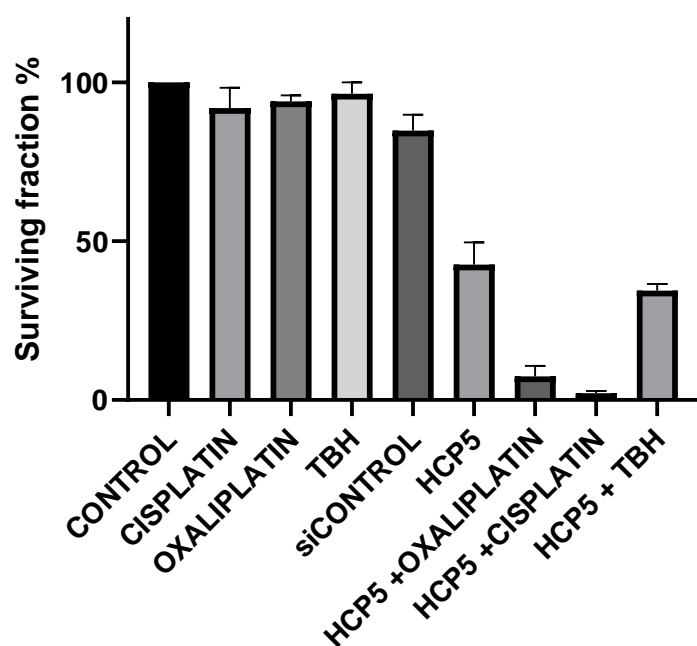
Figure 4.18 -**Effect of combination treatment of anticancer agents and HCP5 knockdown on colony forming ability of DAOY cells.**
DAOY cells were treated with cisplatin, oxaliplatin and TBH alone and in combination HCP5 knockdown for 24 hrs and allowed to grow for 14 days. (A) Colonies were fixed in methanol, stained with crystal violet, and counted. (B) The number of colonies was analysed and data are represented as mean ±standard deviation of the mean (n = 3).

Table 4.5- Comparison of surviving fractions of the different treatment groups in DAOY cells. Statistical analysis was carried out using two-way ANOVA supplemented with Dunnett's multiple comparisons test.

Comparison	p value
CONTROL vs. CISPLATIN	0.1
CONTROL vs. OXALIPLATIN	0.31
CONTROL vs. TBH	0.8
CONTROL vs. siCONTROL	<0.001
CONTROL vs. HCP5	<0.001
CISPLATIN vs. HCP5 +CISPLATIN	<0.001
OXALIPLATIN vs. HCP5 +OXALIPLATIN	<0.001
TBH vs. HCP5 + TBH	<0.001
HCP5 vs. HCP5 +OXALIPLATIN	<0.001
HCP5 vs. HCP5 +CISPLATIN	<0.001
HCP5 vs. HCP5 + TBH	0.09

The DAOY cells were treated with 0.1 μM of oxaliplatin, 0.1 μM of cisplatin and 1 μM of TBH. Comparison of the control colonies and the colonies formed from treatment with the DNA damaging agents only, showed no significant difference. A reduction in the size of colonies formed from the cells transfected for HCP5 knockdown was observed (Figure 4.18). However, comparison of the number of colonies formed from the cells treated with DNA damaging agents only with the colonies formed from the cells treated with the combination treatment, revealed significant decrease in the number of colonies across all the combination treatments. The number of colonies formed in the oxaliplatin and cisplatin combination treatments compared to the HCP5 knockdown group showed a significant decrease in the numbers of colonies, while there was no significant difference in the numbers of colonies formed between the TBH only group and the TBH + HCP5 knockdown group (Table 4.5).
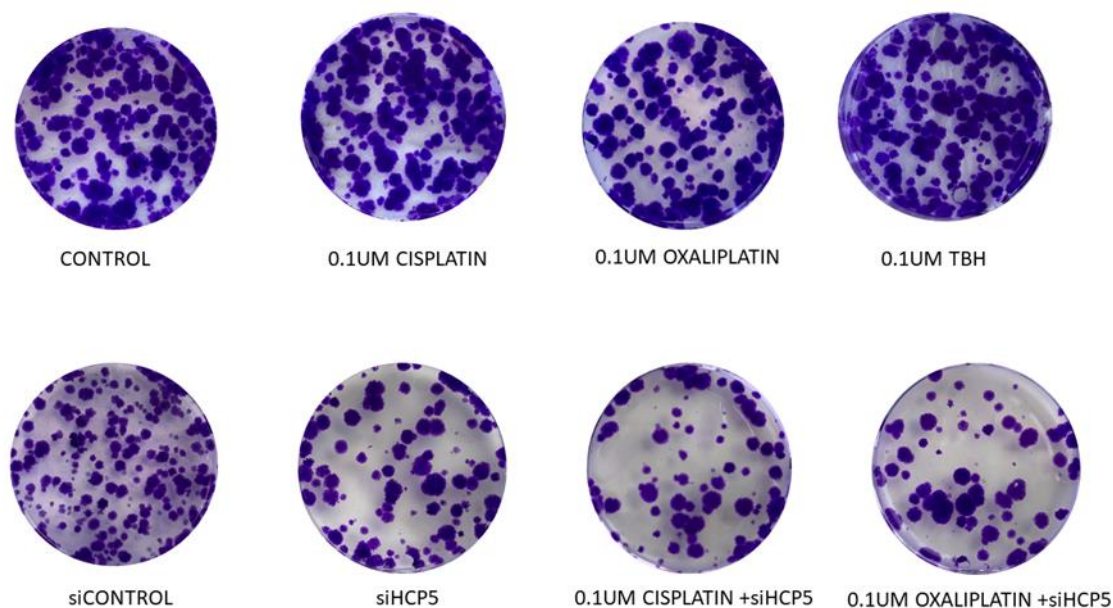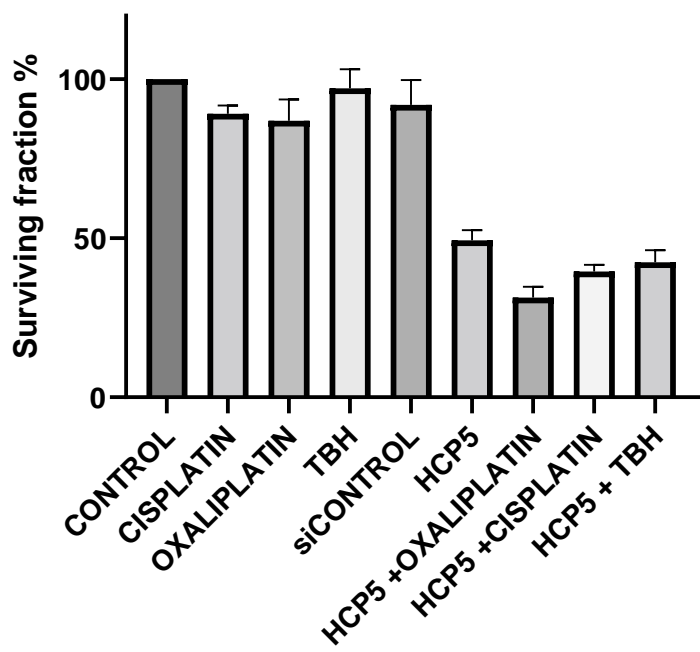
Figure 4.19 -Effect of single and combination treatments of anticancer agents and HCP5 knockdown on colony forming ability of HCT116 cells. HCT116 cells were treated with cisplatin, oxaliplatin and TBH alone and in combination HCP5 knockdown for 24 hrs and allowed to grow for 14 days. (A) Colonies were fixed in methanol, stained with crystal violet, and counted. (B) The number of colonies was analysed and data are represented as mean ±standard deviation of the mean (n = 3).

Table 4.6- Comparison of surviving fractions of the different treatment groups in HCT116 cells. Statistical analysis was carried out using two-way ANOVA supplemented with Dunnett's multiple comparisons test.

Comparison	p value
CONTROL vs. CISPLATIN	0.004
CONTROL vs. OXALIPLATIN	<0.001
CONTROL vs. TBH	0.81
CONTROL vs. siCONTROL	0.03
CONTROL vs. HCP5	<0.001
CISPLATIN vs. HCP5 +CISPLATIN	<0.001
OXALIPLATIN vs. HCP5 +OXALIPLATIN	<0.001
TBH vs. HCP5 + TBH	<0.001
HCP5 vs. HCP5 +OXALIPLATIN	<0.001
HCP5 vs. HCP5 +CISPLATIN	0.008
HCP5 vs. HCP5 + TBH	0.08

For the HCT116 cell line, the cells were treated with 0.1 μM of oxaliplatin, 0.1 μM of cisplatin and 1 μM of TBH (Figure 4.19). There was no significant difference between the number of colonies formed between the control cells and the cells treated with single agents, although there was a small decrease in the number of colonies formed from the cells treated with TBH and cisplatin, this difference was not significant. However, there was a significant decrease in the number of colonies formed after HCP5 knockdown and this decrease was constant when HCP5 knockdown was combined with the anti-cancer agents. When comparing the number of colonies formed from HCP5 knockdown group to the number of colonies formed in the different combination treatments, only the oxaliplatin + HCP5 ($p<0.001$) and the cisplatin + HCP5 ($p=0.008$) combination treatment showed significant decrease in number of colonies, when compared to the HCP5 knockdown only group (Table 4.6).
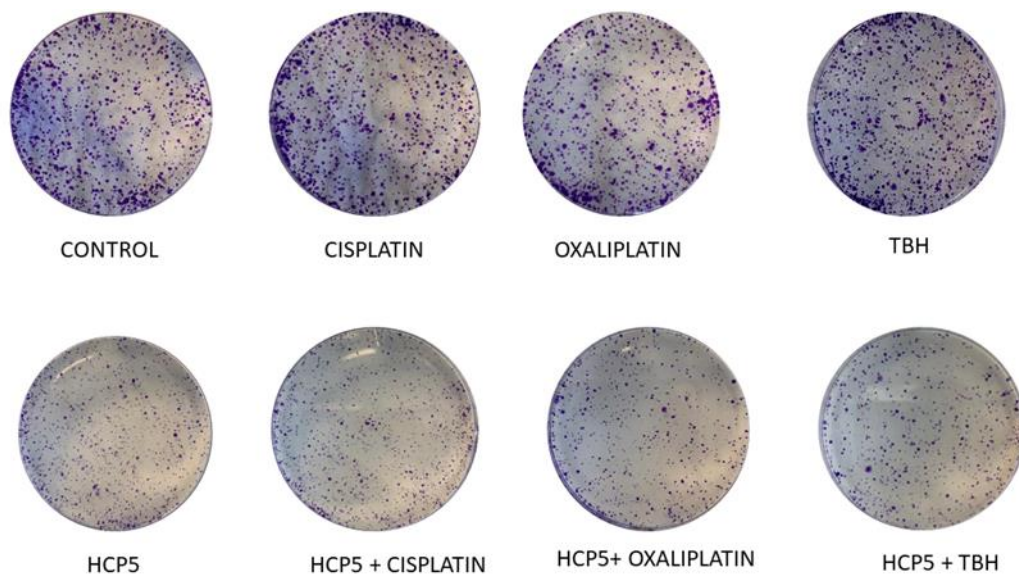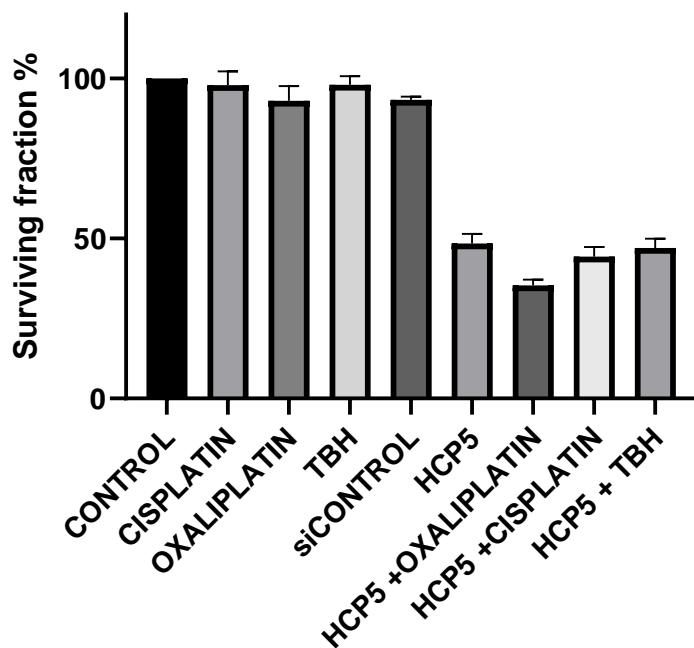
Figure 4.20 -**Effect of single and combination treatments of anticancer agents and HCP5 knockdown on colony forming ability of SW48 cells.**
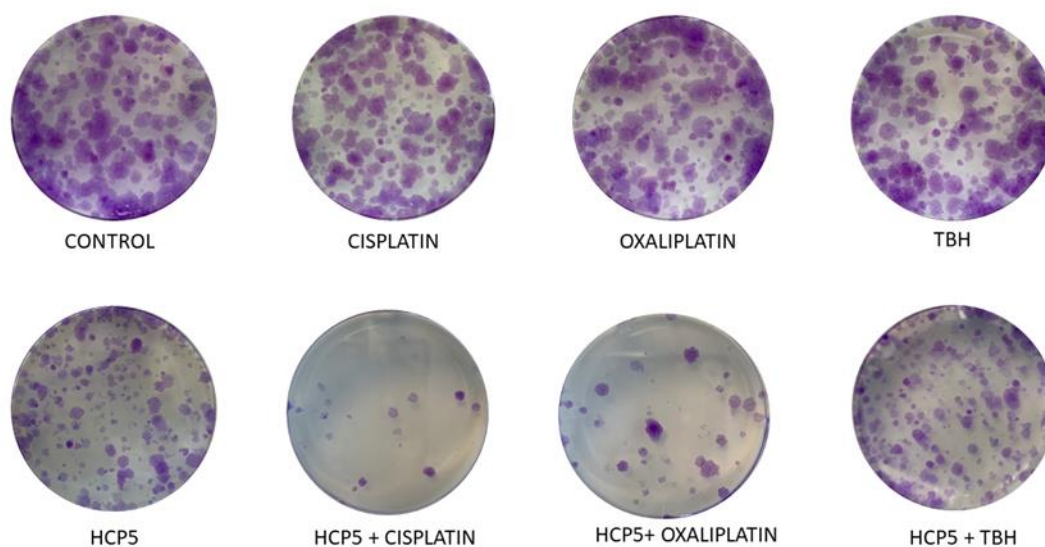SW48 cells were treated with cisplatin, oxaliplatin and TBH alone and in combination HCP5 knockdown for 24 h and allowed to grow for 14 days. (A) Colonies were fixed in methanol, stained with crystal violet, and counted. (B) The number of colonies was analysed and data are represented as mean ±standard deviation of the mean (n = 3).

Table 4.7- Comparison of surviving fractions of the different treatment groups in SW48 cells. Statistical analysis was carried out using two-way ANOVA supplemented with Dunnett's multiple comparisons test.

Comparison	p value
CONTROL vs. CISPLATIN	0.85
CONTROL vs. OXALIPLATIN	0.01
CONTROL vs. TBH	0.87
CONTROL vs. siCONTROL	0.02
CONTROL vs. HCP5	<0.001
CISPLATIN vs. HCP5 +CISPLATIN	<0.001
OXALIPLATIN vs. HCP5 +OXALIPLATIN	<0.001
TBH vs. HCP5 + TBH	<0.001
HCP5 vs. HCP5 +OXALIPLATIN	<0.001
HCP5 vs. HCP5 +CISPLATIN	0.22
HCP5 vs. HCP5 + TBH	0.97

The SW48 cells were treated with 0.1 µM of oxaliplatin, 0.1 µM of cisplatin and 1 µM of TBH. There was no significant difference between the number of colonies formed with single treatments when compared to the control treatment, however there was a slight decrease in number of colonies in the oxaliplatin treatment, however this decrease was not significant. HCP5 knockdown caused a significant reduction in the number of colonies formed when compared to the cells with siRNA-control knockdown. As shown in Figure 4.20, there was however no significant difference between the number of colonies formed when HCP5 was knocked down in combination with the cisplatin and also the TBH combination treatment and the number of colonies from HCP5 knockdown only. However, the oxaliplatin + HCP5 knockdown combination treatment showed a significant reduction in the number of colonies, when compared to the HCP5 knockdown group (Table 4.7).

4.1.10 HCP5 knockdown increases apoptosis.

The predominant cytotoxic mechanism of chemotherapeutic agents is thought to be the activation of apoptosis. Therefore, the apoptotic potential of combining HCP5 knockdown with the genotoxic agents was investigated in the four cell lines. Cells were treated with oxaliplatin, cisplatin or TBH individually or in combination with HCP5 knockdown for 48 hours to investigate the role of HCP5 knockdown on apoptosis. HCP5 was knocked down in the cells

and after 16 hours the cells were treated with cisplatin, oxaliplatin or TBH and subjected to flow cytometry (Annexin V/PI) analysis to determine the effect of HCP5 knockdown on chemotherapy induced apoptosis (Figure 4.21). In the HCT116 cell line, treatment with 5 μM cisplatin alone caused a reduction in the number of viable cells (82.3 ± 2.67%) when compared to the control (92.9 ± 3.8%) and an increase in the cells undergoing late apoptosis (10.9 ± 0.8%) when compared to the control (1.35 ± 0.34%). Treatment with 15 μM TBH resulted in a decrease of viable cells from 92.9 ± 3.8% to 82.8 ± 2.5% and an increase of cells in late apoptosis from 1.28 ± 0.34% to 8.35 ± 1.22% when compared to the control, while treatment with oxaliplatin reduced viable cells from 92.9 ± 3.8% to 76.8 ± 1.88 %, increased late apoptotic cells from 1.28 ± 0.34% to 10.5 ± 0.96% and early apoptotic cells from 1.19 ± 0.82% to 7.51 ± 1.9%. HCP5 knockdown led to an increase in the number of cells undergoing late apoptosis (1.35 ± 0.34% to 7.81 ± 0.9%) which in turn led to a decrease in the number of viable cells from 92.9 ± 3.8% to 87.1 ± 2.9%. When compared to cisplatin only treatment, combination of HCP5 knockdown with cisplatin treatment led to an increase in the number of cells undergoing late apoptosis (10.9 ± 0.8% to 21.7 ± 1.7%), while cells in early apoptosis increased from 4.53 ± 0.76% to 11.8 ± 1.9%, thereby leading to a reduction in the amount of viable from 82.3 ± 2.67% to 64.2 ± 3.4%.
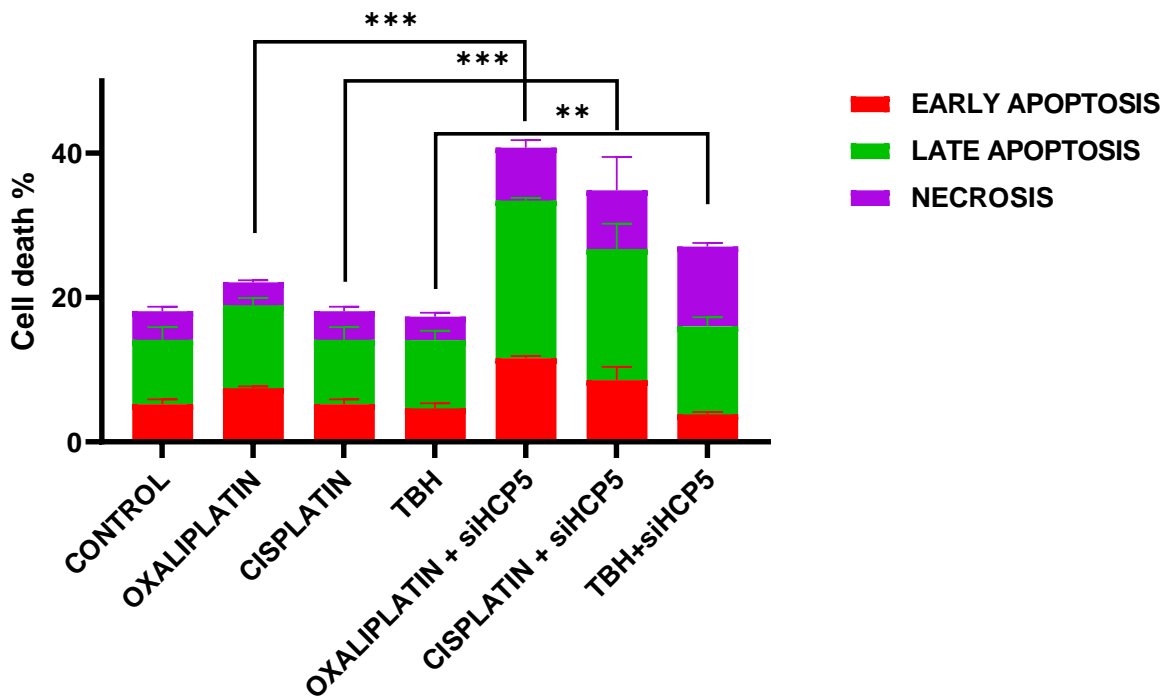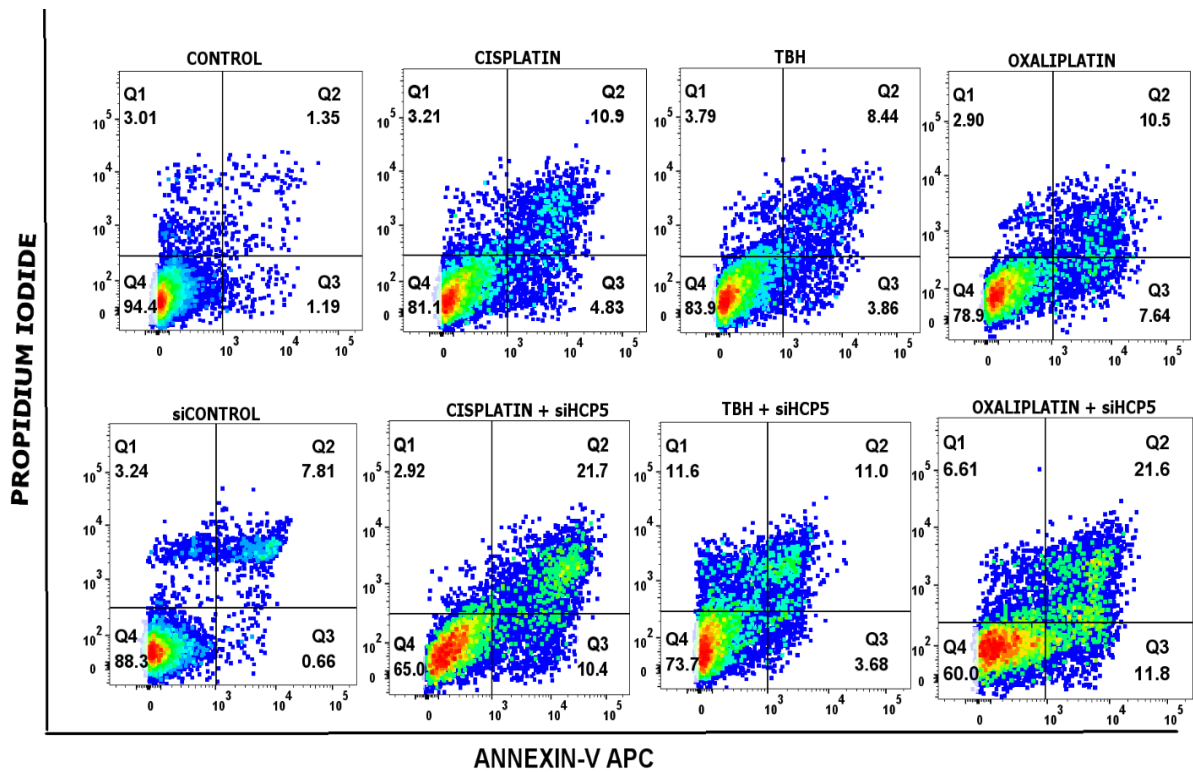
Figure 4.21- Combination of HCP5 knockdown and anticancer agents increases apoptosis in HCT116 cells.

Dual-colour flow cytometry of annexin V- APC/propidium iodide staining of HCT116. HCT116 cells were treated with oxaliplatin, cisplatin and TBH alone and in combination with HCP5 knockdown for 48 hours. In these representative set of plots, Q1(annexin V -/PI+) = necrotic population, Q2 (annexin V +/ PI+) = late apoptosis population, Q3 (annexin V+/ PI-) = early apoptosis population and Q4 (annexin V-/PI-) = viable population. Mean of the

percentage of apoptotic and necrotic population. Data are represented as mean ±standard deviation of the mean (n = 3). ***= p≤ 0.001.

The combination of TBH with HCP5 knockdown when compared to TBH alone resulted in an increase in cells in late apoptosis from 8.35 ± 1.22% to 11.5 ± 1.77%, there was however an increase in the number of necrotic cells from 3.01 ± 0.98% to 10.2 ± 2.2%, due to these increases, there was a reduction in the number of viable cells from 82.8 ± 2.5% to 73.7 ± 3.1%. Treatment with oxaliplatin only was compared to the HCP5 knockdown and oxaliplatin combination treatment and an increase in the late apoptosis population was observed (10.5 ± 0.96% to 19.8 ± 3.3%), an increase from 7.51 ± 1.9% to 10 ± 2.1% in the early apoptosis population and an increase in the necrotic population from 3.01 ± 1.12 % to 6.5 ± 1.33%. These resulted in a decrease in the viable cell population from 76.8 ± 1.88% to 59 ± 4.1%.

Figure 4.22- **Combination of HCP5 knockdown and anticancer agents increases apoptosis in DAOY cells.**
Dual-colour flow cytometry of annexin V- APC/propidium iodide staining of DAOY. DAOY cells were treated with oxaliplatin, cisplatin and TBH alone and in combination with HCP5 knockdown for 48 hours. In these representative set of plots, Q1(annexin V -/PI+) = necrotic population, Q2 (annexin V +/ PI+) = late apoptosis population, Q3 (annexin V+/ PI-) = early apoptosis population and Q4 (annexin V-/PI-) = viable population. Mean of the percentage of apoptotic and necrotic population. Data are represented as mean ±standard deviation of the mean (n = 3). ***= p≤ 0.001.

The DAOY cell line was treated with the various anticancer agents individually and in combination with HCP5 knockdown for 48 h and percentage of apoptosis was determined by flow cytometry (Figure 4.22). In the cisplatin only treatment, the cells were treated with 1 μM cisplatin and compared to the control, there was an increase in the early apoptosis population from $2.9 \pm 0.76\%$ to $7.6 \pm 1\%$, an increase in the late apoptosis population from $2.99 \pm 0.89\%$ to $11.6 \pm 1.56\%$, and the necrotic population from $1.05 \pm 0.6\%$ to $3.9 \pm 2.21\%$, which resulted in a decrease in the viable population from $92.1 \pm 1.57\%$ to $78.2 \pm 2.81\%$. The oxaliplatin treated cells were treated with 5 μM oxaliplatin, this resulted in an increase in the early apoptosis population from $2.9 \pm 0.76\%$ to $8.7 \pm 1.23\%$, an increase in the late apoptosis population from $2.99 \pm 0.89\%$ to $9.03 \pm 1.46\%$, increase in necrotic cells from $1.05 \pm 0.6\%$ to $2.0 \pm 0.2\%$, thus resulting in a decrease in the viable population from $92.1 \pm 1.57\%$ to $79.4 \pm 3.43\%$.

The cells were treated with 12.5 µM TBH which resulted in an increase in early apoptotic cells from 2.9 ± 0.76% to 3.55 ± 1.19%, increase in late apoptosis from 2.99 ± 0.89% to 4.76 ± 1.17%, decrease in necrotic cells from 1.05 ± 0.6% to 0.86 ± 0.34%, which resulted in a decrease of the viable population from 92.1 ± 1.57% to 87.11 ± 3.12. The cisplatin combination treatment with HCP5 knockdown when compared to the cisplatin only treatment, showed an increase in the early apoptosis population from to 7.6 ± 1% to 10.84 ± 1.15% and an increase in the late apoptosis population from 11.6 ±1.56% to 30.86 ± 1.23%, increase in the necrotic population from 3.9 ± 2.21% to 7.5 ± 1.09%, thus resulting in a decrease in the population of viable cells, from 78.6 ± 2.81% to 47.91 ± 3.33%.

The TBH + HCP5 knockdown combination treatment when compared to the TBH only treatment, resulted in an increase in the early apoptosis population from 3.55 ± 1.19% to 11.01 ± 1.99%, an increase in the late apoptosis population from 4.76 ± 1.17% to 18.17 ± 2.16%, an increase in the necrotic population from 0.86 ± 0.34% to 3.81 ± 1.37% which when combined resulted in a decrease in the viable cells population from 87.11 ± 3.12% to 64.22 ± 2.98%. While the oxaliplatin +siHCP5 treatment when compared to the oxaliplatin only treatment resulted in an increase in the early apoptosis population, from 8.7 ± 1.23% to 12.8 ± 5.9%, an increase in the late apoptosis population from 9.03 ± 1.46% to 27.03 ± 1.36%, an increase in the necrotic population from 2.0 ± 0.2% to 5.93 ± 2.96%, which in turn resulted in a reduction in the viable cell population, from 79.4 ± 2.43% to 53.8 ± 1.3%.

Figure 4.23- Combination of HCP5 knockdown and anticancer agents increases apoptosis in SW48 cells.

Dual-colour flow cytometry of annexin V- APC/propidium iodide staining of SW48. SW48 cells were treated with oxaliplatin, cisplatin and TBH alone and in combination with HCP5

knockdown for 48 hours. In these representative set of plots, Q1 (annexin V -/PI+) = necrotic population, Q2 (annexin V +/ PI+) = late apoptosis population, Q3 (annexin V+/ PI-) = early apoptosis population and Q4 (annexin V-/PI-) = viable population. Mean of the percentage of apoptotic and necrotic population. Data are represented as mean ±standard deviation of the mean (n = 3). ***= p≤ 0.001.

As shown in Figure 4.23, treatment with 5 µM cisplatin alone in the SW48 cell line caused a reduction in the number of viable cells from 93.1 ± 2.67% to 80.9 ± 1.9%, due to an increase in the early apoptosis population 1.52 ± 0.88% to 4.86 ±1.1%, increase in late apoptosis population 1.42 ±0.6% to 8.49 ± 2.1%, increase in the necrotic population from 1.92 ± 0.9% to 4.58 ±1.5% when compared to the control group. Treatment with 25 µM TBH resulted in a decrease of the viable population from 93.1 ± 2.67% to 86.9 ± 2.4% due to an increase of cells in early apoptosis from 1.52 ± 0.88% to 5.01 ± 1.88%, late apoptosis from 1.42 ± 0.6% to 3.98 ± 2% and a decrease in the necrotic population from 1.92 ± 0.9% to 1.62 ± 1.1%, when compared to the control. While treatment with oxaliplatin reduced viable cells from 93.1 ± 2.67% to 81.4 ± 2.8% resulting from an increase in early apoptotic cells from 1.52 ± 0.88% to 4.77 ± 2.1%, late apoptotic cells from 1.42 ± 0.6% to 8.26 ± 2.2% and necrotic cells from 1.92 ± 0.9% to 5 ± 1.82%. HCP5 knockdown led to an increase in the number of cells undergoing early apoptosis (1.52 ± 0.88% to 4.28 ± 1.12%), late apoptosis (1.42 ± 0.6% to 6.47 ± 1.6%) and necrotic cells (1.92 ± 0.9% to 4.01 ± 1.3%) which in turn led to a decrease in the number of viable cells from 93.1 ± 2.67% to 85.2 ± 3.1%. When compared to the cisplatin only treatment, combination of HCP5 knockdown with cisplatin treatment led to an increase in the number of cells undergoing early apoptosis (4.86 ± 1.1% to 15 ± 2.31%), while cells in late apoptosis increased from 8.49 ± 2.1% to 23.8 ± 3.12%, thereby leading to a reduction in the viable population from 93.1 ± 2.67% to 56.9 ± 3.9%.

The combination of TBH with HCP5 knockdown when compared to TBH alone resulted in an increase of cells in early apoptosis from 5.01 ± 1.88% to 7.09 ± 2.11%, late apoptosis 3.98 ± 2% to 21 ± 3.3% and necrotic cells from 1.62 ± 1.1% to 4.56 ± 1.89%, due to these increases, there was a reduction in the number of viable cells from 86.9 ± 2.4 % to 67.7 ± 2.15%. Comparison of the oxaliplatin only treatment with the HCP5 knockdown and oxaliplatin combination treatment resulted in an increase in the early apoptosis population from 4.77 ± 2.1% to 19 ± 3.1%, an increase from 8.26 ± 2.2% to 29 ± 3.32% in the late apoptosis population and a decrease in the necrotic population from 5 ± 1.82% to 2.68 ± 0.98%. These resulted in a decrease in the viable cells population from 81.4 ± 2.8% to 49.3 ± 4.4%.
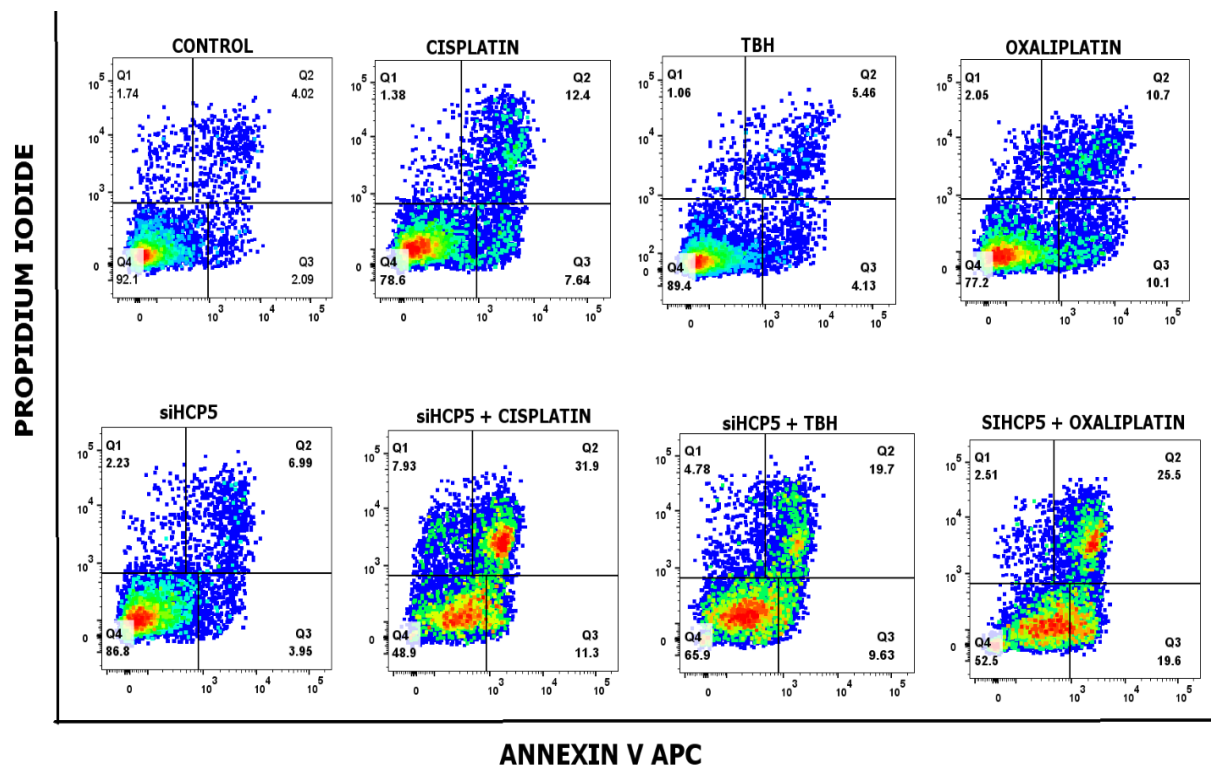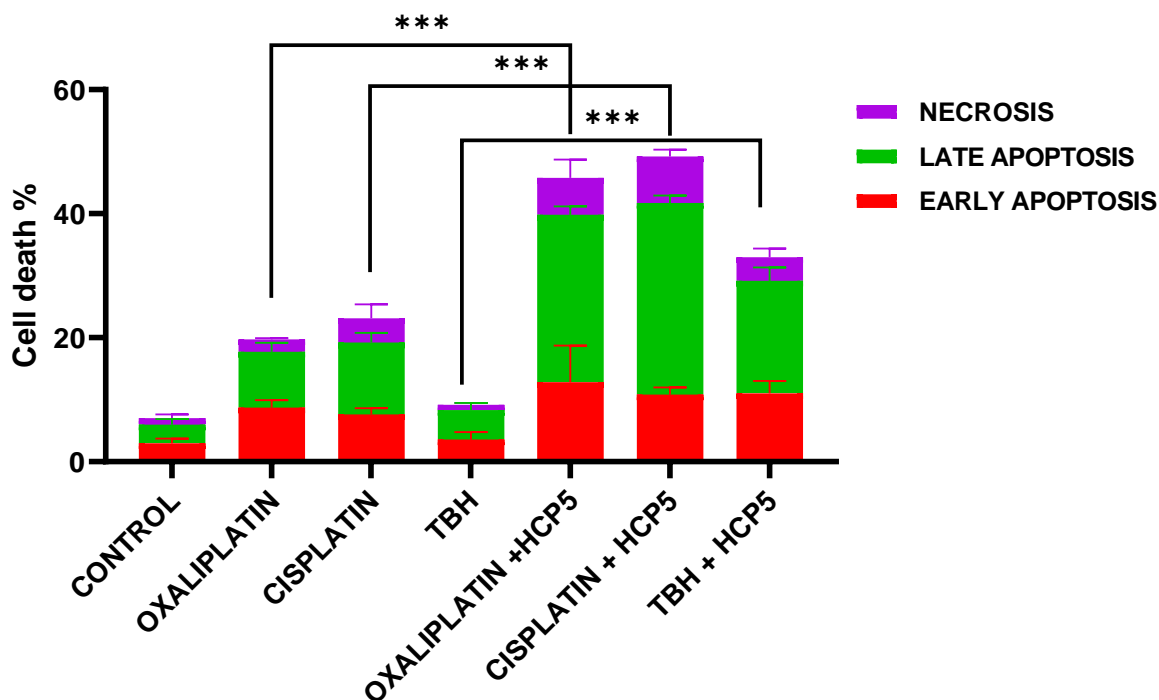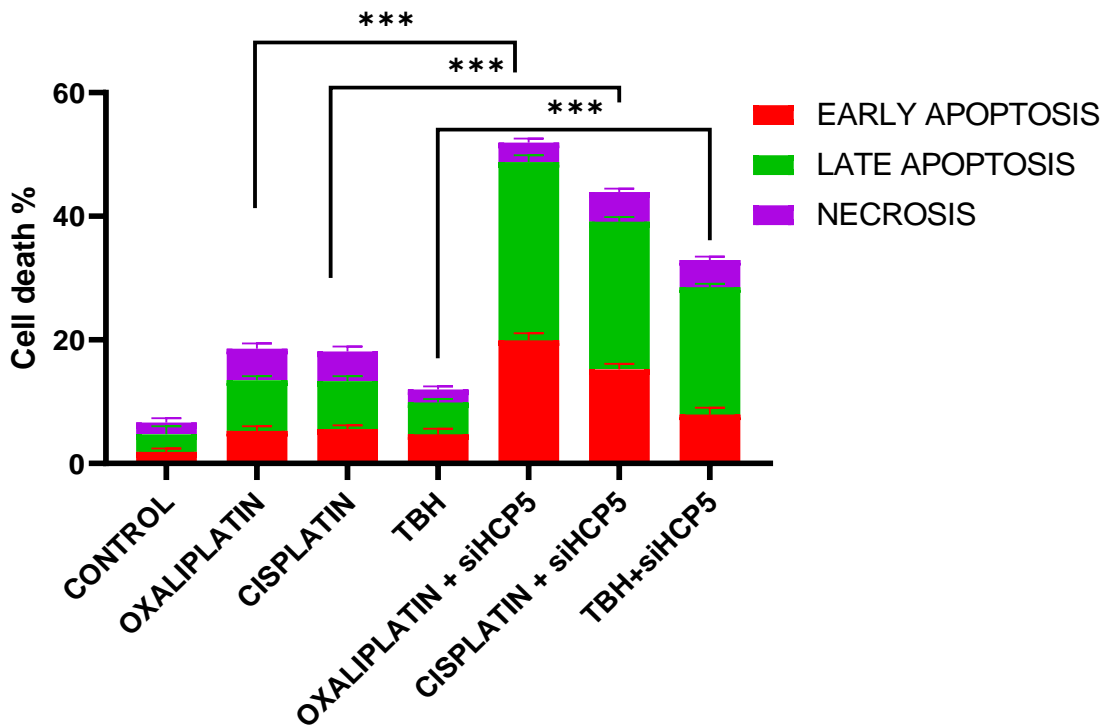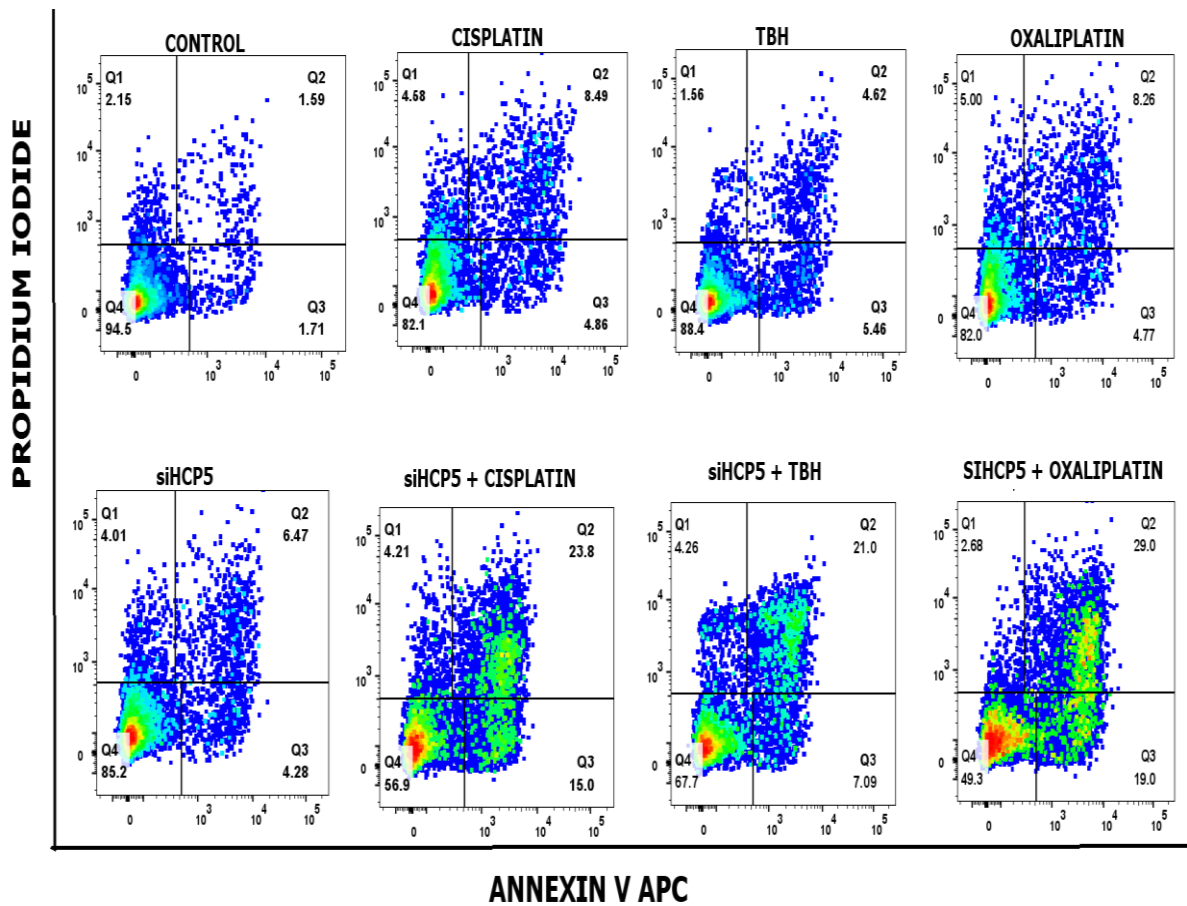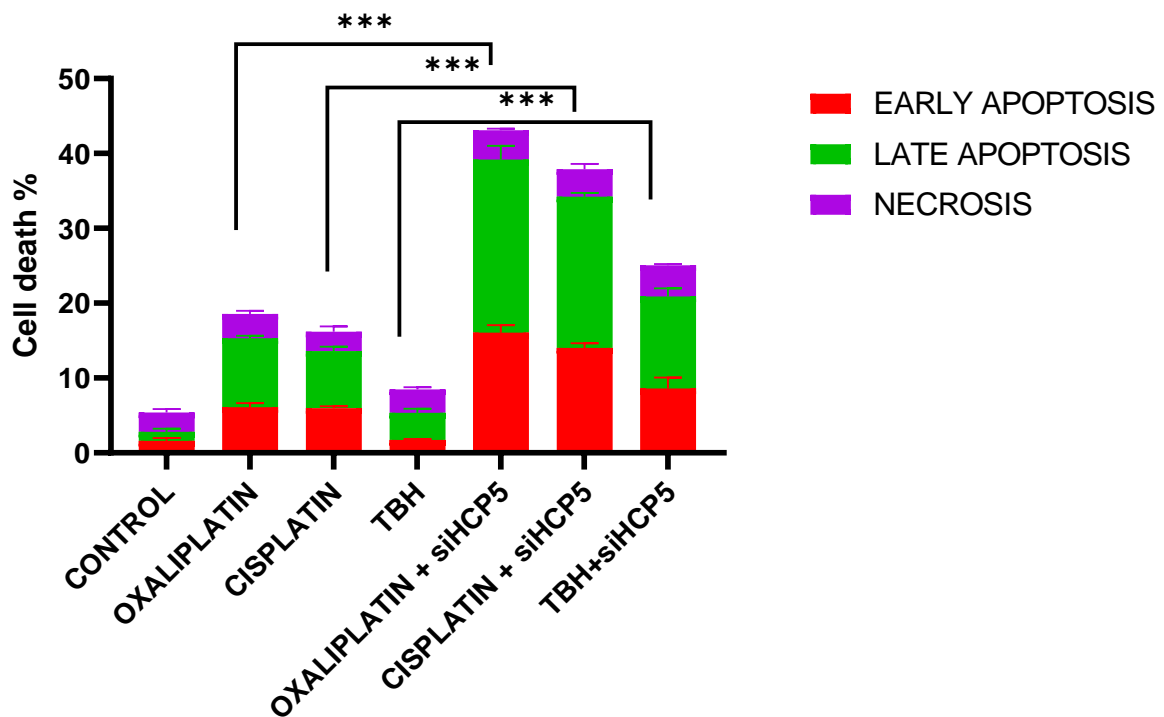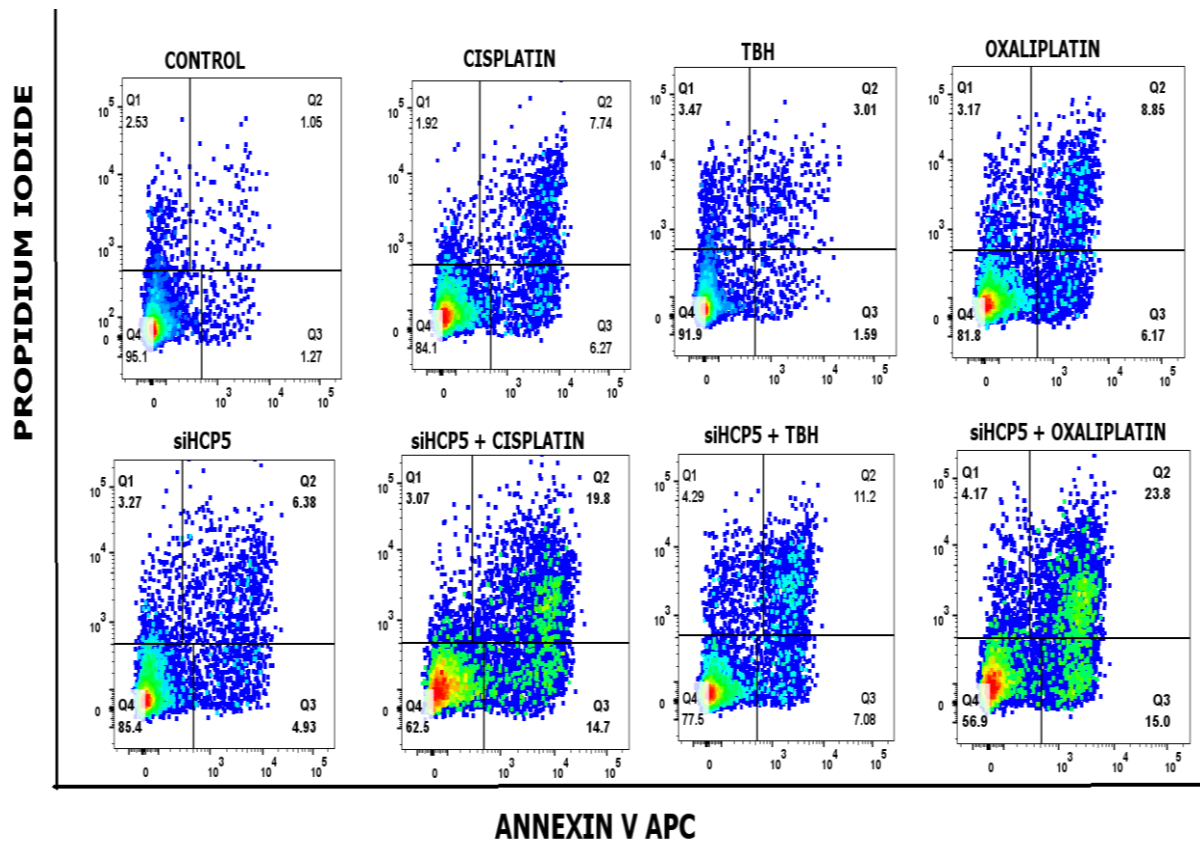
Figure 4.24 - **Combination of HCP5 knockdown and anticancer agents increases apoptosis in SW480 cells.**

Dual-colour flow cytometry of annexin V- APC/propidium iodide staining of SW480. SW480 cells were treated with oxaliplatin, cisplatin and TBH alone and in combination with HCP5 knockdown for 48 hours. In these representative set of plots, Q1(annexin V -/PI+) = necrotic

population, Q2 (Annexin V +/ PI+) = late apoptosis population, Q3 (Annexin V+/ PI-) = early apoptosis population and Q4 (Annexin V-/PI-) = viable population. Mean of the percentage of apoptotic and necrotic population. Data are represented as mean ±standard deviation of the mean (n = 3) ***= p≤ 0.001.

The SW480 cell line was treated with the various DNA damaging agents individually and in combination with HCP5 knockdown for 48 hours and the percentage of apoptosis was determined by flow cytometry (Figure 4.24). In the cisplatin only treatment, the cells were treated with 5 µM cisplatin and compared to the control, there was an increase in the early apoptosis population from $1.19 \pm 0.9\%$ to $7.31 \pm 1.89\%$, an increase in the late apoptosis population from $1.31 \pm 0.78\%$ to $6.83 \pm 2.1\%$, a decrease in the necrotic population from $2.15 \pm 1.92\%$ to $1.63 \pm 1.01\%$, which resulted in a decrease in the viable population from $93.6 \pm 2.9\%$ to $84.5 \pm 1.4\%$. The oxaliplatin treated cells were treated with 1 µM oxaliplatin, this resulted in an increase in the early apoptosis population from $1.19 \pm 0.9\%$ to $6.33 \pm 2\%$, an increase in the late apoptosis population from $1.31 \pm 0.78\%$ to $7.62 \pm 1.91\%$, increase in necrotic cells from $2.15 \pm 1.92\%$ to $3.05 \pm 0.84\%$, thus resulting in a decrease in the viable population from $93.6 \pm 2.9\%$ to $81.6 \pm 1.8\%$. The cells treated with 25 µM TBH showed an increase in early apoptotic cells from $1.19 \pm 0.9\%$ to 1.42%, increase in late apoptosis from $1.31 \pm 0.78\%$ to $3.01 \pm 1.6\%$, necrotic cells from $2.15 \pm 1.92\%$ to $2.81 \pm 1.89\%$, which resulted in a decrease of the viable population from $93.6 \pm 2.9\%$ to 89.2 ± 2.3 %. The cisplatin combination treatment with HCP5 knockdown when compared to the cisplatin only treatment, showed an increase in the early apoptosis population from $7.31 \pm 1.89\%$ to $12.3 \pm 3\%$, an increase in the late apoptosis population from $6.83 \pm 2.1\%$ to $20.65 \pm 2.12\%$, increase in the necrotic population from 1.92% to $2.76 \pm 2.1\%$, thus resulting in a decrease in the population of viable cells, from $84.5 \pm 1.4\%$ to 62.5%.

The TBH + HCP5 knockdown combination treatment when compared to the TBH only treatment, resulted in an increase in the early apoptosis population from 1.42% to 7.08%, an increase in the late apoptosis population from $3.01 \pm 1.6\%$ to $10.1 \pm 2.1\%$, an increase in the necrotic population from $2.81 \pm 1.89\%$ to $4.63 \pm 1.5\%$ which when combined resulted in a decrease in the viable cells population from $89.2 \pm 2.3\%$ to $75.3 \pm 2.12\%$. While the oxaliplatin +siHCP5 treatment when compared to the oxaliplatin only treatment resulted in an increase in the early apoptosis population, from 6.17% to $13.8 \pm 2.15\%$, an increase in the late apoptosis population from $7.62 \pm 1.91\%$ to $22.8 \pm 2.6\%$, an increase in the necrotic population from 3.05

± 0.84% to 4.3 ± 1.1%, which in turn resulted in a reduction in the viable cells population, from 81.6 ± 1.8% to 55.4 ± 3.6%.

4.1.11 HCP5 plays a pivotal role in YB-1 localisation to the nucleus.

To explore the regulatory role of HCP5 on YB-1, which has been shown to interact with HCP5, the expression level of YB-1 was determined by qPCR after HCP5 knockdown. The results shown in Figure 4.25 indicate that there was no change in the expression of YB-1 after knockdown of HCP5.
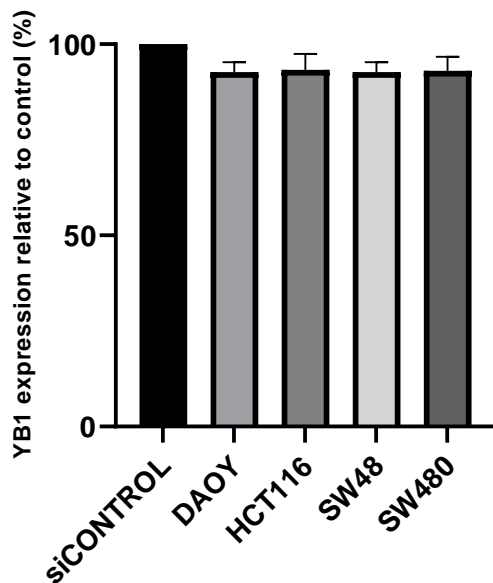
Figure 4.25 – Expression of YB-1 in cell lines after HCP5 knockdown.
Expression level of YB-1 in reference to actin after HCP5 knockdown was determined by qPCR. Each data point represents three independent experiments, carried out in triplicates (n=9). Analysis of data was carried out using the $2^{-\Delta\Delta Ct}$ method. Data are represented as mean and error bars ± standard deviation.

This was further explored by monitoring the movement of YB-1 in the cell, as it has been shown that YB-1 exerts its activity by travelling from the cytoplasm to the nucleus (Mehta *et al*., 2020). To determine this, immunofluorescence assay was used to determine the location of YB-1 in the cell. To begin, possible autofluorescence of each cell line was ruled out by running control experiments and also, preliminary experiments confirming that YB-1could be detected in the cytoplasm and nucleus of the cell lines used was carried out. Once this was confirmed, HCP5 was knocked down in the four cell lines and after 24 hours the location of HCP5 was determined using an immunofluorescence assay. The location of HCP5 in the control cells was

compared to its location in the HCP5 knockdown cells. It can be seen in all three cell lines shown in Figure 4.26 that YB-1 is found predominantly in the cytoplasm after HCP5 knockdown.

A
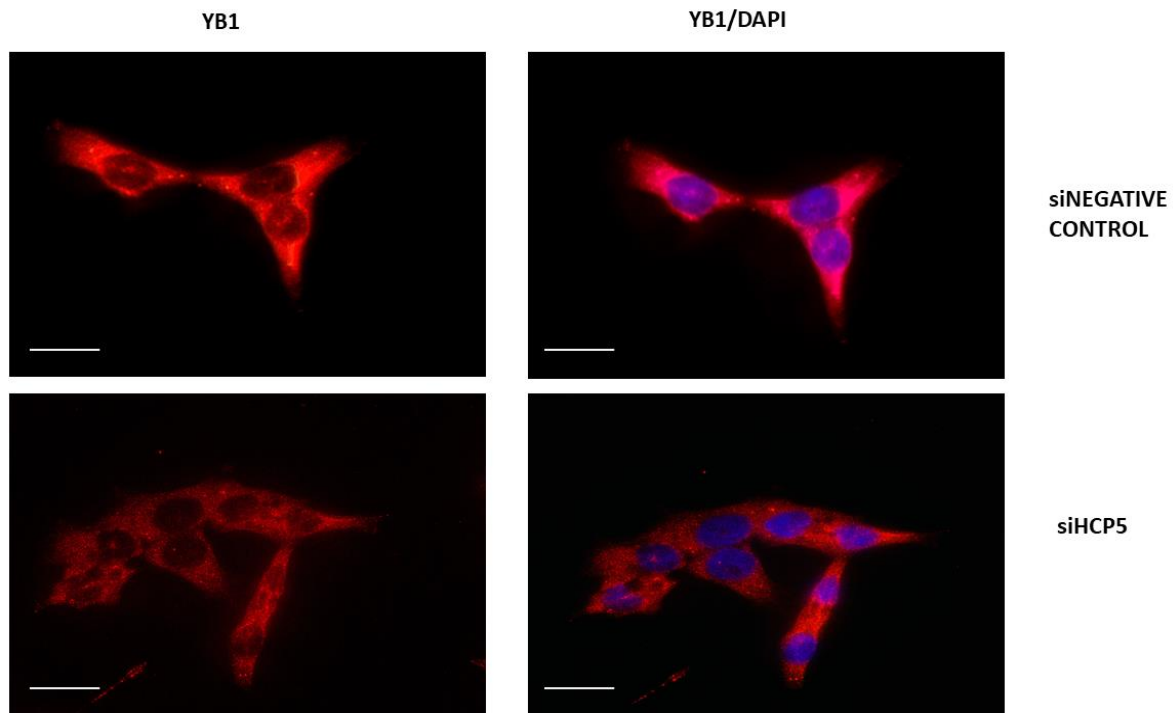
B
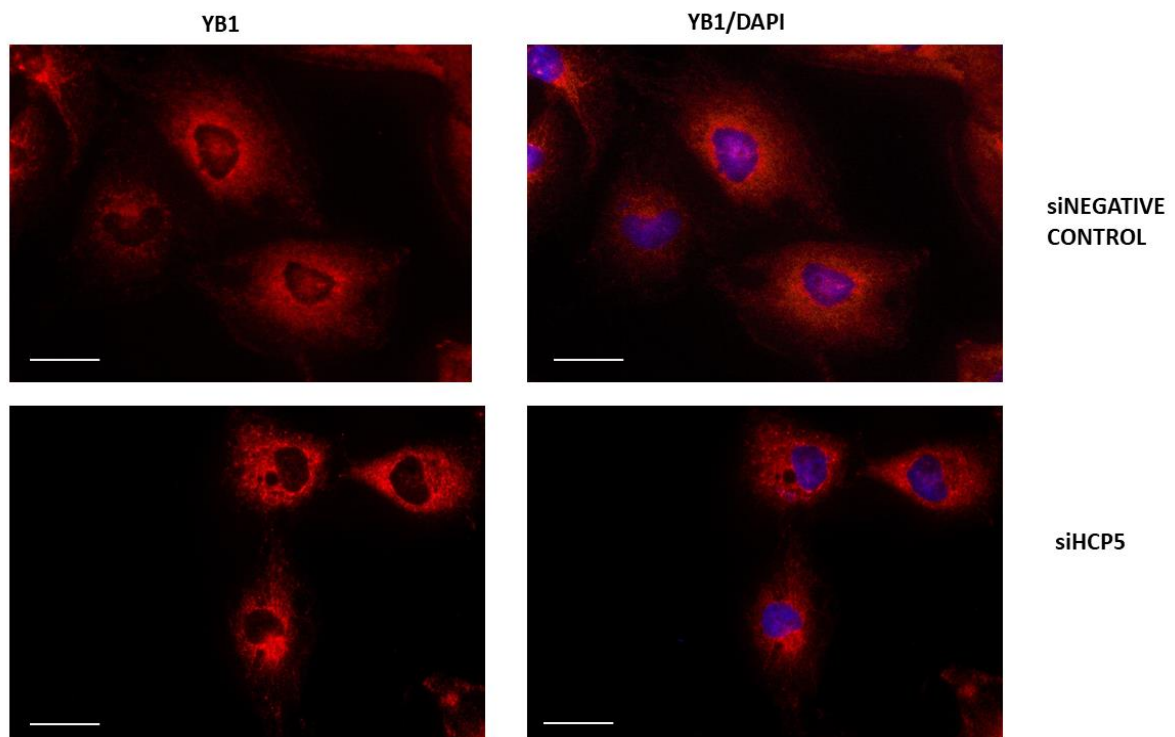
C
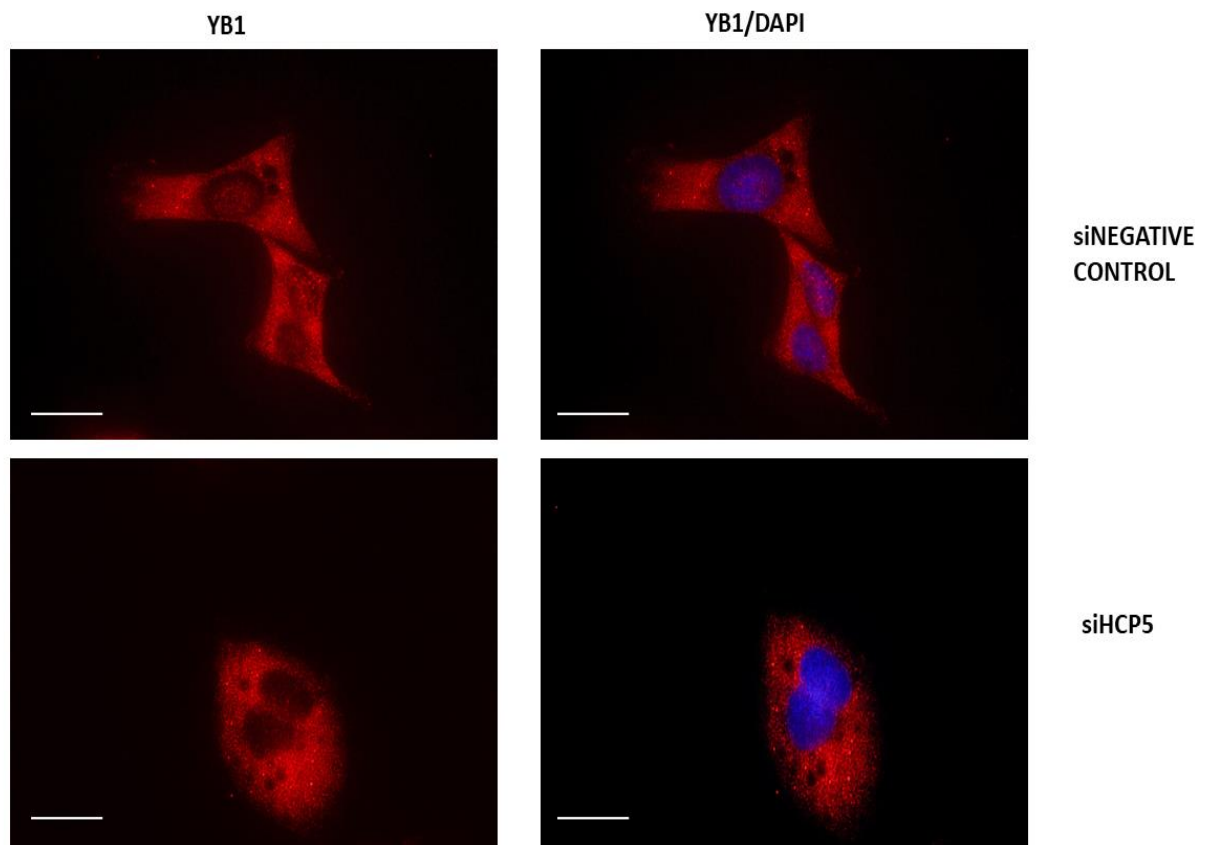
D
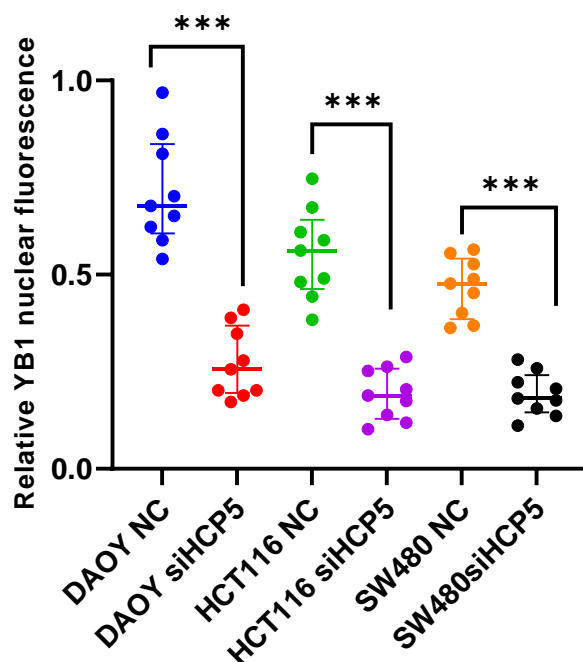
Figure 4.26 – YB-1 is found predominantly in the cytoplasm after HCP5 knockdown.
Immunofluorescence assay for YB-1 in (A)HCT116, (B) DAOY and (C) SW480 cells before
and after HCP5 knockdown. (D) Intensity of the nuclear immunofluorescence was quantified
using imageJ, ten images from four independent experiments were analysed (n=4). Scale bar

is 100 µm and magnification is 40X. Data is presented as the median ± interquartile range. ***= p≤ 0.001.

4.1.12 HCP5 knockdown increases double-strand breaks.

A characteristic feature of double-strand breaks in cells is the accumulation of γH2AX (Collins *et al*., 2020). To determine the effect of HCP5 knockdown on DNA damage and formation of double strand breaks, the four cell lines were treated with the platinum compounds cisplatin and oxaliplatin. The cells were treated with either only cisplatin or oxaliplatin for 24 h and then another batch of cells where HCP5 was knocked down with oligo4 were also treated with oxaliplatin or cisplatin for 24 h and the result analysed by western blot assay to determine the expression level of γH2AX before and after HCP5 knockdown. The cells were treated with varying concentrations of oxaliplatin and cisplatin (as shown in Figure 4.27) as all the cell lines responded differently to each treatment. The expression of γH2AX a marker for the induction of double-strand breaks was analysed and γH2AX expression was found to be higher in the cells where HCP5 had been knocked down prior to treatment with oxaliplatin or cisplatin. This result was the same across the four cell lines for both cisplatin and oxaliplatin.
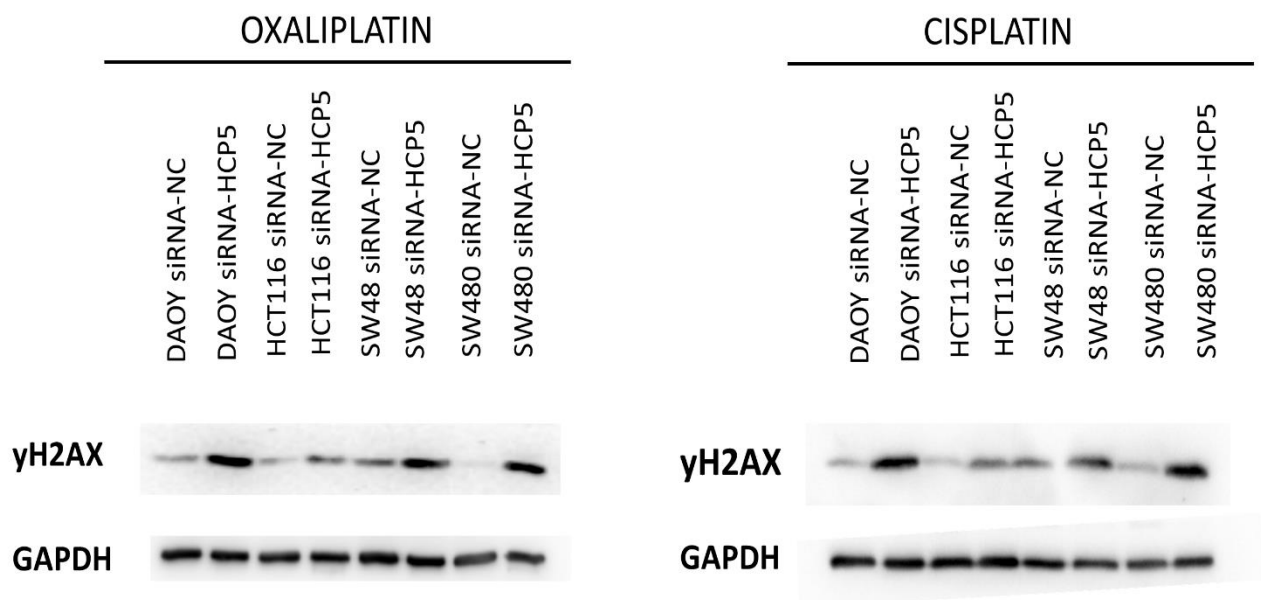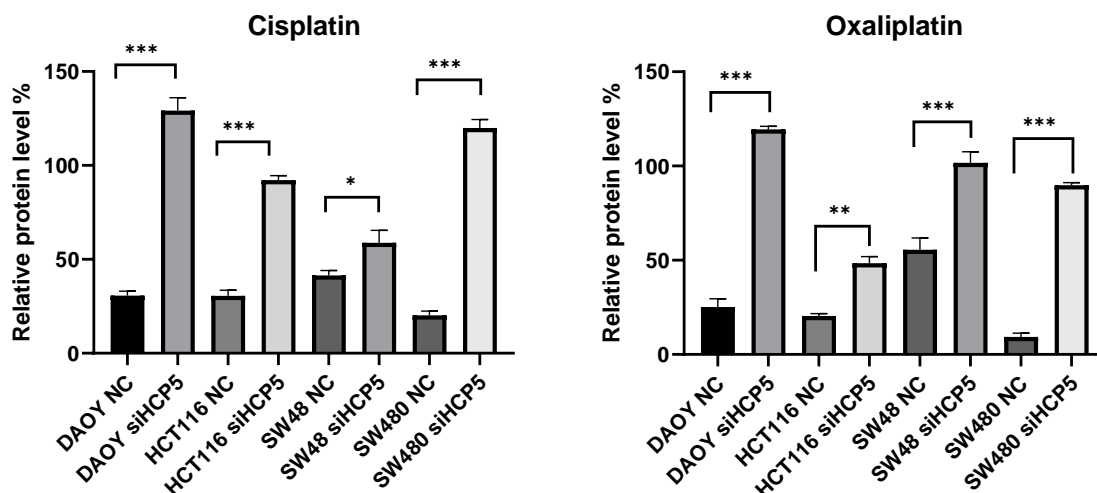
Figure 4.27- **HCP5 knockdown increases double-strand break formation when combined with oxaliplatin and cisplatin.**
Cells were treated with cisplatin and oxaliplatin separately for 24 hours and results compared to cells treated with combination of HCP5 knockdown and the platinum compounds. Expression level of γ-H2AX was obtained by western blot using GAPDH as a loading control. Each band was quantified by densitometric analysis in relation to GAPDH. Each data point represents three independent experiments (n=3). Data are represented as mean ±standard deviation of the mean. ns = p>0.05, * = p ≤0.05, ** = p≤ 0.01, ***= p≤ 0.001.

4.2 Discussion

Cancer is one of the major causes of death in the United Kingdom and the world at large and it is a significant impediment to a higher life expectancy (Bray *et al.*, 2021). Although treatment for cancer has evolved over time, with new advances in radiotherapy, immunotherapy and most especially adjuvant chemotherapy, most of the success of these treatments has been flawed by drug resistance, patient relapse and severe side effects (Zugazagoitia,*et al.*, 2016). Despite an increase in the number of cancer treatment options in the past few years, the clinical outcome for certain cancers is still poor. One of the main reasons for this is the absence of a sensitive and specific biomarker for early tumour detection; in a high percentage of cancer patients, the cancer is only detected when it has progressed to an advanced stage, thus making treatment difficult (Shi *et al.*, 2021). Early detection and improved therapy regimen are critical for improving the prognosis of cancer patients, hence finding new biomarkers and therapeutic targets for cancer is of critical clinical importance (Hu *et al.*, 2021).

HCP5 a long non-coding RNA which has been identified as an oncogene that plays different roles in the proliferation and migration of cancer cells (Zhao & Li, 2019). HCP5 has been "tipped" as a possible biomarker, as well as a therapeutic target, in the diagnosis, prognosis, and treatment of CRC (Qin *et al.*, 2021)). The expression of HCP5, its function, and possible clinical applications have all been studied extensively since its discovery in 1993 (Hu *et al.*, 2021). Nonetheless, both published and unpublished data obtained from online public databanks for this project demonstrated that HCP5 plays a key role in wellness and disease, especially as a ceRNA modulator and biomarker in autoimmune disorders and cancer (Zou et al., 2021, Hu *et al.*, 2021).

It is widely recognised that dysregulated lncRNAs play a key role in the emergence of chemoresistance and chemoresistance has been linked to HCP5 expression (Yang *et al.*, 2019; Bai *et al.*, 2020). For instance, by functioning as a ceRNA to sponge miR-214-3p and thus increase the expression of heparin binding growth factor protein, HCP5 knockdown re-sensitized gemcitabine-resistant pancreatic cancer cells toward gemcitabine by inhibiting proliferation, invasion, migration, and inducing apoptosis and autophagy (Liu *et al.*, 2019). The up-regulation of lncRNA HCP5 facilitated by mesenchymal stem cells promoted stemness and resistance to oxaliplatin and 5-FU in GC cells through the miR-3619-5p/AMPK/PGC1α/CEBPB axis (Wu *et al.*, 2020). HCP5 led to cisplatin resistance in cisplatin-resistant breast cancer cells through PTEN inhibition (Wu *et al.*, 2019). Nonetheless, the role

of HCP5 in resistance to DNA damaging agents has never been studied in medulloblastoma or CRC cells.

Herein, an *in-silico* analysis of RNA-seq data from the TCGA STAD dataset was carried out, which revealed that HCP5 was up-regulated in tumour tissue when compared to healthy normal tissues in different types of cancer (Figure 4.1). To investigate further, an *in-silico* analysis to compare the expression of HCP5 in 223 medulloblastoma samples and 315 CRC samples was carried out (Figure 4.2). This revealed that HCP5 expression was significantly higher in CRC compared to medulloblastoma. Based on this data, the expression level of HCP5 in three medulloblastoma cell lines and five CRC cell lines was determined and as seen in Figure 4.3, expression of HCP5 was generally higher in the CRC cell lines than the medulloblastoma and that the CRC cell line SW48 had a significantly higher expression of HCP5 when compared to the other cell lines (Figure 4.3). Four cell lines were then chosen for further research based on this data (DAOY, HCT116, SW48 and SW480). One medulloblastoma cell line was chosen to determine if the results of HCP5 experiments in the CRC cell lines could be replicated in other types of cancers.

The multifunctional protein YB-1 was discovered to play a key role in the function of HCP5 and Wang *et al*. (2020) showed that HCP5 binds directly to YB-1 and therefore, that one of the ways HCP5 carries out its function is via YB-1 activity. Of interest here, YB-1 has been shown to interact with the DNA glycosylases NTH1, NEIL1 and NEIL2 and Das *et al*. (2007) reported that YB-1 was directly linked to NEIL2 and improved the rate of base excision repair initiated by NEIL2. Thus, due to the interaction of YB-1 with these key DNA repair proteins, it was decided to determine the expression levels of selected DNA repair genes. This included the three proteins known to interact with YB-1 and NEIL3, ERCC1 and OGG1 that are also involved in the repair of DNA damage induced by the genotoxic agents used in these experiments.

As shown in Figure 4.7, the four cell lines did not show a consistent expression pattern for the different genes analysed. For example, the CRC cell lines HCT116 and SW48 showed a higher expression level for all the genes tested except ERCC1 when compared to the other two cell lines. Thus, HCT116 had the highest expression of NEIL1, 2 and 3, while SW48 had the highest expression of OGG1, YB-1 and NTH1, which was interesting, as SW48 also had the highest expression levels of HCP5 (Figure 4.3). Interestingly, Guay *et al*. (2008) showed that NTH1 is a target of YB-1 and confers resistance to cisplatin in breast cancer cells and that there was an

increase in the amount of NTH1/YB-1 complex formed in cells overexpressing YB-1 after treatment with cisplatin. Therefore, at this point it was of interest to know if SW48 was resistant to cisplatin as it showed a high mRNA level for both YB-1 and NTH1. It was also of interest to determine if knockdown of HCP5 had any effect on the expression of the DNA repair genes and if knockdown of HCP5 could sensitise these cells to genotoxic agents.

Heterogeneity in sensitivity of cancer cells to DNA damaging agents.

The main issue facing pharmaceutical development particularly in oncology and immune therapy, is variability in patient responses to even the most effective and tailored medicines (Yang *et al.*, 2010). The data obtained from the MTT assay (Figure 4.8) clearly revealed that the four cell lines responded differently to treatment with TBH, oxaliplatin and cisplatin. When comparing the response of the four cell lines to cisplatin, the DAOY cells were more sensitive to the cisplatin treatment when compared to the CRC cell lines, with the SW48 cells being the least sensitive. An investigation into the possible source of resistance to cisplatin, revealed that a number of genes have been shown to play a key role in cisplatin resistance, including ERCC1 (Zhang *et al.*, 2006). Previous studies *in vitro* have connected cisplatin resistance to the expression of ERCC1 mRNA in cervical cancer cell lines (Britten *et al.*, 2000). ERCC1, which is a subunit of the ERCC1-XPF endonuclease is essential for NER, which is the process used to repair intra-strand crosslinks formed by cisplatin (Arora *et al.*, 2010). This was, however, conflicting with the data derived from this experiment as the DAOY cells had the highest expression of ERCC1 but were the most sensitive to cisplatin (Figure 4.7). However, contrary to this, it must also be taken into consideration that the high ERCC1 expression shown in the DAOY cells was also shown to confer resistance to oxaliplatin treatment (Hector *et al.*, 2001). Thus, these experiments just confirm the multiple pathways of resistance to genotoxic agents that exist in tumour cells and that it is rare for one protein (or other macromolecule) to confer resistance uniquely.

A further study into the possible cause of resistance displayed by the CRC cell lines to cisplatin might be due to the over expression of YB-1 in the CRC cell lines when compared to the DAOY cell line as shown in Figure 4.7, as numerous studies have shown that secondary resistance to cisplatin is associated with the overexpression of YB-1 in melanoma, ovarian and breast cancer cells (Yahata *et al.*, 2002; Janz *et al.*, 2002; Schittek *et al.*, 2007). Additional research has shown that cisplatin-modified DNA is a preferred target for YB-1 (Ise *et al.*, 1999) and YB-1 aggressively encourages strand separation of duplex DNA that has either cisplatin alterations

or mismatches, regardless of the nucleotide sequence (Gaudreault *et al*., 2004). Applying this hypothesis to the results from these studies and comparing the expression level of YB-1 to the sensitivity of the cells to cisplatin, it can be seen that the CRC cells which were resistant to cisplatin had a higher expression of YB-1 (Figure 4.7).

Another gene that has been shown to confer resistance to cisplatin in cancer cells is the DNA glycosylase NEIL3 (Wang *et al*., 2021). The NEIL family, which includes NEIL3, are DNA glycosylase / lyases that remove oxidised bases to initiate BER in order to preserve genomic integrity (Makasheva *et al*., 2020). Wang *et al* (2021a) showed that knockdown of NEIL3 in prostate cancer cells resulted in an increased sensitivity to cisplatin which was attributed to its high homology, through the GRF zinc finger domain, which activates the ATR pathway (Wallace *et al*., 2017). Phosphorylation of ATR was also found to be accelerated by NEIL3 and NEIL3 also directly increases the protein level of ataxia telangiectasia and Rad3-related protein (Wang *et al*., 2021a; Wang *et al*., 2021b). When comparing the expression of NEIL3 in the various cell lines and the sensitivity of each cell line to cisplatin, the DAOY cell line which was the most sensitive to cisplatin had the lowest expression of NEIL3, while the CRC cell lines which were resistant to cisplatin had a higher expression of NEIL3 (Figure 4.7). However, the HCT116 cell line had the highest expression of NEIL3 out of the four cell lines, but it was the most sensitive to cisplatin out of the three CRC cell lines, therefore based on the results of this study, NEIL3 might have played a part in the sensitivity of the cells to cisplatin, but it was not applicable across all the cell lines. It is also important to take into consideration the previous studies by Tran *et al*. (2020) that showed that patients from six different types of cancer with NEIL3 overexpression had considerably worse clinical outcomes. High NEIL3 expression, on the other hand, was linked to higher cancer-specific survival in patients with colorectal and stomach cancer. As a result, several investigations have demonstrated that NEIL3 overexpression may play a very varied role in malignancies originating from different organs (Tran *et al*., 2020).

Furthermore, considering the oxaliplatin treatment, the CRC cell lines were more sensitive to oxaliplatin when compared to the DAOY cell line, with the HCT116 cell line being the most sensitive (Figure 4.8). As mentioned, various genes have been cited to play a part in the resistance of cells to oxaliplatin with ERCC1 being at the forefront. Hector *et al*. (2001) proposed that the sensitivity or resistance to oxaliplatin may be determined by the relative expression of ERCC1. Therefore, a cancer cell in which oxaliplatin induces ERCC1 will be resistant to its cytotoxic effects (Seetharam *et al*., 2010). Results from this study showed that

DAOY cells had the highest expression of ERCC1 and were also highly resistant to oxaliplatin which signifies ERCC1 expression might play a role in oxaliplatin resistance in DAOY medulloblastoma cells. However, this pattern was not observed with the CRC cell lines, as the HCT116 cells also had a high expression of ERCC1 when compared to the SW480 and SW48 cell lines but were the most sensitive to oxaliplatin amongst the four cell lines (Figure 4.7). Therefore, from these results, it is clear again, that multiple factors must be involved in the resistance of CRC cells to oxaliplatin, and it is difficult to infer the contribution of ERCC1 on oxaliplatin resistance in these cells.

It is well known that oxidative damage induced by ROS, destroys cellular macromolecules, including DNA, RNA, proteins, and lipids and is one of the contributing factors to the onset of various malignancies (Alia *et al*., 2005). The TBH treatment revealed that the SW48 cells were highly resistant to TBH (which is used to induce ROS in cells) with no IC50 value obtained even at 100 µM, while the DAOY cell line was the most sensitive to TBH when comparing the four cell lines. The BER pathway is crucial in preventing the build-up of oxidative DNA damage, a damage-specific DNA glycosylase must identify and remove the affected base in the initial step of BER (Jacobs & Schär, 2012). 8-oxoguanine DNA glycosylase and endonuclease III-like protein 1 are the two main DNA glycosylases that participate in the repair of oxidised DNA bases, together with the NEIL family of proteins (Parsons & Dianov, 2013). Taking this into consideration, it was interesting to see that the SW48 cell line, which was the most resistant to TBH had a high expression of OGG1 and NTH1 (Figure 4.7). This is in line with results by Yang *et al*. (2006) who showed that in H_2O_2 treated cells with a high percentage of individually damaged sites, overexpression of NTH1 and OGG1 enhanced resistance to the cytotoxic effects of H_2O_2, whereas cells with lower expression of NTH1 and OGG1 were more vulnerable. A closer investigation into how these DNA glycosylases confer this resistance revealed that although OGG1 speeds up the rate of repairing 8-oxoguanine, overexpression of OGG1 had no impact on the amount of endogenous oxidative DNA damage (Hollenbach *et al*., 1999). Similar findings were reported by Dahle *et al*. (2008) who conclude that OGG1 may play a part in preserving genomic stability in cancer cells after oxidative stress. Therefore, if increased OGG1 expression speeds up the repair of the DNA damage in the cell before the induction of apoptosis, the more cells evading apoptosis and surviving oxidation induced DNA damage treatment. Comparing the function of both DNA glycosylases, it was believed that since NTH1 is capable of repairing a number of cytotoxic DNA lesions, including the frequently occurring oxidised pyrimidine thymine glycol, it may partake in a more significant

191

role in H_2O_2 cytotoxicity (Yang *et al*., 2006). OGG1 primarily eliminates the pre-mutagenic lesion 8-oxoguanine and, to a lesser extent, Fapy-G which is also a substrate for NTH1 (Ba *et al*., 2018) and NTH1 has been shown to provide backup for OGG1 to release Fapy-G (Asagoshi *et al*., 2000). From the results of this study, it can be noted that the higher the expression of OGG1, the more resistant the cell line is to TBH, and therefore based on these results and hypotheses from other studies, it can be proposed that high expression of OGG1 and NTH1 confers resistance to oxidative stress induced by certain DNA damaging agents (ROS).

HCP5 knockdown combined with DNA damaging agents inhibits cell proliferation, colony formation in cancer cells and encourages the induction of apoptosis.

Drug resistance, whether intrinsic or acquired, is the principal barrier to effective cancer treatment (Vasan *et al*., 2019). To combat drug resistance in medulloblastoma and CRC cells, it is important to find relevant indicators for anticipating chemoresistance and modifying treatment plans for individual patients (Begg *et al*., 2011). Here, evidence is provided that indicates that HCP5 silencing might be a useful tool for combating genotoxic agent chemotherapeutic resistance. In the present study, the antiproliferative capacity of the combination of HCP5 knockdown with the DNA damaging agent treatment was examined. The results show that treatment with cisplatin, oxaliplatin or TBH induced dose-dependent inhibition of growth in CRC and medulloblastoma cells (Figures 4.8). More interestingly, for the first time it was shown that the combination of HCP5 knockdown and DNA damaging agent treatment had a significant anti-proliferative effect in the CRC and medulloblastoma cancer cell lines as shown in Figure 4.13- 4.16. This was also demonstrated by the MTT assay IC50 values, which showed that the knockdown of HCP5 before exposure to DNA damaging agents resulted in a lower IC50 value when compared to genotoxin treatment alone (Table 4.1). In line with the MTT assay, observations from the colony formation assay indicated the synergistic effect of HCP5 knockdown and the DNA damaging agents. When HCP5 knockdown was combined with treatment with DNA damaging, a considerable decrease in the number of cell colonies was observed when compared with normal HCP5 levels (Figures 4.17- 4.20). These results are consistent with study by Zhang and Wang (2021), published during the execution of these experiments, in which the administration of cisplatin plus HCP5 knockdown led to a considerable increase in apoptosis (40%) and decreased cell growth in gastric cancer cells (Zhang & Wang, 2021).

Since a previous study had reported that nuclear YB-1 can activate PARP-1 and PARP-2 and moreover, serve as a cofactor for PARP-1 in BER (Alemasova *et al*., 2016), it was decided to study the mechanism of action of HCP5 further, utilizing a combination treatment including the PARP inhibitor, olaparib, HCP5 knockdown and DNA damaging agent treatment. The results, shown in Figure 4.13- 4.16, showed no significant additional increase in sensitivity of the cells to the DNA damaging agents. However, on reflection, the results obtained can be easily explained and indeed indicate the efficiency of HCP5 knockdown and the requirement for HCP5 to bind to YB-1 for translocation through the nuclear pore complex.

Since YB-1 exerts its function through activation of PARP in the nucleus and HCP5 knockdown may already result in a reduction in PARP activity, olaparib will not have any additional effect on the sensitivity of the cells to the DNA damaging agents, as HCP5 knockdown already limits PARP activation via YB-1. PARP-1 has also been implicated as one of the genes that confers cisplatin resistance on cancer cells (Wang *et al*., 2017). Cisplatin treatment has been shown to result in the over expression and hyperactivation of PARP-1 in different cancer cells (Prasad *et al*., 2017). Cisplatin treatment also resulted in an increase in the accumulation of PARP-1 in the nucleus and, therefore the interaction of YB-1 with PARP-1 might play a role in how HCP5 sensitizes cancer cells to cisplatin: as YB-1 is needed for the activation of PARP-1 in the nucleus and if YB-1 is absent from the nucleus, PARP-1 cannot be activated.

Various studies have demonstrated that DNA damaging agents exert their cytotoxic effect through the induction of apoptosis (Mortezaee *et al*., 2019; Faivre *et al*., 2003). Loss of plasma membrane asymmetry, which occurs early in apoptosis, results in the exposure of phosphatidylserine residues at the outer plasma membrane with which annexin v binds (Chaudhry *et al*., 2020). Furthermore, the plasma and nuclear membranes become less stable as apoptosis progresses into its final stage, allowing propidium iodide, a DNA binding dye to enter the cell and interact with nucleic acid (Riccardi, & Nicoletti, 2006). In this study, it was discovered across the four cell lines that combination of HCP5 knockdown with DNA damaging agent treatment resulted in an increase in the number of cells undergoing apoptosis when compared to the DNA damaging agent treatment alone (Figure 4.). The underlying molecular mechanism of apoptosis is still only partially understood and several genes, including p53, Bcl-2, Bax, and p21WAF1 have been shown to act intracellularly to orchestrate the activation of apoptosis (Li *et al*., 1999). Previous studies have shown that the capacity of p53 to induce cell death and transactivate proapoptotic proteins is inhibited by YB-1

(Sangermano *et al*., 2020). YB-1 binds directly to p53 and this interaction limits the accessibility to the p53 binding site of pro-apoptotic promoters such as CDKN1A and MDM2 (Homer *et al*., 2005). Therefore, if nuclear YB-1 binds to, and inhibits p53 activity, while HCP5 knockdown prevents YB-1 entry into the nucleus, it can be deduced that knockdown of HCP5 will result in the inability of YB-1 to inhibit p53, thus resulting in an increase in apoptosis.

HCP5 is essential for YB-1 localisation in the nucleus.

The Y-box (5´ -CTGATTGGC/TC/TAA-3´) is a DNA sequence found in the promoter region of many genes, and the multifunctional protein YB-1 gets its name from its capacity to bind to it (Alkrekshi *et al*., 2021). Thus, YB-1 is either directly or indirectly involved in the production of these genes that contain the Y-box sequence (Lyabin *et al*., 2014). Although initially identified as a DNA transcription factor, YB-1 has since been linked to a number of other processes, including pre-mRNA splicing, translation, and mRNA stability (Ceman *et al*., 2000). As mentioned, previous studies suggested a crosstalk between YB-1 and the lncRNA HCP5 (Shi *et al*., 2022). Wang *et al*. (2020) confirmed this relationship by showing that YB-1 was a direct binding protein of HCP5. This discovery was interesting as YB-1 plays a pivotal role in the regulation and activity of different proteins, such as the BER proteins mentioned previously (Wang *et al*., 2020). Therefore, to determine the effect of HCP5 knockdown on YB-1, initial experiments were undertaken to analyse the effect of HCP5 knockdown on the expression of YB-1. As shown in Figure 4.25, HCP5 knockdown had no effect on the expression of YB-1 in all four cell lines used.

Previous studies have shown that YB-1 shuttles between the nucleus and cytoplasm and that increased accumulation of YB-1 in the nucleus is a trait associated with cancer cells and drug resistance (Kuwano *et al*., 2004). Nuclear YB-1 controls the transcription of numerous genes, such as those responsible for cell growth and division as well as DNA repair and replication (Evdokimova *et al*, 2001), while cytoplasmic YB-1 is essential for the transformation of mRNA into messenger ribonucleoprotein particles (Skabkin *et al*., 2004). It was therefore important to determine the effect of HCP5 knockdown on the translocation of YB-1 from the cytoplasm to the nucleus. As shown in Figure 4.26, upon knockdown of HCP5, the amount of YB-1 in the nucleus was reduced in all cell lines tested, indicating that translocation from the cytoplasm to the nucleus was restricted and further evidence that HCP5 might play a role in the translocation of YB-1 through the nuclear pore complex.

194

The mechanism of YB-1 transport into the nucleus has been investigated by several groups and various hypotheses have been proposed (Mordovkina *et al*., 2016; Zhang *et al*., 2003). Thus, it has been demonstrated that YB-1 has two different kinds of signalling sequences, including a cytoplasmic retention site (CRS) and a nuclear localization signal (NLS) (Bader & Vogt, 2005). It was proposed that under normal cellular circumstances, the CRS would predominate over the NLS, favouring YB-1 localization mostly in the cytoplasm. However, as YB-1 was also found in cell nuclei, it appears that CRS dominance over NLS can be overcome in some situations (Stewart, 2007).

Macromolecules are actively transported through the nuclear pore complex bound to karyopherin protein family members, called importins and exportins. Importins are karyopherins that are involved nuclear import of cargo proteins while exportins help transport their cargo out of the nucleus (Soniat & Chook, 2015). In the cargo protein, importins identify a specific NLS, which is a short amino acid sequence required to direct the protein to the nucleus and transportin-1 is the importin responsible for YB-1 nuclear import (Mordovkina *et al*., 2016). Based on this discovery, a few hypotheses have been developed to account for the nuclear translocation of YB-1. One of them involves the movement of full-length YB-1 to the nucleus when YB-1 is phosphorylated at S102 by AKT or other protein kinases (Basak *et al*., 2007). Another method involves the accumulation of truncated YB-1 lacking the CRS in the nuclei of DNA damaged cells as a result of proteasome-mediated cleavage of YB-1 between NLS and CRS (Sorokin *et al*., 2007).

However, from the recent reports from Wang *et al*., (2020) showing a role for HCP5 in the translocation of YB-1, it can be expected that HCP5 knockdown will prohibit, or at least restrict the translocation of YB-1 from the cytoplasm to the nucleus. This should then impact on the activity of the DNA glycosylases mentioned previously that have been found to interact with YB-1. In this scenario, HCP5 knockdown should have no direct effect on the expression of the DNA glycosylase genes, and this was confirmed in this study. Nuclear expression of YB-1 was significantly reduced when HCP5 was knocked down, as shown in Figure 4.26. However, as there is considerable nuclear staining for YB-1 in the wildtype cells, it is interesting to speculate the fate of the YB-1 already present in the nucleus as YB-1 has not been shown to translocate from the nucleus to the cytoplasm. An interesting discovery which could possibly explain this phenomenon is the ubiquitination and degradation of YB-1 by retinoblastoma binding protein 6 (Chibi *et al*., 2008). RBBp6 has been found in nuclear speckles and is believed to translocate to the nucleus due to its extremely basic charge and C-terminal NLS (Mabonga & Kappo,

2019). Ubiquitination of YB-1 by RBBp6 represents a biological strategy for preserving appropriate quantities of functional, non-ubiquitinated YB-1 in the cell (Chibi *et al*., 2008).

Nuclear YB-1 has been associated with binding, interacting and activating DNA repair proteins and Das *et al*., (2007) showed that in addition to its direct interaction and activation of NEIL2, nuclear YB-1 also promotes a seven-fold increase in the base excision activity of NEIL2, nuclear YB-1 also binds to and activates NTH1 and NEIL1 (Alemasova *et al*., 2016) (Guay *et al*., 2008). Therefore, combining its activation of DNA repair enzymes and inhibition of p53 activity, nuclear YB-1 is considered to be a key player in conferring resistance to chemotherapy in cancer cells. The inhibition of nuclear YB-1 activation of DNA repair enzymes might also play a role in HCP5 ability to sensitize cancer cells to chemotherapy as reduction in nuclear YB-1 which results in the inhibition of the activation of the repair enzymes, which in turn translates to less repair of DNA damage acquired during treatment with chemotherapeutic agents, thus resulting in cell death.
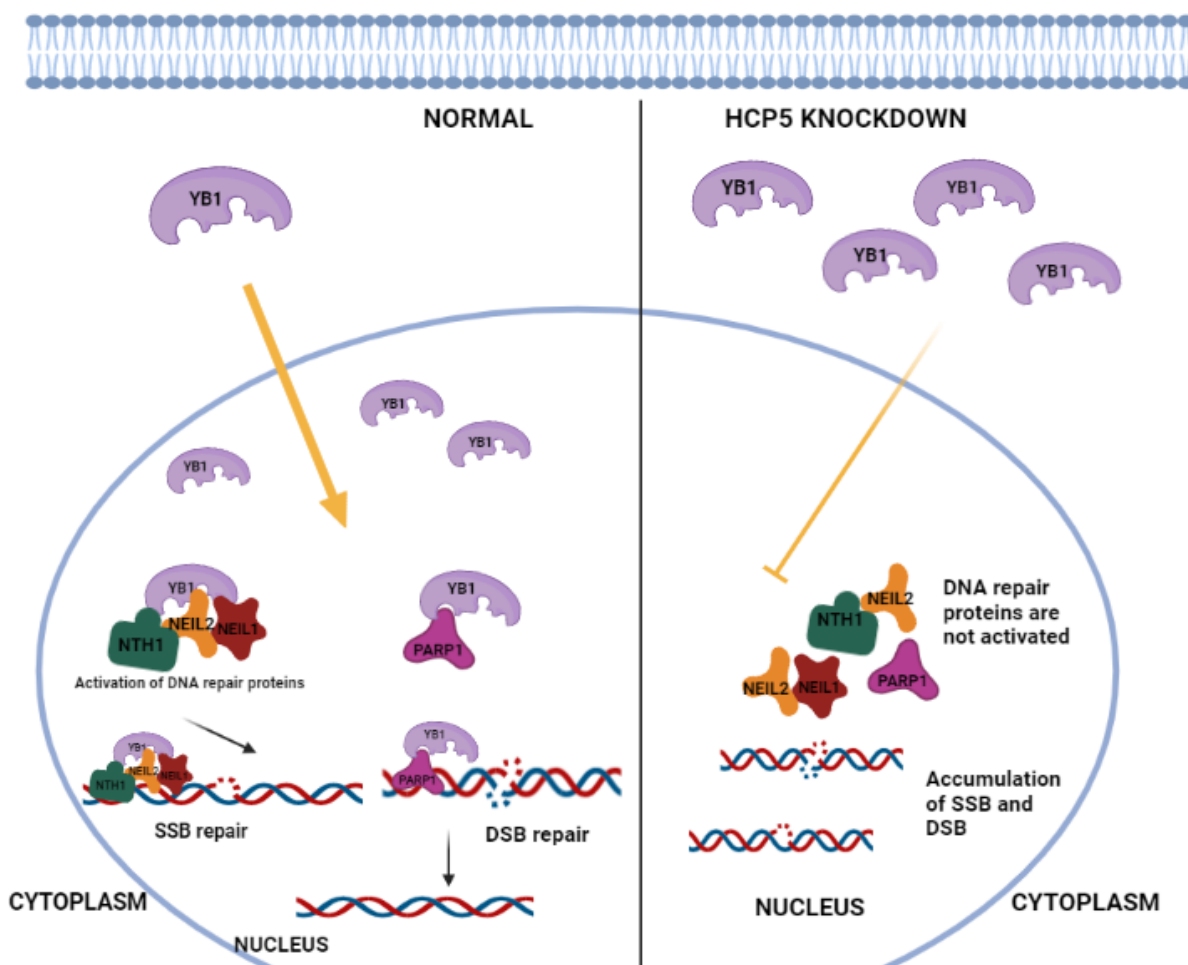
Figure 4.28- Schematic representation of the effect of HCP5 knockdown on YB-1 and DNA repair enzymes.

HCP5 knockdown leads to DNA double-strand breaks

As shown in Figure 4.27, treatment of HCP5 knockdown cells with cisplatin or oxaliplatin resulted in an increase in DNA double-strand break formation when compared to similar treatment of wildtype cells, as measured by γH2AX foci. BRCA1 and BRCA2 are tumour suppressor genes that encode proteins that participate primarily in the repair of double-strand breaks through NHEJ and HR but have also been implicated in the repair of DNA adducts by NER (Bernstein *et al*., 2002; MacLachlan *et al*., 2002). Relevant to this study, mutation of BRCA1/2 has been shown to lead to the accumulation of DNA double-strand breaks in cisplatin - treated pancreatic tumour xenografts (Lohse *et al*., 2015). Another important gene to take into consideration is PARP-1. Inactivation of PARP-1 might be responsible for the increase in double-strand breaks when HCP5 knockdown is combined with cisplatin. Previous studies

have shown that the inconsistent activation of DNA repair pathways might play a role in the variability of cancer cells response to chemotherapy (Shao *et al*., 2008) and the upregulation of components in the non-homologous end joining/homologous recombination pathways have been shown to promote cisplatin resistance by increasing the double strand breaks repair capability in cancer cells (Rocha *et al*., 2018). To further highlight the role of PARP-1 in resistance to platinum agents, Wang *et al*., (2021) showed that in cisplatin-resistant gastric cancer cells, PARP-1 inhibition increased cisplatin sensitivity by suppressing the NHEJ pathway. The activation of DNA-PKcs, a component of NHEJ, has also been shown to be a major resistance factor to cisplatin treatment (Weterings *et al*., 2004). These authors showed that cisplatin resistance may be caused by activation of the NHEJ pathway due to the discovery of increased expression levels of DNA-PKcs in cisplatin-resistant GC cells compared to sensitive cells. Also, in cisplatin-resistant gastric cancer cells, down-regulation of DNA-PKcs expression and suppression of DNA-PKcs activation occurred after PARP-1 activity was inhibited (Wang *et al*., 2017). Prasad *et al*., (2017) showed that due to a lack of PARP activity (which controls the recruitment of replication protein A via MRE11), when PARP is inhibited, both PARP-depleted and inhibited cervical cancer cells displayed loss of RPA foci after cisplatin treatment. Open DNA ends, the production of DNA DSBs, and prolonged 53BP1 recruitment occur when appropriate RPA recruitment is inhibited.

Conclusion

In conclusion, dysregulation of HCP5 is substantially associated with both prognosis and advanced clinicopathological characteristics in most malignancies. Based on results from this study, HCP5 silencing reduced oxaliplatin and cisplatin resistance in CRC and medulloblastoma cells, as indicated by a decline in cell viability and an increase in cell apoptosis, indicating the role of HCP5 as a promising target to restore chemosensitivity in CRC. HCP5 may therefore serve as a unique potential prognostic biomarker and therapeutic target in cancer treatment.

4.3 Limitations and challenges

At the beginning of this study several attempts were made over a period of time to quantify HCP5 expression in the various cell lines, this was due to the reverse transcription kit used at the time (Quantinova reverse transcription kit) not being sensitive enough to transcribe the lncRNA which is naturally expressed at low levels. This was replaced with the Takara bio

reverse transcription kit which was more sensitive and produced good detection of HCP5. During the knockdown of HCP5 some challenges were encountered, the first one being the most effective antisense oligonucleotide (ASO) for HCP5 knockdown had a high toxicity rate (70%) therefore, this ASO could not be utilised. Another challenge encountered was with the SW48 cell line as it was difficult to transfect, thus multiple failed attempts at transfecting the HCP5 ASO, after a lot of optimisation was carried out, which constituted of optimising the concentration of each reagent. HCP5 knockdown was finally detected in the SW48 cells, however the knockdown efficiency was lower compared to the other cell lines.

4.4 Future work

Further studies are required to complete the overview on the sensitization of cancer cells to DNA damaging agents by HCP5 knockdown. To further elucidate this, this hypothesis will have to be tested on a broader range of cell lines (including metastatic and primary cell lines) from various cancer types with various expression of HCP5. To accurately model the native environment of cells *in vivo* and better represent the numerous cell-cell interactions that have a profound effect on the behaviour of cells, further testing using 3D models such as 3D spheroids and organoids can be carried out.

Preliminary results from this study showed HCP5 knockdown with cisplatin and oxaliplatin increased the accumulation γH2AX which is an indicator of double-strand breaks. However, recent studies have shown that detection of γH2AX foci may not necessarily be linked with double-strand DNA damage, making the use of γH2AX foci alone to quantify DSBs ambiguous. Further studies investigating this can be carried out using the detection of γH2AX and colocalised proteins such as 53bp1 (γH2AX /53bp1). The comet assay, which is another method of effectively detecting and quantifying chemotherapy induced double-strand breaks can also be used.

4.5 Final Discussion and Conclusion

Since their discovery, microtubule targeting agents such as vincristine have been considered the gold standard for treating numerous malignant types (Mohammadgholi *et al*., 2013). However, they do have some drawbacks, such as their toxicity toward healthy tissues such as the brain (Škubník *et al*., 2021). The Bcl-2 family is a critical player in the efficiency of

vincristine because they are important mediators for cellular death during mitosis and significant regulators of programmed cell death (Luo *et al*., 1998). The effectiveness of vincristine in particular can now be improved thanks to the recent development of small compounds that can precisely target the Bcl-2 family.

Results from this study showed that vincristine and the Bcl-xL inhibitor WEHI 539 had anticancer effects when used sequentially in ONS76 cell lines. Additionally, this sequential combination will enable a reduction in chemotherapeutic dose, which is necessary to minimize the therapy's side effects. These results demonstrate the significance of logically combining anti-cancer medications with BH3 mimetics. They also highlight the current efforts to target the anti-apoptotic protein Bcl-xL, which is being investigated in clinical trials (Arulanda *et al*., 2021). If these innovative therapeutic approaches are supported by a functional predictive biomarker like DBP, they may enhance the management of medulloblastoma patients in the clinic, particularly for those who relapse. Although the therapeutic potential of combining vincristine with Bclxl inhibition is still being investigated, this preliminary research suggests several interesting new combinations using the different Bcl-2 family proteins that can be taken advantage of to improve targeted cancer cell death, enable lower vincristine dosages, and lead to reduced toxicity. However, in this study, knockdown of Bcl-xL was only effective in sensitizing cells that over expressed Bcl-xL (ONS76) to vincristine, while cells with low expression of the protein showed no significant difference in cell viability after treatment with vincristine. This indicated that this combination treatment would not be effective in sensitizing cancer cells across different cancer types which might have varied expression of Bcl-xL. It was therefore important to investigate other means by which cancer cells can be sensitized to chemotherapy.

Recent research has demonstrated that lncRNA plays a role in multiple stages of the development of cancer by influencing important genes that regulate cell proliferation, apoptosis, and invasion (Chen *et al*., 2021). A newly identified lncRNA called HCP5 is overexpressed in numerous malignancies, and new research suggests that HCP5 may play a role in chemoresistance (Hu *et al*., 2021). Gene expression analysis carried out using RT-PCR revealed that CRC cells had higher levels of HCP5 compared to the medulloblastoma cells. Furthermore, in the four medulloblastoma and CRC cell lines used, HCP5 knockdown sensitized the cells to DNA damaging agents by reduced cell growth and increasing the rate of apoptosis. Thus, indicating a close connection between HCP5 and cancer formation and chemoresistance in medulloblastoma and CRC cells. It has been established that interactions

with RNA-binding proteins are the primary method that lncRNAs carry out their biological activity (Sun *et al*., 2015). Previous studies found that YB-1 and HCP5 are direct binding partners (Wang *et al*., 2020). YB-1 is a pleiotropic protein that shuttles back and forth between the nucleus and the cytoplasm to take part in DNA transcription, mRNA splicing, mRNA stability, and mRNA translation (Lyabin *et al*., 2014). Although the overall expression of YB-1 was unaffected by HCP5 knockdown, the nuclear localisation of YB-1 was much reduced, confirming earlier reports that the lncRNA HCP5 is involved in the transport of YB-1 into the nucleus.

In conclusion, based on data from this research a probable mechanism of action for the lncRNA HCP5 in sensitizing CRC and medulloblastoma cells to DNA-damaging chemicals is proposed. Also highlighted was HCP5 expression in medulloblastoma and CRC cells function by directly interacting with YB-1 and modifying its subcellular location. This research suggests novel lncRNA HCP5 as a potential contributor to the dysfunctionality of medulloblastoma and CRC by transcriptionally controlling the activation of DNA damage repair proteins via YB-1. This potential discovery offers a novel epigenetic mechanism for cancer aetiology.

REFERENCES

Abdelkader, A., Hartley, C., & Hagen, C. (2017). Tubulovillous adenomas with serrated features are precursors to KRAS mutant colorectal carcinoma. in laboratory investigation (Vol. 97, pp. 157A-157A). *Nature*.

Abraha, A. M., & Ketema, E. B. (2016). Apoptotic pathways as a therapeutic target for colorectal cancer treatment. *World Journal of Gastrointestinal Oncology*, 8(8), 583–591. https://doi.org/10.4251/wjgo.v8.i8.583

Abraham,R.T. (2001) Cell cycle checkpoint signaling through the ATM and ATR kinases. *Genes Dev*. , 15 , 2177 –2196.

Acehan, D., Jiang, X., Morgan, D., Heuser, J., Wang, X., & Akey, C. (2002). Three-Dimensional Structure of the Apoptosome. *Molecular Cell*, 9(2), 423-432. doi: 10.1016/s10972765(02)00442-2.

Adams, M. M., & Carpenter, P. B. (2006). Tying the loose ends together in DNA double strand break repair with 53BP1. *Cell division*, 1, 19. https://doi.org/10.1186/1747-1028-1-19

Ahmad, S. (2017). Kinetic aspects of platinum anticancer agents. *Polyhedron*, 138, 109-124.

Ahmed, D., Eide, P. W., Eilertsen, I. A., Danielsen, S. A., Eknæs, M., Hektoen, M., Lind, G. E., & Lothe, R. A. (2013). Epigenetic and genetic features of 24 colon cancer cell lines. *Oncogenesis*, 2(9), e71. https://doi.org/10.1038/oncsis.2013.35

Aissaoui, N., Lai-Kee-Him, J., Mills, A., Declerck, N., Morichaud, Z., Brodolin, K., ... & Bellot, G. (2021). Modular Imaging Scaffold for Single-Particle Electron Microscopy. ACS nano, 15(3), 4186-4196.

Alam, M. M., Naeem, M., Khan, M. M. A., & Uddin, M. (2017). Vincristine and vinblastine anticancer catharanthus alkaloids: Pharmacological applications and strategies for yield improvement. Catharanthus roseus: Current Research and Future Prospects, 277-307.

Alberts, B., Johnson, A., Lewis, J., Raff, M., Roberts, K., & Walter, P. (2002). Programmed cell death (apoptosis). In Molecular Biology of the Cell. 4th edition. Garland Science.

Alcindor, T., & Beauger, N. (2011). Oxaliplatin: a review in the era of molecularly targeted therapy. *Current Oncology* (Toronto, Ont.), 18(1), 18–25. https://doi.org/10.3747/co.v18i1.708

Alemasova, E. E., Moor, N. A., Naumenko, K. N., Kutuzov, M. M., Sukhanova, M. V., Pestryakov, P. E., & Lavrik, O. I. (2016). Y-box-binding protein 1 as a non-canonical factor of base excision repair. *Biochimica et Biophysica Acta (BBA)-Proteins and Proteomics*, 1864(12), 1631-1640.

Alía, M., Ramos, S., Mateos, R., Bravo, L., & Goya, L. (2005). Response of the antioxidant defense system to tert-butyl hydroperoxide and hydrogen peroxide in a human hepatoma cell line (HepG2). *Journal of Biochemical and Molecular Toxicology*, 19(2), 119-128.

Alison, M. R., Lim, S. M., & Nicholson, L. J. (2011). Cancer stem cells: problems for therapy?. *The Journal of Pathology*, 223(2), 147–161. https://doi.org/10.1002/path.2793

Alkrekshi, A., Wang, W., Rana, P. S., Markovic, V., & Sossey-Alaoui, K. (2021). A comprehensive review of the functions of YB-1 in cancer stemness, metastasis and drug resistance. *Cellular Signalling*, 85, 110073.

Allan, L., & Clarke, P. (2007). Phosphorylation of Caspase-9 by CDK1/Cyclin B1 Protects Mitotic Cells against Apoptosis. *Molecular Cell*, 26(2), 301-310.doi:10.1016/j.molcel.2007.03.019

Al-Taee, A., Almukhtar, R., Lai, J., & Jallad, B. (2016). Metastatic signet ring cell carcinoma of unknown primary origin: a case report and review of the literature. Annals of translational medicine, 4(15), 283. https://doi.org/10.21037/atm.2016.07.24

 Álvarez, P., Marchal, J. A., Boulaiz, H., Carrillo, E., Vélez, C., Rodríguez-Serrano, F., Melguizo, C., Prados, J., Madeddu, R., & Aranega, A. (2012). 5-Fluorouracil derivatives: a patent review. Expert opinion on therapeutic patents, 22(2), 107–123. https://doi.org/10.1517/13543776.2012.661413.

Amin, M., Kobayashi, K., & Tanaka, K. (2015). CLIP-170 tethers kinetochores to microtubule plus ends against poleward force by dynein for stable kinetochore-microtubule attachment. *FEBS Letters*, *589*(19PartB), 2739-2746. doi: 10.1016/j.febslet.2015.07.036

Amundson, S.A., Myers, T.G., Scudiero, D., Kitada, S., Reed, J.C., Fornace, A.J. (2000) An informatics approach identifying markers of chemosensitivity in human cancer cell lines. *Cancer Research*,60(21),6101–6110.

Andrezálová, L., & Országhová, Z. (2021). Covalent and noncovalent interactions of coordination compounds with DNA: An overview. *Journal of Inorganic Biochemistry*, 225, 111624.

Apetoh, L., Ghiringhelli, F., Tesniere, A., Obeid, M., Ortiz, C., Criollo, A., Mignot, G., Maiuri, M. C., Ullrich, E., Saulnier, P., Yang, H., Amigorena, S., Ryffel, B., Barrat, F. J., Saftig, P., Levi, F., Lidereau, R., Nogues, C., Mira, J. P., Chompret, A., … Zitvogel, L. (2007). Toll-like receptor 4-dependent contribution of the immune system to anticancer chemotherapy and radiotherapy. *Nature Medicine*, 13(9), 1050–1059. https://doi.org/10.1038/nm1622

Apps, M. G., Choi, E. H., & Wheate, N. J. (2015). The state-of-play and future of platinum drugs. *Endocrine-related Research*.

Armaghany, T., Wilson, J. D., Chu, Q., & Mills, G. (2012). Genetic alterations in colorectal cancer. *Gastrointestinal Cancer Research* : GCR, 5(1), 19–27.

Arnesano, F., & Natile, G. (2009). Mechanistic insight into the cellular uptake and processing of cisplatin 30 years after its approval by FDA. *Coordination Chemistry Reviews*, 253(15-16), 2070-2081.

Arora, S., Kothandapani, A., Tillison, K., Kalman-Maltese, V., & Patrick, S. M. (2010). Downregulation of XPF–ERCC1 enhances cisplatin efficacy in cancer cells. *DNA Repair*, 9(7), 745-753.

Arulananda, S., O'Brien, M., Evangelista, M., Jenkins, L. J., Poh, A. R., Walkiewicz, M., ... & Fairlie, W. D. (2021). A novel BH3-mimetic, AZD0466, targeting BCL-XL and BCL-2 is effective in pre-clinical models of malignant pleural mesothelioma. *Cell death discovery*, 7(1), 1-9.

Asagoshi, K., Yamada, T., Okada, Y., Terato, H., Ohyama, Y., Seki, S., & Ide, H. (2000). Recognition of formamidopyrimidine by Escherichia coli and mammalian thymine glycol glycosylases: distinctive paired base effects and biological and mechanistic implications. *Journal of Biological Chemistry*, 275(32), 24781-24786.

Ashton, T. M., Mankouri, H. W., Heidenblut, A., McHugh, P. J., & Hickson, I. D. (2011). Pathways for Holliday junction processing during homologous recombination in Saccharomyces cerevisiae. *Molecular and Cellular Biology*, 31(9), 1921–1933. https://doi.org/10.1128/MCB.01130-10

Ba, X., & Boldogh, I. (2018). 8-Oxoguanine DNA glycosylase 1: Beyond repair of the oxidatively modified base lesions. *Redox Biology*, 14, 669-678.

Bader, A. G., & Vogt, P. K. (2005). Inhibition of protein synthesis by Y box-binding protein 1 blocks oncogenic cell transformation. *Molecular and Cellular biology*, 25(6), 2095–2106. https://doi.org/10.1128/MCB.25.6.2095-2106.2005

Baiken, Y., Kanayeva, D., Taipakova, S., Groisman, R., Ishchenko, A. A., Begimbetova, D., ... & Saparbaev, M. (2021). Role of base excision repair pathway in the processing of complex DNA damage generated by oxidative stress and anticancer drugs. *Frontiers in Cell and Developmental Biology*, 8, 617884.

Bailey, P., Cushing, H. (1925). Medulloblastoma cerebelli: a common type of midcerebellar glioma of childhood. *Arch Neurol Psychiatry* 14(2),192-224.

Bakhoum, S. F., Kabeche, L., Compton, D. A., Powell, S. N., & Bastians, H. (2017). Mitotic DNA damage response: at the crossroads of structural and numerical cancer chromosome instabilities. *Trends In Cancer*, 3(3), 225-234.

Balachandran, R., Heighington, C., Starostina, N., Anderson, J., Owen, D., Vasudevan, S., & Kipreos, E. (2016). The ubiquitin ligase CRL2 ZYG11 targets cyclin B1 for degradation in a conserved pathway that facilitates mitotic slippage. *The Journal Of Cell Biology*, 215(2), 151166. doi: 10.1083/jcb.201601083.

Balas, M. M., & Johnson, A. M. (2018). Exploring the mechanisms behind long non-coding RNAs and cancer. *Non-coding RNA Research*, 3(3), 108–117. https://doi.org/10.1016/j.ncrna.2018.03.001

Bandaru V, Sunkara S, Wallace SS, Bond JP.(2002). A novel human DNA glycosylase that removes oxidative DNA damage and is homologous to Escherichia coli endonuclease VIII. *DNA Repair Amst* ;1:517–529.

Banerjee A, Santos WL, Verdine GL.(2006). Structure of a DNA glycosylase searching for lesions. *Science*,311:1153–1157

Banerjee D, Mandal SM, Das A, Hegde ML, Das S, Bhakat KK, Boldogh I, Sarkar PS, Mitra S, Hazra TK. (2011) Preferential repair of oxidized base damage in the transcribed genes of mammalian cells. *J Biol Chem*. 286:6006–6016.

Baptista, B., Riscado, M., Queiroz, J. A., Pichon, C., & Sousa, F. (2021). Non-coding RNAs: Emerging from the discovery to therapeutic applications. *Biochemical Pharmacology*, 189, 114469.

Bartek,J., Falck,J. and Lukas,J. (2001) CHK2 kinase—a busy messenger. Nature Reviews, *Molecular Cell Biology*, 2 , 877 –886.

Basaki, Y., Hosoi, F., Oda, Y., Fotovati, A., Maruyama, Y., Oie, S., Ono, M., Izumi, H., Kohno, K., Sakai, K., Shimoyama, T., Nishio, K., & Kuwano, M. (2007). Akt-dependent nuclear localization of Y-box-binding protein 1 in acquisition of malignant characteristics by human ovarian cancer cells. *Oncogene*, 26(19), 2736–2746. https://doi.org/10.1038/sj.onc.1210084

Basu, A. (2022). The interplay between apoptosis and cellular senescence: Bcl-2 family proteins as targets for cancer therapy. *Pharmacology & Therapeutics*, 230, 107943.

Batlle, E., & Clevers, H. (2017). Cancer stem cells revisited. *Nature Medicine*, 23(10), 1124-1134.

Begg, A. C., Stewart, F. A., & Vens, C. (2011). Strategies to improve radiotherapy with targeted drugs. *Nature Reviews Cancer*, 11(4), 239-253.

Belli, S., Aytac, H. O., Karagulle, E., Yabanoglu, H., Kayaselcuk, F., & Yildirim, S. (2014). Outcomes of surgical treatment of primary signet ring cell carcinoma of the colon and rectum: 22 cases reviewed with literature. *International Surgery*, 99(6), 691–698. https://doi.org/10.9738/INTSURG-D-14-00067.1

Benesch, M., & Mathieson, A. (2020). Epidemiology of Signet Ring Cell Adenocarcinomas. Cancers, 12(6), 1544. https://doi.org/10.3390/cancers12061544

Bennett, A., Sloss, O., Topham, C., Nelson, L., Tighe, A., & Taylor, S. (2016). Inhibition of Bcl-xL sensitizes cells to mitotic blockers, but not mitotic drivers. *Open Biology*, 6(8), 160134. doi: 10.1098/rsob.160134

Berg, K., Sveen, A., Høland, M., Alagaratnam, S., Berg, M., Danielsen, S. A., Nesbakken, A., Søreide, K., & Lothe, R. A. (2019). Gene expression profiles of CMS2-epithelial/canonical colorectal cancers are largely driven by DNA copy number gains. *Oncogene*, 38(33), 6109–6122. https://doi.org/10.1038/s41388-019-0868-5

Bernstein, B. E., Birney, E., Dunham, I., Green, E. D., Gunter, C., Snyder, M., ENCODE Project Consortium, & Hubbard, T. (2012). An integrated encyclopedia of DNA elements in the human genome. *Nature,* 489(7414), 57-74. https://doi.org/10.1038/nature11247

Bernstein, C., Bernstein, H., Payne, C. M., & Garewal, H. (2002). DNA repair/pro-apoptotic dual-role proteins in five major DNA repair pathways: fail-safe protection against carcinogenesis. *Mutation Research/Reviews in Mutation Research*, 511(2), 145-178.

Beroukhim R., Mermel C. H., Porter D., Wei G., Raychaudhuri S., Donovan J., Barretina J., Boehm J. S., Dobson J., Urashima M., Mc Henry K. T., Pinchback R. M., Ligon A. H.,

Berretta, J., & Morillon, A. (2009). Pervasive transcription constitutes a new level of eukaryotic genome regulation. *EMBO Reports*, 10(9), 973–982. https://doi.org/10.1038/embor.2009.181

Bertone, P., Stolc, V., Royce, T. E., Rozowsky, J. S., Urban, A. E., Zhu, X., Rinn, J. L., Tongprasit, W., Samanta, M., Weissman, S., Gerstein, M., & Snyder, M. (2004). Global identification of human transcribed sequences with genome tiling arrays. *Science* (New York, N.Y.), 306(5705), 2242–2246. https://doi.org/10.1126/science.1103388

Bétermier, M., Bertrand, P., & Lopez, B. S. (2014). Is non-homologous end-joining really an inherently error-prone process?. *PLoS Genetics*, 10(1), e1004086.

Bizard, A. H., & Hickson, I. D. (2014). The dissolution of double Holliday junctions. Cold Spring *Harbor Perspectives in Biology*, 6(7), a016477. https://doi.org/10.1101/cshperspect.a016477

Block WD, Yu Y, Merkle D, *et al*. Autophosphorylation-dependent remodeling of the DNA-dependent protein kinase catalytic subunit regulates ligation of DNA ends. *Nucleic Acids Res* 2004; 32:4351–4357.

Boland, C. R., & Goel, A. (2010). Microsatellite instability in colorectal cancer. *Gastroenterology*, 138(6), 2073–2087.e3. https://doi.org/10.1053/j.gastro.2009.12.064

Borghaei, H., Smith, M. R., & Campbell, K. S. (2009). Immunotherapy of cancer. *European Journal of pharmacology*, 625(1-3), 41-54.

Bourdon, J., Surget, S., & Khoury, M. (2013). Uncovering the role of p53 splice variants in human malignancy: a clinical perspective. *Oncotargets And Therapy*, 57. doi:10.2147/ott.s53876

Brabec, V., & Kasparkova, J. (2005). Modifications of DNA by platinum complexes. Relation to resistance of tumors to platinum antitumor drugs. Drug resistance updates : reviews and commentaries in antimicrobial and anticancer chemotherapy, 8(3), 131–146. https://doi.org/10.1016/j.drup.2005.04.006

Bray, F., Laversanne, M., Weiderpass, E., & Soerjomataram, I. (2021). The ever-increasing importance of cancer as a leading cause of premature death worldwide. *Cancer*, 127(16), 3029–3030. https://doi.org/10.1002/cncr.33587

Briggs, K. J., Corcoran-Schwartz, I. M., Zhang, W., Harcke, T., Devereux, W. L., Baylin, S. B., Eberhart, C. G., & Watkins, D. N. (2008). Cooperation between the Hic1 and Ptch1 tumor suppressors in medulloblastoma. *Genes & Development*, 22(6), 770–785. https://doi.org/10.1101/gad.1640908

Brito, D., & Rieder, C. (2006). Mitotic Checkpoint Slippage in Humans Occurs via Cyclin B Destruction in the Presence of an Active Checkpoint. *Current Biology*, 16(12), 1194-1200. doi: 10.1016/j.cub.2006.04.043.

Britten, R. A., Liu, D., Tessier, A., Hutchison, M. J., & Murray, D. (2000). ERCC1 expression as a molecular marker of cisplatin resistance in human cervical tumor cells. *International Journal of Cancer*, 89(5), 453–457.

Brunner, A. L., Beck, A. H., Edris, B., Sweeney, R. T., Zhu, S. X., Li, R., Montgomery, K., Varma, S., Gilks, T., Guo, X., Foley, J. W., Witten, D. M., Giacomini, C. P., Flynn, R. A., Pollack, J. R., Tibshirani, R., Chang, H. Y., van de Rijn, M., & West, R. B. (2012). Transcriptional profiling of long non-coding RNAs and novel transcribed regions across a diverse panel of archived human cancers. *Genome Biology*, 13(8), R75. https://doi.org/10.1186/gb-2012-13-8-r75

Bunting, S. F., & Nussenzweig, A. (2013). End-joining, translocations and cancer. *Nature reviews Cancer*, 13(7), 443-454.

Buqué, A., Bloy, N., Aranda, F., Castoldi, F., Eggermont, A., Cremer, I., Fridman, W. H., Fucikova, J., Galon, J., Marabelle, A., Spisek, R., Tartour, E., Zitvogel, L., Kroemer, G., & Galluzzi, L. (2015). Trial Watch: Immunomodulatory monoclonal antibodies for oncological indications. *Oncoimmunology*, 4(4), e1008814. https://doi.org/10.1080/2162402X.2015.1008814

Burgess, A., Rasouli, M., & Rogers, S. (2014). Stressing mitosis to death. Frontiers in *Oncology*, 4, 140.

Burma, S., Chen, B. P., & Chen, D. J. (2006). Role of non-homologous end joining (NHEJ) in maintaining genomic integrity. *DNA Repair*, 5(9-10), 1042–1048. https://doi.org/10.1016/j.dnarep.2006.05.026

Bushati, N., & Cohen, S. M. (2007). microRNA functions. *Annual review of cell and developmental biology*, 23, 175–205. https://doi.org/10.1146/annurev.cellbio.23.090506.123406

Cahill, D., Connor, B., & Carney, J. P. (2006). Mechanisms of eukaryotic DNA double strand break repair. *Frontiers in Bioscience* : a journal and virtual library, 11, 1958–1976. https://doi.org/10.2741/1938

Cairns, J. (1975). Mutation selection and the natural history of cancer. *Nature*, 255(5505), 197-200.

Caldecott K. W. (2007). Mammalian single-strand break repair: mechanisms and links with chromatin. *DNA Repair*, 6(4), 443–453. https://doi.org/10.1016/j.dnarep.2006.10.006

Cancer Research UK (2015) How cancer starts. http://www.cancerresearchuk.org/aboutcancer/what-is-cancer/how-cancer-starts. [Accessed 15 May 2018].

Cannan, W. J., & Pederson, D. S. (2016). Mechanisms and Consequences of Double-Strand DNA Break Formation in Chromatin. *Journal of Cellular Physiology*, 231(1), 3–14. https://doi.org/10.1002/jcp.25048

Cao J. (2014). The functional role of long non-coding RNAs and epigenetics. *Biol Proced Online*. 16:11. doi: 10.1186/1480-9222-16-11

Caracciolo, D., Riillo, C., Di Martino, M. T., Tagliaferri, P., & Tassone, P. (2021). Alternative non-homologous end-joining: error-prone DNA repair as cancer's achilles' heel. *Cancers*, 13(6), 1392.

Carberry, S., D'Orsi, B., Monsefi, N., Salvucci, M., Bacon, O., Fay, J., Rehm, M., McNamara, D., Kay, E. W., & Prehn, J. (2018). The BAX/BAK-like protein BOK is a prognostic marker in colorectal cancer. *Cell Death & Disease*, 9(2), 125. https://doi.org/10.1038/s41419-017-0140-2

Carninci, P., Kasukawa, T., Katayama, S., Gough, J., Frith, M. C., Maeda, N., Oyama, R., Ravasi, T., Lenhard, B., Wells, C., Kodzius, R., Shimokawa, K., Bajic, V. B., Brenner, S. E., Batalov, S., Forrest, A. R., Zavolan, M., Davis, M. J., Wilming, L. G., Aidinis, V., … RIKEN Genome Exploration Research Group and Genome Science Group (Genome Network Project Core Group) (2005). The transcriptional landscape of the mammalian genome. *Science* (New York, N.Y.), 309(5740), 1559–1563. https://doi.org/10.1126/science.1112014

Carrato A. (2008). Adjuvant treatment of colorectal cancer. *Gastrointestinal Cancer Research* : GCR, 2(4 Suppl), S42–S46.

Castedo, M., Perfettini, J. L., Roumier, T., Andreau, K., Medema, R., & Kroemer, G. (2004). Cell death by mitotic catastrophe: a molecular definition. *Oncogene*, 23(16), 2825-2837.

Ceman, S., Nelson, R., & Warren, S. T. (2000). Identification of mouse YB1/p50 as a component of the FMRP-associated mRNP particle. *Biochemical and Biophysical Research Communications*, 279(3), 904-908.

Chabner, B. A., & Roberts, T. G., Jr (2005). Timeline: Chemotherapy and the war on cancer. Nature reviews. *Cancer*, 5(1), 65–72. https://doi.org/10.1038/nrc1529

Chaleshi, V., Irani, S., Alebouyeh, M., Mirfakhraie, R., & Aghdaei, H. A. (2020). Association of lncRNA-p53 regulatory network (lincRNA-p21, lincRNA-ROR and MALAT1) and p53 with the clinicopathological features of colorectal primary lesions and tumors. *Oncology Letters*, 19(6), 3937–3949. https://doi.org/10.3892/ol.2020.11518

Chan, K. S., Koh, C. G., & Li, H. Y. (2012). Mitosis-targeted anti-cancer therapies: where they stand. *Cell Death & Disease*, 3(10), e411. https://doi.org/10.1038/cddis.2012.148

Chatterjee, N., & Walker, G. C. (2017). Mechanisms of DNA damage, repair, and mutagenesis. *Environmental and Molecular Mutagenesis*, 58(5), 235–263. https://doi.org/10.1002/em.22087

Chaudhari, S., Ware, A. P., Jayaram, P., Gorthi, S. P., El-Khamisy, S. F., & Satyamoorthy, K. (2021). Apurinic/Apyrimidinic Endonuclease 2 (APE2): An ancillary enzyme for contextual base excision repair mechanisms to preserve genome stability. *Biochimie,* 190, 70-90.

Chaudhry, F., Kawai, H., Johnson, K. W., Narula, N., Shekhar, A., Chaudhry, F., ... & Narula, J. (2020). Molecular imaging of apoptosis in atherosclerosis by targeting cell membrane phospholipid asymmetry. *Journal of the American College of Cardiology*, 76(16), 1862-1874.

Chen, B., Dragomir, M. P., Yang, C., Li, Q., Horst, D., & Calin, G. A. (2022). Targeting non-coding RNAs to overcome cancer therapy resistance. Signal transduction and targeted therapy, 7(1), 121.

Chen, J., Jin, S., Abraham, V., Huang, X., Liu, B., Mitten, M. J., ... & Elmore, S. W. (2011). The Bcl-2/Bcl-XL/Bcl-w Inhibitor, Navitoclax, Enhances the Activity of Chemotherapeutic Agents In Vitro and In VivoNavitoclax Enhances the Activity of Chemotherapeutic Agents. *Molecular Cancer Therapeutics*, 10(12), 2340-2349.

Chen, R., Xin, G., & Zhang, X. (2019). Long non-coding RNA HCP5 serves as a ceRNA sponging miR-17-5p and miR-27a/b to regulate the pathogenesis of childhood obesity via the MAPK signaling pathway. *Journal of Pediatric Endocrinology & Metabolism* : JPEM, 32(12), 1327–1339. https://doi.org/10.1515/jpem-2018-0432

Chen, S., Ren, C., Zheng, H., Sun, X., & Dai, J. (2020). The Effect of Long Non-Coding RNA (lncRNA) HCP5 on Regulating Epithelial-Mesenchymal Transition (EMT)-Related Markers in Gastric Carcinoma Is Partially Reversed by miR-27b-3p. *Medical science monitor : International Medical Journal of Experimental and Clinical Research*, 26, e921383. https://doi.org/10.12659/MSM.921383

Chen, W., Zhang, K., Yang, Y., Guo, Z., Wang, X., Teng, B., Zhao, Q., Huang, C., & Qiu, Z. (2021). MEF2A-mediated lncRNA HCP5 Inhibits Gastric Cancer Progression via MiR-106b-5p/p21 Axis. *International Journal of Biological Sciences*, 17(2), 623–634. https://doi.org/10.7150/ijbs.55020

Cheng J., Kapranov P., Drenkow J., Dike J., Brubaker S., Patel S., (2005) Transcriptional maps of 10 human chromosomes at 5-nucleotide resolution. *Science*, 308 pp. 1149-1154

Cheng, B., & Crasta, K. (2017). Consequences of mitotic slippage for antimicrotubule drug therapy. *Endocrine-related Cancer*, 24(9), T97-T106.

Chetsanga, C. J., & Lindahl, T. (1979). Release of 7-methylguanine residues whose imidazole rings have been opened from damaged DNA by a DNA glycosylase from Escherichia coli. *Nucleic acids Research*, 6(11), 3673–3684. https://doi.org/10.1093/nar/6.11.3673

Cheung-Ong, K., Giaever, G., & Nislow, C. (2013). DNA-damaging agents in cancer chemotherapy: serendipity and chemical biology. *Chemistry & Biology*, 20(5), 648–659. https://doi.org/10.1016/j.chembiol.2013.04.007

Chibi, M., Meyer, M., Skepu, A., G Rees, D. J., Moolman-Smook, J. C., & Pugh, D. J. (2008). RBBP6 interacts with multifunctional protein YB-1 through its RING finger domain, leading to ubiquitination and proteosomal degradation of YB-1. *Journal of Molecular Biology*, 384(4), 908–916. https://doi.org/10.1016/j.jmb.2008.09.060

Children with Cancer UK. (2018). Childhood cancer facts and figures. https://www.childrenwithcancer.org.uk/childhood-cancer-info/childhood-cancer-factsfigures/ [Accessed 15 May 2018].

Cho Y. J., Haery L., Greulich H., Reich M., Winckler W., Lawrence M. S., Weir B. A., Tanaka K. E., Chiang D. Y., Bass A. J., Loo A., Hoffman C., Prensner J., Liefeld T., Gao Q., Yecies D., Signoretti S., Maher E., Kaye F. J., Sasaki H., Tepper J. E., Fletcher J. A., Tabernero J., Baselga J., Tsao M. S., Demichelis F., Rubin M. A., Janne P. A., Daly M. J., Nucera C., Levine R. L., Ebert B. L., Gabriel S., Rustgi A. K., Antonescu C. R., Ladanyi M., Letai A., Garraway L. A., Loda M., Beer D. G., True L. D., Okamoto A., Pomeroy S.

L., Singer S., Golub T. R., Lander E. S., Getz G., Sellers W. R., Meyerson M. (2010) The landscape of somatic copy number alteration across human cancers. *Nature* 463, 899–905

Cho, Y. J., Tsherniak, A., Tamayo, P., Santagata, S., Ligon, A., Greulich, H., Berhoukim, R., Amani, V., Goumnerova, L., Eberhart, C. G., Lau, C. C., Olson, J. M., Gilbertson, R. J., Gajjar, A., Delattre, O., Kool, M., Ligon, K., Meyerson, M., Mesirov, J. P., & Pomeroy, S. L. (2011). Integrative genomic analysis of medulloblastoma identifies a molecular subgroup that drives poor clinical outcome. *Journal of Clinical Oncology* : official journal of the American Society of Clinical Oncology, 29(11), 1424–1430. https://doi.org/10.1200/JCO.2010.28.5148

Ciccia, A., & Elledge, S. J. (2010). The DNA damage response: making it safe to play with knives. *Molecular Cell,* 40(2), 179-204.

Ciombor, K. K., Wu, C., & Goldberg, R. M. (2015). Recent therapeutic advances in the treatment of colorectal cancer. *Annual Review of Medicine,* 66, 83–95. https://doi.org/10.1146/annurev-med-051513-102539

Clancy, S. (2008) DNA damage & repair: mechanisms for maintaining DNA integrity. *Nature Education* 1(1):10

Cleare, M. J., & Hoeschele, J. D. (1973). Antilt umour Platinum Compounds. *Platinum Metals Rev*, 17(1), 2-13.

Clifford, S. C., Lusher, M. E., Lindsey, J. C., Langdon, J. A., Gilbertson, R. J., Straughton, D., & Ellison, D. W. (2006). Wnt/Wingless pathway activation and chromosome 6 loss characterize a distinct molecular sub-group of medulloblastomas associated with a favorable prognosis. *Cell Cycle* (Georgetown, Tex.), 5(22), 2666–2670. https://doi.org/10.4161/cc.5.22.3446

Coebergh van den Braak, R., Ten Hoorn, S., Sieuwerts, A. M., Tuynman, J. B., Smid, M., Wilting, S. M., Martens, J., Punt, C., Foekens, J. A., Medema, J. P., IJzermans, J., & Vermeulen, L. (2020). Interconnectivity between molecular subtypes and tumor stage in colorectal cancer. *BMC Cancer*, 20(1), 850. https://doi.org/10.1186/s12885-020-07316-z

Compton, C. C., & Greene, F. L. (2004). The staging of colorectal cancer: 2004 and beyond. CA: a cancer journal for clinicians, 54(6), 295-308.

Correia, J. J., & Lobert, S. (2001). Physiochemical aspects of tubulin-interacting antimitotic drugs. *Current Pharmaceutical Design,* 7(13), 1213–1228. https://doi.org/10.2174/1381612013397438

Corrette-Bennett, S. E., Borgeson, C., Sommer, D., Burgers, P. M., & Lahue, R. S. (2004). DNA polymerase delta, RFC and PCNA are required for repair synthesis of large looped heteroduplexes in Saccharomyces cerevisiae. *Nucleic acids Research*, 32(21), 6268–6275. https://doi.org/10.1093/nar/gkh965

Costantini, S., Woodbine, L., Andreoli, L., Jeggo, P. A., & Vindigni, A. (2007). Interaction of the Ku heterodimer with the DNA ligase IV/Xrcc4 complex and its regulation by DNA-PK. *DNA Repair*, 6(6), 712–722. https://doi.org/10.1016/j.dnarep.2006.12.007

Coward, J., & Harding, A. (2014). Size Does Matter: Why Polyploid Tumor Cells are Critical Drug Targets in the War on Cancer. *Frontiers in Oncology*, 4, 123. https://doi.org/10.3389/fonc.2014.00123

Croop, J. M., Raymond, M., Haber, D., Devault, A., Arceci, R. J., Gros, P., & Housman, D. E. (1989). The three mouse multidrug resistance (mdr) genes are expressed in a tissue-specific manner in normal mouse tissues. *Molecular and Cellular Biology*, 9(3), 1346–1350. https://doi.org/10.1128/mcb.9.3.1346-1350.1989

Crosslin, D. R., Carrell, D. S., Burt, A., Kim, D. S., Underwood, J. G., Hanna, D. S., ... & Jarvik, G. P. (2015). Genetic variation in the HLA region is associated with susceptibility to herpes zoster. *Genes & Immunity*, 16(1), 1-7.

Culy, C. R., Clemett, D., & Wiseman, L. R. (2000). Oxaliplatin. *Drugs*, 60(4), 895-924.

Cunningham J, Kantekure K, Saif MW. (2014). Medullary Carcinoma of the Colon: A Case Series and Review of the Literature. *In Vivo*. 28:311–314.

D'Arcy, M. S. (2019). Cell death: a review of the major forms of apoptosis, necrosis and autophagy. *Cell Biology International*, 43(6), 582-592.

Dagoglu, N., Mahadevan, A., Nedea, E., Poylin, V., & Nagle, D. (2015). Stereotactic body radiotherapy (SBRT) reirradiation for pelvic recurrence from colorectal cancer. *Journal of Surgical Oncology*, 111(4), 478-482.

Dahle, J., Brunborg, G., Svendsrud, D. H., Stokke, T., & Kvam, E. (2008). Overexpression of human OGG1 in mammalian cells decreases ultraviolet A induced mutagenesis. *Cancer Letters*, 267(1), 18-25.

Danielsen, H. E., Pradhan, M., & Novelli, M. (2016). Revisiting tumour aneuploidy - the place of ploidy assessment in the molecular era. *Nature reviews. Clinical oncology*, 13(5), 291–304. https://doi.org/10.1038/nrclinonc.2015.208

Dasari, S., & Tchounwou, P. B. (2014). Cisplatin in cancer therapy: molecular mechanisms of action. *European Journal of Pharmacology,* 740, 364–378. https://doi.org/10.1016/j.ejphar.2014.07.025

Dasgupta, A., Gupta, T., Sridhar, E., Shirsat, N., Krishnatry, R., Goda, J. S., Chinnaswamy, G., & Jalali, R. (2019). Pediatric Patients With SHH Medulloblastoma Fail Differently as Compared With Adults: Possible Implications for Treatment Modifications. *Journal of Paediatric Haematology/Oncology*, 41(8), e499–e505. https://doi.org/10.1097/MPH.0000000000001484

Davis, A. J., & Chen, D. J. (2013). DNA double strand break repair via non-homologous end-joining. *Translational Cancer Research*, 2(3), 130–143. https://doi.org/10.3978/j.issn.2218-676X.2013.04.02

De Braganca, K. C., & Packer, R. J. (2013). Treatment Options for Medulloblastoma and CNS Primitive Neuroectodermal Tumor (PNET). *Current Treatment Options in Neurology*, 15(5), 593–606. https://doi.org/10.1007/s11940-013-0255-4

de Martel, C., Ferlay, J., Franceschi, S., Vignat, J., Bray, F., Forman, D., & Plummer, M. (2012). Global burden of cancers attributable to infections in 2008: a review and synthetic

analysis. *The Lancet. Oncology*, 13(6), 607–615. https://doi.org/10.1016/S1470-2045(12)70137-7

De Sousa E Melo, F., Wang, X., Jansen, M., Fessler, E., Trinh, A., de Rooij, L. P., de Jong, J. H., de Boer, O. J., van Leersum, R., Bijlsma, M. F., Rodermond, H., van der Heijden, M., van Noesel, C. J., Tuynman, J. B., Dekker, E., Markowetz, F., Medema, J. P., & Vermeulen, L. (2013). Poor-prognosis colon cancer is defined by a molecularly distinct subtype and develops from serrated precursor lesions. *Nature Medicine*, 19(5), 614–618. https://doi.org/10.1038/nm.3174

de Vree, J. M., Jacquemin, E., Sturm, E., Cresteil, D., Bosma, P. J., Aten, J., Deleuze, J. F., Desrochers, M., Burdelski, M., Bernard, O., Oude Elferink, R. P., & Hadchouel, M. (1998). Mutations in the MDR3 gene cause progressive familial intrahepatic cholestasis. Proceedings of the National Academy of Sciences of the United States of America, 95(1), 282–287. https://doi.org/10.1073/pnas.95.1.282

del Charco, J.O., Bolek, T.W., McCollough, W.M. (1998). Medulloblastoma: time-dose relationship based on a 30-year review. *Int J Radiat Oncol Biol Phys*.,42(1),147-154.

Denisenko, T., Sorokina, I., Gogvadze, V., & Zhivotovsky, B. (2016). Mitotic catastrophe and cancer drug resistance: A link that must to be broken. *Drug Resistance Updates*, *24*, 1-12. doi: 10.1016/j.drup.2015.11.002

Deriano, L., & Roth, D. B. (2013). Modernizing the nonhomologous end-joining repertoire: alternative and classical NHEJ share the stage. Annual review of genetics, 47, 433-455.

Derrien, T., Johnson, R., Bussotti, G., Tanzer, A., Djebali, S., Tilgner, H., Guernec, G., Martin, D., Merkel, A., Knowles, D. G., Lagarde, J., Veeravalli, L., Ruan, X., Ruan, Y., Lassmann, T., Carninci, P., Brown, J. B., Lipovich, L., Gonzalez, J. M., Thomas, M., … Guigó, R. (2012). The GENCODE v7 catalog of human long non-coding RNAs: analysis of their gene structure, evolution, and expression. Genome research, 22(9), 1775–1789. https://doi.org/10.1101/gr.132159.111

Desoize, B., & Madoulet, C. (2002). Particular aspects of platinum compounds used at present in cancer treatment. Critical reviews in oncology/hematology, 42(3), 317-325.

DeSouza, R., Jones, B., Lowis, S., & Kurian, K. (2014). Paediatric Medulloblastoma "Update on Molecular Classification Driving Targeted Therapies. *Frontiers In Oncology*, *4*. doi: 10.3389/fonc.2014.00176

Dhall, G. (2009). Medulloblastoma. *Journal of Child Neurology*, 24(11), 1418-1430.

Dhyani, P., Quispe, C., Sharma, E., Bahukhandi, A., Sati, P., Attri, D. C., ... & Cho, W. C. (2022). Anticancer potential of alkaloids: a key emphasis to colchicine, vinblastine, vincristine, vindesine, vinorelbine and vincamine. *Cancer Cell International*, 22(1), 1-20.

Di Francesco, A. M., Ruggiero, A., & Riccardi, R. (2002). Cellular and molecular aspects of drugs of the future: oxaliplatin. *Cellular and Molecular Life Sciences* : CMLS, 59(11), 1914–1927. https://doi.org/10.1007/pl00012514

Di, L., Artursson, P., Avdeef, A., Benet, L. Z., Houston, J. B., Kansy, M., ... & Sugano, K. (2020). The critical role of passive permeability in designing successful drugs. *ChemMedChem*, 15(20), 1862-1874.

Dienstmann, R., Vermeulen, L., Guinney, J., Kopetz, S., Tejpar, S., & Tabernero, J. (2017). Consensus molecular subtypes and the evolution of precision medicine in colorectal cancer. *Nature reviews. Cancer*, 17(4), 268. https://doi.org/10.1038/nrc.2017.24

DiTullio, R. A., Jr, Mochan, T. A., Venere, M., Bartkova, J., Sehested, M., Bartek, J., & Halazonetis, T. D. (2002). 53BP1 functions in an ATM-dependent checkpoint pathway that is constitutively activated in human cancer. *Nature Cell Biology*, 4(12), 998–1002. https://doi.org/10.1038/ncb892

Djebali, S., Davis, C. A., Merkel, A., Dobin, A., Lassmann, T., Mortazavi, A., Tanzer, A., Lagarde, J., Lin, W., Schlesinger, F., Xue, C., Marinov, G. K., Khatun, J., Williams, B. A., Zaleski, C., Rozowsky, J., Röder, M., Kokocinski, F., Abdelhamid, R. F., Alioto, T., … Gingeras, T. R. (2012). Landscape of transcription in human cells. *Nature*, 489(7414), 101–108. https://doi.org/10.1038/nature11233

Dolce, V., Dusi, S., Giannattasio, M., Joseph, C. R., Fumasoni, M., & Branzei, D. (2022). Parental histone deposition on the replicated strands promotes error-free DNA damage tolerance and regulates drug resistance. *Genes & Development*, 36(3-4), 167-179.

Dolznig, H., Grebien, F., Sauer, T., Beug, H., & Müllner, E. W. (2004). Evidence for a size-sensing mechanism in animal cells. *Nature Cell Biology*, 6(9), 899–905. https://doi.org/10.1038/ncb1166

Dou H, Mitra S, Hazra TK. (2003). Repair of oxidized bases in DNA bubble structures by human DNA glycosylases NEIL1 and NEIL2. *J Biol Chem*.278:49679–49684.

Downs, I., Vijayan, S., Sidiq, T., & Kobayashi, K. S. (2016). CITA/NLRC5: a critical transcriptional regulator of MHC class I gene expression. *Biofactors,* 42(4), 349-357.

Downs, J. A., & Jackson, S. P. (2004). A means to a DNA end: the many roles of Ku. Nature reviews. *Molecular Cell Biology*, 5(5), 367–378. https://doi.org/10.1038/nrm1367

Drewinko, B., Romsdahl, M. M., Yang, L. Y., Ahearn, M. J., & Trujillo, J. M. (1976). Establishment of a human carcinoembryonic antigen-producing colon adenocarcinoma cell line. *Cancer Research*, 36(2 Pt 1), 467–475.

Dudley, D. D., Chaudhuri, J., Bassing, C. H., and Alt, F. W. (2005). Mechanism and control of V(D)J recombination versus class switch recombination: similarities and differences. *Advanced Immunology* 86, 43–112. doi: 10.1016/S0065-2776(04)86002-4

Duman-Scheel M. (2012). Deleted in Colorectal Cancer (DCC) pathfinding: axon guidance gene finally turned tumor suppressor. *Current Drug Targets*, 13(11), 1445–1453. https://doi.org/10.2174/138945012803530215

Eberhart, C. G., Tihan, T., & Burger, P. C. (2000). Nuclear localization and mutation of β-catenin in medulloblastomas. *Journal of Neuropathology & Experimental Neurology*, 59(4), 333-337.

Ehrlich, M. (2019). DNA hypermethylation in disease: mechanisms and clinical relevance. *Epigenetics,* 14(12), 1141-1163.

Eide, P. W., Moosavi, S. H., Eilertsen, I. A., Brunsell, T. H., Langerud, J., Berg, K. C., ... & Sveen, A. (2021). Metastatic heterogeneity of the consensus molecular subtypes of colorectal cancer. *NPJ Genomic Medicine*, 6(1), 1-9.

El Hussein, S., & Khader, S. N. (2019). Primary signet ring cell carcinoma of the pancreas: Cytopathology review of a rare entity. *Diagnostic Cytopathology*, 47(12), 1314–1320. https://doi.org/10.1002/dc.24324

Elbakry, A., & Löbrich, M. (2021). Homologous Recombination Subpathways: A Tangle to Resolve. *Frontiers in Genetics*, 12, 723847. https://doi.org/10.3389/fgene.2021.723847

Ellis, B. C., Molloy, P. L., & Graham, L. D. (2012). CRNDE: A Long Non-Coding RNA Involved in CanceR, Neurobiology, and Development. *Frontiers in Genetics*, 3, 270. https://doi.org/10.3389/fgene.2012.00270

Ellison, D. W., Dalton, J., Kocak, M., Nicholson, S. L., Fraga, C., Neale, G., Kenney, A. M., Brat, D. J., Perry, A., Yong, W. H., Taylor, R. E., Bailey, S., Clifford, S. C., & Gilbertson, R. J. (2011). Medulloblastoma: clinicopathological correlates of SHH, WNT, and non-SHH/WNT molecular subgroups. *Acta neuropathologica*, 121(3), 381–396. https://doi.org/10.1007/s00401-011-0800-8

Ellison, D. W., Onilude, O. E., Lindsey, J. C., Lusher, M. E., Weston, C. L., Taylor, R. E., Pearson, A. D., Clifford, S. C., & United Kingdom Children's Cancer Study Group Brain Tumour Committee (2005). beta-Catenin status predicts a favorable outcome in childhood medulloblastoma: the United Kingdom Children's Cancer Study Group Brain Tumour Committee. *Journal of clinical oncology : official journal of the American Society of Clinical Oncology*, 23(31), 7951–7957. https://doi.org/10.1200/JCO.2005.01.5479

Ensminger, M., & Löbrich, M. (2020). One end to rule them all: Non-homologous end-joining and homologous recombination at DNA double-strand breaks. *The British Journal of Radiology*, 93(1115), 20191054.

Esteller M. (2011). Non-coding RNAs in human disease. Nature reviews. *Genetics*, 12(12), 861–874. https://doi.org/10.1038/nrg3074

Evdokimova, V., Ruzanov, P., Imataka, H., Raught, B., Svitkin, Y., Ovchinnikov, L. P., & Sonenberg, N. (2001). The major mRNA-associated protein YB-1 is a potent 5′ cap-dependent mRNA stabilizer. *The EMBO Journal*, 20(19), 5491-5502.

Fabris, L., & Calin, G. A. (2017). Understanding the genomic ultraconservations: T-UCRs and cancer. *International Review of Cell and Molecular Biology*, 333, 159-172.

Faivre, S., Chan, D., Salinas, R., Woynarowska, B., & Woynarowski, J. M. (2003). DNA strand breaks and apoptosis induced by oxaliplatin in cancer cells. *Biochemical Pharmacology*, 66(2), 225–237. https://doi.org/10.1016/s0006-2952(03)00260-0

Fajka-Boja, R., Marton, A., Tóth, A., Blazsó, P., Tubak, V., Bálint, B., Nagy, I., Hegedűs, Z., Vizler, C., & Katona, R. L. (2018). Increased insulin-like growth factor 1 production by polyploid adipose stem cells promotes growth of breast cancer cells. *BMC Cancer*, 18(1), 872. https://doi.org/10.1186/s12885-018-4781-z

Fan, J., Xing, Y., Wen, X., Jia, R., Ni, H., He, J., ... & Fan, X. (2015). Long non-coding RNA ROR decoys gene-specific histone methylation to promote tumorigenesis. *Genome Biology*, 16(1), 1-17.

Fang, Y., & Fullwood, M. J. (2016). Roles, Functions, and Mechanisms of Long Non-coding RNAs in cancer. *Genomics, Proteomics & Bioinformatics*, 14(1), 42–54. https://doi.org/10.1016/j.gpb.2015.09.006

Fatica, A., & Bozzoni, I. (2014). Long non-coding RNAs: new players in cell differentiation and development. Nature reviews. *Genetics*, 15(1), 7–21. https://doi.org/10.1038/nrg3606

Fatima, Z., Sharma, P., Youssef, B., & Krishnan, K. (2021). Medullary Carcinoma of the Colon: A Histopathologic Challenge. *Cureus*, 13(6), e15831. https://doi.org/10.7759/cureus.15831

Fearon, E. R. (2011). Molecular genetics of colorectal cancer. Annual Review of Pathology: *Mechanisms of Disease*, 6, 479-507.

Fearon, E. R., & Vogelstein, B. (1990). A genetic model for colorectal tumorigenesis. *Cell*, 61(5), 759–767. https://doi.org/10.1016/0092-8674(90)90186-i

Fei, F., Zhang, M., Li, B., Zhao, L., Wang, H., Liu, L., ... & Zhang, S. (2019). Formation of polyploid giant cancer cells involves in the prognostic value of neoadjuvant chemoradiation in locally advanced rectal cancer. *Journal of Oncology*, 2019.

Fernandez-Capetillo, O., Chen, H. T., Celeste, A., Ward, I., Romanienko, P. J., Morales, J. C., Naka, K., Xia, Z., Camerini-Otero, R. D., Motoyama, N., Carpenter, P. B., Bonner, W. M., Chen, J., & Nussenzweig, A. (2002). DNA damage-induced G2-M checkpoint activation by histone H2AX and 53BP1. *Nature Cell Biology*, 4(12), 993–997. https://doi.org/10.1038/ncb884

Fessler, E., Drost, J., van Hooff, S. R., Linnekamp, J. F., Wang, X., Jansen, M., De Sousa E Melo, F., Prasetyanti, P. R., IJspeert, J. E., Franitza, M., Nürnberg, P., van Noesel, C. J., Dekker, E., Vermeulen, L., Clevers, H., & Medema, J. P. (2016). TGFβ signaling directs serrated adenomas to the mesenchymal colorectal cancer subtype. *EMBO Molecular Medicine*, 8(7), 745–760. https://doi.org/10.15252/emmm.201606184

Field, J. J., Waight, A. B., & Senter, P. D. (2014). A previously undescribed tubulin binder. *Proceedings of the National Academy of Sciences of the United States of America*, 111(38), 13684–13685. https://doi.org/10.1073/pnas.1414572111

Fiorenzano, A., Pascale, E., Gagliardi, M., Terreri, S., Papa, M., Andolfi, G., ... & Fico, A. (2018). An ultraconserved element containing lncRNA preserves transcriptional dynamics and maintains ESC self-renewal. *Stem Cell Reports*, 10(3), 1102-1114.

Fischel, J. L., Formento, P., Ciccolini, J., Rostagno, P., Etienne, M. C., Catalin, J., & Milano, G. (2002). Impact of the oxaliplatin-5 fluorouracil-folinic acid combination on respective intracellular determinants of drug activity. *British Journal of Cancer,* 86(7), 1162–1168. https://doi.org/10.1038/sj.bjc.6600185

Florea, A. M., & Büsselberg, D. (2011). Cisplatin as an anti-tumor drug: cellular mechanisms of activity, drug resistance and induced side effects. Cancers, 3(1), 1351-1371.

Fontana, E., Eason, K., Cervantes, A., Salazar, R., & Sadanandam, A. (2019). Context matters-consensus molecular subtypes of colorectal cancer as biomarkers for clinical trials. *Annals of oncology : official journal of the European Society for Medical Oncology*, 30(4), 520–527. https://doi.org/10.1093/annonc/mdz052

Fortini P & Dogliotti E (2007). "Base damage and single-strand break repair: mechanisms and functional significance of short- and long-patch repair subpathways". *DNA Repair*. 6 (4): 398–409. doi:10.1016/j.dnarep.2006.10.008

Fortini, P., Pascucci, B., Parlanti, E., Sobol, R. W., Wilson, S. H., & Dogliotti, E. (1998). Different DNA polymerases are involved in the short-and long-patch base excision repair in mammalian cells. *Biochemistry*, 37(11), 3575-3580.

Fromme JC, Banerjee A, Verdine GL (2004). "DNA glycosylase recognition and catalysis". *Curr. Opin. Struct. Biol.* 14 (1): 43–9. doi:10.1016/j.sbi.2004.01.003

Fuertes, M. A., Alonso, C., & Pérez, J. M. (2003). Biochemical modulation of cisplatin mechanisms of action: enhancement of antitumor activity and circumvention of drug resistance. *Chemical Reviews*, 103(3), 645-662.

Fuertes, M. A., Castilla, J., Alonso, C., & Perez, J. M. (2002). Novel concepts in the development of platinum antitumor drugs. *Current Medicinal Chemistry-Anti-Cancer Agents*, 2(4), 539-551.

Fukui Y. (2014). Mechanisms behind signet ring cell carcinoma formation. *Biochemical and Biophysical Research Communications*, 450(4), 1231–1233. https://doi.org/10.1016/j.bbrc.2014.07.025.

Gajjar, A., & Robinson, G. (2014). Medulloblastoma—translating discoveries from the bench to the bedside. *Nature Reviews Clinical Oncology*, *11*(12), 714-722. doi: 10.1038/nrclinonc.2014.181

Galán-Malo, P., Vela, L., Gonzalo, O., Calvo-Sanjuán, R., Gracia-Fleta, L., Naval, J., & Marzo, I. (2012). Cell fate after mitotic arrest in different tumour cells is determined by the balance between slippage and apoptotic threshold. *Toxicology And Applied Pharmacology*, *258*(3), 384-393. doi: 10.1016/j.taap.2011.11.021

Galanski, M., Jakupec, M. A., & Keppler, B. K. (2005). Update of the preclinical situation of anticancer platinum complexes: novel design strategies and innovative analytical approaches. *Current Medicinal Chemistry,* 12(18), 2075–2094. https://doi.org/10.2174/0929867054637626

Galluzzi, L., Linkermann, A., Kepp, O., & Kroemer, G. (2020). Pathophysiology of cancer cell death. *In Abeloff's Clinical Oncology* (pp. 74-83). Elsevier.

Ganem, N., Cornils, H., Chiu, S., O'Rourke, K., Arnaud, J., & Yimlamai, D. *et al*. (2014).Cytokinesis Failure Triggers Hippo Tumour Suppressor Pathway Activation. *Cell*, 158(4), 833848. doi: 10.1016/j.cell.2014.06.029

Ganem, N., Storchova, Z., & Pellman, D. (2007). Tetraploidy, aneuploidy and cancer. *Current Opinion In Genetics & Development*, 17(2), 157-162. doi: 10.1016/j.gde.2007.02.011

Gao, N., Li, Y., Li, J., Gao, Z., Yang, Z., Li, Y., ... & Fan, T. (2020). Long non-coding RNAs: the regulatory mechanisms, research strategies, and future directions in cancers. *Frontiers in Oncology*, 10, 598817.

Gao, W. G., Pu, S. P., Liu, W. P., Liu, Z. D., & Yang, Y. K. (2003). The aquation of oxaliplatin and the effect of acid. *Acta Pharmaceutica Sinica*, 38(3), 223-226.

Garcia-Lopez, J., Kumar, R., Smith, K. S., & Northcott, P. A. (2021). Deconstructing Sonic Hedgehog Medulloblastoma: Molecular Subtypes, Drivers, and Beyond. *Trends in Genetics : TIG*, 37(3), 235–250. https://doi.org/10.1016/j.tig.2020.11.001

Gascoigne, K. E., & Taylor, S. S. (2008) Cancer cells display profound intra- and interline variation following prolonged exposure to antimitotic drugs. *Cancer Cell* 14, 111-122

Gascoigne, K., & Taylor, S. (2009). How do anti-mitotic drugs kill cancer cells?. *Journal Of Cell Science*, *122*(15), 2579-2585. doi: 10.1242/jcs.039719

Gaudreault, I., Guay, D., & Lebel, M. (2004). YB-1 promotes strand separation in vitro of duplex DNA containing either mispaired bases or cisplatin modifications, exhibits endonucleolytic activities and binds several DNA repair proteins. *Nucleic acids Research*, 32(1), 316–327. https://doi.org/10.1093/nar/gkh170

Gayan, S., Teli, A., & Dey, T. (2017). Inherent aggressive character of invasive and non-invasive cells dictates the in vitro migration pattern of multicellular spheroid. *Scientific Reports*, 7(1), 11527. https://doi.org/10.1038/s41598-017-10078-7

Geyer J.R., Sposto R., & Jennings M, *et al*. Multiagent chemotherapy and deferred radiotherapy in infants with malignant brain tumors: a report from the Children's Cancer Group. *Journal of Clinical Oncology*;23(30),7621-7631.

Ghosh S. (2019). Cisplatin: The first metal based anticancer drug. *Bioorganic Chemistry*, 88, 102925. https://doi.org/10.1016/j.bioorg.2019.102925

Ghosh, D., & Raghavan, S. C. (2021). 20 years of DNA polymerase μ, the polymerase that still surprises. *The FEBS Journal,* 288(24), 7230-7242.

Gibert Jr, M. K., Sarkar, A., Chagari, B., Roig-Laboy, C., Saha, S., Bednarek, S., ... & Abounader, R. (2022). Transcribed Ultraconserved Regions in Cancer. *Cells*, 11(10), 1684.

Gibson, P., Tong, Y., Robinson, G., Thompson, M., Currle, D., & Eden, C. *et al*. (2010). Subtypes of medulloblastoma have distinct developmental origins. *Nature*, 468(7327), 10951099. doi: 10.1038/nature09587

Gilbertson R. J. (2004). Medulloblastoma: signalling a change in treatment. *The Lancet. Oncology*, 5(4), 209–218. https://doi.org/10.1016/S1470-2045(04)01424-X

Gilbertson, R. J., & Ellison, D. W. (2008). The origins of medulloblastoma subtypes. *Annual Review of Pathology*, 3, 341–365. https://doi.org/10.1146/annurev.pathmechdis.3.121806.151518

Gomber, S., Dewan, P., & Chhonker, D. (2010). Vincristine induced neurotoxicity in cancer patients. *The Indian Journal of Pediatrics*, 77(1), 97-100.

Gómez-Ruiz, S., Maksimović-Ivanić, D., Mijatović, S., & Kaluđerović, G. N. (2012). On the discovery, biological effects, and use of Cisplatin and metallocenes in anticancer chemotherapy. *Bioinorganic Chemistry and Applications*, 2012, 140284. https://doi.org/10.1155/2012/140284

Goschzik, T., Zur Mühlen, A., Kristiansen, G., Haberler, C., Stefanits, H., Friedrich, C., ... & Pietsch, T. (2015). Molecular stratification of medulloblastoma: comparison of histological and genetic methods to detect Wnt activated tumours. *Neuropathology and Applied Neurobiology*, 41(2), 135-144.

Grady, W. M., & Carethers, J. M. (2008). Genomic and epigenetic instability in colorectal cancer pathogenesis. *Gastroenterology*, 135(4), 1079–1099. https://doi.org/10.1053/j.gastro.2008.07.076

Green, D. R. (2022). Cell death and cancer. *Cold Spring Harbor Perspectives in Biology*, 14(9), a041103.

Gros, F., Gilbert, W., Hiatt, H. H., Attardi, G., Spahr, P. F., & Watson, J. D. (1961). Molecular and biological characterization of messenger RNA. *In Cold Spring Harbor symposia on quantitative biology* (Vol. 26, pp. 111-132). Cold Spring Harbor Laboratory Press.

Grosshans D. R. (2016). Proton therapy for paediatric medulloblastoma. *The Lancet. Oncology*, 17(3), 258–259. https://doi.org/10.1016/S1470-2045(15)00217-X

Grote P,. Wittler L., Hendrix D., Koch F., Wahrisch S., Beisaw A., (2013) The tissue-specific lncRNA Fendrr is an essential regulator of heart and body wall development in the mouse *Dev Cell,* 24, pp. 206-214

Grundy, G. J., Rulten, S. L., Zeng, Z., Arribas-Bosacoma, R., Iles, N., Manley, K., Oliver, A., & Caldecott, K. W. (2013). APLF promotes the assembly and activity of non-homologous end joining protein complexes. *The EMBO Journal*, 32(1), 112–125. https://doi.org/10.1038/emboj.2012.304

Gu, C., Shi, X., Huang, Z., Chen, J., Yang, J., Shi, J., & Pan, X. (2020). A comprehensive study of construction and analysis of competitive endogenous RNA networks in lung adenocarcinoma. *Biochimica et Biophysica Acta (BBA)-Proteins and Proteomics*, 1868(8), 140444.

Guay, D., Garand, C., Reddy, S., Schmutte, C., & Lebel, M. (2008). The human endonuclease III enzyme is a relevant target to potentiate cisplatin cytotoxicity in Y-box-binding protein-1 overexpressing tumor cells. *Cancer Science*, 99(4), 762-769.

Guerrini-Rousseau, L., Dufour, C., Varlet, P., Masliah-Planchon, J., Bourdeaut, F., Guillaud-Bataille, M., Abbas, R., Bertozzi, A. I., Fouyssac, F., Huybrechts, S., Puget, S., Bressac-De Paillerets, B., Caron, O., Sevenet, N., Dimaria, M., Villebasse, S., Delattre, O., Valteau-Couanet, D., Grill, J., & Brugières, L. (2018). Germline SUFU mutation carriers and medulloblastoma: clinical characteristics, cancer risk, and prognosis. *Neuro-oncology*, 20(8), 1122–1132. https://doi.org/10.1093/neuonc/nox228

Guinney, J., Dienstmann, R., Wang, X., de Reyniès, A., Schlicker, A., Soneson, C., Marisa, L., Roepman, P., Nyamundanda, G., Angelino, P., Bot, B. M., Morris, J. S., Simon, I. M.,

Gerster, S., Fessler, E., De Sousa E Melo, F., Missiaglia, E., Ramay, H., Barras, D., Homicsko, K., … Tejpar, S. (2015). The consensus molecular subtypes of colorectal cancer. *Nature Medicine*, 21(11), 1350–1356. https://doi.org/10.1038/nm.3967

Guirouilh-Barbat, J., Lambert, S., Bertrand, P., & Lopez, B. S. (2014). Is homologous recombination really an error-free process?. *Frontiers in Genetics*, 5, 175.

Gunturi, A., & McDermott, D. F. (2015). Nivolumab for the treatment of cancer. *Expert opinion on investigational drugs*, 24(2), 253-260.

Gupta, R. A., Shah, N., Wang, K. C., Kim, J., Horlings, H. M., Wong, D. J., Tsai, M. C., Hung, T., Argani, P., Rinn, J. L., Wang, Y., Brzoska, P., Kong, B., Li, R., West, R. B., van de Vijver, M. J., Sukumar, S., & Chang, H. Y. (2010). Long non-coding RNA HOTAIR reprograms chromatin state to promote cancer metastasis. *Nature,* 464(7291), 1071–1076. https://doi.org/10.1038/nature08975

Gutschner, T., & Diederichs, S. (2012). The hallmarks of cancer: a long non-coding RNA point of view. *RNA Biology*, 9(6), 703–719. https://doi.org/10.4161/rna.20481

Guttman, M., Garber, M., Levin, J. Z., Donaghey, J., Robinson, J., Adiconis, X., Fan, L., Koziol, M. J., Gnirke, A., Nusbaum, C., Rinn, J. L., Lander, E. S., & Regev, A. (2010). Ab initio reconstruction of cell type-specific transcriptomes in mouse reveals the conserved multi-exonic structure of lincRNAs. *Nature Biotechnology*, 28(5), 503–510. https://doi.org/10.1038/nbt.1633

Grundy, G. J., & Parsons, J. L. (2020). Base excision repair and its implications to cancer therapy. *Essays in Biochemistry*, 64(5), 831-843.

Haber, J. E. (2014). Genome Stability: DNA Repair and Recombinaition. New York, NY: Garland Science.

Häfner, M. F., & Debus, J. (2016). Radiotherapy for colorectal cancer: current standards and future perspectives. *Visceral Medicine*, 32(3), 172-177.

Haider, K., Rahaman, S., Yar, M. S., & Kamal, A. (2019). Tubulin inhibitors as novel anticancer agents: an overview on patents (2013-2018). *Expert opinion on therapeutic patents*, 29(8), 623-641.

Hamilton, L. E., Jones, K., Church, N., & Medlicott, S. (2013). Synchronous appendiceal and intramucosal gastric signet ring cell carcinomas in an individual with CDH1-associated hereditary diffuse gastric carcinoma: a case report of a novel association and review of the literature. *BMC Gastroenterology*, 13(1), 1-6.

Hanaoka, F., and Sugasawa, K., (eds.) (2016). DNA Replication, recombination, and repair: *Molecular Mechanisms and Pathology*. Tokyo: Springer.

Hangauer, M. J., Vaughn, I. W., & McManus, M. T. (2013). Pervasive transcription of the human genome produces thousands of previously unidentified long intergenic non-coding RNAs. *PLoS genetics*, 9(6), e1003569. https://doi.org/10.1371/journal.pgen.1003569

Hans, F., Senarisoy, M., Bhaskar Naidu, C., & Timmins, J. (2020). Focus on DNA Glycosylases—A Set of Tightly Regulated Enzymes with a High Potential as Anticancer Drug Targets. *International Journal of Molecular Sciences*, 21(23), 9226.

Hao, N. B., He, Y. F., Li, X. Q., Wang, K., & Wang, R. L. (2017). The role of miRNA and lncRNA in gastric cancer. *Oncotarget*, 8(46), 81572.

Hao, Y., Samuels, Y., Li, Q., Krokowski, D., Guan, B. J., Wang, C., Jin, Z., Dong, B., Cao, B., Feng, X., Xiang, M., Xu, C., Fink, S., Meropol, N. J., Xu, Y., Conlon, R. A., Markowitz, S., Kinzler, K. W., Velculescu, V. E., Brunengraber, H., … Wang, Z. (2016). Oncogenic PIK3CA mutations reprogram glutamine metabolism in colorectal cancer. *Nature* communications, 7, 11971. https://doi.org/10.1038/ncomms11971

Haraldsdottir, S., Einarsdottir, H. M., Smaradottir, A., Gunnlaugsson, A., & Halfdanarson, T. R. (2014). *Colorectal cancer-review*. Laeknabladid, 100(2), 75-82.

Harley, M., Allan, L., Sanderson, H., & Clarke, P. (2010). Phosphorylation of Mcl-1 by CDK1– cyclin B1 initiates its Cdc20-dependent destruction during mitotic arrest. *The EMBO Journal*, 29(14), 2407-2420. doi: 10.1038/emboj.2010.112

Hartmann, J. T., & Lipp, H. P. (2003). Toxicity of platinum compounds. *Expert opinion on pharmacotherapy*, 4(6), 889-901.

Hatten, M. E., & Roussel, M. F. (2011). Development and cancer of the cerebellum. *Trends in Neurosciences*, 34(3), 134–142. https://doi.org/10.1016/j.tins.2011.01.002

Hauer, M. H., & Gasser, S. M. (2017). Chromatin and nucleosome dynamics in DNA damage and repair. *Genes & Development*, 31(22), 2204-2221.

Havas, A. P., Rodrigues, K. B., Bhakta, A., Demirjian, J. A., Hahn, S., Tran, J., ... & Smith, C. L. (2016). Belinostat and vincristine demonstrate mutually synergistic cytotoxicity associated with mitotic arrest and inhibition of polyploidy in a preclinical model of aggressive diffuse large B cell lymphoma. *Cancer Biology & Therapy*, 17(12), 1240-1252.

He, L., & Hannon, G. J. (2004). MicroRNAs: small RNAs with a big role in gene regulation. *Nature Reviews. Genetics*, 5(7), 522–531. https://doi.org/10.1038/nrg1379

Hector, S., Bolanowska-Higdon, W., Zdanowicz, J., Hitt, S., & Pendyala, L. (2001). In vitro studies on the mechanisms of oxaliplatin resistance. *Cancer Chemotherapy and Pharmacology*, 48(5), 398–406. https://doi.org/10.1007/s002800100363

Hengartner, M. O. (2000). The biochemistry of apoptosis. *Nature*, 407(6805), 770-776.

Heo, J. B., & Sung, S. (2011). Vernalization-mediated epigenetic silencing by a long intronic non-coding RNA. *Science* (New York, N.Y.), 331(6013), 76–79. https://doi.org/10.1126/science.1197349

Hildrestrand GA, Neurauter CG, Diep DB, Castellanos CG, Krauss S, Bjoras M, Luna L. (2009). Expression patterns of Neil3 during embryonic brain development and neoplasia. BMC *Neurosci.* 10:45.

Hindi, N. N., Elsakrmy, N., & Ramotar, D. (2021). The base excision repair process: Comparison between higher and lower eukaryotes. *Cellular and Molecular Life Sciences*, 1-23.

Hoeijmakers JH (2009). "DNA damage, aging, and cancer". *The New England Journal of Medicine*. 361 (15): 1475–85. doi:10.1056/NEJMra0804615.

Hollenbach, S., Dhénaut, A., Eckert, I., Radicella, J. P., & Epe, B. (1999). Overexpression of Ogg1 in mammalian cells: effects on induced and spontaneous oxidative DNA damage and mutagenesis. *Carcinogenesis,* 20(9), 1863-1868.

Hollingsworth M.A., Swanson B.J.(2004). Mucins in Cancer: Protection and Control of the Cell Surface. *Nat. Rev. Cancer.*4:45–60. doi: 10.1038/nrc1251.

Homer, C., Knight, D. A., Hananeia, L., Sheard, P., Risk, J., Lasham, A., ... & Braithwaite, A. W. (2005). Y-box factor YB1 controls p53 apoptotic function. *Oncogene*, 24(56), 8314-8325.

Hoskin, P. J., de Canha, S. M., Bownes, P., Bryant, L., & Jones, R. G. (2004). High dose rate afterloading intraluminal brachytherapy for advanced inoperable rectal carcinoma. *Radiotherapy and Oncology*, 73(2), 195-198.

Housman, G., Byler, S., Heerboth, S., Lapinska, K., Longacre, M., Snyder, N., & Sarkar, S. (2014). Drug resistance in cancer: an overview. *Cancers,* 6(3), 1769–1792. https://doi.org/10.3390/cancers6031769

Hu, S. P., Ge, M. X., Gao, L., Jiang, M., & Hu, K. W. (2021). LncRNA HCP5 as a potential therapeutic target and prognostic biomarker for various cancers: a meta-analysis and bioinformatics analysis. *Cancer Cell International*, 21(1), 686. https://doi.org/10.1186/s12935-021-02404-x

Hu, X., Sood, A. K., Dang, C. V., & Zhang, L. (2018). The role of long non-coding RNAs in cancer: the dark matter matters. *Current opinion in Genetics & Development*, 48, 8–15. https://doi.org/10.1016/j.gde.2017.10.004

Huang, D., & Strasser, A. (2000). BH3-Only Proteins—Essential Initiators of Apoptotic Cell Death. *Cell*, *103*(6), 839-842. doi: 10.1016/s0092-8674(00)00187-2

Huang, R. X., & Zhou, P. K. (2020). DNA damage response signaling pathways and targets for radiotherapy sensitization in cancer. *Signal transduction and targeted therapy*, 5(1), 1-27.

Huarte, M., Guttman, M., Feldser, D., Garber, M., Koziol, M. J., Kenzelmann-Broz, D., Khalil, A. M., Zuk, O., Amit, I., Rabani, M., Attardi, L. D., Regev, A., Lander, E. S., Jacks, T., & Rinn, J. L. (2010). A large intergenic non-coding RNA induced by p53 mediates global gene repression in the p53 response. *Cell*, 142(3), 409–419. https://doi.org/10.1016/j.cell.2010.06.040

Huerta, S., Harris, D. M., Jazirehi, A., Bonavida, B., Elashoff, D., Livingston, E. H., & Heber, D. (2003). Gene expression profile of metastatic colon cancer cells resistant to cisplatin-induced apoptosis. *International Journal of Oncology*, 22(3), 663-670.

Huffman, J. L., Sundheim, O., & Tainer, J. A. (2005). DNA base damage recognition and removal: new twists and grooves. *Mutation Research*, 577(1-2), 55–76. https://doi.org/10.1016/j.mrfmmm.2005.03.012

Hughes, E.N., Shillito, J., Sallan, S.E., Loeffler, J.S., Cassady, J.R., Tarbell, N.J. (1988) Medulloblastoma at the joint center for radiation therapy between 1968 and 1984. The influence of radiation dose on the patterns of failure and survival. *Cancer*,61(10), 1992-1998.

Hughes, J. R., & Parsons, J. L. (2020). FLASH radiotherapy: current knowledge and future insights using proton-beam therapy. International Journal of Molecular Sciences, 21(18), 6492.

Hung, T., Wang, Y., Lin, M. F., Koegel, A. K., Kotake, Y., Grant, G. D., Horlings, H. M., Shah, N., Umbricht, C., Wang, P., Wang, Y., Kong, B., Langerød, A., Børresen-Dale, A. L., Kim, S. K., van de Vijver, M., Sukumar, S., Whitfield, M. L., Kellis, M., Xiong, Y., … Chang, H. Y. (2011). Extensive and coordinated transcription of non-coding RNAs within cell-cycle promoters. *Nature Genetics*, 43(7), 621–629. https://doi.org/10.1038/ng.848

Iaccarino, I. (2017). lncRNAs and MYC: an intricate relationship. *International Journal of Molecular Sciences*, 18(7), 1497.

Iliakis, G., Murmann, T., & Soni, A. (2015). Alternative end-joining repair pathways are the ultimate backup for abrogated classical non-homologous end-joining and homologous recombination repair: Implications for the formation of chromosome translocations. *Mutation Research/Genetic Toxicology and Environmental Mutagenesis*, 793, 166-175.

Inaguma, S., Lasota, J., Felisiak-Golabek, A., Kowalik, A., Wang, Z., Zieba, S., ... & Miettinen, M. (2017). Histopathological and genotypic characterization of metastatic colorectal carcinoma with PD-L1 (CD274)-expression: Possible roles of tumour micro environmental factors for CD274 expression. *The Journal of Pathology: Clinical Research*, 3(4), 268-278.

Ise, T., Nagatani, G., Imamura, T., Kato, K., Takano, H., Nomoto, M., Izumi, H., Ohmori, H., Okamoto, T., Ohga, T., Uchiumi, T., Kuwano, M., & Kohno, K. (1999). Transcription factor Y-box binding protein 1 binds preferentially to cisplatin-modified DNA and interacts with proliferating cell nuclear antigen. *Cancer Research*, 59(2), 342–346.

Itatani, Y., Kawada, K., & Sakai, Y. (2019). Transforming Growth Factor-β Signaling Pathway in Colorectal Cancer and Its Tumor Microenvironment. *International Journal of Molecular Sciences,* 20(23), 5822. https://doi.org/10.3390/ijms20235822

Ito, J., Sugimoto, R., Nakaoka, H., Yamada, S., Kimura, T., Hayano, T., & Inoue, I. (2017). Systematic identification and characterization of regulatory elements derived from human endogenous retroviruses. *PLoS Genetics*, 13(7), e1006883.

Ivanov, D., Coyle, B., Walker, D., & Grabowska, A. (2016). In vitro models of medulloblastoma: Choosing the right tool for the job. *Journal Of Biotechnology*, *236*, 10-25. doi: 10.1016/j.jbiotec.2016.07.028

Jacobs, A. L., & Schär, P. (2012). DNA glycosylases: in DNA repair and beyond. *Chromosoma*, 121(1), 1–20. https://doi.org/10.1007/s00412-011-0347-4

Jamieson, E. R., & Lippard, S. J. (1999). Structure, recognition, and processing of cisplatin−DNA adducts. *Chemical Reviews*, 99(9), 2467-2498.

Jan, R., & Chaudhry, G. E. (2019). Understanding Apoptosis and Apoptotic Pathways Targeted Cancer Therapeutics. *Advanced Pharmaceutical Bulletin*, 9(2), 205–218. https://doi.org/10.15171/apb.2019.024

Janz, M., Harbeck, N., Dettmar, P., Berger, U., Schmidt, A., Jürchott, K., Schmitt, M., & Royer, H. D. (2002). Y-box factor YB-1 predicts drug resistance and patient outcome in breast cancer independent of clinically relevant tumor biologic factors HER2, uPA and PAI-1. *International Journal of Cancer*, 97(3), 278–282. https://doi.org/10.1002/ijc.1610

Jasin, M., & Rothstein, R. (2013). Repair of strand breaks by homologous recombination. *Cold Spring Harbor perspectives in Biology*, 5(11), a012740.

Jeng, P. S., Inoue-Yamauchi, A., Hsieh, J. J., & Cheng, E. H. (2018). BH3-Dependent and Independent Activation of BAX and BAK in Mitochondrial Apoptosis. *Current Opinion in Physiology*, 3, 71–81. https://doi.org/10.1016/j.cophys.2018.03.005

Jiang, Q., Ma, R., Wang, J., Wu, X., Jin, S., Peng, J., Tan, R., Zhang, T., Li, Y., & Wang, Y. (2015). LncRNA2Function: a comprehensive resource for functional investigation of human lncRNAs based on RNA-seq data. *BMC Genomics*, 16 Suppl 3(Suppl 3), S2. https://doi.org/10.1186/1471-2164-16-S3-S2

Jones, P. A., & Laird, P. W. (1999). Cancer epigenetics comes of age. *Nature Genetics*, 21(2), 163–167. https://doi.org/10.1038/5947

Jordan, M., & Wilson, L. (2004). Microtubules as a target for anticancer drugs. *Nature Reviews Cancer*, *4*(4), 253-265. doi: 10.1038/nrc1317

Joza, N., Susin, S. A., Daugas, E., Stanford, W. L., Cho, S. K., Li, C. Y., ... & Penninger, J. M. (2001). Essential role of the mitochondrial apoptosis-inducing factor in programmed cell death. *Nature*, 410(6828), 549-554.

Juliano, R. L., & Ling, V. (1976). A surface glycoprotein modulating drug permeability in Chinese hamster ovary cell mutants. *Biochimica et Biophysica acta*, 455(1), 152–162. https://doi.org/10.1016/0005-2736(76)90160-7

Jun, Y. W., & Kool, E. T. (2022). Chemical Tools for the Study of DNA Repair. Accounts of Chemical Research, 55(23), 3495-3506.

Jung, D., and Alt, F. W. (2004). Unraveling V(D)J recombination; insights into gene regulation. *Cell* 116, 299–311. doi: 10.1016/S0092-8674(04)00039-X

Junop MS, Obmolova G, Rausch K, Hsieh P, Yang W. (2001) Composite active site of an ABC ATPase: MutS uses ATP to verify mismatch recognition and authorize *DNA Repair*. *Mol Cell*; **7**:1–12

Kang, S., Na, Y., Joung, S. Y., Lee, S. I., Oh, S. C., & Min, B. W. (2018). The significance of microsatellite instability in colorectal cancer after controlling for clinicopathological factors. *Medicine*, 97(9), e0019. https://doi.org/10.1097/MD.0000000000010019

Kartha, R. V., & Subramanian, S. (2014). Competing endogenous RNAs (ceRNAs): new entrants to the intricacies of gene regulation. *Frontiers in Genetics*, 5, 8. https://doi.org/10.3389/fgene.2014.00008

Kastan, M. B., & Bartek, J. (2004). Cell-cycle checkpoints and cancer. *Nature*, 432(7015), 316–323. https://doi.org/10.1038/nature03097

Kay, J., Thadhani, E., Samson, L., & Engelward, B. (2019). Inflammation-induced DNA damage, mutations and cancer. *DNA Repair*, 83, 102673.

Kelland L. (2007). The resurgence of platinum-based cancer chemotherapy. *Nature Reviews. Cancer*, 7(8), 573–584. https://doi.org/10.1038/nrc2167

Kelso, A. A., Goodson, S. D., Watts, L. E., Ledford, L. L., Waldvogel, S. M., Diehl, J. N., ... & Sehorn, M. G. (2017). The β-isoform of BCCIP promotes ADP release from the RAD51 presynaptic filament and enhances homologous DNA pairing. *Nucleic acids Research*, 45(2), 711-725.

Kennedy, R. D., Quinn, J. E., Mullan, P. B., Johnston, P. G., & Harkin, D. P. (2004). The role of BRCA1 in the cellular response to chemotherapy. *Journal of the National Cancer Institute*, 96(22), 1659-1668.

Kent, T., Chandramouly, G., McDevitt, S. M., Ozdemir, A. Y., & Pomerantz, R. T. (2015). Mechanism of microhomology-mediated end-joining promoted by human DNA polymerase θ. *Nature Structural & Molecular Biology*, 22(3), 230-237.

Khalil, A. M., Guttman, M., Huarte, M., Garber, M., Raj, A., Rivea Morales, D., ... & Rinn, J. L. (2009). Many human large intergenic non-coding RNAs associate with chromatin-modifying complexes and affect gene expression. *Proceedings of the National Academy of Sciences*, 106(28), 11667-11672.

Khanna KK, Jackson SP. DNA double-strand breaks: signaling, repair and the cancer connection. *Nature Genetics*. 2001 Mar;27(3):247-54. doi: 10.1038/85798.

Kidani, Y., Inagaki, K., Iigo, M., Hoshi, A., and Kuretani, K. (1978) Anti-tumor Activity of 1,2-Diaminocyclohexane-Platinum Complexes Against Sarcoma-180 Ascite Form. *J. Med. Chem.* 21, 1315–1318.

Kijima, N., & Kanemura, Y. (2016). Molecular Classification of Medulloblastoma. *Neurologia Medico-Chirurgica*, *56*(11), 687-697. doi: 10.2176/nmc.ra.2016-0016

Kikuchi A. (2003). Tumor formation by genetic mutations in the components of the Wnt signaling pathway. *Cancer Science*, 94(3), 225–229. https://doi.org/10.1111/j.1349-7006.2003.tb01424.x

Kim, M. S., Choi, C., Yoo, S., Cho, C., Seo, Y., Ji, Y., ... & Kang, H. (2008). Stereotactic body radiation therapy in patients with pelvic recurrence from rectal carcinoma. *Japanese Journal of Clinical Oncology*, 38(10), 695-700.

Kish, T., & Uppal, P. (2016). Trifluridine/Tipiracil (Lonsurf) for the Treatment of Metastatic Colorectal Cancer. *P & T : a peer-reviewed journal for formulary management*, 41(5), 314–325.

Kishikawa T, Otsuka M, Ohno M, Yoshikawa T, Takata A, Koike K. (2015). Circulating RNAs as new biomarkers for detecting pancreatic cancer. *World J Gastroenterol.* 21:8527–8540. doi: 10.3748/wjg.v21.i28.8527

Klase, Z., Yedavalli, V. S., Houzet, L., Perkins, M., Maldarelli, F., Brenchley, J., Strebel, K., Liu, P., & Jeang, K. T. (2014). Activation of HIV-1 from latent infection via synergy of RUNX1 inhibitor Ro5-3335 and SAHA. *PLoS Pathogens*, 10(3), e1003997. https://doi.org/10.1371/journal.ppat.1003997

Kleefstra, T., Brunner, H. G., Amiel, J., Oudakker, A. R., Nillesen, W. M., Magee, A., Geneviève, D., Cormier-Daire, V., van Esch, H., Fryns, J. P., Hamel, B. C., Sistermans, E. A., de Vries, B. B., & van Bokhoven, H. (2006). Loss-of-function mutations in euchromatin histone methyl transferase 1 (EHMT1) cause the 9q34 subtelomeric deletion syndrome. *American Journal of Human Genetics*, 79(2), 370–377. https://doi.org/10.1086/505693

Knop M . (2011).Yeast cell morphology and sexual reproduction—a short overview and some considerations. *C R Biol* **334**: 599–606.

Kogo R, Shimamura T, Mimori K, Kawahara K, Imoto S, Sudo T, Tanaka F, Shibata K, Suzuki A, Komune S. (2011). Long non-coding RNA HOTAIR regulates polycomb-dependent chromatin modification and is associated with poor prognosis in colorectal cancers. *Cancer Research.*71:6320–6326. doi: 10.1158/0008-5472.CAN-11-1021

Köhler K, Ferreira P, Pfander B, Boos D (2016). The Initiation of DNA Replication in Eukaryotes. Springer, Cham. pp. 443–460. doi:10.1007/978-3-319-24696-3_22

Koike, K., Uchiumi, T., Ohga, T., Toh, S., Wada, M., Kohno, K., & Kuwano, M. (1997). Nuclear translocation of the Y-box binding protein by ultraviolet irradiation. *FEBS letters*, 417(3), 390-394.

Kondo, Y., & Issa, J. P. (2004). Epigenetic changes in colorectal cancer. *Cancer Metastasis Reviews,* 23(1-2), 29–39. https://doi.org/10.1023/a:1025806911782

Kool, M., Korshunov, A., Remke, M., Jones, D., Schlanstein, M., & Northcott, P. *et al*. (2012). Molecular subgroups of medulloblastoma: an international meta-analysis of transcriptome, genetic aberrations, and clinical data of WNT, SHH, Group 3, and Group 4 medulloblastomas. *Acta Neuropathologica*, 123(4), 473-484. doi: 10.1007/s00401-012-0958-8

Korshunov, A., Remke, M., Kool, M., Hielscher, T., Northcott, P. A., Williamson, D., Pfaff, E., Witt, H., Jones, D. T., Ryzhova, M., Cho, Y. J., Wittmann, A., Benner, A., Weiss, W. A., von Deimling, A., Scheurlen, W., Kulozik, A. E., Clifford, S. C., Peter Collins, V., Westermann, F., … Pfister, S. M. (2012). Biological and clinical heterogeneity of MYCN-amplified medulloblastoma. *Acta neuropathologica*, 123(4), 515–527. https://doi.org/10.1007/s00401-011-0918-8

Kothari, A., Hittelman, W. N., & Chambers, T. C. (2016). Cell Cycle-Dependent Mechanisms Underlie Vincristine-Induced Death of Primary Acute Lymphoblastic Leukemia Cells. *Cancer Research*, 76(12), 3553–3561. https://doi.org/10.1158/0008-5472.CAN-15-2104

Koyuncu, D., Sharma, U., Goka, E. T., & Lippman, M. E. (2021). Spindle assembly checkpoint gene BUB1B is essential in breast cancer cell survival. *Breast Cancer Research and Treatment*, 185, 331-341.

Krasikova, Y. S., Rechkunova, N. I., Maltseva, E. A., & Lavrik, O. I. (2018). RPA and XPA interaction with DNA structures mimicking intermediates of the late stages in nucleotide excision repair. *PloS one*, 13(1), e0190782. https://doi.org/10.1371/journal.pone.0190782

Krejci, L., Altmannova, V., Spirek, M., & Zhao, X. (2012). Homologous recombination and its regulation. *Nucleic acids Research*, 40(13), 5795–5818. https://doi.org/10.1093/nar/gks270

Kufe D.W. Mucins in Cancer: Function, Prognosis and Therapy. (2009). *Nature Reviews Cancer.* 9:874–885. doi: 10.1038/nrc2761.

Kulski, J. K. (2019). Long non-coding RNA HCP5, a hybrid HLA class I endogenous retroviral gene: structure, expression, and disease associations. *Cells*, 8(5), 480.

Kulski, J. K., & Dawkins, R. L. (1999). The P5 multicopy gene family in the MHC is related in sequence to human endogenous retroviruses HERV-L and HERV-16. *Immunogenetics*, 49(5), 404-412.

Kulski, J. K., Gaudieri, S., Inoko, H., & Dawkins, R. L. (1999). Comparison between two human endogenous retrovirus (HERV)-rich regions within the major histocompatibility complex. *Journal of Molecular Evolution*, 48(6), 675-683.

Kulski, J. K., Gaudieri, S., Martin, A., & Dawkins, R. L. (1999). Coevolution of PERB11 (MIC) and HLA class I genes with HERV-16 and retroelements by extended genomic duplication. *Journal of Molecular Evolution*, 49(1), 84-97.

Kung, J. T., Colognori, D., & Lee, J. T. (2013). Long non-coding RNAs: past, present, and future. *Genetics*, 193(3), 651–669. https://doi.org/10.1534/genetics.112.146704

Kunkel TA, Erie DA . (2005). DNA mismatch repair. *Annu Rev Biochem.* **74**:681–710

Kunschner, L. (2002). Harvey Cushing and Medulloblastoma. *Archives Of Neurology*, 59(4), 642. doi: 10.1001/archneur.59.4.642

Kuo, L. J., & Yang, L. X. (2008). Gamma-H2AX - a novel biomarker for DNA double-strand breaks. *In vivo* (Athens, Greece), 22(3), 305–309.

Kuwano, M., Oda, Y., Izumi, H., Yang, S. J., Uchiumi, T., Iwamoto, Y., Toi, M., Fujii, T., Yamana, H., Kinoshita, H., Kamura, T., Tsuneyoshi, M., Yasumoto, K., & Kohno, K. (2004). The role of nuclear Y-box binding protein 1 as a global marker in drug resistance. *Molecular Cancer Therapeutics*, 3(11), 1485–1492.

Kweekel, D. M., Gelderblom, H., & Guchelaar, H. J. (2005). Pharmacology of oxaliplatin and the use of pharmacogenomics to individualize therapy. *Cancer Treatment Reviews*, 31(2), 90–105. https://doi.org/10.1016/j.ctrv.2004.12.006

Kwong, L. N., & Dove, W. F. (2009). APC and its modifiers in colon cancer. Advances in *Experimental Medicine and Biology*, 656, 85–106. https://doi.org/10.1007/978-1-4419-1145-2_8

Labianca, R., & Merelli, B. (2010). Screening and diagnosis for colorectal cancer: present and future. *Tumour Journal*, 96(6), 889-901.

Lambert, M., Benmoussa, A., & Provost, P. (2019). Small non-coding RNAs derived from eukaryotic ribosomal RNA. *Non-coding RNA*, 5(1), 16.

Lander, E. S., Linton, L. M., Birren, B., Nusbaum, C., Zody, M. C., Baldwin, J., Devon, K., Dewar, K., Doyle, M., FitzHugh, W., Funke, R., Gage, D., Harris, K., Heaford, A.,

Howland, J., Kann, L., Lehoczky, J., LeVine, R., McEwan, P., McKernan, K., … International Human Genome Sequencing Consortium (2001). Initial sequencing and analysis of the human genome. *Nature*, 409(6822), 860–921. https://doi.org/10.1038/35057062

Lane, L. C., Kuś, A., Bednarczuk, T., Bossowski, A., Daroszewski, J., Jurecka-Lubieniecka, B., ... & Mitchell, A. L. (2020). An intronic HCP5 variant is associated with age of onset and susceptibility to Graves disease in UK and Polish cohorts. *The Journal of Clinical Endocrinology & Metabolism*, 105(9), e3277-e3284.

Lanzillotti, C., De Mattei, M., Mazziotta, C., Taraballi, F., Rotondo, J. C., Tognon, M., & Martini, F. (2021). Long Non-coding RNAs and MicroRNAs Interplay in Osteogenic Differentiation of Mesenchymal Stem Cells. *Frontiers in Cell and Developmental Biology*, 9, 646032. https://doi.org/10.3389/fcell.2021.646032

Lanzós, A., Carlevaro-Fita, J., Mularoni, L., Reverter, F., Palumbo, E., Guigó, R., & Johnson, R. (2017). Discovery of Cancer Driver Long Non-coding RNAs across 1112 Tumour Genomes: New Candidates and Distinguishing Features. *Scientific Reports*, 7, 41544. https://doi.org/10.1038/srep41544

Laprie, A., Hu, Y., Alapetite, C., Carrie, C., Habrand, J. L., Bolle, S., ... & Balosso, J. (2015). Paediatric brain tumours: a review of radiotherapy, state of the art and challenges for the future regarding protontherapy and carbontherapy. *Cancer/Radiothérapie*, 19(8), 775-789.

Lara-Gonzalez, P., Westhorpe, F., & Taylor, S. (2012). The Spindle Assembly Checkpoint. *Current Biology*, *22*(22), R966-R980. doi: 10.1016/j.cub.2012.10.006

Lazow, M. A., Palmer, J. D., Fouladi, M., & Salloum, R. (2022). Medulloblastoma in the Modern Era: Review of Contemporary Trials, Molecular Advances, and Updates in Management. *Neurotherapeutics*, *19*(6), 1733-1751.

Lawley, P. D., & Brookes, P. (1967). Interstrand cross-linking of DNA by difunctional alkylating agents. *Journal of Molecular Biology*, 25(1), 143-160.

Lee N.K., Kim S., Kim H.S., Jeon T.Y., Kim G.H., Kim D.U., Park D.Y., Kim T.U., Kang D.H. (2011). Spectrum of Mucin-Producing Neoplastic Conditions of the Abdomen and Pelvis: Cross-Sectional Imaging Evaluation. *World Journal Gastroenterol*. 17:4757–4771. doi: 10.3748/wjg.v17.i43.4757.

Lee, C. D., Snee, A. J., Perkins, K., Jelley, F. E., & Wong, H. (2007). High dose rate brachytherapy as a boost after preoperative chemoradiotherapy for more advanced rectal tumours: the Clatterbridge experience. *Clinical Oncology* (Royal College of Radiologists (Great Britain)), 19(9), 711-719.

Leibovitz, A., Stinson, J. C., McCombs III, W. B., McCoy, C. E., Mazur, K. C., & Mabry, N. D. (1976). Classification of human colorectal adenocarcinoma cell lines. *Cancer Research*, 36(12), 4562-4569.

Leopoldo, S., Lorena, B., Cinzia, A., Gabriella, D. C., Angela Luciana, B., Renato, C., ... & Cesare, B. (2008). Two subtypes of mucinous adenocarcinoma of the colorectum: clinicopathological and genetic features. *Annals of Surgical Oncology*, 15(5), 1429-1439.

Lepoivre C., Belhocine M., Bergon A., Griffon A., Yammine M., Vanhille L., Divergent transcription is associated with promoters of transcriptional regulators BMC *Genomics*, 14 (2013), p. 914

Lévi, F., Metzger, G., Massari, C., & Milano, G. (2000). Oxaliplatin. *Clinical Pharmacokinetics*, 38(1), 1-21.

Levine, A., Momand, J., & Finlay, C. (1991). The p53 tumour suppressor gene. *Nature*, *351*(6326), 453-456. doi: 10.1038/351453a0

Leygue E. (2007). Steroid receptor RNA activator (SRA1): unusual bifaceted gene products with suspected relevance to breast cancer. *Nuclear Receptor Signalling*, 5, e006. https://doi.org/10.1621/nrs.05006

Li, GM. (2008). Mechanisms and functions of DNA mismatch repair. *Cell Research* **18,** 85–98 https://doi.org/10.1038/cr.2007.115

Li, P., Zhou, L., Liu, X., Jin, X., Zhao, T., Ye, F., Liu, X., Hirayama, R., & Li, Q. (2014). Mitotic DNA damages induced by carbon-ion radiation incur additional chromosomal breaks in polyploidy. *Toxicology Letters*, 230(1), 36–47. https://doi.org/10.1016/j.toxlet.2014.08.006

Li, T., & Chen, Z. J. (2018). The cGAS-cGAMP-STING pathway connects DNA damage to inflammation, senescence, and cancer. *The Journal of Experimental Medicine*, 215(5), 1287–1299. https://doi.org/10.1084/jem.20180139

Li, W., Jie, Z., Li, Z., Liu, Y., Gan, Q., Mao, Y., & Wang, X. (2014). ERCC1 siRNA ameliorates drug resistance to cisplatin in gastric carcinoma cell lines. *Molecular Medicine Reports*, 9(6), 2423-2428.

Li, Y., Upadhyay, S., Bhuiyan, M., & Sarkar, F. H. (1999). Induction of apoptosis in breast cancer cells MDA-MB-231 by genistein. *Oncogene*, 18(20), 3166-3172.

Li, Z., Shen, J., Chan, M. T., & Wu, W. K. (2016). TUG1: a pivotal oncogenic long non-coding RNA of human cancers. *Cell Proliferation*, 49(4), 471–475. https://doi.org/10.1111/cpr.12269

Liang, L., Xu, J., Wang, M., Xu, G., Zhang, N., Wang, G., & Zhao, Y. (2018). LncRNA HCP5 promotes follicular thyroid carcinoma progression via miRNAs sponge. *Cell Death & Disease*, 9(3), 372. https://doi.org/10.1038/s41419-018-0382-7

Libri, A., Marton, T., & Deriano, L. (2022). The (lack of) DNA double-strand break repair pathway choice during V (D) J recombination. *Frontiers in Genetics*, 12, 2726.

Lindahl T. (1974). An N-glycosidase from *Escherichia coli* that releases free uracil from DNA containing deaminated cytosine residues. *Proc Natl Acad Sci USA*. 71:3649–3653. doi: 10.1073/pnas.71.9.3649.

Lindahl, T. (1986). DNA glycosylases in DNA repair. In Mechanisms of DNA Damage and Repair (pp. 335-340). Springer, Boston, MA.

Lindahl, T., & Barnes, D. E. (2000). Repair of endogenous DNA damage. In Cold Spring Harbor symposia on quantitative biology (Vol. 65, pp. 127-134). Cold Spring Harbor Laboratory Press.

Lindsey, J. C., Hill, R. M., Megahed, H., Lusher, M. E., Schwalbe, E. C., Cole, M., Hogg, T. L., Gilbertson, R. J., Ellison, D. W., Bailey, S., & Clifford, S. C. (2011). TP53 mutations in favorable-risk Wnt/Wingless-subtype medulloblastomas. *Journal of Clinical Oncology* : official journal of the American Society of Clinical Oncology, 29(12), e344–e348. https://doi.org/10.1200/JCO.2010.33.8590

Liu, F., Huang, J., & Liu, Z. (2019). Vincristine impairs microtubules and causes neurotoxicity in cerebral organoids. *Neuroscience*, 404, 530-540.

Liu, H., Wu, Y., He, F., Cheng, Z., Zhao, Z., Xiang, C., Feng, X., Bai, X., Takeda, S., Wu, X., & Qing, Y. (2019). Brca1 is involved in tolerance to adefovir dipivoxil-induced DNA damage. *International Journal of Molecular Medicine*, 43(6), 2491–2498. https://doi.org/10.3892/ijmm.2019.4164

Liu, S. T., & Zhang, H. (2016). The mitotic checkpoint complex (MCC): looking back and forth after 15 years. AIMS *Molecular Science*, 3(4), 597.

Liu, Y., Wang, J., Dong, L., Xia, L., Zhu, H., Li, Z., & Yu, X. (2019). Long non-coding RNA HCP5 regulates pancreatic cancer gemcitabine (GEM) resistance by sponging Hsa-miR-214-3p to target HDGF. *Oncotargets and Therapy*, 12, 8207.

Livak, K. J., & Schmittgen, T. D. (2001). Analysis of relative gene expression data using real-time quantitative PCR and the 2(-Delta Delta C(T)) Method. *Methods* (San Diego, Calif.), 25(4), 402–408. https://doi.org/10.1006/meth.2001.1262

Loehrer, P. J., & Einhorn, L. H. (1984). Cisplatin. *Annals of Internal Medicine*, 100(5), 704-713.

Lohse, I., Borgida, A., Cao, P., Cheung, M., Pintilie, M., Bianco, T., ... & Hedley, D. W. (2015). BRCA1 and BRCA2 mutations sensitize to chemotherapy in patient-derived pancreatic cancer xenografts. *British Journal of Cancer*, 113(3), 425-432.

Lok, T. M., Wang, Y., Xu, W. K., Xie, S., Ma, H. T., & Poon, R. (2020). Mitotic slippage is determined by p31comet and the weakening of the spindle-assembly checkpoint. *Oncogene*, 39(13), 2819–2834. https://doi.org/10.1038/s41388-020-1187-6

Longley, D. B., Harkin, D. P., & Johnston, P. G. (2003). 5-fluorouracil: mechanisms of action and clinical strategies. *Nature reviews. Cancer*, 3(5), 330–338. https://doi.org/10.1038/nrc1074

Lopez de Saro FJ, Marinus MG, Modrich P, O'Donnell M. (1994). The beta sliding clamp binds to multiple sites within MutL and MutS. *J Biol Chem*. **281**:14340–14349.

Lord, C. J., & Ashworth, A. (2012). The DNA damage response and cancer therapy. *Nature*, 481(7381), 287-294.

Louro, R., Smirnova, A. S., & Verjovski-Almeida, S. (2009). Long intronic non-coding RNA transcription: expression noise or expression choice?. *Genomics*, 93(4), 291–298. https://doi.org/10.1016/j.ygeno.2008.11.009

Lovejoy, K. S., & Lippard, S. J. (2009). Non-traditional platinum compounds for improved accumulation, oral bioavailability, and tumor targeting. *Dalton Transactions* (Cambridge, England : 2003), (48), 10651–10659. https://doi.org/10.1039/b913896j

Lowe, S. W., & Lin, A. W. (2000). Apoptosis in cancer. Carcinogenesis, 21(3), 485-495.

Lu, G., Duan, J., Shu, S., Wang, X., Gao, L., Guo, J., & Zhang, Y. (2016). Ligase I and ligase III mediate the DNA double-strand break ligation in alternative end-joining. *Proceedings of the National Academy of Sciences*, 113(5), 1256-1260.

Lujambio, A., & Lowe, S. W. (2012). The microcosmos of cancer. *Nature*, 482(7385), 347-355.

Luo, X., Budihardjo, I., Zou, H., Slaughter, C., & Wang, X. (1998). Bid, a Bcl-2 Interacting protein, mediates Cytochrome c Release from mitochondria in response to activation of cell Surface Death Receptors. *Cell*, 94(4), 481-490. doi: 10.1016/s0092-8674(00)81589-5

Lyabin, D. N., Eliseeva, I. A., & Ovchinnikov, L. P. (2014). YB-1 protein: functions and regulation. *Wiley Interdisciplinary Reviews: RNA*, 5(1), 95-110.

Ma, L., Bajic, V. B., & Zhang, Z. (2013). On the classification of long non-coding RNAs. *RNA Biology*, 10(6), 925–933. https://doi.org/10.4161/rna.24604

Mabonga, L., & Kappo, A. P. (2019). The oncogenic potential of small nuclear ribonucleoprotein polypeptide G: a comprehensive and perspective view. *American Journal of Translational Research*, 11(11), 6702.

Macheret, M., & Halazonetis, T. D. (2015). DNA replication stress as a hallmark of cancer. *Annual Review of Pathology: Mechanisms of Disease*, 10, 425-448.

MacLachlan, T. K., Takimoto, R., & El-Deiry, W. S. (2002). BRCA1 directs a selective p53-dependent transcriptional response towards growth arrest and DNA repair targets. *Molecular and Cellular Biology*, 22(12), 4280-4292.

Mahoney, J. A., & Rosen, A. (2005). Apoptosis and autoimmunity. *Current Opinion in Immunology,* 17(6), 583–588. https://doi.org/10.1016/j.coi.2005.09.018

Maier, H., Dalianis, T., & Kostopoulou, O. N. (2021). New approaches in targeted therapy for medulloblastoma in children. *Anticancer Research*, 41(4), 1715-1726.

Mailand, N., Bekker-Jensen, S., Faustrup, H., Melander, F., Bartek, J., Lukas, C., & Lukas, J. (2007). RNF8 ubiquitylates histones at DNA double-strand breaks and promotes assembly of repair proteins. *Cell*, 131(5), 887-900

Makasheva, K. A., Endutkin, A. V., & Zharkov, D. O. (2020). Requirements for DNA bubble structure for efficient cleavage by helix-two-turn-helix DNA glycosylases. *Mutagenesis*, 35(1), 119–128. https://doi.org/10.1093/mutage/gez047

Mandel, C. R., Bai, Y., & Tong, L. (2008). Protein factors in pre-mRNA 3′-end processing. *Cellular and Molecular Life Sciences*, 65(7), 1099-1122.

Manic, G., Corradi, F., Sistigu, A., Siteni, S., & Vitale, I. (2017). Molecular regulation of the spindle assembly checkpoint by kinases and phosphatases. *International Review of Cell and Molecular Biology*, 328, 105-161.

Marash, L., Liberman, N., Henis-Korenblit, S., Sivan, G., Reem, E., Elroy-Stein, O., & Kimchi, A. (2008). DAP5 Promotes Cap-Independent Translation of Bcl-2 and CDK1 to

Facilitate Cell Survival during Mitosis. *Molecular Cell*, *30*(4), 447-459. doi: 10.1016/j.molcel.2008.03.018

Markowitz, S. D., & Bertagnolli, M. M. (2009). Molecular basis of colorectal cancer. *New England Journal of Medicine*, 361(25), 2449-2460.

Mármol, I., Sánchez-de-Diego, C., Pradilla Dieste, A., Cerrada, E., & Rodriguez Yoldi, M. J. (2017). Colorectal Carcinoma: A General Overview and Future Perspectives in Colorectal Cancer. *International Journal of Molecular Sciences*, 18(1), 197. https://doi.org/10.3390/ijms18010197

Marnett, L. J. (2000). Oxyradicals and DNA damage. *Carcinogenesis*, 21(3), 361-370.

Martinez-Balibrea, E., Martínez-Cardús, A., Ginés, A., Ruiz de Porras, V., Moutinho, C., Layos, L., ... & Abad, A. (2015). Tumor-related molecular mechanisms of oxaliplatin resistance. *Molecular Cancer Therapeutics*, 14(8), 1767-1776.

Marzo, I., & Naval, J. (2013). Antimitotic drugs in cancer chemotherapy: Promises and pitfalls. *Biochemical Pharmacology*, 86(6), 703-710. doi: 10.1016/j.bcp.2013.07.010

Massagué, J., Blain, S. W., & Lo, R. S. (2000). TGFbeta signaling in growth control, cancer, and heritable disorders. *Cell*, 103(2), 295–309. https://doi.org/10.1016/s0092-8674(00)00121-5

Mathiasen, D. P., & Lisby, M. (2014). Cell cycle regulation of homologous recombination in Saccharomyces cerevisiae. FEMS *Microbiology Reviews*, 38(2), 172–184. https://doi.org/10.1111/1574-6976.12066

Matson, D., & Stukenberg, P. (2011). Spindle Poisons and Cell Fate: A Tale of Two Pathways. *Molecular Interventions*, 11(2), 141-150. doi: 10.1124/mi.11.2.12.

Matzaraki, V., Kumar, V., Wijmenga, C., & Zhernakova, A. (2017). The MHC locus and genetic susceptibility to autoimmune and infectious diseases. *Genome Biology*, 18(1), 76. https://doi.org/10.1186/s13059-017-1207-1

Mauger, D. M., Cabral, B. J., Presnyak, V., Su, S. V., Reid, D. W., Goodman, B., ... & McFadyen, I. J. (2019). mRNA structure regulates protein expression through changes in functional half-life. *Proceedings of the National Academy of Sciences*, 116(48), 24075-24083

Maximov, G., & Maximov, K. (2008). The Role of p53 Tumour-Suppressor Protein in Apoptosis and Cancerogenesis. *Biotechnology & Biotechnological Equipment*, 22(2), 664-668.

McKinney, P. (2004). Brain tumours: incidence, survival, and aetiology. *Journal Of Neurology, Neurosurgery & Psychiatry,* 75(suppl 2), ii12-ii17.

McKinnon, P. J., & Caldecott, K. W. (2007). DNA strand break repair and human genetic disease. *Annu. Rev. Genomics Hum. Genet*., 8, 37-55.

McNeill, D. R., Paramasivam, M., Baldwin, J., Huang, J., Vyjayanti, V. N., Seidman, M. M., & Wilson, D. M. (2013). NEIL1 responds and binds to psoralen-induced DNA interstrand crosslinks. *Journal of Biological Chemistry*, 288(18), 12426-12436.

McNeill, D. R., Whitaker, A. M., Stark, W. J., Illuzzi, J. L., McKinnon, P. J., Freudenthal, B. D., & Wilson III, D. M. (2020). Functions of the major abasic endonuclease (APE1) in cell viability and genotoxin resistance. *Mutagenesis*, 35(1), 27-38.

Mehmood, R. K., Parker, J., Ahmed, S., Qasem, E., Mohammed, A. A., Zeeshan, M., & Jehangir, E. (2014). Review of cisplatin and oxaliplatin in current immunogenic and monoclonal antibodies perspective. *World Journal of Oncology*, 5(3), 97.

Mehta, S., McKinney, C., Algie, M., Verma, C. S., Kannan, S., Harfoot, R., ... & Woolley, A. G. (2020). Dephosphorylation of YB-1 is required for nuclear localisation during G2 phase of the cell cycle. *Cancers*, *12*(2), 315.

Meijers, R., Smock, R. G., Zhang, Y., & Wang, J. H. (2020). Netrin synergizes signaling and adhesion through DCC. *Trends in Biochemical Sciences*, 45(1), 6-12.

Melamede RJ, Hatahet Z, Kow YW, Ide H, Wallace SS. (1994). Isolation and characterization of endonuclease VIII from *Escherichia coli*. *Biochemistry*. 33:1255–1264.

Menyhárt, O., Giangaspero, F., & Győrffy, B. (2019). Molecular markers and potential therapeutic targets in non-WNT/non-SHH (group 3 and group 4) medulloblastomas. *Journal of Hematology & Oncology*, 12(1), 1-17.

Mercer, T. R., Dinger, M. E., & Mattick, J. S. (2009). Long non-coding RNAs: insights into functions. *Nature Reviews. Genetics*, 10(3), 155–159. https://doi.org/10.1038/nrg2521

Merchant, T., Kun, L., Krasin, M., Wallace, D., Chintagumpala, M., & Woo, S. *et al.* (2008). Multi-Institution Prospective Trial of Reduced-Dose Craniospinal Irradiation (23.4 Gy) Followed by Conformal Posterior Fossa (36 Gy) and Primary Site Irradiation (55.8 Gy) and Dose-Intensive Chemotherapy for Average-Risk Medulloblastoma. *International Journal Of Radiation Oncology Biology Physics*, *70*(3),782787. doi:10.1016/j.ijrobp.2007.07.2342

Mezencev, R. (2014). Interactions of cisplatin with non-DNA targets and their influence on anticancer activity and drug toxicity: the complex world of the platinum complex. *Current Cancer Drug Targets*, 14(9), 794-816.

Miquel, C., Borrini, F., Grandjouan, S., Aupérin, A., Viguier, J., Velasco, V., Duvillard, P., Praz, F., & Sabourin, J. C. (2005). Role of bax mutations in apoptosis in colorectal cancers with microsatellite instability. *American Journal of Clinical Pathology*, 123(4), 562–570. https://doi.org/10.1309/JQ2X-3RV3-L8F9-TGYW

Mirman, Z., & de Lange, T. (2020). 53BP1: a DSB escort. *Genes & Development*, 34(1-2), 7-23. doi: 10.1080/13102818.2008.10817532

Mirzayans, R., Andrais, B., & Murray, D. (2018). Roles of Polyploid/Multinucleated Giant Cancer Cells in Metastasis and Disease Relapse Following Anticancer Treatment. *Cancers*, 10(4), 118. https://doi.org/10.3390/cancers10040118

Misset, J. L., Bleiberg, H., Sutherland, W., Bekradda, M., & Cvitkovic, E. (2000). Oxaliplatin clinical activity: a review. *Critical reviews in Oncology/Haematology*, 35(2), 75–93. https://doi.org/10.1016/s1040-8428(00)00070-6

Mladenova, V., Mladenov, E., Stuschke, M., & Iliakis, G. (2022). DNA Damage Clustering after Ionizing Radiation and Consequences in the Processing of Chromatin Breaks. *Molecules,* 27(5), 1540.

Mohammadgholi, A., Rabbani-Chadegani, A., & Fallah, S. (2013). Mechanism of the interaction of plant alkaloid vincristine with DNA and chromatin: spectroscopic study. *DNA and Cell biology*, 32(5), 228–235. https://doi.org/10.1089/dna.2012.1886

Montero, J., & Letai, A. (2017). Why do BCL-2 inhibitors work and where should we use them in the clinic?. *Cell Death And Differentiation*, *25*(1), 56-64. doi: 10.1038/cdd.2017.183

Moore, J. B., 4th, & Uchida, S. (2020). Functional characterization of long non-coding RNAs. *Current Opinion in Cardiology,* 35(3), 199–206. https://doi.org/10.1097/HCO.0000000000000725

Mordovkina, D. A., Kim, E. R., Buldakov, I. A., Sorokin, A. V., Eliseeva, I. A., Lyabin, D. N., & Ovchinnikov, L. P. (2016). Transportin-1-dependent YB-1 nuclear import. *Biochemical and Biophysical Research Communications*, 480(4), 629–634. https://doi.org/10.1016/j.bbrc.2016.10.107

Morgan, David (2006). Cell Cycle: Principles of Control. London: New Science Press

Mortezaee, K., Salehi, E., Mirtavoos-mahyari, H., Motevaseli, E., Najafi, M., Farhood, B., ... & Sahebkar, A. (2019). Mechanisms of apoptosis modulation by curcumin: Implications for cancer therapy. *Journal of Cellular Physiology*, 234(8), 12537-12550.

Moudi, M., Go, R., Yien, C. Y. S., & Nazre, M. (2013). Vinca alkaloids. *International Journal of Preventive Medicine*, 4(11), 1231.

Mousavi, M., Ilkhani, A. R., Sharifi, S., Mehrzad, J., Eghdami, A., & Monajjemi, M. (2013). DFT studies of nano anticancer on vinblastine and vincristine molecules. *International Journal of Microbiology Research Reviews*, 1(2), 31-8.

Mudgapalli, N., Shaw, B. P., Chava, S., & Challagundla, K. B. (2019). The transcribed-ultra conserved regions: novel non-coding RNA players in neuroblastoma progression. *Non-coding RNA*, 5(2), 39.

Mullins, E. A., Rodriguez, A. A., Bradley, N. P., & Eichman, B. F. (2019). Emerging roles of DNA glycosylases and the base excision repair pathway. *Trends in Biochemical Sciences*, 44(9), 765-781.

Musacchio, A., & Salmon, E. (2007). The spindle-assembly checkpoint in space and time. *Nature Reviews Molecular Cell Biology*, *8*(5), 379-393. doi: 10.1038/nrm2163

Muto, T., Bussey, H. J., & Morson, B. C. (1975). The evolution of cancer of the colon and rectum. *Cancer,* 36(6), 2251–2270. https://doi.org/10.1002/cncr.2820360944

Nano, M., Gemble, S., Simon, A., Pennetier, C., Fraisier, V., Marthiens, V., & Basto, R. (2019). Cell-Cycle Asynchrony Generates DNA Damage at Mitotic Entry in Polyploid Cells. *Current Biology* : CB, 29(22), 3937–3945.e7. https://doi.org/10.1016/j.cub.2019.09.041

Nasmyth, K., & Haering, C. H. (2009). Cohesin: its roles and mechanisms. *Annual Review of Genetics,* 43, 525–558. https://doi.org/10.1146/annurev-genet-102108-134233

Navin N., Krasnitz A., Rodgers L., Cook K., Meth J., Kendall J., Riggs M., Eberling Y., Troge J., Grubor V., *et al*. Inferring tumor progression from genomic heterogeneity. *Genome Research*. 2010;20:68–80. doi: 10.1101/gr.099622.109

Nazarkina, Z. K., Khodyreva, S. N., Marsin, S., Lavrik, O. I., & Radicella, J. P. (2007). XRCC1 interactions with base excision repair DNA intermediates. *DNA Repair*, 6(2), 254–264. https://doi.org/10.1016/j.dnarep.2006.10.002

Nezi, L., & Musacchio, A. (2009). Sister chromatid tension and the spindle assembly checkpoint. *Current Opinion In Cell Biology*,21(6),785-795.doi:10.1016/j.ceb.2009.09.007

Nikanjam, M., Arguello, D., Gatalica, Z., Swensen, J., Barkauskas, D. A., & Kurzrock, R. (2020). Relationship between protein biomarkers of chemotherapy response and microsatellite status, tumor mutational burden and PD-L1 expression in cancer patients. *International Journal of Cancer*, 146(11), 3087–3097. https://doi.org/10.1002/ijc.32661

Nimonkar, A. V., Genschel, J., Kinoshita, E., Polaczek, P., Campbell, J. L., Wyman, C., ... & Kowalczykowski, S. C. (2011). BLM–DNA2–RPA–MRN and EXO1–BLM–RPA–MRN constitute two DNA end resection machineries for human DNA break repair. *Genes & Development*, 25(4), 350-362.

Nishiyama, A., & Nakanishi, M. (2021). Navigating the DNA methylation landscape of cancer. *Trends in Genetics*, 37(11), 1012-1027.

Nojadeh, J. N., Behrouz Sharif, S., & Sakhinia, E. (2018). Microsatellite instability in colorectal cancer. *EXCLI Journal*, 17, 159–168. https://doi.org/10.17179/excli2017-948

Northcott, P. A., Korshunov, A., Witt, H., Hielscher, T., Eberhart, C. G., Mack, S., Bouffet, E., Clifford, S. C., Hawkins, C. E., French, P., Rutka, J. T., Pfister, S., & Taylor, M. D. (2011). Medulloblastoma comprises four distinct molecular variants. *Journal of Clinical Oncology* : official journal of the American Society of Clinical Oncology, 29(11), 1408–1414. https://doi.org/10.1200/JCO.2009.27.4324

Northcott, P. A., Nakahara, Y., Wu, X., Feuk, L., Ellison, D. W., Croul, S., Mack, S., Kongkham, P. N., Peacock, J., Dubuc, A., Ra, Y. S., Zilberberg, K., McLeod, J., Scherer, S. W., Sunil Rao, J., Eberhart, C. G., Grajkowska, W., Gillespie, Y., Lach, B., Grundy, R., … Taylor, M. D. (2009). Multiple recurrent genetic events converge on control of histone lysine methylation in medulloblastoma. *Nature Genetics*, 41(4), 465–472. https://doi.org/10.1038/ng.336

O'Brown, Z. K., & Greer, E. L. (2022). N6-methyladenine: A Rare and Dynamic DNA Mark. In DNA Methyltransferases-Role and Function (pp. 177-210). Cham: Springer International Publishing.

O'Connor, M. J. (2015). Targeting the DNA damage response in cancer. *Molecular Cell*, 60(4), 547-560.

O'Connor, P. M., Jackman, J., Bae, I., Myers, T. G., Fan, S., Mutoh, M., Scudiero, D., Monks, A., Sausville, E. A., Weinstein, J. N., Friend, S., Fornace, A. J., Kohn K. W. (1997). Characterization of the *p53* tumour suppressor pathway in cell lines of the National Cancer

Institute anticancer drug screen and correlations with the growth-inhibitory potency of 123 anticancer agents. *Cancer Research*, 57,4285-4300.

O'Hagan HM, Mohammad HP, Baylin SB (2008). "Double strand breaks can initiate gene silencing and SIRT1-dependent onset of DNA methylation in an exogenous promoter CpG island". *PLOS Genetics.* 4 (8): e1000155. doi:10.1371/journal.pgen.1000155

Oltersdorf, T., Elmore, S. W., Shoemaker, A. R., Armstrong, R. C., Augeri, D. J., Belli, B. A., Bruncko, M., Deckwerth, T. L., Dinges, J., Hajduk, P. J., Joseph, M. K., Kitada, S., Korsmeyer, S. J., Kunzer, A. R., Letai, A., Li, C., Mitten, M. J., Nettesheim, D. G., Ng, S., Nimmer, P. M., … Rosenberg, S. H. (2005). An inhibitor of Bcl-2 family proteins induces regression of solid tumours. *Nature*, 435(7042), 677–681. https://doi.org/10.1038/nature03579

Opferman, J. (2015). Attacking cancer's Achilles heel: antagonism of anti-apoptotic BCL-2 family members. *The FEBS Journal*, *283*(14), 2661-2675. doi: 10.1111/febs.13472

Orth, J.D., Kohler, R.H., Foijer, F., Sorger, P.K., Weissleder, R., Mitchison, T.J. (2011). Analysis of mitosis and antimitotic drug responses in tumours by in vivo microscopy and single-cell pharmacodynamics. *Cancer Research*,71,4608-16.

Osielska, M. A., & Jagodziński, P. P. (2018). Long non-coding RNA as potential biomarkers in non-small-cell lung cancer: What do we know so far?. *Biomedicine & Pharmacotherapy*, 101, 322-333.

Oskarsson, T., Batlle, E., & Massagué, J. (2014). Metastatic stem cells: sources, niches, and vital pathways. *Cell Stem Cell*, 14(3), 306–321. https://doi.org/10.1016/j.stem.2014.02.002

Pachano, T., Sánchez-Gaya, V., Ealo, T., Mariner-Faulí, M., Bleckwehl, T., Asenjo, H. G., ... & Rada-Iglesias, A. (2021). Orphan CpG islands amplify poised enhancer regulatory activity and determine target gene responsiveness. *Nature Genetics*, 53(7), 1036-1049.

Packer RJ, Macdonald T, Vezina G, Keating R, Santi M. Medulloblastoma and primitive neuroectodermal tumors. *Handbook of Clinical Neurology*. 2012;105:529-48. doi: 10.1016/B978-0-444-53502-3.00007-0.

Packer, R. J., Gajjar, A., Vezina, G., Rorke-Adams, L., Burger, P. C., Robertson, P. L., Bayer, L., LaFond, D., Donahue, B. R., Marymont, M. H., Muraszko, K., Langston, J., & Sposto, R. (2006). Phase III study of craniospinal radiation therapy followed by adjuvant chemotherapy for newly diagnosed average-risk medulloblastoma. *Journal of Clinical Oncology* : official journal of the American Society of Clinical Oncology, 24(25), 4202–4208. https://doi.org/10.1200/JCO.2006.06.4980

Pal, R., Paul, N., Bhattacharya, D., Rakshit, S., Shanmugam, G., & Sarkar, K. (2022). XPG in the Nucleotide Excision Repair and Beyond: a study on the different functional aspects of XPG and its associated diseases. *Molecular Biology Reports*, 49(8), 7995–8006. https://doi.org/10.1007/s11033-022-07324-1

Panier, S., Boulton, S. Double-strand break repair: 53BP1 comes into focus. Nat Rev Mol *Cell Biology* 15, 7–18 (2014). https://doi.org/10.1038/nrm3719

Pannunzio, N. R., Watanabe, G., & Lieber, M. R. (2018). Nonhomologous DNA end-joining for repair of DNA double-strand breaks. *Journal of Biological Chemistry*, 293(27), 10512-10523.

Pardoll D. M. (2012). The blockade of immune checkpoints in cancer immunotherapy. Nature reviews. *Cancer*, 12(4), 252–264. https://doi.org/10.1038/nrc3239

Parkin, D. M., Bray, F., Ferlay, J., & Pisani, P. (2005). Global cancer statistics, 2002. *CA: a Cancer Journal for Clinicians*, 55(2), 74-108.

Parsons, D. W., Li, M., Zhang, X., Jones, S., Leary, R. J., Lin, J. C., Boca, S. M., Carter, H., Samayoa, J., Bettegowda, C., Gallia, G. L., Jallo, G. I., Binder, Z. A., Nikolsky, Y., Hartigan, J., Smith, D. R., Gerhard, D. S., Fults, D. W., VandenBerg, S., Berger, M. S., … Velculescu, V. E. (2011). The genetic landscape of the childhood cancer medulloblastoma. *Science* (New York, N.Y.), 331(6016), 435–439. https://doi.org/10.1126/science.1198056

Parsons, J. L., & Dianov, G. L. (2013). Co-ordination of base excision repair and genome stability. *DNA Repair*, 12(5), 326–333. https://doi.org/10.1016/j.dnarep.2013.02.001

Paterson, E., Farr, R.F. (1953). Cerebellar medulloblastoma: treatment by irradiation of the whole central nervous system. *Acta radiol*. 39(4),323-336.

Pereira Zambalde, E., Bayraktar, R., Schultz Jucoski, T., Ivan, C., Rodrigues, A. C., Mathias, C., ... & Carvalhode Oliveira, J. (2021). A novel lncRNA derived from an ultraconserved region: Lnc-uc. 147, a potential biomarker in luminal A breast cancer. *RNA Biology*, 18(sup1), 416-429.

Perez E. A. (2009). Microtubule inhibitors: Differentiating tubulin-inhibiting agents based on mechanisms of action, clinical activity, and resistance. *Molecular Cancer Therapeutics*, 8(8), 2086–2095. https://doi.org/10.1158/1535-7163.MCT-09-0366

Pérez-Figueroa, E., Álvarez-Carrasco, P., Ortega, E., & Maldonado-Bernal, C. (2021). Neutrophils: many ways to die. *Frontiers in Immunology*, 12, 631821.

Pfaff, E., Remke, M., Sturm, D., Benner, A., Witt, H., Milde, T., von Bueren, A. O., Wittmann, A., Schöttler, A., Jorch, N., Graf, N., Kulozik, A. E., Witt, O., Scheurlen, W., von Deimling, A., Rutkowski, S., Taylor, M. D., Tabori, U., Lichter, P., Korshunov, A., … Pfister, S. M. (2010). TP53 mutation is frequently associated with CTNNB1 mutation or MYCN amplification and is compatible with long-term survival in medulloblastoma. *Journal of Clinical Oncology* : official journal of the American Society of Clinical Oncology, 28(35), 5188–5196. https://doi.org/10.1200/JCO.2010.31.1670

Pfister, S., Remke, M., Benner, A., Mendrzyk, F., Toedt, G., Felsberg, J., Wittmann, A., Devens, F., Gerber, N. U., Joos, S., Kulozik, A., Reifenberger, G., Rutkowski, S., Wiestler, O. D., Radlwimmer, B., Scheurlen, W., Lichter, P., & Korshunov, A. (2009). Outcome prediction in pediatric medulloblastoma based on DNA copy-number aberrations of chromosomes 6q and 17q and the MYC and MYCN loci. *Journal of Clinical Oncology* : official journal of the American Society of Clinical Oncology, 27(10), 1627–1636. https://doi.org/10.1200/JCO.2008.17.9432

Phi, L. T. H., Sari, I. N., Yang, Y. G., Lee, S. H., Jun, N., Kim, K. S., ... & Kwon, H. Y. (2018). Cancer stem cells (CSCs) in drug resistance and their therapeutic implications in cancer treatment. *Stem cells International*, 2018.

Pino, M. S., & Chung, D. C. (2010). The chromosomal instability pathway in colon cancer. *Gastroenterology*, 138(6), 2059–2072. https://doi.org/10.1053/j.gastro.2009.12.065

Pomeroy, S., Tamayo, P., Gaasenbeek, M., Sturla, L., Angelo, M., & McLaughlin, M. *et al*. (2002). Prediction of central nervous system embryonal tumour outcome based on gene expression. *Nature*, 415(6870), 436-442. doi: 10.1038/415436a

Pommier Y. (2013). Drugging topoisomerases: lessons and challenges. *ACS Chemical Biology*, 8(1), 82–95. https://doi.org/10.1021/cb300648v

Ponting, C. P., Oliver, P. L., & Reik, W. (2009). Evolution and functions of long non-coding RNAs. *Cell*, 136(4), 629–641. https://doi.org/10.1016/j.cell.2009.02.006

Portnoy, L. M. (2006). Radiologic diagnosis of gastric cancer. Springer Medizin Verlag Heidelberg.

Postow, L., & Funabiki, H. (2013). An SCF complex containing Fbxl12 mediates DNA damage-induced Ku80 ubiquitylation. *Cell Cycle*, 12(4), 587–595. https://doi.org/10.4161/cc.23408

Postow, L., Ghenoiu, C., Woo, E. M., Krutchinsky, A. N., Chait, B. T., & Funabiki, H. (2008). Ku80 removal from DNA through double strand break-induced ubiquitylation. The *Journal of Cell Biology*, 182(3), 467–479. https://doi.org/10.1083/jcb.200802146

Prakash A, Doublié S, Wallace SS. (2012). The Fpg/Nei family of DNA glycosylases: substrates, structures, and search for damage. *Prog Mol Biol Transl Sci*.110:71-91. doi: 10.1016/B978-0-12-387665-2.00004-3

Prasad, C. B., Prasad, S. B., Yadav, S. S., Pandey, L. K., Singh, S., Pradhan, S., & Narayan, G. (2017). Olaparib modulates DNA repair efficiency, sensitizes cervical cancer cells to cisplatin and exhibits anti-metastatic property. *Scientific Reports*, 7(1), 12876. https://doi.org/10.1038/s41598-017-13232-3

Price, B. D., & D'Andrea, A. D. (2013). Chromatin remodeling at DNA double-strand breaks. *Cell*, 152(6), 1344-1354.

Prieto-Vila, M., Takahashi, R. U., Usuba, W., Kohama, I., & Ochiya, T. (2017). Drug Resistance Driven by Cancer Stem Cells and Their Niche. *International Journal of Molecular Sciences,* 18(12), 2574. doi:10.3390/ijms18122574

Pryczynicz, A., Gryko, M., Niewiarowska, K., Cepowicz, D., Ustymowicz, M., Kemona, A., & Guzińska-Ustymowicz, K. (2014). Bax protein may influence the invasion of colorectal cancer. *World Journal of Gastroenterology*, 20(5), 1305–1310. https://doi.org/10.3748/wjg.v20.i5.1305

Puig, P. E., Guilly, M. N., Bouchot, A., Droin, N., Cathelin, D., Bouyer, F., Favier, L., Ghiringhelli, F., Kroemer, G., Solary, E., Martin, F., & Chauffert, B. (2008). Tumor cells can escape DNA-damaging cisplatin through DNA endoreduplication and reversible

polyploidy. *Cell Biology International*, 32(9), 1031–1043. https://doi.org/10.1016/j.cellbi.2008.04.021

Putnam, C. D. (2021). Strand discrimination in DNA mismatch repair. *DNA repair*, *105*, 10316

Putti, S., Giovinazzo, A., Merolle, M., Falchetti, M. L., & Pellegrini, M. (2021). ATM Kinase Dead: From Ataxia Telangiectasia Syndrome to Cancer. *Cancers*, 13(21), 5498.

Qin, C., Pan, Y., Li, Y., Li, Y., Long, W., & Liu, Q. (2021). Novel Molecular Hallmarks of Group 3 Medulloblastoma by Single-Cell Transcriptomics. *Frontiers in Oncology*, 11, 810.

Qin, S., Yang, L., Kong, S., Xu, Y., Liang, B., & Ju, S. (2021). LncRNA HCP5 : A Potential Biomarker for Diagnosing Gastric Cancer. *Frontiers in Oncology*, 11, 684531. https://doi.org/10.3389/fonc.2021.684531

Quagliata, L., Matter, M. S., Piscuoglio, S., Arabi, L., Ruiz, C., Procino, A., Kovac, M., Moretti, F., Makowska, Z., Boldanova, T., Andersen, J. B., Hämmerle, M., Tornillo, L., Heim, M. H., Diederichs, S., Cillo, C., & Terracciano, L. M. (2014). Long non-coding RNA HOTTIP/HOXA13 expression is associated with disease progression and predicts outcome in hepatocellular carcinoma patients. *Hepatology* (Baltimore, Md.), 59(3), 911–923. https://doi.org/10.1002/hep.26740

Radulescu, S., Ridgway, R. A., Cordero, J., Athineos, D., Salgueiro, P., Poulsom, R., Neumann, J., Jung, A., Patel, S., Woodgett, J., Barker, N., Pritchard, D. M., Oien, K., & Sansom, O. J. (2013). Acute WNT signalling activation perturbs differentiation within the adult stomach and rapidly leads to tumour formation. *Oncogene*, 32(16), 2048–2057. https://doi.org/10.1038/onc.2012.224

Ragu, S., Matos-Rodrigues, G., Thomas, M., & Lopez, B. S. (2021). Homologous recombination in mammalian cells: From molecular mechanisms to pathology. In Genome Stability (pp. 367-392). Academic Press.

Ramaswamy, V., Nör, C., & Taylor, M. D. (2015). p53 and Meduloblastoma. Cold Spring Harbor perspectives in medicine, 6(2), a026278. https://doi.org/10.1101/cshperspect.a026278

Ramaswamy, V., Remke, M., Bouffet, E., Faria, C., Perreault, S., & Cho, Y. *et al*. (2013). Recurrence patterns across medulloblastoma subgroups: an integrated clinical and molecular analysis. *The Lancet Oncology*, *14*(12), 1200-1207. doi: 10.1016/s1470-2045(13)70449-2

Ramilo C, Gu L, Guo S. (2002). Partial reconstitution of human DNA mismatch repair *in vitro*: characterization of the role of human replication protein A. *Mol Cell Biol* 2002; **22**:2037–2046.

Rao, C. V., Yang, Y. M., Swamy, M. V., Liu, T., Fang, Y., Mahmood, R., Jhanwar-Uniyal, M., & Dai, W. (2005). Colonic tumorigenesis in BubR1+/-ApcMin/+ compound mutant mice is linked to premature separation of sister chromatids and enhanced genomic instability. *Proceedings of the National Academy of Sciences of the United States of America*, 102(12), 4365–4370. https://doi.org/10.1073/pnas.0407822102

Rass, E., Grabarz, A., Plo, I., Gautier, J., Bertrand, P., & Lopez, B. S. (2009). Role of Mre11 in chromosomal nonhomologous end joining in mammalian cells. *Nature Structural & Molecular Biology*, 16(8), 819-824.

Rathore, S., Datta, G., Kaur, I., Malhotra, P., & Mohmmed, A. (2015). Disruption of cellular homeostasis induces organelle stress and triggers apoptosis like cell-death pathways in malaria parasite. *Cell Death & Disease*, 6(7), e1803-e1803. doi: 10.1038/cddis.2015.142

Raymond, E., Faivre, S., Chaney, S., Woynarowski, J., and Cvitkovic, E. (2002) Cellular and molecular pharmacology of oxaliplatin. *Molecular Cancer Therapeutics*. 1, 227–235.

Rebersek M. (2020). Consensus molecular subtypes (CMS) in metastatic colorectal cancer - personalized medicine decision. *Radiology and Oncology*, 54(3), 272–277. https://doi.org/10.2478/raon-2020-0031

Rebuzzi, S. E., Pesola, G., Martelli, V., & Sobrero, A. F. (2020). Adjuvant Chemotherapy for Stage II Colon Cancer. *Cancers*, 12(9), 2584. https://doi.org/10.3390/cancers12092584

Reinhardt, H. C., & Yaffe, M. B. (2013). Phospho-Ser/Thr-binding domains: navigating the cell cycle and DNA damage response. *Nature Reviews*. Molecular cell biology, 14(9), 563–580. https://doi.org/10.1038/nrm3640

Remke, M., Hielscher, T., Korshunov, A., Northcott, P. A., Bender, S., Kool, M., Westermann, F., Benner, A., Cin, H., Ryzhova, M., Sturm, D., Witt, H., Haag, D., Toedt, G., Wittmann, A., Schöttler, A., von Bueren, A. O., von Deimling, A., Rutkowski, S., Scheurlen, W., … Pfister, S. M. (2011). FSTL5 is a marker of poor prognosis in non-WNT/non-SHH medulloblastoma. *Journal of Clinical Oncology* : official journal of the American Society of Clinical Oncology, 29(29), 3852–3861. https://doi.org/10.1200/JCO.2011.36.2798

Requena, D. O., & Garcia-Buitrago, M. (2020). Molecular insights into colorectal carcinoma. *Archives of Medical Research*, 51(8), 839-844.

Riccardi, C., & Nicoletti, I. (2006). Analysis of apoptosis by propidium iodide staining and flow cytometry. *Nature Protocols*, 1(3), 1458-1461.

Richard, J. L. C., & Eichhorn, P. J. A. (2018). Platforms for investigating LncRNA functions. *SLAS Technology*, 23(6), 493-506.

Rinn JL, Chang HY. (2012). Genome regulation by long non-coding RNAs. *Annu Rev Biochem.* 81:145–166. doi: 10.1146/annurev-biochem-051410-092902

Rivard, M. J., Venselaar, J. L., & Beaulieu, L. (2009). The evolution of brachytherapy treatment planning. *Medical Physics*, 36(6Part1), 2136-2153.

Rodgers, K., & McVey, M. (2016). Error-prone repair of DNA double-strand breaks. *Journal of Cellular Physiology*, 231(1), 15-24.

Rodriguez, A. A., Wojtaszek, J. L., Greer, B. H., Haldar, T., Gates, K. S., Williams, R. S., & Eichman, B. F. (2020). An autoinhibitory role for the GRF zinc finger domain of DNA glycosylase NEIL3. *The Journal of Biological Chemistry*, 295(46), 15566–15575. https://doi.org/10.1074/jbc.RA120.015541

Rodríguez-Nóvoa, S., Cuenca, L., Morello, J., Córdoba, M., Blanco, F., Jiménez-Nácher, I., & Soriano, V. (2010). Use of the HCP5 single nucleotide polymorphism to predict hypersensitivity reactions to abacavir: correlation with HLA-B* 5701. *Journal of Antimicrobial Chemotherapy*, 65(8), 1567-1569.

Roepman, P., Schlicker, A., Tabernero, J., Majewski, I., Tian, S., Moreno, V., Snel, M. H., Chresta, C. M., Rosenberg, R., Nitsche, U., Macarulla, T., Capella, G., Salazar, R., Orphanides, G., Wessels, L. F., Bernards, R., & Simon, I. M. (2014). Colorectal cancer intrinsic subtypes predict chemotherapy benefit, deficient mismatch repair and epithelial-to-mesenchymal transition. *International Journal of Cancer*, 134(3), 552–562. https://doi.org/10.1002/ijc.28387

Rohdenburg, M., Martinović, P., Ahlenhoff, K., Koch, S., Emmrich, D., Gölzhäuser, A., & Swiderek, P. (2019). Cisplatin as a potential platinum focused electron beam induced deposition precursor: NH3 ligands enhance the electron-induced removal of chlorine. *The Journal of Physical Chemistry* , 123(35), 21774-21787.

Roma, C., Rachiglio, A. M., Pasquale, R., Fenizia, F., Iannaccone, A., Tatangelo, F., Antinolfi, G., Parrella, P., Graziano, P., Sabatino, L., Colantuoni, V., Botti, G., Maiello, E., & Normanno, N. (2016). BRAF V600E mutation in metastatic colorectal cancer: Methods of detection and correlation with clinical and pathologic features. *Cancer biology & Therapy*, 17(8), 840–848. https://doi.org/10.1080/15384047.2016.1195048

Rood, B. R., MacDonald, T. J., & Packer, R. J. (2004, October). Current treatment of medulloblastoma: recent advances and future challenges. *Seminars in Oncology* (Vol. 31, No. 5, pp. 666-675). WB Saunders.

Rosenberg, B., Van Camp, L., & Krigas, T. (1965). Inhibition of cell division in Escherichia coli by electrolysis products from a platinum electrode. *Nature*, 205(4972), 698-699.

Rossi, A., Caracciolo, V., Russo, G., Reiss, K., & Giordano, A. (2008). Medulloblastoma: from molecular pathology to therapy. *Clinical Cancer Research* : an official journal of the American Association for Cancer Research, 14(4), 971–976. https://doi.org/10.1158/1078-0432.CCR-07-2072

Roth D. B. (2014). V(D)J Recombination: Mechanism, Errors, and Fidelity. *Microbiology Spectrum*, 2(6), 10.1128/microbiolspec.MDNA3-0041-2014. https://doi.org/10.1128/microbiolspec.MDNA3-0041-2014

Roth, D. B. (2015). V (D) J recombination: mechanism, errors, and fidelity. *Mobile DNA III*, 311-324.

Rottenberg, S., Disler, C., & Perego, P. (2021). The rediscovery of platinum-based cancer therapy. *Nature Reviews Cancer*, 21(1), 37-50.

Roussel, M. F., & Robinson, G. W. (2013). Role of MYC in Medulloblastoma. Cold Spring Harbor perspectives in medicine, 3(11), a014308. https://doi.org/10.1101/cshperspect.a014308

Roussel, M. F., & Stripay, J. L. (2018). Epigenetic Drivers in Pediatric Medulloblastoma. *Cerebellum* (London, England), 17(1), 28–36. https://doi.org/10.1007/s12311-017-0899-9

Ruan, X., Li, P., Chen, Y., Shi, Y., Pirooznia, M., Seifuddin, F., ... & Cao, H. (2020). In vivo functional analysis of non-conserved human lncRNAs associated with cardiometabolic traits. *Nature Communications*, 11(1), 1-13.

Rubin, J. B., & Rowitch, D. H. (2002). Medulloblastoma: a problem of developmental biology. *Cancer Cell*, 2(1), 7–8. https://doi.org/10.1016/s1535-6108(02)00090-9

Rulten, S. L., & Caldecott, K. W. (2013). DNA strand break repair and neurodegeneration. *DNA Repair*, 12(8), 558-567.

Rupnik, A., Lowndes, N. F., & Grenon, M. (2010). MRN and the race to the break. *Chromosoma*, 119(2), 115–135. https://doi.org/10.1007/s00412-009-0242-4

Ryan, D. P., Hong, T. S., & Bardeesy, N. (2014). Pancreatic adenocarcinoma. *New England Journal of Medicine*, 371(11), 1039-1049.

Rycenga, H. B., & Long, D. T. (2018). The evolving role of DNA inter-strand crosslinks in chemotherapy. *Current Opinion in Pharmacology*, 41, 20-26.

Saintigny, Y., Delacote, F., Vares, G., Petitot, F., Lambert, S., Averbeck, D., *et al*. (2001). Characterization of homologous recombination induced by replication inhibition in mammalian cells. *EMBO Journals*. 20, 3861–3870. doi: 10.1093/emboj/20.14.3861

Sakurikar, N., Eichhorn, J., & Chambers, T. (2012). Cyclin-dependent Kinase-1 (Cdk1)/Cyclin B1 Dictates Cell Fate after Mitotic Arrest via Phosphoregulation of Antiapoptotic Bcl-2 Proteins. *Journal Of Biological Chemistry*, 287(46), 39193-39204. doi: 10.1074/jbc.m112.391854.

Salguero, I., Belotserkovskaya, R., Coates, J., Sczaniecka-Clift, M., Demir, M., Jhujh, S., ... & Jackson, S. P. (2019). MDC1 PST-repeat region promotes histone H2AX-independent chromatin association and DNA damage tolerance. *Nature Communications*, 10(1), 5191.

Salmena, L., Poliseno, L., Tay, Y., Kats, L., & Pandolfi, P. P. (2011). A ceRNA hypothesis: the Rosetta Stone of a hidden RNA language?. *Cell*, 146(3), 353–358. https://doi.org/10.1016/j.cell.2011.07.014

Saltz, L. B., Cox, J. V., Blanke, C., Rosen, L. S., Fehrenbacher, L., Moore, M. J., Maroun, J. A., Ackland, S. P., Locker, P. K., Pirotta, N., Elfring, G. L., & Miller, L. L. (2000). Irinotecan plus fluorouracil and leucovorin for metastatic colorectal cancer. Irinotecan Study Group. *The New England Journal of Medicine*, 343(13), 905–914. https://doi.org/10.1056/NEJM200009283431302

Sameer, A. S., Nissar, S., and Fatima, K. (2014). Mismatch repair pathway: molecules, functions, and role in colorectal carcinogenesis. *Eur. J. Cancer Prev*. 23, 246–257. doi: 10.1097/CEJ.0000000000000019

Sammons, M. A., Nguyen, T. A. T., McDade, S. S., & Fischer, M. (2020). Tumor suppressor p53: from engaging DNA to target gene regulation. *Nucleic Acids Research*, *48*(16), 8848-8869.

Sangermano, F., Delicato, A., & Calabrò, V. (2020). Y box binding protein 1 (YB-1) oncoprotein at the hub of DNA proliferation, damage and cancer progression. *Biochimie*, 179, 205-216.

Santagostino, S. F., Assenmacher, C. A., Tarrant, J. C., Adedeji, A. O., & Radaelli, E. (2021). Mechanisms of regulated cell death: Current perspectives. *Veterinary Pathology*, 58(4), 596-623.

Satake, Y., Kuwano, Y., Nishikawa, T., Fujita, K., Saijo, S., Itai, M., ... & Rokutan, K. (2018). Nucleolin facilitates nuclear retention of an ultraconserved region containing TRA2β4 and accelerates colon cancer cell growth. *Oncotarget*, 9(42), 26817.

Sayers, T. J. (2011). Targeting the extrinsic apoptosis signaling pathway for cancer therapy. *Cancer Immunology, Immunotherapy*, 60(8), 1173-1180.

Schärer O. D. (2013). Nucleotide excision repair in eukaryotes. Cold Spring Harbor Perspectives in Biology, 5(10), a012609. https://doi.org/10.1101/cshperspect.a012609

Scheel, C., Eaton, E. N., Li, S. H., Chaffer, C. L., Reinhardt, F., Kah, K. J., Bell, G., Guo, W., Rubin, J., Richardson, A. L., & Weinberg, R. A. (2011). Paracrine and autocrine signals induce and maintain mesenchymal and stem cell states in the breast. *Cell*, 145(6), 926–940. https://doi.org/10.1016/j.cell.2011.04.029

Schittek, B., Psenner, K., Sauer, B., Meier, F., Iftner, T., & Garbe, C. (2007). The increased expression of Y box-binding protein 1 in melanoma stimulates proliferation and tumor invasion, antagonizes apoptosis and enhances chemoresistance. *International Journal of Cancer*, 120(10), 2110–2118. https://doi.org/10.1002/ijc.22512

Schuch, A. P., Garcia, C. C., Makita, K., & Menck, C. F. (2013). DNA damage as a biological sensor for environmental sunlight. *Photochemical & Photobiological Sciences* : Official journal of the European Photochemistry Association and the European Society for Photobiology, 12(8), 1259–1272. https://doi.org/10.1039/c3pp00004d

Seetharam, R. N., Sood, A., Basu-Mallick, A., Augenlicht, L. H., Mariadason, J. M., & Goel, S. (2010). Oxaliplatin resistance induced by ERCC1 up-regulation is abrogated by siRNA-mediated gene silencing in human colorectal cancer cells. *Anticancer Research*, 30(7), 2531-2538.

Sengupta, S., Pomeranz Krummel, D., & Pomeroy, S. (2017). The evolution of medulloblastoma therapy to personalized medicine. F1000Research, 6, 490. https://doi.org/10.12688/f1000research.10859.1

Shakeri, R., Kheirollahi, A., & Davoodi, J. (2017). Apaf-1: Regulation and function in cell death. *Biochimie*, 135, 111-125.

Shao, C. J., Fu, J., Shi, H. L., Mu, Y. G., & Chen, Z. P. (2008). Activities of DNA-PK and Ku86, but not Ku70, may predict sensitivity to cisplatin in human gliomas. *Journal of Neuro-oncology*, 89(1), 27-35.

Sharma, M. G. (2022). RNA Transcription. In Genetics Fundamentals Notes (pp. 491-535). Singapore: Springer Nature Singapore.

Sherrill, K., Byrd, M., Van Eden, M., & Lloyd, R. (2004). BCL-2 Translation Is Mediated via Internal Ribosome Entry during Cell Stress. *Journal Of Biological Chemistry*, 279(28), 2906629074. doi: 10.1074/jbc.m402727200

Shi, J., & Mitchison, T. J. (2017). Cell death response to anti-mitotic drug treatment in cell culture, mouse tumor model and the clinic. *Endocrine-related Cancer*, 24(9), T83–T96. https://doi.org/10.1530/ERC-17-0003

Shi, S. B., Cheng, Q. H., Gong, S. Y., Lu, T. T., Guo, S. F., Song, S. M., Yang, Y. P., Cui, Q., Yang, K. H., & Qian, Y. W. (2021). PCAT6 may be a new prognostic biomarker in various cancers: a meta-analysis and bioinformatics analysis. *Cancer Cell International*, 21(1), 370. https://doi.org/10.1186/s12935-021-02079-4

Shiina, T., Tamiya, G., Oka, A., Yamagata, T., Yamagata, N., Kikkawa, E., Goto, K., Mizuki, N., Watanabe, K., Fukuzumi, Y., Taguchi, S., Sugawara, C., Ono, A., Chen, L., Yamazaki, M., Tashiro, H., Ando, A., Ikemura, T., Kimura, M., & Inoko, H. (1998). Nucleotide sequencing analysis of the 146-kilobase segment around the IkBL and MICA genes at the centromeric end of the HLA class I region. *Genomics*, 47(3), 372–382. https://doi.org/10.1006/geno.1997.5114

Shiloh, Y., & Ziv, Y. (2013). The ATM protein kinase: regulating the cellular response to genotoxic stress, and more. Nature reviews. *Molecular Cell Biology*, 14(4), 197–210. https://doi.org/10.1038/nrm3546

Siddik, Z. H. (2003). Cisplatin: mode of cytotoxic action and molecular basis of resistance. *Oncogene*, 22(47), 7265-7279.

Siddiqui, M. S., François, M., Fenech, M. F., & Leifert, W. R. (2015). Persistent γH2AX: A promising molecular marker of DNA damage and aging. *Mutation Research*. Reviews in mutation research, 766, 1–19. https://doi.org/10.1016/j.mrrev.2015.07.001

Silva, R. d., Marie, S. K., Uno, M., Matushita, H., Wakamatsu, A., Rosemberg, S., & Oba-Shinjo, S. M. (2013). CTNNB1, AXIN1 and APC expression analysis of different medulloblastoma variants. *Clinics,* 68(2), 167–172. https://doi.org/10.6061/clinics/2013(02)oa08

Silvestri R. (2013). New prospects for vinblastine analogues as anticancer agents. *Journal of Medicinal Chemistry*, 56(3), 625–627. https://doi.org/10.1021/jm400002j

Simpson, J., & Scholefield, J. H. (2008). Treatment of colorectal cancer: surgery, chemotherapy and radiotherapy. *Surgery*, 26(8), 329-333.

Sinha, D., Duijf, P. H., & Khanna, K. K. (2019). Mitotic slippage: an old tale with a new twist. *Cell Cycle*, 18(1), 7-15.

Sinicrope, F. A., Foster, N. R., Thibodeau, S. N., Marsoni, S., Monges, G., Labianca, R., Kim, G. P., Yothers, G., Allegra, C., Moore, M. J., Gallinger, S., & Sargent, D. J. (2011). DNA mismatch repair status and colon cancer recurrence and survival in clinical trials of 5-fluorouracil-based adjuvant therapy. *Journal of the National Cancer Institute*, 103(11), 863–875. https://doi.org/10.1093/jnci/djr153

Sitas, F., Parkin, M., Chirenje, Z., Stein, L., Mqoqi, N., & Wabinga, H. (2006). Cancers. Disease and Mortality in Sub-Saharan Africa. 2nd edition.

Skabkin, M. A., Kiselyova, O. I., Chernov, K. G., Sorokin, A. V., Dubrovin, E. V., Yaminsky, I. V., ... & Ovchinnikov, L. P. (2004). Structural organization of mRNA

complexes with major core mRNP protein YB-1. *Nucleic acids Research*, 32(18), 5621-5635.

Skowron, P., Farooq, H., Cavalli, F. M., Morrissy, A. S., Ly, M., Hendrikse, L. D., ... & Taylor, M. D. (2021). The transcriptional landscape of Shh medulloblastoma. *Nature Communications*, 12(1), 1-17.

Skowronek, J. (2017). Current status of brachytherapy in cancer treatment–short overview. *Journal of Contemporary Brachytherapy*, 9(6), 581-589.

Škubník, J., Pavlíčková, V. S., Ruml, T., & Rimpelová, S. (2021). Vincristine in Combination Therapy of Cancer: Emerging Trends in Clinics. *Biology*, 10(9), 849. https://doi.org/10.3390/biology10090849

Skvortsova, K., Stirzaker, C., & Taberlay, P. (2019). The DNA methylation landscape in cancer. *Essays in Biochemistry*, 63(6), 797-811.

Slade, I., Murray, A., Hanks, S., Kumar, A., Walker, L., Hargrave, D., Douglas, J., Stiller, C., Izatt, L., & Rahman, N. (2011). Heterogeneity of familial medulloblastoma and contribution of germline PTCH1 and SUFU mutations to sporadic medulloblastoma. *Familial Cancer*, 10(2), 337–342. https://doi.org/10.1007/s10689-010-9411-0

Sloss, O., Topham, C., Diez, M., & Taylor, S. (2016). Mcl-1 dynamics influence mitotic slippage and death in mitosis. *Oncotarget*, *7*(5). doi: 10.18632/oncotarget.6894

Smoll, N. (2011). Relative survival of childhood and adult medulloblastomas and primitive neuroectodermal tumours (PNETs). *Cancer*, 118(5), 1313-1322. doi: 10.1002/cncr.26387

Snyder, M., Iraola-Guzmán, S., Saus, E., & Gabaldón, T. (2022). Discovery and Validation of Clinically Relevant Long Non-Coding RNAs in Colorectal Cancer. *Cancers*, 14(16), 3866. https://doi.org/10.3390/cancers14163866

Sobhy, M. A., Bralić, A., Raducanu, V. S., Takahashi, M., Tehseen, M., Rashid, F., ... & Hamdan, S. M. (2019). Resolution of the Holliday junction recombination intermediate by human GEN1 at the single-molecule level. *Nucleic acids Research*, 47(4), 1935-1949.

Soderquist, R., & Eastman, A. (2016). BCL-2 Inhibitors as Anticancer Drugs: A Plethora of Misleading BH3 Mimetics. *Molecular Cancer Therapeutics*, *15*(9), 2011-2017. doi: 10.1158/1535-7163.mct-16-0031

Soniat, M., & Chook, Y. M. (2015). Nuclear localization signals for four distinct karyopherin-β nuclear import systems. *Biochemical Journal*, 468(3), 353-362.

Sorokin, A. V., Selyutina, A. A., Skabkin, M. A., Guryanov, S. G., Nazimov, I. V., Richard, C., Th'ng, J., Yau, J., Sorensen, P. H., Ovchinnikov, L. P., & Evdokimova, V. (2005). Proteasome-mediated cleavage of the Y-box-binding protein 1 is linked to DNA-damage stress response. *The EMBO Journal*, 24(20), 3602–3612. https://doi.org/10.1038/sj.emboj.7600830

Souers, A. J., Leverson, J. D., Boghaert, E. R., Ackler, S. L., Catron, N. D., Chen, J., Dayton, B. D., Ding, H., Enschede, S. H., Fairbrother, W. J., Huang, D. C., Hymowitz, S. G., Jin, S., Khaw, S. L., Kovar, P. J., Lam, L. T., Lee, J., Maecker, H. L., Marsh, K. C., Mason, K. D., … Elmore, S. W. (2013). ABT-199, a potent and selective BCL-2 inhibitor,

achieves antitumor activity while sparing platelets. *Nature Medicine*, 19(2), 202–208. https://doi.org/10.1038/nm.3048

Spingler, B., Whittington, D. A., & Lippard, S. J. (2001). 2.4 A crystal structure of an oxaliplatin 1,2-d(GpG) intrastrand cross-link in a DNA dodecamer duplex. *Inorganic Chemistry*, 40(22), 5596–5602. https://doi.org/10.1021/ic010790t

Spivak G. (2016). Transcription-coupled repair: an update. *Archives of Toxicology*, 90(11), 2583–2594. https://doi.org/10.1007/s00204-016-1820-x

Squillaro, T., Finicelli, M., Alessio, N., Del Gaudio, S., Di Bernardo, G., Melone, M. A. B., ... & Galderisi, U. (2019). A rapid, safe, and quantitative in vitro assay for measurement of uracil-DNA glycosylase activity. *Journal of Molecular Medicine*, 97, 991-1001.

Statello, L., Guo, C. J., Chen, L. L., & Huarte, M. (2021). Gene regulation by long non-coding RNAs and its biological functions. *Nature reviews*. *Molecular Cell Biology*, 22(2), 96–118. https://doi.org/10.1038/s41580-020-00315-9

Stewart, M. (2007). Molecular mechanism of the nuclear protein import cycle. *Nature reviews Molecular Cell Biology*, 8(3), 195-208.

Stingele, J., Bellelli, R., & Boulton, S. J. (2017). Mechanisms of DNA–protein crosslink repair. *Nature Reviews Molecular Cell Biology*, 18(9), 563-573.

Stinson, B. M., Moreno, A. T., Walter, J. C., & Loparo, J. J. (2020). A mechanism to minimize errors during non-homologous end joining. *Molecular cell*, 77(5), 1080-1091.

Stintzing, S., Wirapati, P., Lenz, H. J., Neureiter, D., Fischer von Weikersthal, L., Decker, T., Kiani, A., Kaiser, F., Al-Batran, S., Heintges, T., Lerchenmüller, C., Kahl, C., Seipelt, G., Kullmann, F., Moehler, M., Scheithauer, W., Held, S., Modest, D. P., Jung, A., Kirchner, T., … Heinemann, V. (2019). Consensus molecular subgroups (CMS) of colorectal cancer (CRC) and first-line efficacy of FOLFIRI plus cetuximab or bevacizumab in the FIRE3 (AIO KRK-0306) trial. *Annals of Oncology* : official journal of the European Society for Medical Oncology, 30(11), 1796–1803. https://doi.org/10.1093/annonc/mdz387

Stojic L, Brun R, Jiricny J. (2004). Mismatch repair and DNA damage signalling. *DNA Repair (Amst)* **3**:1091–1101.

Stracker, T. H., & Petrini, J. H. (2011). The MRE11 complex: starting from the ends. *Nature reviews. Molecular cell biology*, 12(2), 90–103. https://doi.org/10.1038/nrm3047

Stromecki, M., Tatari, N., Morrison, L. C., Kaur, R., Zagozewski, J., Palidwor, G., ... & Werbowetski-Ogilvie, T. E. (2018). Characterization of a novel OTX 2-driven stem cell program in Group 3 and Group 4 medulloblastoma. *Molecular Oncology*, 12(4), 495-513.

Stucki, M., Clapperton, J. A., Mohammad, D., Yaffe, M. B., Smerdon, S. J., & Jackson, S. P. (2005). MDC1 directly binds phosphorylated histone H2AX to regulate cellular responses to DNA double-strand breaks. *Cell*, 123(7), 1213-1226.

Sullivan, K., Galbraith, M., Andrysik, Z. (2018). Mechanisms of transcriptional regulation by p53. *Cell Death Differ* **25**, 133–143. https://doi.org/10.1038/cdd.2017.174

Sun, J., Wang, X., Gao, P., Song, Y., Chen, X., Sun, Y., ... & Wang, Z. (2018). Prognosis and efficiency of adjuvant therapy in resected colon signet-ring cell carcinoma. *Translational Cancer Research*, 7(4), 1006-1025.

Sundaram M, Guernsey DL, Rajaraman MM, Rajaraman R. (2004). Neosis: a novel type of cell division in cancer. *Cancer Biol Ther* 2004; **3**: 207–218

Sung, P., & Klein, H. (2006). Mechanism of homologous recombination: mediators and helicases take on regulatory functions. *Nature reviews Molecular Cell Biology*, 7(10), 739-750.

Svoboda M, Slyskova J, Schneiderova M, Makovicky P, Bielik L, Levy M, Lipska L, Hemmelova B, Kala Z, Protivankova M. (2014). HOTAIR long non-coding RNA is a negative prognostic factor not only in primary tumors, but also in the blood of colorectal cancer patients. *Carcinogenesis*. 2014;35:1510–1515. doi: 10.1093/carcin/bgu055

Sznarkowska, A., Mikac, S., & Pilch, M. (2020). MHC class I regulation: the origin perspective. *Cancers*, 12(5), 1155.

Tait, S. W., & Green, D. R. (2010). Mitochondria and cell death: outer membrane permeabilization and beyond. *Nature reviews Molecular Cell Biology*, 11(9), 621-632.

Tam, S. Y., & Wu, V. (2019). A Review on the Special Radiotherapy Techniques of Colorectal Cancer. *Frontiers in Oncology*, 9, 208. https://doi.org/10.3389/fonc.2019.00208

Tam, S. Y., & Wu, V. W. (2019). A review on the special radiotherapy techniques of colorectal cancer. *Frontiers in Oncology*, 9, 208.

Tamura, Y., Simizu, S., Muroi, M., Takagi, S., Kawatani, M., Watanabe, N., & Osada, H. (2008). Polo-like kinase 1 phosphorylates and regulates Bcl-xL during pironetin-induced apoptosis. *Oncogene*, 28(1), 107-116. doi: 10.1038/onc.2008.368

Tan, B. S., Tiong, K. H., Choo, H. L., Fei-Lei Chung, F., Hii, L. W., Tan, S. H., ... & Leong, C. O. (2015). Mutant p53-R273H mediates cancer cell survival and anoikis resistance through AKT-dependent suppression of BCL-2-modifying factor (BMF). *Cell death & Disease*, 6(7), e1826-e1826.

Tao, Z., Hasvold, L., Wang, L., Wang, X., Petros, A., & Park, C. *et al*. (2014). Discovery of a Potent and Selective BCL-XL Inhibitor with in Vivo Activity. *ACS Medicinal Chemistry Letters*, 5(10), 1088-1093. doi: 10.1021/ml5001867

Taylor, M. D., Liu, L., Raffel, C., Hui, C. C., Mainprize, T. G., Zhang, X., Agatep, R., Chiappa, S., Gao, L., Lowrance, A., Hao, A., Goldstein, A. M., Stavrou, T., Scherer, S. W., Dura, W. T., Wainwright, B., Squire, J. A., Rutka, J. T., & Hogg, D. (2002). Mutations in SUFU predispose to medulloblastoma. *Nature Genetics*, 31(3), 306–310. https://doi.org/10.1038/ng916

Taylor, M. D., Mainprize, T. G., & Rutka, J. T. (2000). Molecular insight into medulloblastoma and central nervous system primitive neuroectodermal tumor biology from hereditary syndromes: a review. *Neurosurgery*, 47(4), 888–901. https://doi.org/10.1097/00006123-200010000-00020

Taylor, R., Bailey, C., Robinson, K., Weston, C., Walker, D., & Ellison, D. *et al*. (2005). Outcome for patients with metastatic (M2–3) medulloblastoma treated with SIOP/UKCCSG PNET-3 chemotherapy. *European Journal Of Cancer*, *41*(5), 727-734. doi: 10.1016/j.ejca.2004.12.017

Temmink, O. H., Emura, T., de Bruin, M., Fukushima, M., & Peters, G. J. (2007). Therapeutic potential of the dual-targeted TAS-102 formulation in the treatment of gastrointestinal malignancies. *Cancer Science*, 98(6), 779–789. https://doi.org/10.1111/j.1349-7006.2007.00477.x

Teng, H., Wang, P., Xue, Y., Liu, X., Ma, J., Cai, H., ... & Liu, Y. (2016). Role of HCP5-miR-139-RUNX1 feedback loop in regulating malignant behavior of glioma cells. *Molecular Therapy*, 24(10), 1806-1822.

Tesniere, A., Schlemmer, F., Boige, V., Kepp, O., Martins, I., Ghiringhelli, F., Aymeric, L., Michaud, M., Apetoh, L., Barault, L., Mendiboure, J., Pignon, J. P., Jooste, V., van Endert, P., Ducreux, M., Zitvogel, L., Piard, F., & Kroemer, G. (2010). Immunogenic death of colon cancer cells treated with oxaliplatin. *Oncogene*, 29(4), 482–491. https://doi.org/10.1038/onc.2009.356

Testa, U., Pelosi, E., & Castelli, G. (2018). Colorectal cancer: genetic abnormalities, tumor progression, tumor heterogeneity, clonal evolution and tumor-initiating cells. *Medical Sciences*, 6(2), 31.

Thanki, K., Nicholls, M. E., Gajjar, A., Senagore, A. J., Qiu, S., Szabo, C., Hellmich, M. R., & Chao, C. (2017). Consensus Molecular Subtypes of Colorectal Cancer and their Clinical Implications. *International Biological and Biomedical Journal*, 3(3), 105–111.

Theriot CA, Hegde ML, Hazra TK, Mitra S. (2010). RPA physically interacts with the human DNA glycosylase NEIL1 to regulate excision of oxidative DNA base damage in primer-template structures. *DNA Repair (Amst)* 9:643–652.

Thirion, P., Michiels, S., Pignon, J. P., Buyse, M., Braud, A. C., Carlson, R. W., ... & Piedbois, P. (2004). Modulation of fluorouracil by leucovorin in patients with advanced colorectal cancer: an updated meta-analysis. *Journal of Clinical Oncology*: official journal of the American Society of Clinical Oncology, 22(18), 3766-3775.

Thirunavukarusu P, Sathaiah M, Singla S. (2010). Medullary carcinoma of the large intestine: a population based analysis. *Int J Oncol*. 37(4):901–907.

Thompson, M. C., Fuller, C., Hogg, T. L., Dalton, J., Finkelstein, D., Lau, C. C., Chintagumpala, M., Adesina, A., Ashley, D. M., Kellie, S. J., Taylor, M. D., Curran, T., Gajjar, A., & Gilbertson, R. J. (2006). Genomics identifies medulloblastoma subgroups that are enriched for specific genetic alterations. Journal of clinical oncology : official journal of the American Society of Clinical Oncology, 24(12), 1924–1931. https://doi.org/10.1200/JCO.2005.04.4974

Thompson, P. S., & Cortez, D. (2020). New insights into abasic site repair and tolerance. *DNA Repair*, 90, 102866.

Timerbaev, A. R., Hartinger, C. G., Aleksenko, S. S., & Keppler, B. K. (2006). Interactions of antitumor metallodrugs with serum proteins: advances in characterization using modern

analytical methodology. *Chemical Reviews*, 106(6), 2224–2248. https://doi.org/10.1021/cr040704h

Todd, R. C., & Lippard, S. J. (2009). Inhibition of transcription by platinum antitumor compounds. *Metallomics* : integrated biometal science, 1(4), 280–291. https://doi.org/10.1039/b907567d

Topham, C., & Taylor, S. (2013). Mitosis and apoptosis: how is the balance set?. *Current Opinion In Cell Biology*, *25*(6), 780-785. doi: 10.1016/j.ceb.2013.07.003.

Tran, O. T., Tadesse, S., Chu, C., & Kidane, D. (2020). Overexpression of NEIL3 associated with altered genome and poor survival in selected types of human cancer. *Tumour Biology* : the journal of the International Society for Oncodevelopmental Biology and Medicine, 42(5), 1010428320918404. https://doi.org/10.1177/1010428320918404

Trasvina-Arenas, C. H., Demir, M., Lin, W. J., & David, S. S. (2021). Structure, function and evolution of the Helix-hairpin-Helix DNA glycosylase superfamily: Piecing together the evolutionary puzzle of DNA base damage repair mechanisms. *DNA Repair*, 108, 103231.

Trédan, O., Galmarini, C. M., Patel, K., & Tannock, I. F. (2007). Drug resistance and the solid tumor microenvironment. *Journal of the National Cancer Institute*, 99(19), 1441–1454. https://doi.org/10.1093/jnci/djm135

Trisciuoglio, D., Tupone, M. G., Desideri, M., Di Martile, M., Gabellini, C., Buglioni, S., ... & Del Bufalo, D. (2017). BCL-XL overexpression promotes tumor progression-associated properties. *Cell Death & Disease*, 8(12), 1-15.

Um H. D. (2016). Bcl-2 family proteins as regulators of cancer cell invasion and metastasis: a review focusing on mitochondrial respiration and reactive oxygen species. *Oncotarget*, 7(5), 5193–5203. https://doi.org/10.18632/oncotarget.640

Uren, R. T., Iyer, S., & Kluck, R. M. (2017). Pore formation by dimeric Bak and Bax: an unusual pore?. *Philosophical transactions of the Royal Society of London*. Series B, Biological sciences, 372(1726), 20160218. https://doi.org/10.1098/rstb.2016.0218

Uszczynska-Ratajczak, B., Lagarde, J., Frankish, A., Guigó, R., & Johnson, R. (2018). Towards a complete map of the human long non-coding RNA transcriptome. *Nature reviews. Genetics*, 19(9), 535–548. https://doi.org/10.1038/s41576-018-0017-y

Uzunova, K., Dye, B. T., Schutz, H., Ladurner, R., Petzold, G., Toyoda, Y., Jarvis, M. A., Brown, N. G., Poser, I., Novatchkova, M., Mechtler, K., Hyman, A. A., Stark, H., Schulman, B. A., & Peters, J. M. (2012). APC15 mediates CDC20 autoubiquitylation by APC/C(MCC) and disassembly of the mitotic checkpoint complex. *Nature Structural & Molecular Biology*, 19(11), 1116–1123. https://doi.org/10.1038/nsmb.2412

Vakifahmetoglu H, Olsson M, Zhivotovsky B. (2008). Death through a tragedy: mitotic catastrophe. *Cell Death Differ*. **15**: 1153–1162.

van Heemst D, den Reijer PM, Westendorp RG. Ageing or cancer: a review on the role of caretakers and gatekeepers. *European Journal of Cancer*. 2007 Oct;43(15):2144-52. doi: 10.1016/j.ejca.2007.07.011

Van Meerloo, J., Kaspers, G. J., & Cloos, J. (2011). Cell sensitivity assays: the MTT assay. *Cancer cell culture: methods and protocols*, 237-245.

van Sluis, M., & McStay, B. (2015). A localized nucleolar DNA damage response facilitates recruitment of the homology-directed repair machinery independent of cell cycle stage. *Genes & Development*, 29(11), 1151-1163.

van Vuuren, R. J., Visagie, M. H., Theron, A. E., & Joubert, A. M. (2015). Antimitotic drugs in the treatment of cancer. *Cancer Chemotherapy and Pharmacology*, 76(6), 1101–1112. https://doi.org/10.1007/s00280-015-2903-8

Vanhoefer, U., Harstrick, A., Achterrath, W., Cao, S., Seeber, S., & Rustum, Y. M. (2001). Irinotecan in the treatment of colorectal cancer: clinical overview. *Journal of Clinical Oncology* : official journal of the American Society of Clinical Oncology, 19(5), 1501–1518. https://doi.org/10.1200/JCO.2001.19.5.1501

Vasan, N., Baselga, J., & Hyman, D. M. (2019). A view on drug resistance in cancer. *Nature,* 575(7782), 299-309.

Vijapura, C., Saad Aldin, E., Capizzano, A. A., Policeni, B., Sato, Y., & Moritani, T. (2017). Genetic syndromes associated with central nervous system tumors. *Radiographics*, 37(1), 258-280.

Visconti, R., & Grieco, D. (2009). New insights on oxidative stress in cancer. *Current Opinion in Drug Discovery & Development*, 12(2), 240–245.

Vitti, E. T., & Parsons, J. L. (2019). The radiobiological effects of proton beam therapy: Impact on DNA damage and repair. *Cancers*, 11(7), 946.

Vodenkova, S., Buchler, T., Cervena, K., Veskrnova, V., Vodicka, P., & Vymetalkova, V. (2020). 5-fluorouracil and other fluoropyrimidines in colorectal cancer: Past, present and future. *Pharmacology & Therapeutics*, 206, 107447.

Vogelstein, B., Lane, D., & Levine, A. (2000). Surfing the p53 network. *Nature*, 408(6810), 307-310. doi: 10.1038/35042675

Walker JR, Corpina RA, Goldberg J. Structure of the Ku heterodimer bound to DNA and its implications for double-strand break repair. *Nature*. 2001 Aug 9;412(6847):607-14. doi: 10.1038/35088000.

Wallace SS, Bandaru V, Kathe SD, Bond JP. (2003). The enigma of endonuclease VIII. *DNA Repair (Amst)*. 2:441–453.

Wallace, B. D., Berman, Z., Mueller, G. A., Lin, Y., Chang, T., Andres, S. N., Wojtaszek, J. L., DeRose, E. F., Appel, C. D., London, R. E., Yan, S., & Williams, R. S. (2017). APE2 Zf-GRF facilitates 3′-5′ resection of DNA damage following oxidative stress. *Proceedings of the National Academy of Sciences of the United States of America*, 114(2), 304–309. https://doi.org/10.1073/pnas.1610011114

Wang, B., Matsuoka, S., Carpenter, P. B., & Elledge, S. J. (2002). 53BP1, a mediator of the DNA damage checkpoint. *Science*, 298(5597), 1435–1438. https://doi.org/10.1126/science.1076182

Wang, K. C., & Chang, H. Y. (2011). Molecular mechanisms of long non-coding RNAs. *Molecular Cell*, 43(6), 904–914. https://doi.org/10.1016/j.molcel.2011.08.018

Wang, L., Cho, K. B., Li, Y., Tao, G., Xie, Z., & Guo, B. (2019). Long non-coding RNA (lncRNA)-mediated competing endogenous RNA networks provide novel potential biomarkers and therapeutic targets for colorectal cancer. *International Journal of Molecular Sciences*, 20(22), 5758.

Wang, P., Ren, Z., & Sun, P. (2012). Overexpression of the long non-coding RNA MEG3 impairs in vitro glioma cell proliferation. *Journal of Cellular Biochemistry*, 113(6), 1868–1874. https://doi.org/10.1002/jcb.24055

Wang, Q., Li, Z., Yang, J., Peng, S., Zhou, Q., Yao, K., ... & Huang, H. (2021). Loss of NEIL3 activates radiotherapy resistance in the progression of prostate cancer. *Cancer Biology & Medicine.*

Wang, Q., Xiong, J., Qiu, D., Zhao, X., Yan, D., Xu, W., ... & Zhou, J. (2017). Inhibition of PARP1 activity enhances chemotherapeutic efficiency in cisplatin-resistant gastric cancer cells. *The international journal of biochemistry & cell biology*, 92, 164-172.

Wang, X., Dubuc, A., Ramaswamy, V., Mack, S., Gendoo, D., & Remke, M. *et al.* (2015). Medulloblastoma subgroups remain stable across primary and metastatic compartments. *Acta Neuropathologica*, *129*(3), 449-457. doi: 10.1007/s00401-015-1389-0

Wang, X., Zhang, X., Dang, Y., Li, D., Lu, G., Chan, W. Y., ... & Chen, Z. J. (2020). Long non-coding RNA HCP5 participates in premature ovarian insufficiency by transcriptionally regulating MSH5 and DNA damage repair via YB1. *Nucleic acids Research*, 48(8), 4480-4491.

Wang, Y., Xu, L., Shi, S., Wu, S., Meng, R., Chen, H., & Jiang, Z. (2021). Deficiency of NEIL3 Enhances the Chemotherapy Resistance of Prostate Cancer. *International Journal of Molecular Sciences*, 22(8), 4098. https://doi.org/10.3390/ijms22084098

Wei, X., Gu, X., Ma, M., & Lou, C. (2019). Long non-coding RNA HCP5 suppresses skin cutaneous melanoma development by regulating RARRES3 gene expression via sponging miR-12. *Oncotargets and Therapy*, 12, 6323.

Weterings, E., & Chen, D. J. (2008). The endless tale of non-homologous end-joining. *Cell Research*, 18(1), 114–124. https://doi.org/10.1038/cr.2008.3

Weterings, E., & van Gent, D. C. (2004). The mechanism of non-homologous end-joining: a synopsis of synapsis. *DNA Repair*, 3(11), 1425–1435. https://doi.org/10.1016/j.dnarep.2004.06.003

White, A. C., & Lowry, W. E. (2015). Refining the role for adult stem cells as cancer cells of origin. *Trends in Cell Biology*, 25(1), 11-20.

Wiltshaw, E. (1979). Cisplatin in the treatment of cancer. *Platinum Metals Review*, 23(3), 90-98.

Wolf, P., Schoeniger, A., & Edlich, F. (2022). Pro-apoptotic complexes of BAX and BAK on the outer mitochondrial membrane. Biochimica et Biophysica Acta (BBA)-Molecular Cell Research, 119317.

Wong, R. S. (2011). Apoptosis in cancer: from pathogenesis to treatment. *Journal of Experimental & Clinical Cancer Research*, 30(1), 1-14.

Wood, L. D., Parsons, D. W., Jones, S., Lin, J., Sjöblom, T., Leary, R. J., Shen, D., Boca, S. M., Barber, T., Ptak, J., Silliman, N., Szabo, S., Dezso, Z., Ustyanksky, V., Nikolskaya, T., Nikolsky, Y., Karchin, R., Wilson, P. A., Kaminker, J. S., Zhang, Z., … Vogelstein, B. (2007). The genomic landscapes of human breast and colorectal cancers. *Science* (New York, N.Y.), 318(5853), 1108–1113. https://doi.org/10.1126/science.1145720

Woynarowski, J. M., Faivre, S., Herzig, M. C., Arnett, B., Chapman, W. G., Trevino, A. V., Raymond, E., Chaney, S. G., Vaisman, A., Varchenko, M., & Juniewicz, P. E. (2000). Oxaliplatin-induced damage of cellular DNA. Molecular pharmacology, 58(5), 920–927. https://doi.org/10.1124/mol.58.5.920

Wu, G.Y., Fang, Y. Z., Yang, S., Lupton, J. R., and Turner, N. D. (2004) Glutathione metabolism and its implications for health. *Journal of Nutrition*. 134, 489–492.

Wu, H., Yang, L., & Chen, L. L. (2017). The Diversity of Long Non-coding RNAs and Their Generation. *Trends in Genetics* : TIG, 33(8), 540–552. https://doi.org/10.1016/j.tig.2017.05.004

Wu, J., Chen, H., Ye, M., Wang, B., Zhang, Y., Sheng, J., ... & Chen, H. (2019). Downregulation of long non-coding RNA HCP5 contributes to cisplatin resistance in human triple-negative breast cancer via regulation of PTEN expression. *Biomedicine & Pharmacotherapy*, 115, 108869.

Wu, X., Northcott, P., Croul, S., & Taylor, M. (2011). Mouse models of medulloblastoma. *Chinese Journal Of Cancer*, 442-449. doi: 10.5732/cjc.011.10040

Wu, Z., Liu, X., Liu, L., Deng, H., Zhang, J., Xu, Q., ... & Ji, A. (2014). Regulation of lncRNA expression. *Cellular & Molecular Biology Letters*, 19, 561-575.

Wyatt, H. D., Sarbajna, S., Matos, J., & West, S. C. (2013). Coordinated actions of SLX1-SLX4 and MUS81-EME1 for Holliday junction resolution in human cells. *Molecular Cell*, 52(2), 234–247. https://doi.org/10.1016/j.molcel.2013.08.035

Xie X, Tang B, Xiao YF, Xie R, Li BS, Dong H, Zhou JY, Yang SM. Long non-coding RNAs in colorectal cancer. *Oncotarget*. 2016;7:5226–5239.

Xie, M., Zhang, L., He, C. S., Xu, F., Liu, J. L., Hu, Z. H., Zhao, L. P., & Tian, Y. (2012). Activation of Notch-1 enhances epithelial-mesenchymal transition in gefitinib-acquired resistant lung cancer cells. *Journal of Cellular Biochemistry*, 113(5), 1501–1513. https://doi.org/10.1002/jcb.24019

Xu, Q., Karouji, Y., Kobayashi, M., Ihara, S., Konishi, H., & Fukui, Y. (2003). The PI 3-kinase-Rac-p38 MAP kinase pathway is involved in the formation of signet-ring cell carcinoma. *Oncogene*, 22(36), 5537–5544. https://doi.org/10.1038/sj.onc.1206796

Xu, Y., & Pasche, B. (2007). TGF-beta signaling alterations and susceptibility to colorectal cancer. *Human Molecular Genetics*, 16 Spec No 1(SPEC), R14–R20. https://doi.org/10.1093/hmg/ddl486

Xu, Y., Qiu, M., Shen, M., Dong, S., Ye, G., Shi, X., & Sun, M. (2021). The emerging regulatory roles of long non-coding RNAs implicated in cancer metabolism. *Molecular Therapy*, 29(7), 2209-2218.

Xue, C., & Greene, E. C. (2021). DNA repair pathway choices in CRISPR-Cas9-mediated genome editing. *Trends in Genetics*, 37(7), 639-656.

Yahata, H., Kobayashi, H., Kamura, T., Amada, S., Hirakawa, T., Kohno, K., Kuwano, M., & Nakano, H. (2002). Increased nuclear localization of transcription factor YB-1 in acquired cisplatin-resistant ovarian cancer. *Journal of Cancer Research and Clinical Oncology*, 128(11), 621–626. https://doi.org/10.1007/s00432-002-0386-6

Yan, X., Hu, Z., Feng, Y., Hu, X., Yuan, J., Zhao, S. D., Zhang, Y., Yang, L., Shan, W., He, Q., Fan, L., Kandalaft, L. E., Tanyi, J. L., Li, C., Yuan, C. X., Zhang, D., Yuan, H., Hua, K., Lu, Y., Katsaros, D., … Zhang, L. (2015). Comprehensive Genomic Characterization of Long Non-coding RNAs across Human Cancers. *Cancer cell*, 28(4), 529–540. https://doi.org/10.1016/j.ccell.2015.09.006

Yang, C., Sun, J., Liu, W., Yang, Y., Chu, Z., Yang, T., Gui, Y., & Wang, D. (2019). Long non-coding RNA HCP5 contributes to epithelial-mesenchymal transition in colorectal cancer through ZEB1 activation and interacting with miR-139-5p. *American Journal of Translational Research*, 11(2), 953–963.

Yang, G., Liu, C., Chen, S. H., Kassab, M. A., Hoff, J. D., Walter, N. G., & Yu, X. (2018). Super-resolution imaging identifies PARP1 and the Ku complex acting as DNA double-strand break sensors. *Nucleic acids Research*, 46(7), 3446-3457.

Yang, H., Ren, S., Yu, S., Pan, H., Li, T., Ge, S., ... & Xia, N. (2020). Methods favoring homology-directed repair choice in response to CRISPR/Cas9 induced-double strand breaks. *International Journal of Molecular Sciences*, 21(18), 6461.

Yang, M., Davis, T. B., Pflieger, L., Nebozhyn, M. V., Loboda, A., Wang, H., ... & Yeatman, T. J. (2022). An integrative gene expression signature analysis identifies CMS4 KRAS-mutated colorectal cancers sensitive to combined MEK and SRC targeted therapy. *BMC Cancer*, 22(1), 1-21.

Yang, N., Chaudhry, M. A., & Wallace, S. S. (2006). Base excision repair by hNTH1 and hOGG1: a two edged sword in the processing of DNA damage in gamma-irradiated human cells. *DNA Repair*, 5(1), 43–51. https://doi.org/10.1016/j.dnarep.2005.07.003

Yang, R., Niepel, M., Mitchison, T. K., & Sorger, P. K. (2010). Dissecting variability in responses to cancer chemotherapy through systems pharmacology. *Clinical Pharmacology and Therapeutics*, 88(1), 34–38. https://doi.org/10.1038/clpt.2010.96

Yang, S. Y., Sales, K. M., Fuller, B., Seifalian, A. M., & Winslet, M. C. (2009). Apoptosis and colorectal cancer: implications for therapy. *Trends in Molecular Medicine*, 15(5), 225–233. https://doi.org/10.1016/j.molmed.2009.03.003

Yang, Z., Nejad, M. I., Varela, J. G., Price, N. E., Wang, Y., & Gates, K. S. (2017). A role for the base excision repair enzyme NEIL3 in replication-dependent repair of interstrand DNA cross-links derived from psoralen and abasic sites. *DNA Repair*, 52, 1–11. https://doi.org/10.1016/j.dnarep.2017.02.011

Yang, Z., Zhou, L., Wu, L. M., Lai, M. C., Xie, H. Y., Zhang, F., & Zheng, S. S. (2011). Overexpression of long non-coding RNA HOTAIR predicts tumor recurrence in hepatocellular carcinoma patients following liver transplantation. *Annals of Surgical Oncology*, 18(5), 1243–1250. https://doi.org/10.1245/s10434-011-1581-y

Yao, Y., Ma, J., Xue, Y., Wang, P., Li, Z., Liu, J., Chen, L., Xi, Z., Teng, H., Wang, Z., Li, Z., & Liu, Y. (2015). Knockdown of long non-coding RNA XIST exerts tumor-suppressive functions in human glioblastoma stem cells by up-regulating miR-152. *Cancer Letters*, 359(1), 75–86. https://doi.org/10.1016/j.canlet.2014.12.051

Yasuhira, S., Shibazaki, M., Nishiya, M., & Maesawa, C. (2016). Paclitaxel-induced aberrant mitosis and mitotic slippage efficiently lead to proliferative death irrespective of canonical apoptosis and p53. *Cell Cycle*, 15(23), 3268-3277. doi: 10.1080/15384101.2016.1242537

Yauch, R. L., Dijkgraaf, G. J., Alicke, B., Januario, T., Ahn, C. P., Holcomb, T., Pujara, K., Stinson, J., Callahan, C. A., Tang, T., Bazan, J. F., Kan, Z., Seshagiri, S., Hann, C. L., Gould, S. E., Low, J. A., Rudin, C. M., & de Sauvage, F. J. (2009). Smoothened mutation confers resistance to a Hedgehog pathway inhibitor in medulloblastoma. *Science* (New York, N.Y.), 326(5952), 572–574. https://doi.org/10.1126/science.1179386

Ye LC, Zhu X, Qiu JJ, Xu J, Wei Y. (2015). Involvement of long non-coding RNA in colorectal cancer: From benchtop to bedside (Review) *Oncology Letters*. 9:1039–1045. doi: 10.3892/ol.2015.2846

Yildirim, E., Kirby, J. E., Brown, D. E., Mercier, F. E., Sadreyev, R. I., Scadden, D. T., & Lee, J. T. (2013). Xist RNA is a potent suppressor of hematologic cancer in mice. *Cell*, 152(4), 727–742. https://doi.org/10.1016/j.cell.2013.01.034

Yoon, W., Ma, B. J., Fellay, J., Huang, W., Xia, S. M., Zhang, R., Shianna, K. V., Liao, H. X., Haynes, B. F., Goldstein, D. B., & NIAID Center for HIV/AIDS Vaccine Immunology (2010). A polymorphism in the HCP5 gene associated with HLA-B*5701 does not restrict HIV-1 in vitro. *AIDS*, 24(1), 155–157. https://doi.org/10.1097/QAD.0b013e32833202f5

Youle, R. J., & Strasser, A. (2008). The BCL-2 protein family: opposing activities that mediate cell death. *Nature reviews Molecular Cell Biology*, 9(1), 47-59.

Yousefzadeh, M., Henpita, C., Vyas, R., Soto-Palma, C., Robbins, P., & Niedernhofer, L. (2021). DNA damage—how and why we age?. *Elife*, 10, e62852.

Yu J, Zhou Z, Tay-Sontheimer J, Levy RH, Ragueneau-Majlessi I (2017). "Intestinal Drug Interactions Mediated by OATPs: A Systematic Review of Preclinical and Clinical Findings". *Journal of Pharmaceutical Sciences*. 106 (9): 2312–2325. doi:10.1016/j.xphs.2017.04.004.

Yu, W., Lescale, C., Babin, L., Bedora-Faure, M., Lenden-Hasse, H., Baron, L., ... & Deriano, L. (2020). Repair of G1 induced DNA double-strand breaks in S-G2/M by alternative NHEJ. *Nature Communications*, 11(1), 5239.

Yu, X., Fu, S., Lai, M., Baer, R., & Chen, J. (2006). BRCA1 ubiquitinates its phosphorylation-dependent binding partner CtIP. *Genes & Development*, 20(13), 1721-1726.

Zaman, S., Wang, R., & Gandhi, V. (2014). Targeting the apoptosis pathway in hematologic malignancies. *Leukemia & Lymphoma*, 55(9), 1980-1992.

Zamble, D. B., & Lippard, S. J. (1995). Cisplatin and DNA repair in cancer chemotherapy. *Trends in Biochemical Sciences*, 20(10), 435-439.

Zhang, L., & Shay, J. W. (2017). Multiple roles of APC and its therapeutic implications in colorectal cancer. *JNCI: Journal of the National Cancer Institute*, 109(8).

Zhang, L., Ding, P., Lv, H., Zhang, D., Liu, G., Yang, Z., ... & Zhang, S. (2014). Number of polyploid giant cancer cells and expression of EZH2 are associated with VM formation and tumor grade in human ovarian tumor. *Biomed Research International*, 2014.

Zhang, L., Jiang, D., Gan, Q., Shi, H., Miao, L., Gong, Y., & Oger, P. (2021). Identification of a novel bifunctional uracil DNA glycosylase from Thermococcus barophilus Ch5. *Applied Microbiology and Biotechnology*, 105, 5449-5460.

Zhang, P., Zhang, Z., Zhou, X., Qiu, W., Chen, F., & Chen, W. (2006). Identification of genes associated with cisplatin resistance in human oral squamous cell carcinoma cell line. *BMC Cancer*, 6, 224. https://doi.org/10.1186/1471-2407-6-224

Zhang, S., Mercado-Uribe, I., & Liu, J. (2014). Tumor stroma and differentiated cancer cells can be originated directly from polyploid giant cancer cells induced by paclitaxel. *International Journal of Cancer*, 134(3), 508–518. https://doi.org/10.1002/ijc.28319

Zhang, S., Mercado-Uribe, I., Xing, Z., Sun, B., Kuang, J., & Liu, J. (2014). Generation of cancer stem-like cells through the formation of polyploid giant cancer cells. *Oncogene*, 33(1), 116–128. https://doi.org/10.1038/onc.2013.96

Zhang, X., Li, H., Burnett, J. C., & Rossi, J. J. (2014). The role of antisense long non-coding RNA in small RNA-triggered gene activation. *RNA*, 20(12), 1916–1928. https://doi.org/10.1261/rna.043968.113

Zhang, Y. L., Zhang, Z. S., Wu, B. P., & Zhou, D. Y. (2002). Early diagnosis for colorectal cancer in China. *World Journal of Gastroenterology*, 8(1), 21–25. https://doi.org/10.3748/wjg.v8.i1.21

Zhang, Y., Zhang, X. O., Chen, T., Xiang, J. F., Yin, Q. F., Xing, Y. H., Zhu, S., Yang, L., & Chen, L. L. (2013). Circular intronic long non-coding RNAs. *Molecular Cell*, 51(6), 792–806. https://doi.org/10.1016/j.molcel.2013.08.017

Zhang, Z., & Wang, H. (2021). HCP5 promotes proliferation and contributes to cisplatin resistance in gastric cancer through miR-519d/HMGA1 axis. *Cancer Management and Research*, 13, 787.

Zhao, J., Bai, X., Feng, C., Shang, X., & Xi, Y. (2019). Long Non-Coding RNA HCP5 Facilitates Cell Invasion And Epithelial-Mesenchymal Transition In Oral Squamous Cell Carcinoma By miR-140-5p/SOX4 Axis. *Cancer Management and Research*, 11, 10455–10462. https://doi.org/10.2147/CMAR.S230324

Zhao, S. G., Chen, W. S., Li, H., Foye, A., Zhang, M., Sjöström, M., ... & Feng, F. Y. (2020). The DNA methylation landscape of advanced prostate cancer. *Nature Genetics*, 52(8), 778-789.

Zhao, S., Tadesse, S., & Kidane, D. (2021). Significance of base excision repair to human health. *International Review of Cell and Molecular Biology*, 364, 163-193.

Zhao, W., & Li, L. (2019). SP1-induced upregulation of long non-coding RNA HCP5 promotes the development of osteosarcoma. *Pathology-Research and Practice*, 215(3), 439-445.

Zhao, X., Wei, C., Li, J., Xing, P., Li, J., Zheng, S., & Chen, X. (2017). Cell cycle-dependent control of homologous recombination. *Acta biochimica et biophysica Sinica*, 49(8), 655–668. https://doi.org/10.1093/abbs/gmx055

Zheng, L., Rui, C., Zhang, H., Chen, J., Jia, X., & Xiao, Y. (2019). Sonic hedgehog signaling in epithelial tissue development. *Regenerative Medicine Research*, 7, 3. https://doi.org/10.1051/rmr/190004

Zhou, X. J., & Rahmani, R. (1992). Preclinical and clinical pharmacology of vinca alkaloids. *Drugs*, 44 Suppl 4, 1–69. https://doi.org/10.2165/00003495-199200444-00002

Zhou,B.B.S. and Elledge,S.J. (2000) The DNA damage response: putting checkpoints in perspective. *Nature* , 408 , 433 –439.

Zhu, H., Shan, Y., Ge, K., Lu, J., Kong, W., & Jia, C. (2020). Oxaliplatin induces immunogenic cell death in hepatocellular carcinoma cells and synergizes with immune checkpoint blockade therapy. *Cellular Oncology* (Dordrecht), 43(6), 1203–1214. https://doi.org/10.1007/s13402-020-00552-2

Zhukova, N., Ramaswamy, V., Remke, M., Pfaff, E., Shih, D., & Martin, D. *et al*. (2013). Subgroup-Specific Prognostic Implications of TP53 Mutation in Medulloblastoma. *Journal Of Clinical Oncology*, *31*(23), 2927-2935. doi: 10.1200/jco.2012.48.5052.

Ziller, M. J., Gu, H., Müller, F., Donaghey, J., Tsai, L. T. Y., Kohlbacher, O., ... & Meissner, A. (2013). Charting a dynamic DNA methylation landscape of the human genome. *Nature*, 500(7463), 477-481.

Zou, S., Gao, Y., & Zhang, S. (2021). lncRNA HCP5 acts as a ceRNA to regulate EZH2 by sponging miR-138-5p in cutaneous squamous cell carcinoma. *International Journal of Oncology*, 59(2), 56. https://doi.org/10.3892/ijo.2021.5236

Zou, Y., & Chen, B. (2021). Long non-coding RNA HCP5 in cancer. *Clinica chimica acta*, 512, 33-39.

Zugazagoitia, J., Guedes, C., Ponce, S., Ferrer, I., Molina-Pinelo, S., & Paz-Ares, L. (2016). Current challenges in cancer treatment. *Clinical Therapeutics*, 38(7), 1551-1566.

Zurawel, R. H., Chiappa, S. A., Allen, C., & Raffel, C. (1998). Sporadic medulloblastomas contain oncogenic beta-catenin mutations. *Cancer Research*, 58(5), 896–899.
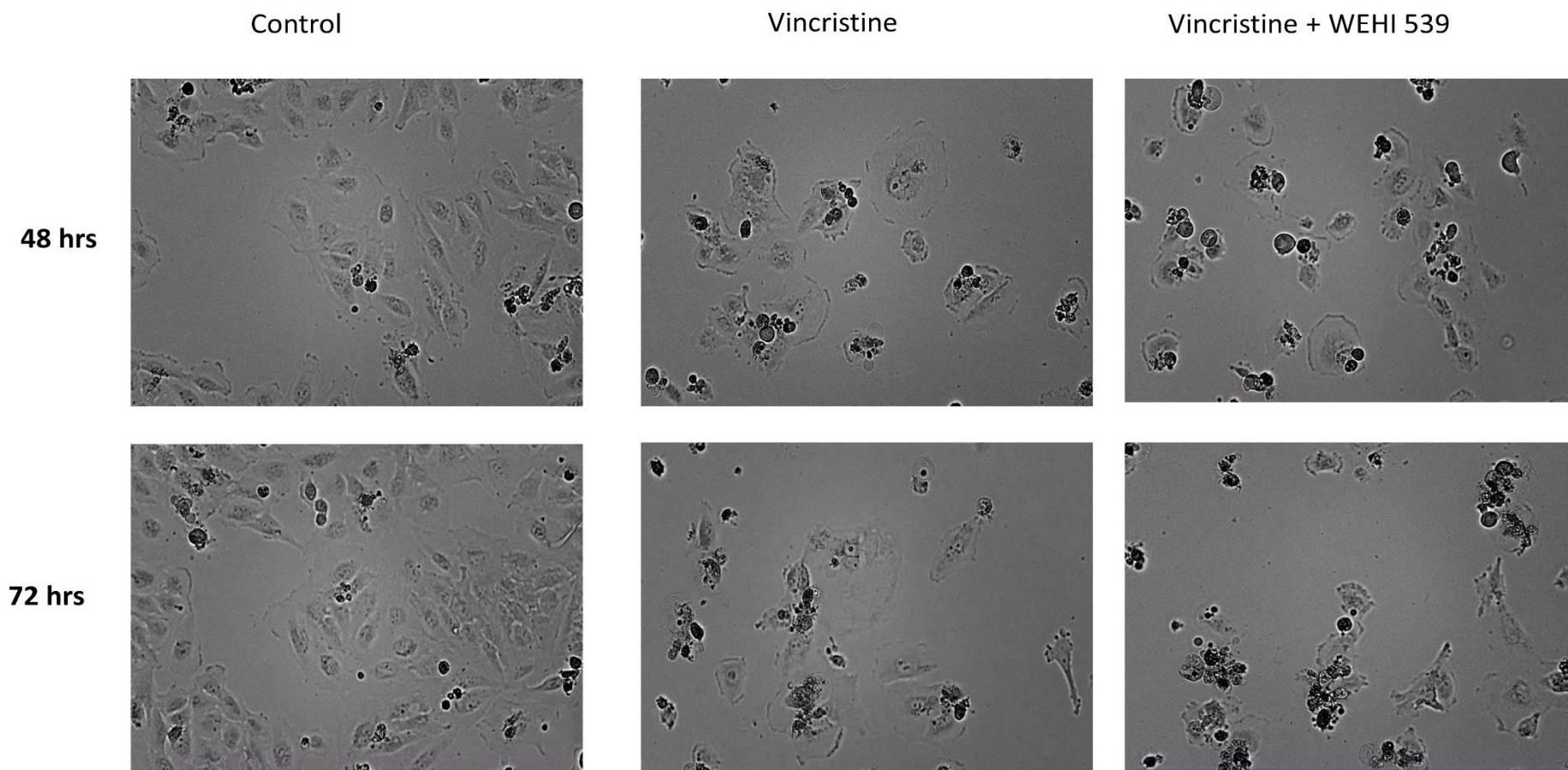
Supplementary data

Time lapse experiment to confirm mitotic slippage.

Subsequent to the treatment of the cells with vincristine, mitotic slippage was confirmed using time lapse microscopy. Time lapse experiment showing mitotic slippage in ONS76 cells after vincristine treatment and combination treatments with WEHI539 and siBcl-xL resulted in a reduction in mitotic slippage and increase in cell death. Time lapse microscopy of the DAOY cell line showed that only a few cells underwent mitotic slippage and in the MBO3 cell lines a higher number of cells were seen to undergo mitotic slippage and treatment with WEHI539 could not rescue all the cells from mitotic slippage. Mitotic slippage was identified by cells exiting mitosis without dividing and change in morphology, while cell death was identified as cells shrivelling up and fragment into apoptotic bodies.
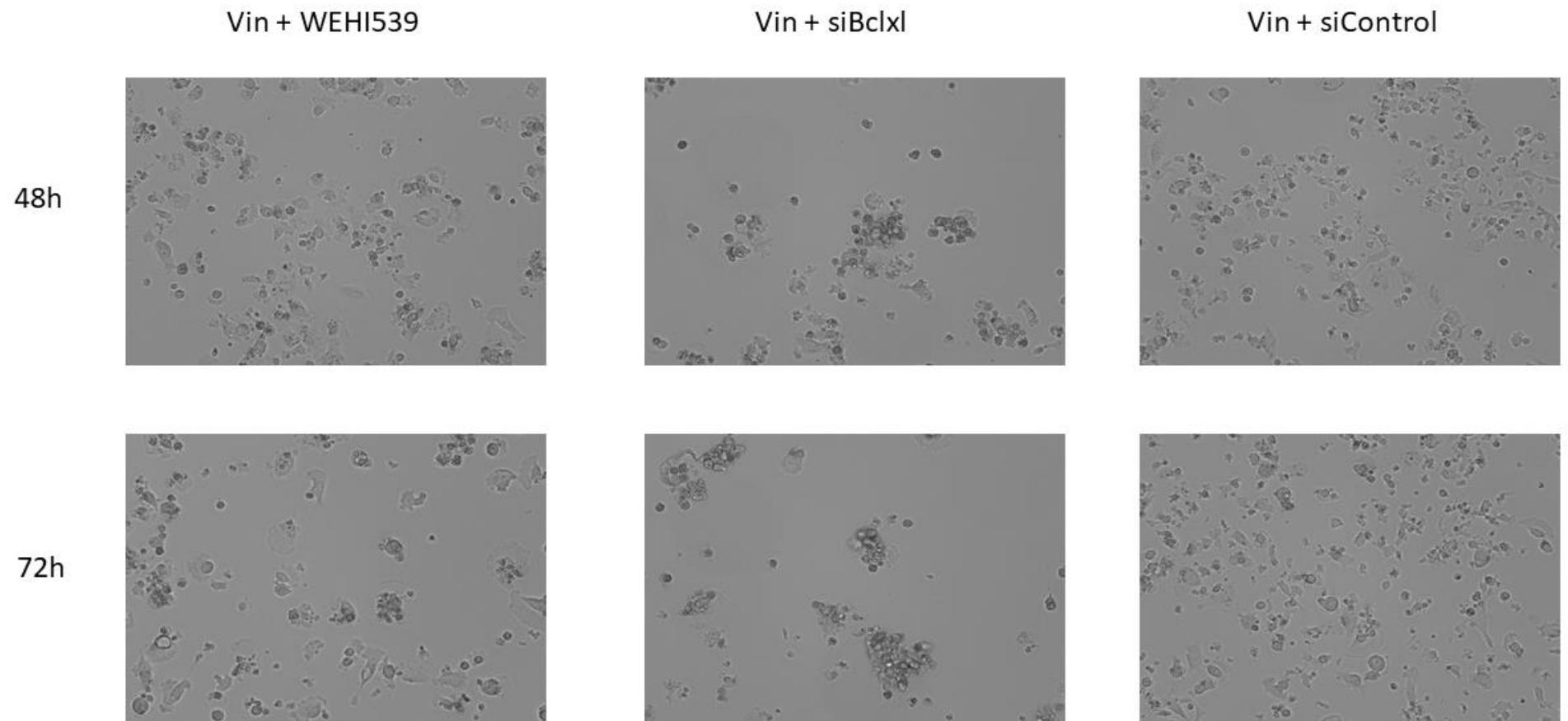
	Control	Vincristine	Vincristine + WEHI 539

48 hrs

72 hrs
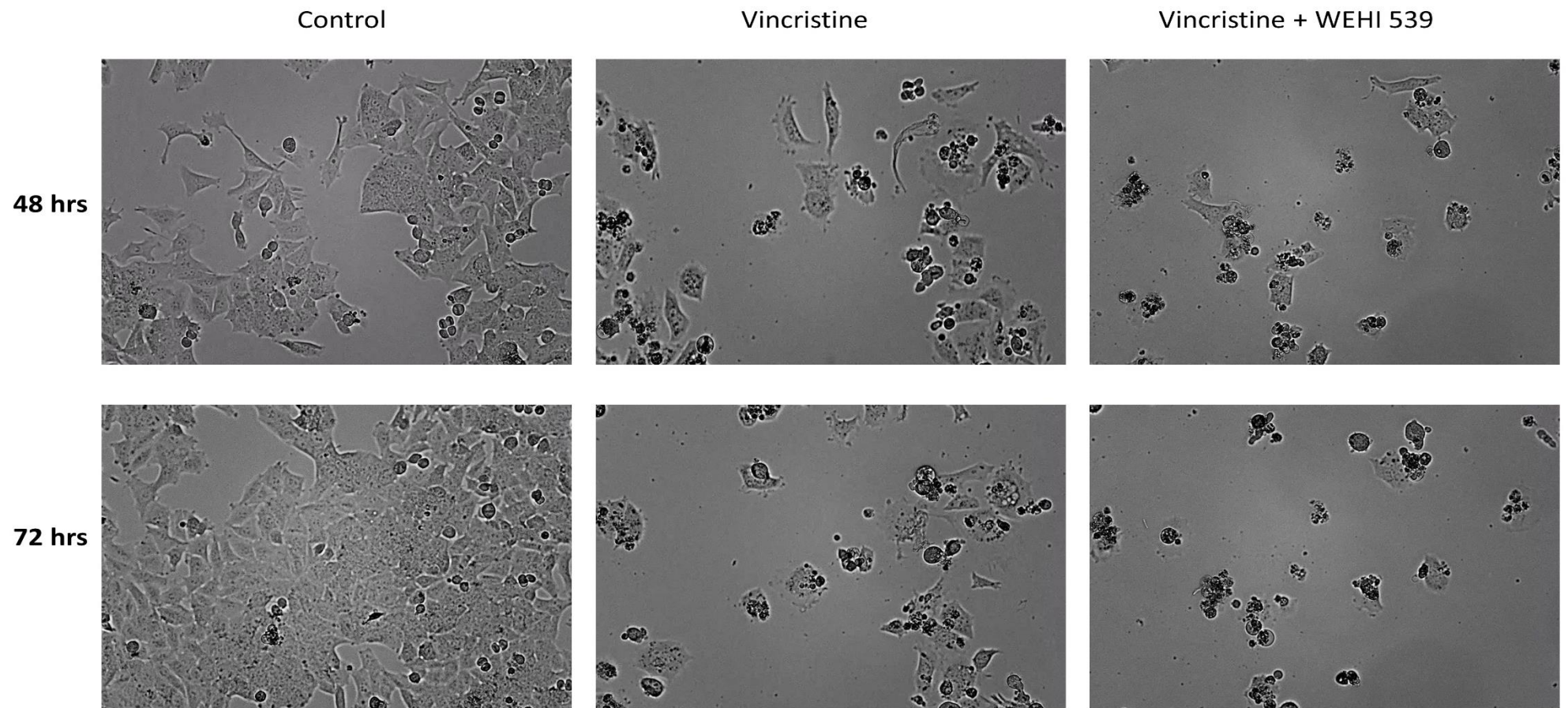
Supplementary data 1- Time lapse microscopy showing the fate of MBO3 cells treated with 15.6 nM vincristine alone and vincristine + WEHI539

	Control	Vincristine	Vincristine + WEHI 539
48 hrs			
72 hrs			

Supplementary data 2- Time lapse microscopy showing the fate of DAOY cells treated with 9.6nM vincristine alone and vincristine + WEHI539

	Mock	siControl	siBclxl	Vincristine
48h				
72h				
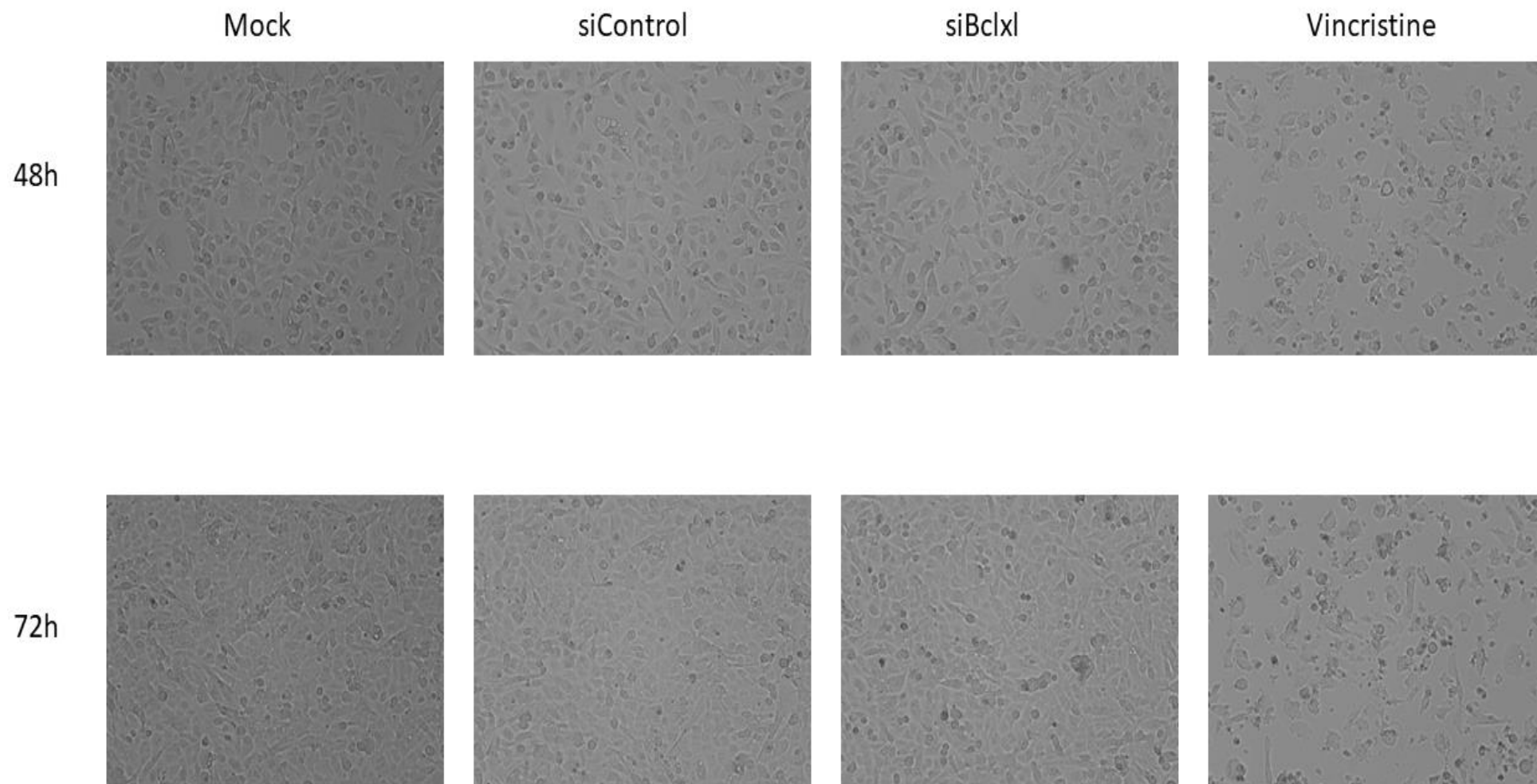
Supplementary data 3- Time lapse microscopy showing the fate of ONS76 cells treated with 39.1 nM vincristine alone, vincristine + WEHI539 and vincristine + si-Bcl-xL.

Cell line	Treatment		
	Cisplatin	Cisplatin + siHCP5	Cisplatin + siHCP5 + olaparib
SW48	17.22 ± 1.15	6.57 ± 2.31	6.23 ± 2.76
SW480	7.295 ± 1.56	3.11 ± 0.72	3.01 ± 0.55
HCT116	3.31 ± 0.98	1.62 ± 0.81	1.51 ± 0.66
DAOY	0.838 ± 0.21	0.33 ± 0.01	0.3 ± 0.02

Cell line	Treatment		
	Oxaliplatin	Oxaliplatin+ siHCP5	Oxaliplatin+ siHCP5 + olaparib
SW48	0.663 ± 0.19	0.321 ± 0.13	0.31 ± 0.1
SW480	1.096 ± 0.23	0.43 ± 0.67	0.38 ± 0.11
HCT116	0.66 ± 0.13	0.37 ± 0.09	0.33 ± 0.12
DAOY	11.48 ± 2.2	6.13 ± 1.8	5.1 ± 1.12

Cell line	Treatment		
	TBH	TBH + siHCP5	TBH + siHCP5 + olaparib
SW48	N/A	70.5 ± 2.31	62.5 ± 3.81
SW480	57.67 ± 2.79	36.5 ± 3.67	28.3 ± 2.9
HCT116	18.28 ± 1.6	14.63 ± 2.11	11.63 ± 2.78
DAOY	13.88± 2.4	8.7 ± 1.9	7.9 ± 2.1

Supplementary data 4- IC50 of cells after treatment with genotoxic agents alone and combination treatments with siHCP5 and siHCP5+ olaparib.